MUTATIONAL ANALYSIS OF THE DNA REPAIR PROTEIN, UvrA

Rachel Mary Albrighton

A dissertation submitted to the University of Bristol in accordance with the requirements for the degree of Doctor of Philosophy in the Faculty of Medical and Veterinary Sciences, Department of Biochemistry, September 2006.

41,110 words.

ABSTRACT

UvrA is an essential component of the *Escherichia coli* nucleotide excision repair (NER) apparatus. Previous studies indicated that the N-terminal region of UvrA interacts with UvrB. UvrB shares a region of sequence and structural homology with Mfd, a transcription-repair coupling factor. UvrB and Mfd are believed to interact with UvrA via this homology region. Mfd recognises stalled transcription complexes and recruits the nucleotide excision repair apparatus via its interaction with UvrA.

In this work the UvrA-UvrB and the UvrA-Mfd interactions have been studied. A bacterial two-hybrid system was used to monitor interactions between the N-terminal domain of UvrA and regions of UvrB or Mfd. Single amino acid substitutions within UvrA that disrupt this interaction have been identified. A second screen, based on UV sensitivity, has been used to identify a further series of *uvrA* mutations that affect a wide range of UvrA functions.

The UvrA mutants identified in these screens have been purified and characterised to determine their nucleotide hydrolysis rates, DNA binding, protein-protein interaction and overall repair capability. $UvrA_{G173}$ and $UvrA_{D205}$ have been identified as potential residues involved in the UvrA-UvrB interaction.

As part of the repair studies site-specific methyltransferase induced labelling (SMILing) of DNA has been used as a novel method of introducing a single site-specific modification within a single strand of a 2.6 kb DNA fragment.

ACKNOWLEDGEMENTS

I am very grateful to my supervisor, Nigel Savery, for all the help, support and enthusiasm he has shown during my time at Bristol. I would also like to thank E. Weinhold, A. Ishihama, and M. Dillingham for gifts of materials used in this work. I am thankful to the BBSRC for funding.

A huge thank you to past and present members of D40, especially to Abby, Anna, Kate, Jacqui and Abdou who have made my time here enjoyable and productive.

Finally I would like to thank all my friends and family especially Mum, Dad and Dan, whose love and support have been invaluable to me over the years.

AUTHORS' DECLARATION

I declare that the work in this dissertation was carried out in accordance with the Regulations of the University of Bristol. The work is original, except where indicated by special reference in the text, and no part of the dissertation has been submitted for any other academic award. Any views expressed in the dissertation are those of the author.

SIGNED:.....R.A.Wright..... DATE:..5th..December.06.

TABLE OF CONTENTS

TABLE OF FIGURES AND TABLES

ABBREVIATIONS

AFM	Atomic Force Microscopy
APS	Ammonium persulphate
ATP	Adenosine triphosphate
ATPase	Adenosine triphosphatase
ATPγS	Adenosine 5'-O-(3-thio) triphosphate
AUC	Analytical ultracentrifuge
B. caldotenax	*Bacillus caldotenax*
BER	Base excision repair
bp	Base pair
BSA	Bovine serum albumin
B. subtilis	*Bacillus subtilis*
CIAP	Calf intestinal alkaline phosphatase
CPD	Cyclobutane pyrimidine dimer
CTD	C-terminal domain
dATP	deoxyadenosine triphosphate
dCTP	deoxycytidine triphosphate
dGTP	deoxyguanosine triphosphate
dNTPs	deoxynucleotide triphosphate
DR	Direct reversal
DTT	Dithiothreitol
dTTP	deoxythymidine triphosphate
E. coli	*Escherichia coli*
EDTA	Ethylenediaminetetraacetate
EMSA	Electrophoretic mobility shift assay
FADH	Flavin adenine dinucleotide (reduced)
Fld-dT	Fluorescein-dT
FPLC	Fast protein liquid chromatography
GTP	Guanosine triphosphate
GTPase	Guanosine triphosphatase
GTPγS	Guanosine 5'-O-(3-thio) triphosphate

HR	Homologous recombination
IPTG	Isopropylthiogalactoside
LB	Leutina Beru
LDH	Lactate dehydrogenase
MMR	Mismatch repair
MWCO	Molecular weight cut-off
NAD	Nicotinamide adenine dinucleotide
NADH	Nicotinamide adenine dinucleotide (reduced)
NER	Nucleotide excision repair
NHEJ	Non-homologous end joining
NTD	N-terminal domain
NTP	Nucleotide triphosphate
PBS	Phosphate buffered saline
PCR	Polymerase chain reaction
PEP	Phosphoenolpyruvate
PK	Pyruvate kinase
RNAP	RNA polymerase
RNase	Ribonuclease
SDS	Sodium dodecyl sulphate
SDS PAGE	SDS polyacrylamide gel electrophoresis
SFM	Scanning force microscopy
SMILing	Sequence-specific methyltransferase induced labelling
T4EV	T4 endonuclease V
TAE	Tris acetic EDTA
TBE	Tris borate EDTA
TCR	Transcription-coupled repair
TE	Tris EDTA
TEMED	Tetramethylethylenediamine
TRCF	Transcription repair-coupling factor
T. thermophilus	*Thermus thermophilus*
UV	Ultraviolet
X-gal	5-Bromo-4-chloro-3-indolyl-b-D-galactoside

CHAPTER 1
INTRODUCTION

DNA is continuously damaged by numerous endogenous and exogenous mutagens (reviewed in (Friedberg *et al.*, 2006)). A wide variety of DNA lesions have now been identified. Damaged DNA can have mutagenic and cytotoxic consequences. Certain types of DNA damage act as roadblocks for DNA polymerase and RNA polymerase (RNAP), preventing DNA replication and transcription respectively (Donahue *et al.*, 1994) (Pages and Fuchs, 2003). If even single base mismatches are not repaired the downstream consequences can be serious with daughter cells potentially inheriting the incorrect DNA sequence. For an individual cell and its progeny to survive it is therefore essential that the damage is efficiently repaired. Organisms recognise and repair the different types of DNA damage using a range of repair pathways (Table 1.1) (reviewed in (Scharer, 2003)).

Mutagens and DNA damage

Endogenous mutagens

Alkylating agents

Many DNA adducts are caused by alkylating agents that modify DNA bases. Alkylating agents are electrophilic and react with the nucleophilic centres of base residues to introduce alkyl groups. The alkylating agents that cause the damage can be mono or bifunctional. Monofunctional alkylating agents include S-adenosylmethionine (AdoMet). Alkylating agents covalently attach alkyl groups to DNA bases at one of a variety of positions (Figure 1.1). Adenine N^3, guanine N^7 and guanine O^6 are the most reactive sites and upon exposure to alkylating agents form products such as N^7-methylguanine, N^3-methyladenine and O^6-methylguanine. The downstream consequences of these three alkylation products are all different. O^6-methylguanine can lead to transition mutations as it is able to base pair with thymine (instead of cytosine) (Snow *et al.*, 1984). N^7-methylguanine base pairs with cytosine as normal and therefore is not as harmful to the cell as O^6-methylguanine. N^3-methyladenine is cytotoxic as it prevents DNA replication (Fronza and Gold, 2004). Alkylating agents can also indirectly cause depurination and depyrimidination as the glycosidic bond of the nucleotide that has been modified is weakened and therefore more susceptible to hydrolysis (reviewed in (Loeb and Preston, 1986)).

Lesion	Principle cause	Principle repair pathway	Effect if not repaired	Reference
CPD	UV irradiation	NER	Cytotoxic	(Franklin and Haseltine, 1984)
6-4 photoproduct	UV irradiation	NER	Cytotoxic	(Franklin and Haseltine, 1984)
Double strand break	Ionizing irradiation	HR or NHEJ	Cytotoxic	(Karagiannis and El-Osta, 2004)
Thymine glycol	Ionizing irradiation/ oxidative damage	NER or BER	cytotoxic	(Weinfeld *et al.*, 2001)
5-hydroxycytosine	Ionizing irradiation	BER	cytotoxic	(D'Ham *et al.*, 1999)
O^6-methylguanine	Alkylating agents	DR	Transition	(Kleibl, 2002)
N^7-methylguanine	Alkylating agents	DR	Limited	(Kleibl, 2002)
N^3-methyladenine	Alkylating agents	DR	Cytotoxic	(Kleibl, 2002)
Intrastrand cross-link	Cross-linking reagents	NER	Cytotoxic	(Van Houten, 1990)
Interstrand cross-link	Cross-linking reagents	NER	Cytotoxic	(Van Houten, 1990)
8-hydroxyguanine	Free radicals	DR	Transversion	(Boiteux and Radicella, 1999)
Uracil (from cytosine)	Deamination	BER	Transition	(Krokan *et al.*, 1997)
Hypoxanthine (from adenine)	Deamination	BER	Transition	(Krokan *et al.*, 1997)
Depurination	Spontaneous	BER	Transition or transversion	(Lindahl, 1993)
Depyrimidination	Spontaneous	BER	Transition or transversion	(Lindahl, 1993)

Table 1.1 Types of DNA damage.

Different types of damage are listed alongside the principle cause of the damage, the main repair pathway and the effect that they would have on the cell if left uncorrected. The principle repair pathways are represented by: NER, nucleotide excision repair; BER, base excision repair; NHEJ, non-homologous end joining; HR, homologous recombination; and DR, direct reversal.

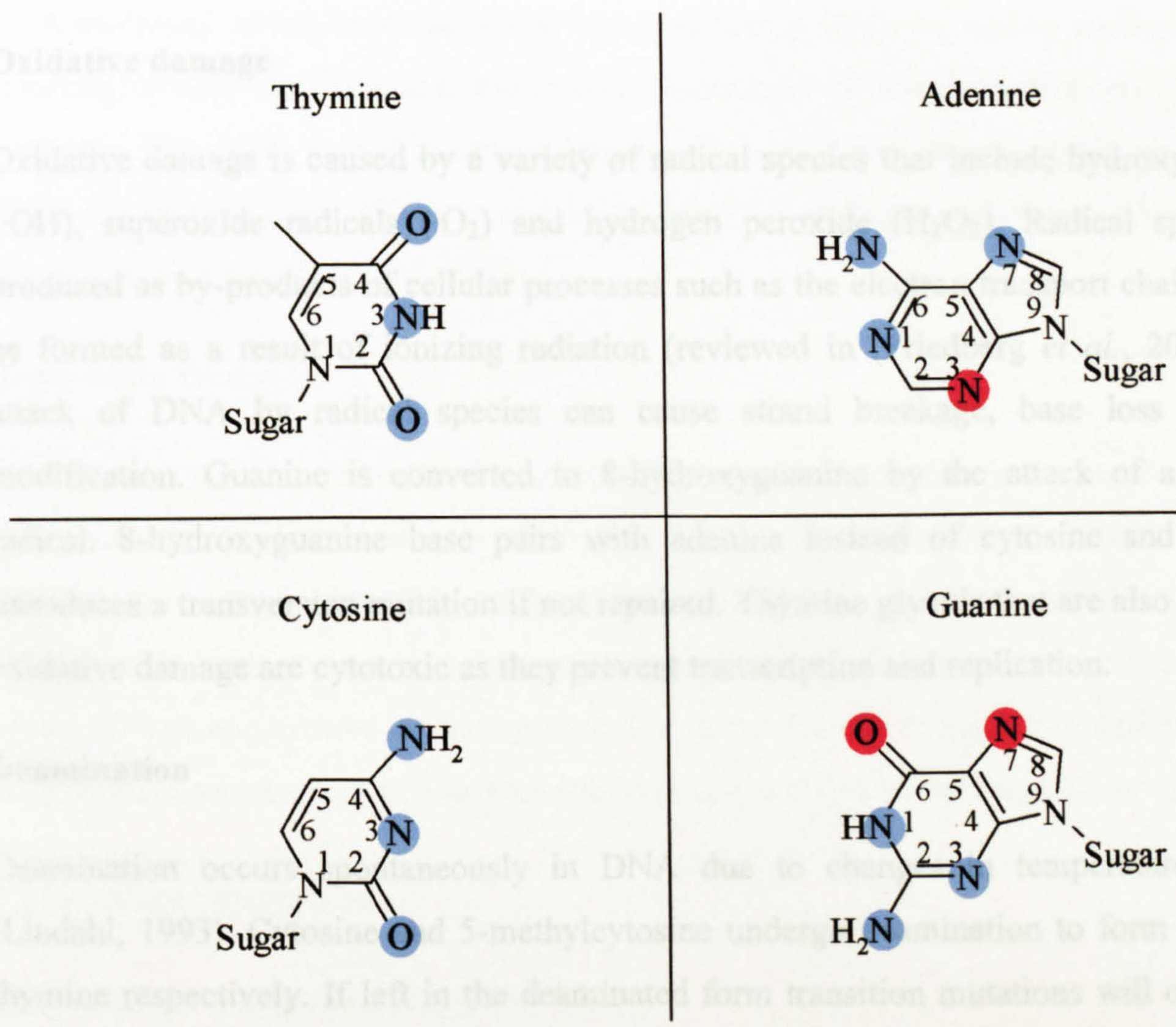

Figure 1.1 Alkylation sites.

The alkylation sites on the four DNA bases are shown in blue and red. The atoms highlighted in red are most susceptible to alkylation (reviewed in (Friedberg *et al.*, 2006)).

Oxidative damage

Oxidative damage is caused by a variety of radical species that include hydroxyl radicals (·OH), superoxide radicals ($\cdot O_2$) and hydrogen peroxide (H_2O_2). Radical species are produced as by-products of cellular processes such as the electron transport chain and can be formed as a result of ionizing radiation (reviewed in (Friedberg *et al.*, 2006)). The attack of DNA by radical species can cause strand breakage, base loss and base modification. Guanine is converted to 8-hydroxyguanine by the attack of a hydroxyl radical. 8-hydroxyguanine base pairs with adenine instead of cytosine and therefore introduces a transversion mutation if not repaired. Thymine glycols that are also a result of oxidative damage are cytotoxic as they prevent transcription and replication.

Deamination

Deamination occurs spontaneously in DNA due to changes in temperature and pH (Lindahl, 1993). Cytosine and 5-methylcytosine undergo deamination to form uracil and thymine respectively. If left in the deaminated form transition mutations will occur upon replication as both uracil and thymine base pair with adenine instead of guanine. However uracil is not a standard component of DNA and is therefore recognised as a DNA lesion that can be repaired (Poole *et al.*, 2001). Thymine is a standard DNA base and therefore it is more difficult to identify which base in the GT base pair is incorrect.

Deamination of purine residues accounts for approximately 2% of all deamination reactions (Karran and Lindahl, 1980). Adenine and guanine are deaminated to form hypoxanthine and xanthine respectively. Hypoxanthine base pairs with cytosine potentially introducing a transition mutation. Xanthine also base pairs with cytosine but because it derives from guanine is not as mutagenic. Overall, deamination events primarily involve cytidine residues and it has been estimated that in a human cell 100 to 500 cytidine bases are deaminated every day (Frederico *et al.*, 1990).

Depurination and depyrimidination

The formation of abasic sites occurs spontaneously within DNA as well as being a secondary consequence in some alkylation reactions. Abasic sites are formed when the glycosidic bond linking the sugar and base is hydrolysed separating the base from the

DNA molecule. If left uncorrected the loss of a base is likely to lead to replication errors resulting in both transition and transversion mutations. Within a human cell it has been estimated that 2000 to 10000 abasic sites are formed every day (Lindahl and Nyberg, 1972) (Nakamura *et al.*, 1998). In approximately 95% of these cases this is due to the loss of a pyrimidine base (Lindahl, 1993).

Replication errors

Mismatches can be introduced during DNA replication and are caused by DNA polymerase incorporating the incorrect base or tautomer (Strazewski, 1988). For DNA polymerases with proof reading activity (such as DNA polymerase I and DNA polymerase III) approximately one error is introduced every 10^6 to 10^7 bases (reviewed in (Kunkel, 1992)). If left uncorrected an incorrect tautomer can lead to transition mutations whereas an incorrect base can lead to either transition or transversion mutations (Strazewski, 1988).

Exogenous mutagens

Exogenous precursors to alkylating agents

Several known chemicals that have no direct effect on the DNA molecule are precursors of DNA alkylating agents. These chemicals can be modified within cells to form mutagens. Within liver cells aflatoxin B_1, a peanut mould toxin, is converted to aflatoxin B_1-8,9,-epoxide that covalently attaches to the N^7 position of guanine (Essigmann *et al.*, 1977). Benzo[a]pyrene, found in cigarette smoke, is converted through a series of reactions to 7,8-diol-9,10-epoxide that will covalently bind the N^2 position of guanine (Phillips, 1983).

Cross-linking reagents

Cross-linking reagents have two reactive centres that can each react with the DNA molecule. Cross-linking reagents include some bifunctional alkylating agents, mitomycin, *cis*-platinum based products (e.g. *cis*-diaminedichloroplatinum) and psoralens. If the two reactive centres interact with the same DNA strand then an intrastrand cross-link is established. If they react with opposite strands then interstrand cross-links are formed (reviewed in (Friedberg *et al.*, 2006)). Interstrand cross-links prevent strand separation of

the DNA molecule preventing DNA replication and thus cell division. Cross-linking reagents have therefore been used as chemotherapy tools to treat cancer (Scharer, 2005).

Psoralens are tricyclic planner molecules that intercalate between DNA bases. Upon exposure to 320 nm to 410 nm ultraviolet (UV) light the psoralen molecules are activated and can react with the C^5-C^6 double bond of pyrimidine bases. Psoralens can be activated at either end and thus can form interstrand cross-links by reacting with a pyrimidine on either strand. The formation of a psoralen induced interstrand cross-link between two pyrimidine bases causes a predicted 47° helical distortion (Pearlman *et al.*, 1985). Angelicin, a psoralen related compound, also intercalates between the bases and is activated upon exposure to UV light (Friedberg *et al.*, 2006). However, angelicin is not a cross-linking reagent as it can only form monoadducts due to its steric positioning within the DNA.

Ultraviolet irradiation

UV light is an exogenous mutagen that can directly lead to the introduction of photoproducts within DNA molecules. Solar UV light is made up of UVA (320 to 400 nm), UVB (280 to 320 nm) and UVC (100 to 280 nm) wavelengths. UVA and UVB light reach the biosphere more frequently than UVC. Despite this, most DNA repair experiments on UV irradiated DNA have been carried out on DNA that has been irradiated using a 254 nm (UVC) wavelength. Studies have shown that the DNA lesions introduced using this monochromatic wavelength are the same as lesions introduced by solar UV and are therefore physiologically relevant (Slieman and Nicholson, 2000).

UV irradiation can cause pyrimidine residues within DNA to become photoexcited. A DNA photoproduct is formed if a photoexcited pyrimidine reacts with an adjacent pyrimidine base. UV irradiated DNA contains a variety of photoproducts of which the cyclobutane pyrimidine dimer (CPD) is the most common (Douki and Cadet, 2001). A CPD consists of a cyclobutane ring formed due to the saturation of the C^5-C^6 double bond of adjacent pyrimidines (Figure 1.2A). TT CPDs are observed more frequently than TC, CT and CC CPDs (written 5′ to 3′) (Douki and Cadet, 2001). The covalent bonds formed between the pyrimidines cause a distortion within the DNA backbone that has been reported to be between 7° and 30° (Husain *et al.*, 1988) (Pearlman *et al.*, 1985) (Wang and Taylor, 1991). A less abundant but significant photoproduct caused by UV irradiation is

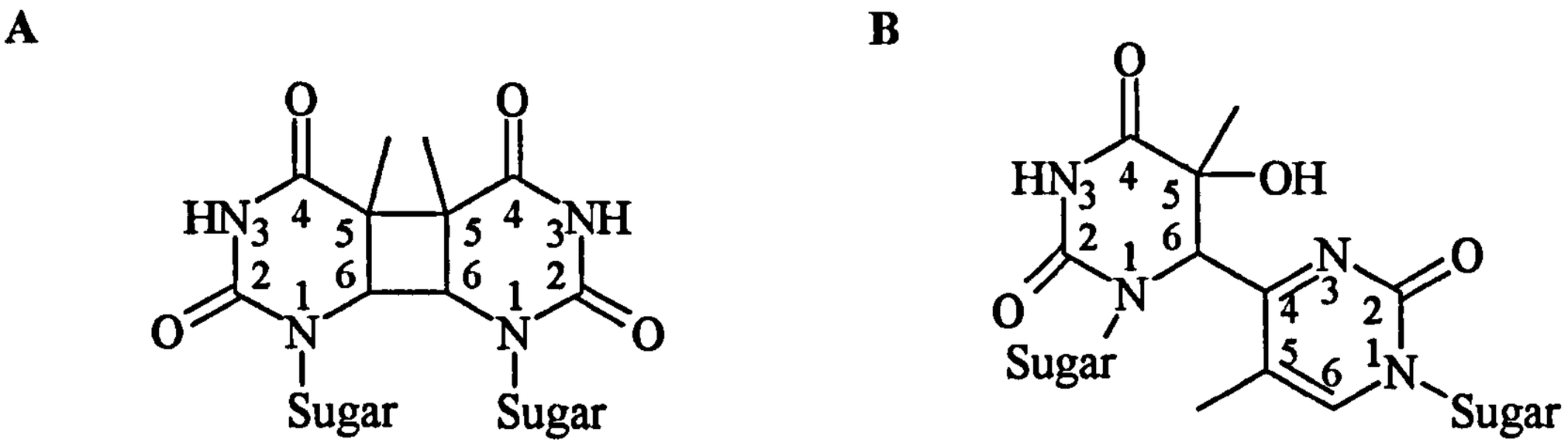

Figure 1.2 UV photoproducts.

Photoproducts are formed as a result of UV irradiation. The two major types of photoproducts are the **(A)** cyclobutane pyrimidine dimer and **(B)** the 6-4 photoproduct. Thymine thymine photoproducts are shown.

the pyrimidine-pyrimidone (6-4) photoproduct in which a single covalent bond is formed between the C^6 and the C^4 position of adjacent pyrimidine bases (Figure 1.2B). On exposure to less than 6.4 kJ/m^2 UVB or UVC light, TC 6-4 photoproducts were observed more frequently then TT and CC 6-4 photoproducts (Douki and Cadet, 2001). CT 6-4 photoproducts were not detected. The formation of the covalent bond between the adjacent pyrimidines causes a 47° distortion in the DNA backbone, greater than the distortion caused by the CPD (Warren *et al.*, 1998). UV irradiation can also cause the formation of several other photoproducts including thymine glycols as well as causing single and double strand breaks (reviewed in (Friedberg *et al.*, 2006)). Lesions arising from UV irradiation can have both cytotoxic and mutagenic effects. The helical distortions caused by the photoproducts stall both DNA polymerase and RNAP preventing the cell from replicating and expressing required proteins (Selby and Sancar, 1990). During DNA synthesis UV induced lesions can be bypassed by DNA polymerase V (Tang *et al.*, 2000). However this can result in permanent transition or transversion mutations being introduced.

Ionizing radiation

Ionizing radiation is an environmental and man made mutagen. It acts on DNA both directly (35%) and indirectly (65%) to cause a variety of lesions (Ward, 1988). Within the cell, ionizing radiation can create free radicals such as ·OH and H_2O_2 that go on to damage the DNA. On exposure to ionizing radiation the C^5-C^6 double bond of pyrimidine bases are often attacked forming modifications such as thymine glycols and 5-hydroxycytosine. Ionizing radiation affects the deoxyribose sugar less frequently. Despite this, sugar modifications can be more harmful to the cell as there is a chance that the DNA strand will be broken. Both the 5′ and 3′ termini of strand breaks are often damaged eliminating the possibility of a straight forward ligation reaction as a form of repair (Henner *et al.*, 1982). Unlike other mutagens, ionizing radiation often introduces DNA lesions in clusters (Sutherland *et al.*, 2000). This subsequently increases the frequency of double strand breaks occurring within the DNA molecule as a single strand break in each strand could occur within a few nucleotides of each other.

Repair Pathways

The vast majority of lesions within a DNA molecule are repaired before the cell suffers any detrimental consequences. There are several repair mechanisms available to a cell: mismatch repair (MMR), base excision repair (BER), nucleotide excision repair (NER), direct reversal (DR), double strand break repair by homologous recombination (HR) and non-homologous end joining (NHEJ). Transcription-coupled repair (TCR) links certain repair pathways to transcription. Each repair mechanism acts in different ways to regenerate the original DNA sequence.

Direct reversal

Certain DNA lesions can be repaired using enzymes that directly restore the DNA to its original state (Figure 1.3). The process is unique amongst repair pathways as only one enzyme is involved in the entire restoration process. Two classes of lesions are known to be repaired in this manner: some photoproducts and certain alkylation products which are restored by the action of specific photolyases and alkyltransferases respectively.

Direct reversal of photoproducts

CPD photolyases recognise and directly repair CPDs by converting the CPD back to its original pyrimidine-pyrimidine sequence using energy from light. All photolyases contain two chromophores: a catalytic and a light harvesting cofactor (Kim and Sancar, 1993). In all reported cases the catalytic cofactor is FADH-. The light harvesting cofactor is either a methenyltetrahydrofolate or an 8-hydroxy-5-deazariboflavin (Yasui *et al.*, 1994). CPD photolyases fall into two categories (class I and class II) depending on their amino acid sequence (Yasui *et al.*, 1994). Class I CPD photolyases are further subcategorised into the folate or deazaflavin class depending on the light harvesting cofactor that they contain. In general, class I photolyases have been found in prokaryotes and type II photolyases have been found in lower eukaryotes (Todo, 1999). No DNA photolyases have been reported in placental mammals.

In a light-independent reaction *Escherichia coli* DNA photolyase recognises and binds thymine dimers 10^4-fold more efficiently than undamaged DNA (Kim and Sancar, 1991). Footprinting studies revealed that the CPD photolyase binds either side of the lesion on both the damaged and undamaged DNA strands (Husain *et al.*, 1987). It is proposed that

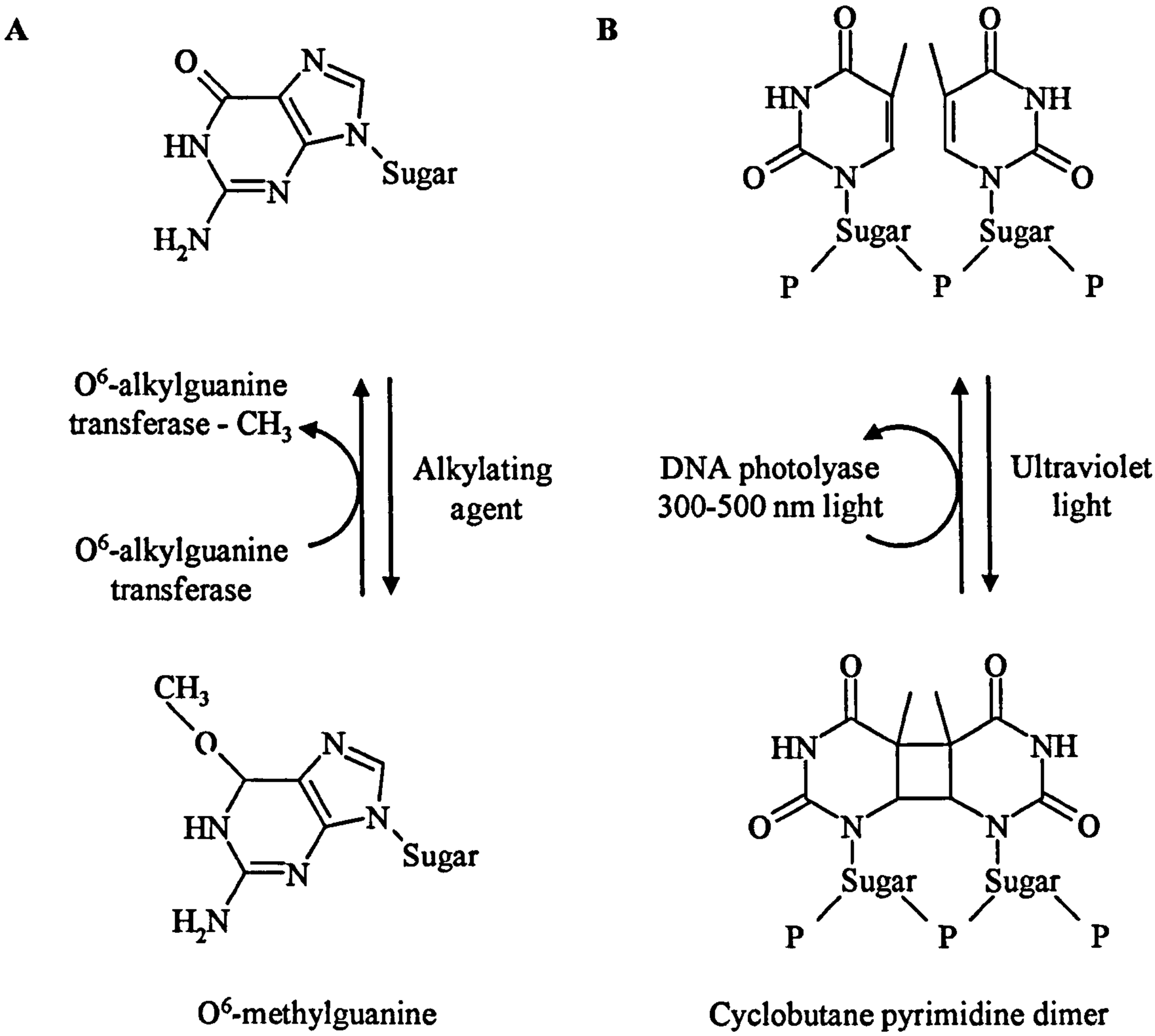

Figure 1.3 Direct reversal.

(A) O^6-methylguanine, which is introduced by alkylating agents, is directly restored to guanine by O^6-alkylguanine transferase. This reaction irreversibly inactivates O^6-alkylguanine transferase. **(B)** Pyrimidine dimers introduced by UV irradiation can be repaired by DNA photolyase that is activated upon exposure to long wavelength UV light (reviewed in (Friedberg *et al.*, 2006)).

the CPD is then flipped out of the helix to position it to readily accept an electron (Christine *et al.*, 2002). To carry out the photoreactivation reaction a photon of light needs to be absorbed by one of the cofactors. The light harvesting cofactor absorbs a photon of light within the 300 to 500 nm range and then transfers an electron to FADH- (Kim and Sancar, 1993). The catalytic cofactor can also weakly absorb a photon of light without the assistance of the light harvesting cofactor. An electron is then transferred from the excited FADH- to the cyclobutane ring (Weber, 2005). The C^5-C^5 bond breaks followed by the C^6-C^6 bond and the transfer of the electron back to the cofactor (Kim and Sancar, 1991). The original DNA sequence is restored. As well as CPD photolyases there are also some 6-4 photolyases that restore 6-4 photoproducts to the original pyrimidine bases (Kim *et al.*, 1994).

Direct reversal of alkylation damage

Alkyltransferases are found in almost all species and remove alkyl groups from modified DNA bases. C-Ada, OGT (both *E. coli*) and hAGT (human) are examples of O^6-alkylguanine alkyltransferases that recognise and bind O^6-alkylguanine before flipping the base from the helical structure (Daniels *et al.*, 2004). This flipping reaction positions the base in close proximity to an active cysteine residue within the O^6-alkylguanine alkyltransferase (Daniels *et al.*, 2004). The active cysteine residue then makes a nucleophilic attack resulting in the transfer of the alkyl group onto the enzyme restoring the base to guanine (Lindahl *et al.*, 1982). The enzyme is degraded after repairing only one lesion as the transfer of the alkyl group onto the cysteine residue renders the enzyme inactive. Other enzymes are used to directly repair other types of alkylation damage. These include N-Ada that repairs methylphosphotriesters and AlkB that repairs N^1-methyladenine and N^3-methylcytosine (reviewed in (Mishina *et al.*, 2006)).

Double strand break repair

Homologous recombination

In prokaryotes HR seems to be the most prevalent double strand break repair mechanism underpinning replication (Figure 1.4). The recombination process uses several enzymes including RecBCD, RecA, RuvAB and RuvC. Upon formation of a double strand break the DNA is unwound by the motors of RecB and RecD. RecBCD has both a 5′ to 3′ and a

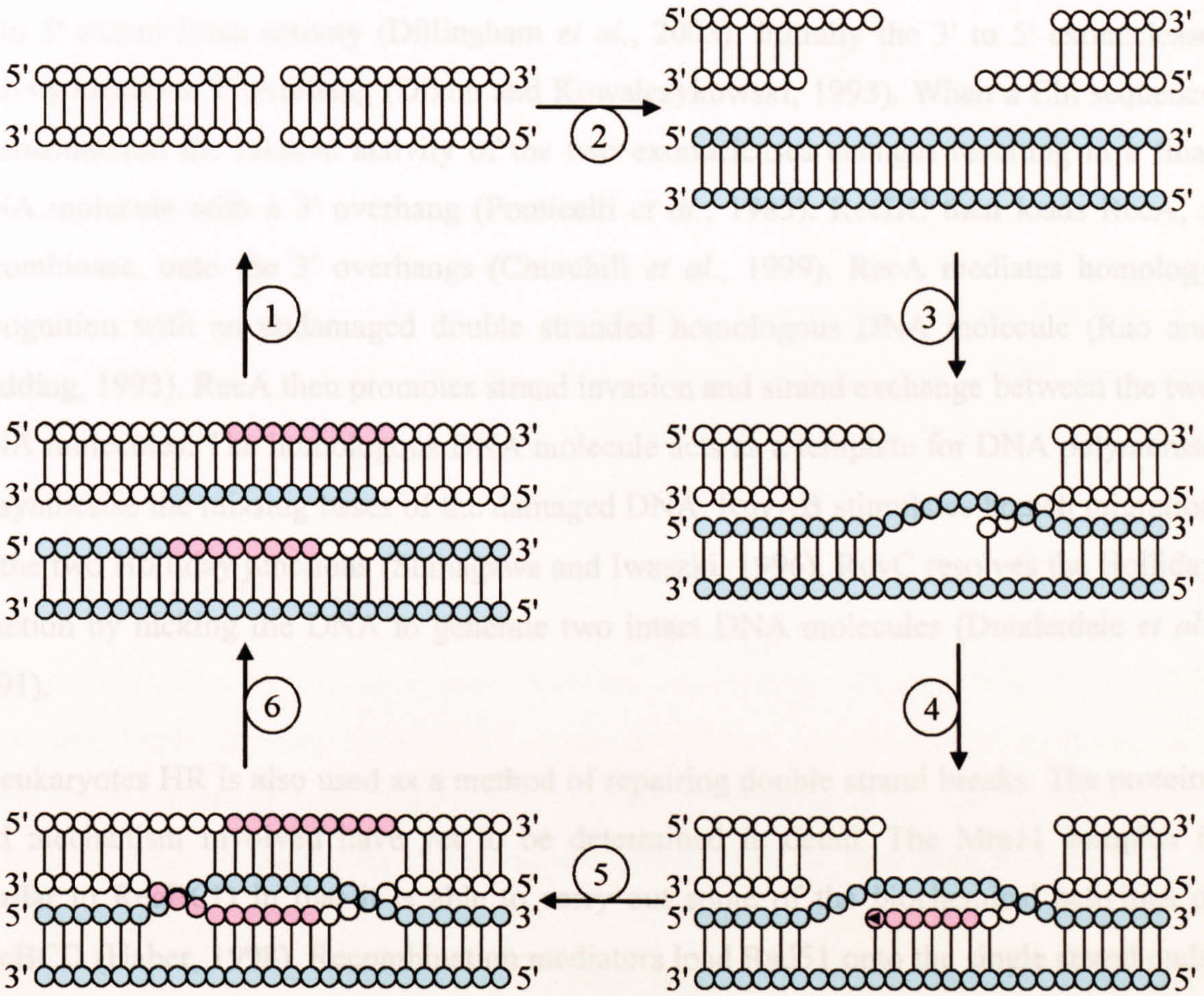

Figure 1.4 Homologous recombination.

(1) Upon exposure to mutagens double strand breaks can be introduced into the DNA. (2) The RecBCD complex recognises the damaged DNA and uses its exonuclease activity to produce 3′ overhangs. (3 - 5) The recombinase RecA recognises and binds the terminal regions and instigates the strand probing with a homologous DNA molecule. DNA polymerase can then synthesise the complementary region of DNA. RuvAB can recognise Holliday junctions and cause branch migration. (6) The resolvase RuvC releases two undamaged homologous DNA strands (reviewed in (Friedberg *et al.*, 2006)). The pink filled circles indicate newly synthesised DNA.

3′ to 5′ exonuclease activity (Dillingham *et al.*, 2003). Initially the 3′ to 5′ exonuclease activity creates a 5′ overhang (Dixon and Kowalczykowski, 1993). When a Chi sequence is encountered the relative activity of the two exonucleases changes resulting in a final DNA molecule with a 3′ overhang (Ponticelli *et al.*, 1985). RecBC then loads RecA, a recombinase, onto the 3′ overhangs (Churchill *et al.*, 1999). RecA mediates homology recognition with an undamaged double stranded homologous DNA molecule (Rao and Radding, 1993). RecA then promotes strand invasion and strand exchange between the two DNA molecules. The homologous DNA molecule acts as a template for DNA polymerase to synthesise the missing bases of the damaged DNA. RuvAB stimulates branch migration of the two Holliday junctions (Shinagawa and Iwasaki, 1996). RuvC resolves the Holliday junction by nicking the DNA to generate two intact DNA molecules (Dunderdale *et al.*, 1991).

In eukaryotes HR is also used as a method of repairing double strand breaks. The proteins and mechanism involved have yet to be determined in detail. The Mre11 complex is similar to RecBCD in that it is able to carry out some of the biochemical activities of RecBCD (Haber, 1998). Recombination mediators load Rad51 onto the single strand ends. Rad51 then requires accessory proteins, like Rad54, for recombination to occur (Baumann and West, 1998). The resolvase has yet to be determined although Rad51C has been proposed to fill this role (Liu *et al.*, 2004).

Non-homologous end joining

NHEJ is the principle method of double strand break repair in mammals (Sonoda *et al.*, 2006). NHEJ also happens in prokaryotes but occurs less frequently than HR (reviewed in (Lieber *et al.*, 2003)). There are several steps involved in NHEJ: the binding of proteins to the DNA ends that stops nucleolytic degradation; the positioning and preparation of the DNA ends using the DNA bound proteins; and finally the ligation of the ends to reconstitute the DNA molecule (reviewed in (Lieber *et al.*, 2003)).

In mammals a Ku complex binds double strand break ends. The Ku complex consists of Ku70 and Ku80 that form a ring like structure through which the DNA can pass (Walker *et al.*, 2001). Ku proteins interact with a DNA protein kinase that interacts with the DNA protein kinase bound to the other section of DNA (reviewed in (Friedberg *et al.*, 2006)). This protein-protein interaction positions the DNA ends ready for ligation. In most cases

the DNA termini need modification before ligation can occur (Chappell *et al.*, 2002). A variety of proteins join the complex, modify the ends and ligate the strands to generate an intact DNA molecule.

Mismatch repair

DNA polymerases are not infallible and can introduce mismatches, insertions or deletions during DNA synthesis. These errors are recognised and repaired by the MMR machinery within the cell. The MMR proteins have to recognise a mismatch, identify which of the two DNA strands are incorrect and then correct the error (Figure 1.5).

Prokaryotic mismatch repair

In *E. coli* MMR there are three main proteins involved in damage recognition: MutS, MutL and MutH. Initially an ADP bound dimer of MutS recognises and asymmetrically binds the mismatched base, insertion or deletion (Obmolova *et al.*, 2000). The binding affinity of MutS to these sites is only approximately 4 to 20-fold more efficient than its binding affinity to matched DNA (Schofield *et al.*, 2001). Common mismatches (GT) are recognised and bound more efficiently than rare mismatches (CC) (Su *et al.*, 1988). ATP replaces the ADP molecule bound to MutS. The ATP bound MutS forms a clamp that slides along the DNA and recruits a MutL dimer (Acharya *et al.*, 2003) (Selmane *et al.*, 2003). MutL recruits MutH to MutS that then activates the endonuclease activity of MutH. The activated MutH acts as an endonuclease and cleaves only the unmethylated (newly synthesised) strand 5′ of a GATC sequence (Welsh *et al.*, 1987). The incision can occur more than 1 kb away from the mismatch in either the 3′ or 5′ direction. MutL loads helicase II (UvrD) onto the nicked site which unwinds the two strands. Excision of the daughter strand is carried out either by a 3′ to 5′ exonuclease (ExoI or ExoX) or a 5′ to 3′ exonuclease (RecJ or ExoVII) that degrades the DNA past the mismatch (Cooper *et al.*, 1993). The parent strand is protected by SSB proteins. DNA polymerase III synthesises a new section of DNA and DNA ligase seals the join (Figure 1.5).

Eukaryotic mismatch repair

The eukaryotic MMR process is similar but not identical to the prokaryotic mechanism. There are several MutS homologues that recognise different types of errors. MSH2 and MSH6 dimerize to form MutSα that is mainly responsible for recognising mismatches and

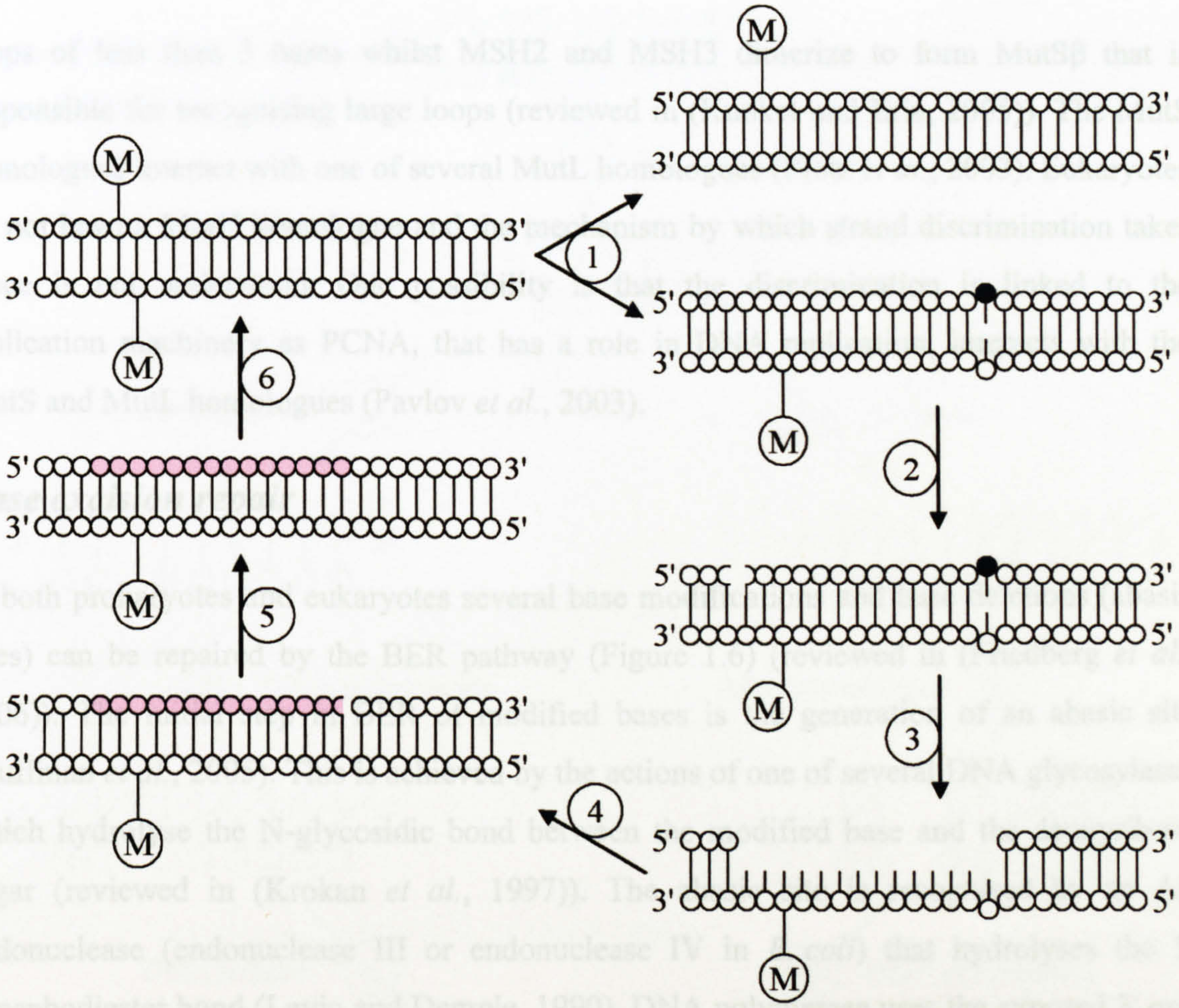

Figure 1.5 Mismatch repair.

(1) An incorrect base can be incorporated into DNA during DNA replication. **(2)** MutS binds the mismatch as a dimer and undergoes a conformational change to form a clamp that can bind MutL. MutL recruits MutH which cleaves the unmethylated DNA strand 5′ of a GATC sequence. **(3)** MutL loads helicase II onto the nick and an exonuclease degrades the unmethylated strand past the mismatch. **(4)** DNA polymerase synthesises a new section of DNA. **(5)** DNA ligase seals the gap to generate an undamaged DNA molecule. **(6)** The DNA is then methylated. MMR is reviewed in Friedberg *et al.* (Friedberg *et al.*, 2006)). M indicates a methylated adenine residue within a GATC sequence, the black filled circle represents an incorrect base and the pink filled circles indicate newly synthesised DNA.

loops of less than 3 bases whilst MSH2 and MSH3 dimerize to form MutSβ that is responsible for recognising large loops (reviewed in (Kunkel and Erie, 2005)). The MutS homologues interact with one of several MutL homologues (Plotz *et al.*, 2003). Eukaryotes do not have a MutH homologue and the mechanism by which strand discrimination takes place is not understood. One possibility is that the discrimination is linked to the replication machinery as PCNA, that has a role in DNA replication, interacts with the MutS and MutL homologues (Pavlov *et al.*, 2003).

Base excision repair

In both prokaryotes and eukaryotes several base modifications and base deletions (abasic sites) can be repaired by the BER pathway (Figure 1.6) (reviewed in (Friedberg *et al.*, 2006)). The initial step in BER of modified bases is the generation of an abasic site (Huffman *et al.*, 2005). This is achieved by the actions of one of several DNA glycosylases which hydrolyse the N-glycosidic bond between the modified base and the deoxyribose sugar (reviewed in (Krokan *et al.*, 1997)). The abasic site is recognised by an AP endonuclease (endonuclease III or endonuclease IV in *E. coli*) that hydrolyses the 5′ phosphodiester bond (Levin and Demple, 1990). DNA polymerase uses the exposed 3′ end of the DNA as a primer and introduces a single nucleotide where the damage had been. A deoxyribosephosphodiesterase (that can be part of DNA polymerase) nicks the DNA 3′ of the damaged site releasing the sugar phosphate (Garcia-Diaz *et al.*, 2005). DNA ligase then ligates the 3′ OH group of the introduced nucleotide to the 5′ phosphate group of the original DNA. Some DNA glycosylases (such as hOGG1) have an associated AP lyase activity that cleaves the DNA 3′ of the damaged site as part of the initial step (van der Kemp *et al.*, 2004). When AP endonuclease cleaves the DNA 5′ of the damaged site the sugar phosphate is therefore released (Wyatt *et al.*, 1999). DNA polymerase then introduces a single nucleotide that is sealed in place by DNA ligase. An alternative BER pathway occurs when DNA polymerase introduces more than one nucleotide, displacing the abasic site and undamaged nucleotides in the process (Klungland and Lindahl, 1997). The displaced nucleotides are excised by an endonuclease (e.g. FEN-I) enabling DNA ligase to seal the join.

Different lesions, predominantly caused by alkylation or oxidation, are recognised by different DNA glycosylases (reviewed in (Friedberg *et al.*, 2006)). Some DNA

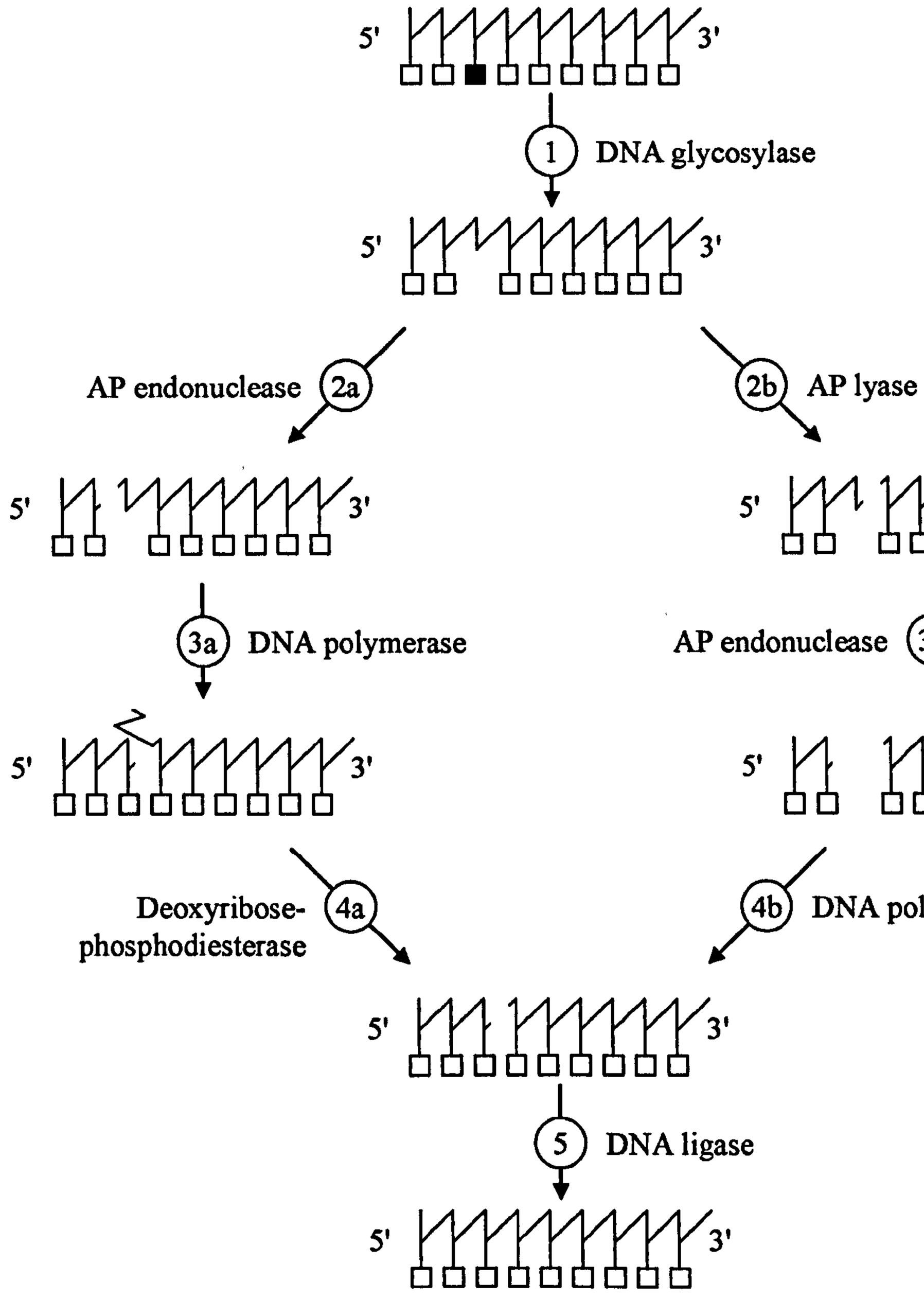

Figure 1.6 Base excision repair.

BER corrects base modifications and abasic sites. **(1)** DNA glycosylase hydrolyses the N-glycosidic bond between the modified base (black box) and the deoxyribose sugar to leave an abasic site. There are then two possible routes. **(2a)** An AP endonuclease hydrolyses the phosphodiester bond 5′ of the damaged site. **(3a)** DNA polymerase introduces a single nucleotide displacing the sugar phosphate of the abasic site. **(4a)** A deoxyribosephosphodiesterase cleaves the DNA 3′ of the damaged site removing the sugar phosphate. Alternatively **(2b)** the DNA glycosylase from step 1 has an associated AP lyase activity that cleaves the phosphodiester bond 3′ to the site of damage. **(3b)** An AP endonuclease cleaves the DNA 5′ of the site of damage resulting in the loss of the sugar phosphate. **(4b)** DNA polymerase introduces a new nucleotide. **(5)** DNA ligase seals the gap to restore the DNA (reviewed in (Friedberg *et al.*, 2006)). The pink box indicates the introduced base.

glycosylases such as T4 endonuclease V (T4EV) specifically recognise pyrimidine dimers (Demple and Linn, 1980). T4EV cleaves the N-glycosidic bond of the 5′ pyrimidine of a dimer. T4EV then uses its associated AP lyase activity to hydrolyse the phosphodiester bond connecting the two nucleotides (McMillan *et al.*, 1981). Pyrimidine dimer DNA glycosylases are the only known type of DNA glycosylases that do not release the modified base into solution, presumably because the pyrimidine is still bound to the other pyrimidine through the cyclobutane ring.

Nucleotide excision repair

NER involves DNA damage recognition, dual incision 3′ and 5′ from the lesion, excision of the damage containing oligonucleotide fragment and finally DNA polymerisation and ligation to yield an undamaged DNA molecule (Figure 1.7). The NER apparatus can detect and repair a wide range of lesions including pyrimidine dimers and psoralen cross-links (Hanawalt *et al.*, 2003).

Overview of prokaryotic nucleotide excision repair

Six proteins are involved in NER in prokaryotes: UvrA, UvrB, UvrC, UvrD (helicase II), DNA polymerase I and DNA ligase. A model for the mechanism of NER proposes that a UvrA dimer acts as the initial damage recognition subunit and in complex with UvrB scans the DNA for damage (Sancar and Hearst, 1993). Once UvrA has located a damaged site it loads UvrB onto the DNA and dissociates (DellaVecchia *et al.*, 2004). UvrC recognises and binds the DNA bound UvrB complex and incises the DNA three to five phosphodiester bonds 3′ and eight phosphodiester bonds 5′ of the lesion (Sancar and Rupp, 1983) (Verhoeven *et al.*, 2000). UvrD unwinds the damage containing oligonucleotide form the DNA and displaces UvrC in the process (Caron *et al.*, 1985) (Husain *et al.*, 1985). DNA polymerase I synthesises a replacement section of DNA and releases UvrB from the undamaged stand (Caron *et al.*, 1985) (Husain *et al.*, 1985). DNA ligase then seals the nick. NER in *E. coli* is discussed in greater detail below.

Overview of eukaryotic nucleotide excision repair

The overall reaction mechanism of eukaryotic NER is similar to prokaryotic NER with damage recognition, incision, excision, synthesis and ligation steps. The scheme is more

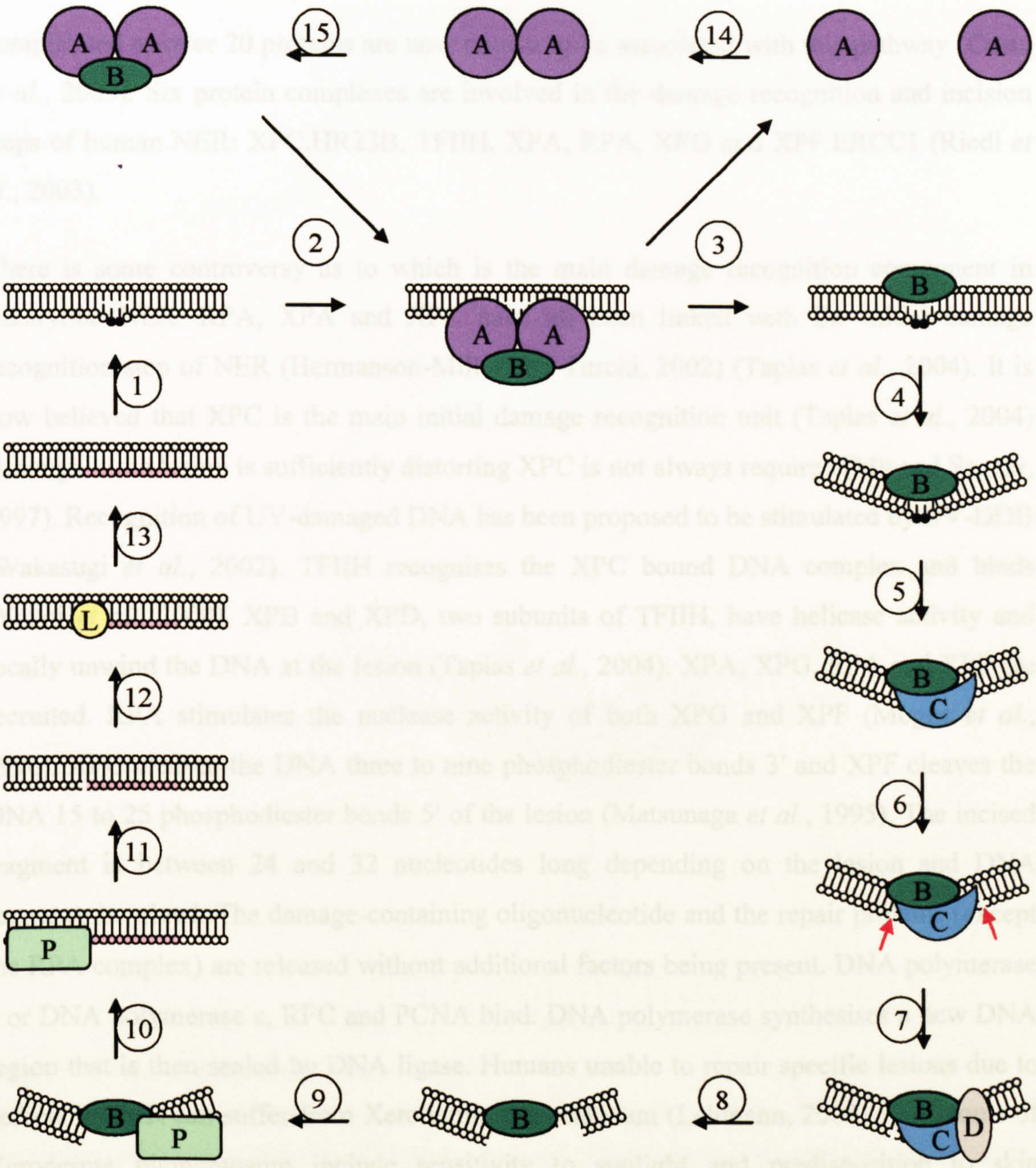

Figure 1.7 Nucleotide excision repair.

In *E. coli* bulky DNA adducts such as pyrimidine dimers are often repaired by the NER pathway. (**1**) DNA is damaged. (**2**) A dimer of UvrA (A) bound to one or two molecules of UvrB (B) recognises and binds the damaged site. (**3**) UvrA loads UvrB onto the DNA and is released. (**4**) The DNA bends and (**5**) UvrC (C) is recruited. (**6**) UvrC incises the DNA first 3′ and then 5′ of the lesion. (**7**) UvrD (D) binds and (**8**) unwinds the DNA releasing the oligonucleotide and UvrC in the process whilst leaving UvrB on the DNA. (**9**) DNA polymerase (P) binds and (**10**) synthesises a new section of DNA displacing UvrB in the process. (**11**) The polymerase is released and (**12**) ligase (L) binds and (**13**) seals the gap. The DNA is now restored to its original undamaged state. The UvrA cycle consists of (**14**) dimerization, (**15**) UvrB binding, (**2**) DNA binding, (**3**) UvrB loading and DNA release. The pink filled circles indicate newly synthesised DNA.

complicated as over 20 proteins are now known to be associated with this pathway (Costa *et al.*, 2003). Six protein complexes are involved in the damage recognition and incision steps of human NER: XPC.HR23B, TFIIH, XPA, RPA, XPG and XPF.ERCC1 (Riedl *et al.*, 2003).

There is some controversy as to which is the main damage recognition component in eukaryotic NER. RPA, XPA and XPC have all been linked with the initial damage recognition step of NER (Hermanson-Miller and Turchi, 2002) (Tapias *et al.*, 2004). It is now believed that XPC is the main initial damage recognition unit (Tapias *et al.*, 2004) although if the lesion is sufficiently distorting XPC is not always required (Mu and Sancar, 1997). Recognition of UV-damaged DNA has been proposed to be stimulated by UV-DDB (Wakasugi *et al.*, 2002). TFIIH recognises the XPC bound DNA complex and binds (Yokoi *et al.*, 2000). XPB and XPD, two subunits of TFIIH, have helicase activity and locally unwind the DNA at the lesion (Tapias *et al.*, 2004). XPA, XPG, RPA and XPF are recruited. RPA stimulates the nuclease activity of both XPG and XPF (Moggs *et al.*, 1996). XPG cleaves the DNA three to nine phosphodiester bonds 3′ and XPF cleaves the DNA 15 to 25 phosphodiester bonds 5′ of the lesion (Matsunaga *et al.*, 1995). The incised fragment is between 24 and 32 nucleotides long depending on the lesion and DNA sequence involved. The damage-containing oligonucleotide and the repair proteins (except the RPA complex) are released without additional factors being present. DNA polymerase δ or DNA polymerase ε, RFC and PCNA bind. DNA polymerase synthesises a new DNA region that is then sealed by DNA ligase. Humans unable to repair specific lesions due to defects in NER can suffer from Xeroderma pigmentosum (Lehmann, 2003). Symptoms of Xeroderma pigmentosum include sensitivity to sunlight and predisposition to skin carcinomas.

Transcription-coupled repair

TCR is the process by which damage located within the template strand of transcribed genes is repaired up to 10 times faster than damaged located within the rest of the genome (Mellon *et al.*, 1987) (Mellon and Hanawalt, 1989) (Terleth *et al.*, 1989). This increase in repair rate is achieved by a transcription repair-coupling factor (TRCF) that links repair to transcription (Figure 1.8). The TRCF is Mfd in *E. coli* (Selby and Sancar, 1993), Rad26 in *S. cerevisiae* (van Gool *et al.*, 1994) and CSB in humans (Venema *et al.*, 1990).

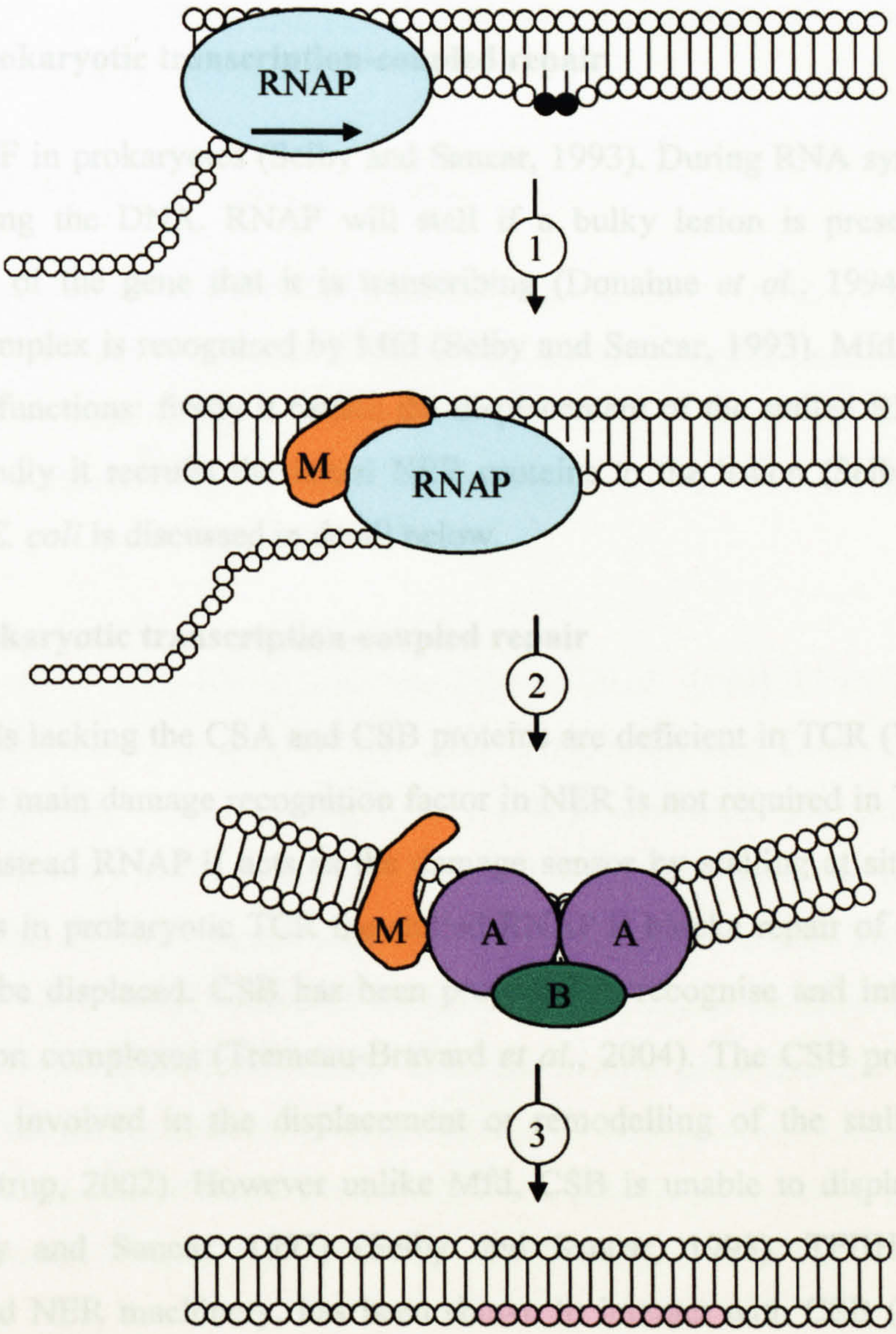

Figure 1.8 Transcription-coupled repair model.

(1) An elongating RNAP complex is stalled by a lesion within the DNA. The stalled elongation complex is recognised and bound by Mfd (M). **(2)** Mfd displaces the stalled elongation complex and recruits the NER proteins to the lesion. **(3)** NER then proceeds. The pink filled circles indicate newly synthesised DNA.

Overview of prokaryotic transcription-coupled repair

Mfd is the TRCF in prokaryotes (Selby and Sancar, 1993). During RNA synthesis RNAP translocates along the DNA. RNAP will stall if a bulky lesion is present within the template strand of the gene that it is transcribing (Donahue *et al.*, 1994). The stalled RNAP-DNA complex is recognised by Mfd (Selby and Sancar, 1993). Mfd is believed to have two main functions: firstly it causes the displacement of the stalled RNAP from the DNA and secondly it recruits the initial NER proteins to the lesion (Selby and Sancar, 1993). TCR in *E. coli* is discussed in detail below.

Overview of eukaryotic transcription-coupled repair

Mammalian cells lacking the CSA and CSB proteins are deficient in TCR (Venema *et al.*, 1990). XPC, the main damage recognition factor in NER is not required in TCR (Venema *et al.*, 1991). Instead RNAP II acts as the damage sensor by stalling at sites of damage. However just as in prokaryotic TCR the stalled RNAP II blocks repair of the lesion and therefore must be displaced. CSB has been proposed to recognise and interact with the stalled elongation complexes (Tremeau-Bravard *et al.*, 2004). The CSB protein has been proposed to be involved in the displacement or remodelling of the stalled elongation complex (Svejstrup, 2002). However unlike Mfd, CSB is unable to displace the stalled complex (Selby and Sancar, 1997) (Selby and Sancar, 1993). TFIIH, part of the transcription and NER machinery, has been shown to interact with CSB (Tantin, 1998). There is relatively little information about how the pathway then leads into NER. Humans deficient in TCR suffer from Cockayne syndrome (Lehmann, 2003). Patients suffering from this syndrome are not sensitive to UV light but do suffer from neurological disorders.

Nucleotide excision repair in *Escherichia coli*

NER was first detected in *E. coli* (Boyce and Howard-Flanders, 1964) (Setlow and Carrier, 1964). UV sensitive strains were found to have defects in or were deficient in one of three genes: *uvrA*, *uvrB* or *uvrC* (Howard-Flanders *et al.*, 1966). Strains deficient in more than one of these genes were no more UV sensitive than strains carrying a single *uvr* gene defect (Howard-Flanders *et al.*, 1966). Complementation assays indicated that the gene products of *uvrA*, *uvrB*, and *uvrC* are required for NER activity (Seeberg *et al.*, 1976).

Furthermore Mg^{2+} and ATP are also essential for NER (Seeberg *et al.*, 1976) (Sancar and Rupp, 1983) (Yeung *et al.*, 1983).

The nucleotide excision repair proteins

There are six essential proteins for NER in *E. coli*: UvrA, UvrB, UvrC, UvrD (helicase II), DNA polymerase I and DNA ligase. UvrA, UvrB and UvrC are required for the damage recognition and incision steps of NER and are described in detail below. Cho, a UvrC homologue that is able to carry out the 3′ incision reaction, is also discussed.

UvrA

UvrA is a 940 amino acid, 104 kDa protein (Husain *et al.*, 1986). UvrA is essential for NER and has been shown to interact with other UvrA molecules, UvrB, DNA and ATP (Mazur and Grossman, 1991) (Yeung *et al.*, 1986a) (Claassen and Grossman, 1991) (Seeberg and Steinum, 1982). It has also been shown to interact with the TRCF, Mfd (Selby and Sancar, 1995a). Primary sequence analysis of UvrA (Figure 1.9) revealed that there are two Walker A and Walker B motifs. Further analysis revealed that UvrA is a member of the ABC transporter family although it only possesses the ABC ATPase domain and not the transmembrane domain common to these proteins (Linton and Higgins, 1998). Sequence analysis of UvrA also revealed two zinc finger motifs, a helix-turn-helix motif and a glycine rich region near its C-terminus (Doolittle *et al.*, 1986).

The *uvrA* gene is under the control of the SOS response. Under normal cellular conditions estimates for the number of UvrA molecules within the cell range from as few as 25 to as many as 1000 (Husain *et al.*, 1986), (Seeberg and Steinum, 1982), (Crowley and Hanawalt, 1998) (Lin *et al.*, 1997). Upon induction of the SOS response the concentration of UvrA within the cell is stimulated between 1.5 and 6-fold (Seeberg and Steinum, 1982) (Crowley and Hanawalt, 1998). This increase in UvrA concentration presumably enhances the cells chances of survival by increasing the frequency of repair reactions.

UvrB

UvrB is a 673 amino acid, 76 kDa protein (Figure 1.9) (Caron and Grossman, 1988). UvrB is a key protein in NER as it interacts with UvrA, UvrC, UvrD, DNA polymerase, DNA and ATP (reviewed in (Van Houten *et al.*, 2005)). Of the three NER proteins required for

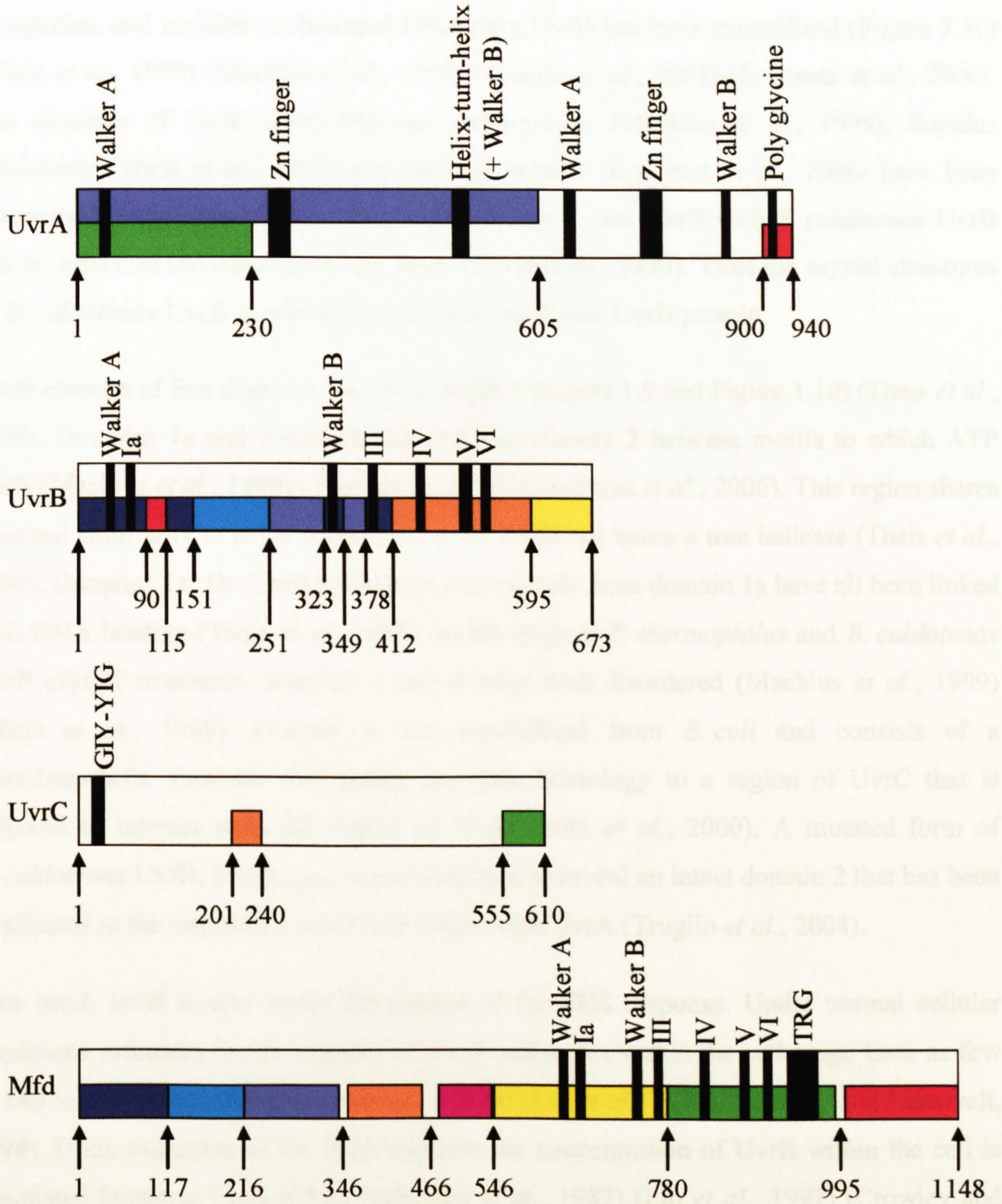

Figure 1.9 Sequence motifs of UvrA, UvrB, UvrC and Mfd.

The primary structure of UvrA, UvrB, UvrC and Mfd are shown. Black boxes represent the structure indicated above each motif. The coloured boxes indicate the following domains. **UvrA** - green, the predicted UvrB interaction domain ($UvrA_{1-230}$); purple, the predicted UvrA dimerization domain ($UvrA_{1-680}$); and red, the damage recognition and stabilisation domain ($UvrA_{900-940}$). **UvrB** - dark blue, domain 1a; purple, domain 1b; aqua, domain 2; orange, domain 3; yellow, domain 4; and red the β-hairpin (Theis *et al.*, 1999). **UvrC** - orange, UvrB interaction domain; and green, a region required for DNA binding. **Mfd** - dark blue, domain 1a; purple, domain 1b; aqua, domain 2; orange, domain 3; pink, domain 4; yellow, domain 5; green, domain 6; and red, domain 7 (Deaconescu *et al.*, 2006).

recognition and incision of damaged DNA only UvrB has been crystallised (Figure 1.10) (Theis *et al.*, 1999) (Machius *et al.*, 1999) (Truglio *et al.*, 2004) (Eryilmaz *et al.*, 2006). The structure of UvrB from *Thermus thermophilus* (Machius *et al.*, 1999), *Bacillus caldotenax* (Theis *et al.*, 1999) and *Bacillus subtilis* (Eryilmaz *et al.*, 2006) have been determined. In *in vitro* excision assays substituting *E. coli* UvrB with *B. caldotenax* UvrB had no effect on the outcome of the assay (Theis *et al.*, 1999). Thus the crystal structures of *B. caldotenax* UvrB is relevant in studying the *E. coli* UvrB protein.

UvrB consists of five domains: 1a, 1b, 2, 3 and 4 (Figure 1.9 and Figure 1.10) (Theis *et al.*, 1999). Domains 1a and 3 contain classical superfamily 2 helicase motifs to which ATP binds (Machius *et al.*, 1999) (Theis *et al.*, 1999) (Eryilmaz *et al.*, 2006). This region shares structual similiarity to many helicases despite UvrB not being a true helicase (Theis *et al.*, 1999). Domains 1a, 1b, 3 and a β-hairpin that extends from domain 1a have all been linked with DNA binding (Theis *et al.*, 1999). In the original *T. thermophilus* and *B. caldotenax* UvrB crystal structures, domains 2 and 4 were both disordered (Machius *et al.*, 1999) (Theis *et al.*, 1999). Domain 4 was crystallised from *E. coli* and consists of a helix-loop-helix structure that shares sequence homology to a region of UvrC that is believed to interact with this region of UvrB (Sohi *et al.*, 2000). A mutated form of *B. caldotenax* UvrB, $UvrB_{YA096}$, was crystallised to reveal an intact domain 2 that has been implicated in the interaction that UvrB makes with UvrA (Truglio *et al.*, 2004).

Like *uvrA*, *uvrB* is also under the control of the SOS response. Under normal cellular conditions estimates for the number of UvrB molecules within the cell range from as few as 140 to as many as 400 (Sancar *et al.*, 1981a) (Lin *et al.*, 1997) (Crowley and Hanawalt, 1998). Upon induction of the SOS response the concentration of UvrB within the cell is stimulated between 5 and 6-fold (Schendel *et al.*, 1982) (Lin *et al.*, 1997) (Crowley and Hanawalt, 1998).

UvrC

UvrC is a 610 amino acid, 66 kDa protein (Sancar *et al.*, 1981b). Primary sequence analysis of UvrC (Figure 1.9) revealed that its N-terminal domain (NTD) shares homology to the GIY-YIG superfamily of intron encoded homing endonucleases (Verhoeven *et al.*, 2000). The NTD of UvrC has been crystallised in both *B. caldotenax* ($UvrC_{1-098}$) and *Thermotoga martima* ($UvrC_{1-097}$) (Truglio *et al.*, 2005). The UvrC C-terminus shares

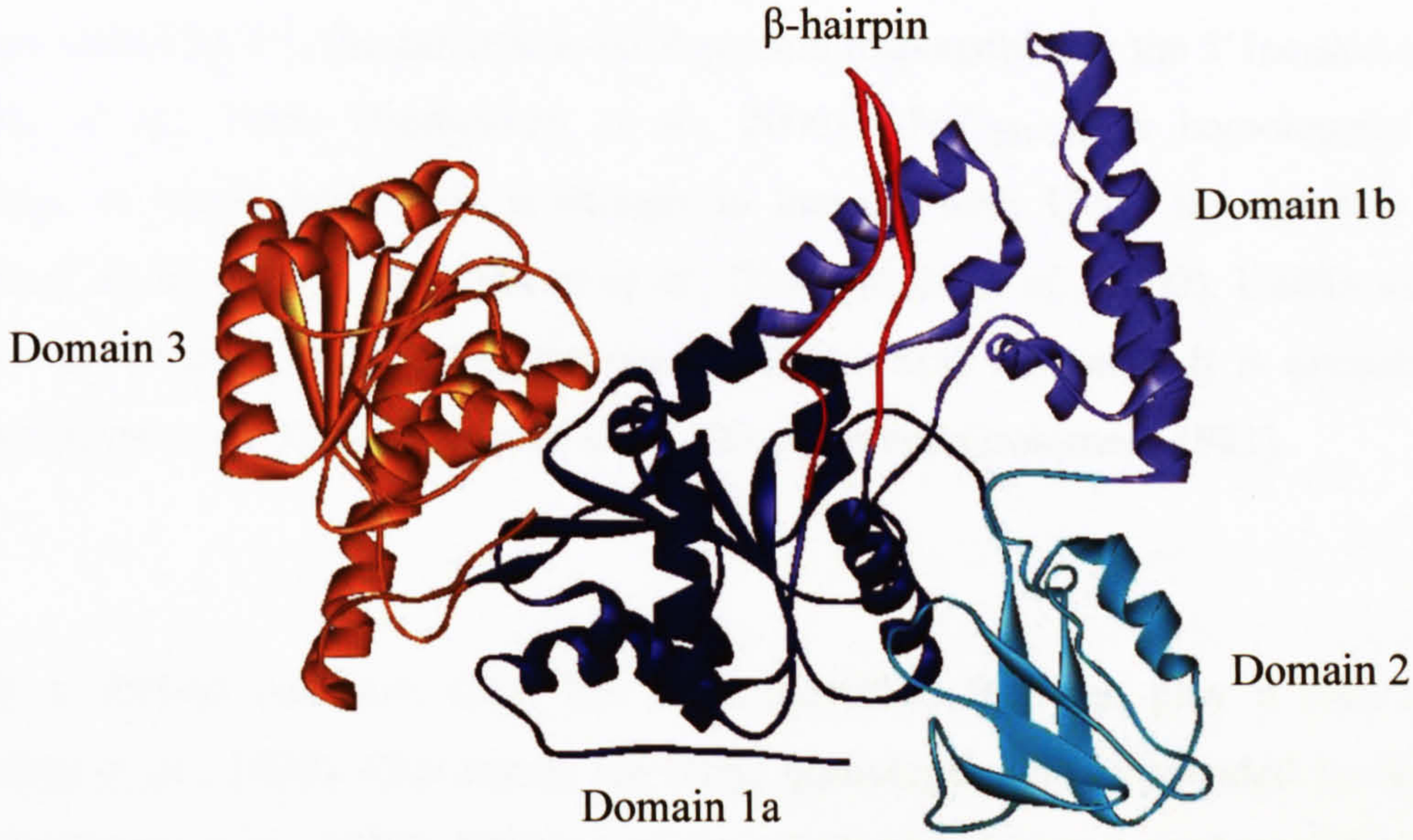

Figure 1.10 Crystal structure of UvrB.

The crystal structure of *B. caldotenax* $UvrB_{YA096}$ is shown (protein data bank number 1D9X). The domains are coloured as follows: dark blue, domain 1a; purple, domain 1b; aqua, domain 2; orange, domain 3 the β-hairpin is shown in red. Domain 4 is not shown. The diagram is adapted from (Truglio *et al.*, 2004).

homology with ERCC1, the eukaryotic NER protein responsible for the 5′ incision reaction (Doolittle *et al.*, 1986) (Verhoeven *et al.*, 2000). $UvrC_{201-240}$ is homologous to the C-terminus of UvrB and UvrC is though to interact with UvrB through this region (Moolenaar *et al.*, 1998b) (Verhoeven *et al.*, 2000) (Sohi *et al.*, 2000). Unlike *uvrA* and *uvrB*, the *uvrC* gene is not under the control of the SOS response. It is estimated that within a cell there are 10 molecules of UvrC (Yoakum and Grossman, 1981).

Cho

Recently a second nuclease, Cho, has been identified that can play a role in NER (Moolenaar *et al.*, 2002). Cho stands for UvrC homologue and is encoded by the *ydgQ* gene (Moolenaar *et al.*, 2002). Deletion of the *ydgQ* gene does not render wild-type cells UV sensitive but does further increase the UV sensitivity of Δ*uvrC* cells (Moolenaar *et al.*, 2002). Unlike *uvrC*, *ydgQ* expression is stimulated by the SOS response. Cho shares homology with the NTD of UvrC (responsible for the 3′ incision reaction) and is a UvrA-UvrB dependent endonuclease that incises the DNA nine phosphodiester bonds 3′ of the lesion (Moolenaar *et al.*, 2002). It is unable to initiate a 5′ incision event. It is believed that Cho interacts with a different region of UvrB than UvrC does since unlike UvrC it is able to incise DNA in the presence of a UvrB C-terminal truncation termed UvrB* (Moolenaar *et al.*, 2002). Cho differs from UvrC in its preferences for lesions and the 3′ incision reaction occurs faster than UvrC on DNA with a cholesterol or menthol group attached (Moolenaar *et al.*, 2002).

The process of nucleotide excision repair

Dimerization, nucleotide binding and nucleotide hydrolysis activity of UvrA

The first step in NER is the dimerization of UvrA (K_a = 10 nM in the absence of ATP) (Mazur and Grossman, 1991). Other members of the ABC transporter family including Rad50 and MutS, two other DNA repair enzymes, dimerize in a head to head orientation (Hopfner *et al.*, 2000) (Obmolova *et al.*, 2000). Truncation studies and gel filtration chromatography have indicated that UvrA dimerizes in a head-to-head orientation involving the N-terminal 605 amino acids (Claassen and Grossman, 1991) (Myles and Sancar, 1991). UvrA truncations that only contain the N-terminal 230, 470 or 560 amino acids are unable to dimerize indicating that a key UvrA dimerization component lies

within $UvrA_{561-605}$ (Claassen and Grossman, 1991). In ABC ATPase domains the ATP binding site is formed at the dimer interface with a Walker A motif from one monomer and a Walker B motif from the other generating the ATP binding site (Hopfner and Tainer, 2003). The UvrA monomer contains two Walker A and Walker B motifs on each molecule (Doolittle *et al.*, 1986). Therefore a potential four ATP molecules could bind at any one time if the dimer interface allowed. However results of nucleotide binding studies showed that 0.57 molecules of ADP bound per UvrA monomer indicating that only one, not four, ATP molecule would bind per UvrA dimer at any one time (Myles *et al.*, 1991). Gel filtration and sedimentation velocity assays indicated that ATP binding stimulates dimerization (K_a = 1 nM) presumably by stabilizing the dimer, whilst ATP hydrolysis promotes dissociation (Mazur and Grossman, 1991) (Orren and Sancar, 1989) (Oh *et al.*, 1989) (Thiagalingam and Grossman, 1991).

UvrA has ATPase activity with reported K_m values between 30 μM and 230 μM (Seeberg and Steinum, 1982), (Caron and Grossman, 1988) (Oh *et al.*, 1989) (Thiagalingam and Grossman, 1991) (Wang and Grossman, 1993) (Wang *et al.*, 1994) (Myles and Sancar, 1991). The reported k_{cat} values were also different (17 min^{-1} to 125 min^{-1}) although this may be due to varying buffer conditions and differences in activity of each separate UvrA preparation (Seeberg and Steinum, 1982) (Thomas *et al.*, 1985) (Caron and Grossman, 1988) (Wang and Grossman, 1993) (Oh *et al.*, 1989). UvrA was also able to hydrolyse GTP (K_m = 910 μM, and k_{cat} = 114 min^{-1}) (Caron and Grossman, 1988). The nucleotide hydrolysis activity of UvrA was inhibited by the addition of excess ATPγS, ADP and GTPγS presumably by preventing ATP or GTP from binding (Seeberg and Steinum, 1982) (Caron and Grossman, 1988).

Single amino acid mutations within the UvrA ABC ATPase motifs ($UvrA_{KA037}$ or $UvrA_{KA646}$) indicated that the N and C-terminal ATP binding sites had different roles in NER (Myles *et al.*, 1991) (Thiagalingam and Grossman, 1991). The two sites act cooperatively as the combined k_{cat} values for each individual site were much lower than the k_{cat} of the whole protein (Thiagalingam and Grossman, 1991). A mutant in which both Walker A motifs had been mutated ($UvrA_{KA037+KA646}$) was unable to hydrolyse ATP (Myles *et al.*, 1991) (Thiagalingam and Grossman, 1991).

UvrA-UvrB complex formation

For successful NER a UvrA-UvrB complex must form. On the basis of centrifuge studies the UvrA-UvrB complex was thought to consist of two molecules of UvrA and one molecule of UvrB (Orren and Sancar, 1989). However recent AFM (atomic force microscopy) evidence suggests that two molecules of UvrB may be present (Verhoeven *et al.*, 2002).

For successful loading of UvrB onto DNA, ATP hydrolysis by UvrB is required. UvrB is unable to hydrolyse ATP by itself (Oh *et al.*, 1989). UvrB will only hydrolyse ATP when it is part of a UvrA-UvrB complex (Caron and Grossman, 1988). As mentioned above UvrA has ATPase activity by itself. However upon complex formation with an ATPase deficient mutant of UvrB ($UvrB_{KA045}$) the ATPase activity decreased indicating that UvrB has an inhibitory effect on the ATPase activity of UvrA (Claassen and Grossman, 1991). Interestingly the ATPase activity of reactions containing wild-type UvrA and wild-type UvrB was stimulated when the UvrA concentration was low and inhibited when the UvrA concentration was high (Claassen and Grossman, 1991). This is presumably due to the initial dimerization state of UvrA. A UvrA monomer has less ATPase activity than a UvrA-UvrB complex which in turn has less ATPase activity than a UvrA dimer. At low UvrA concentrations the majority of the UvrA molecules will be in their monomeric form and thus the addition of UvrB will drive the formation of UvrA-UvrB through the high ATPase intermediate $UvrA_2$ resulting in the detected stimulation of ATPase activity. At high UvrA concentrations the majority of the UvrA molecules will be in their dimeric form and thus the addition of UvrB will drive the formation of the UvrA-UvrB complex that has lower ATPase activity than the UvrA dimer resulting in the detected inhibition of ATPase activity.

The N-terminal 230 amino acids of UvrA are proposed to interact with UvrB as UvrB was able to stimulate the ATPase activity of $UvrA_{1\text{-}230}$ (Claassen and Grossman, 1991). UvrB residues 115-252 and 547-673 (approximately corresponding to domains 2 and 4) interacted with UvrA bound to an affinity column (Hsu *et al.*, 1995). It is not known if these two regions of UvrB interact with the same molecule of UvrA or if they interact with different molecules within the UvrA dimer.

DNA binding in nucleotide excision repair

For successful NER the UvrA-UvrB complex must recognise and bind damaged DNA. Although *in vivo* damage recognition is believed to be carried out by the UvrA-UvrB complex UvrA can bind DNA by itself. Several regions of UvrA have been implicated in DNA binding and damage recognition. Mutation studies of the C-terminal zinc finger motif of UvrA indicated that it has a role in DNA binding, either directly or indirectly whilst mutations of the N-terminal zinc finger had no effect on the DNA binding properties of UvrA (Wang *et al.*, 1994). The C-terminal 40 amino acids of UvrA are also involved in DNA binding as the loss of the residues results in a UvrA protein with a reduced affinity for DNA (Claassen and Grossman, 1991). UvrA with mutations within its helix-turn-helix motif are unable to distinguish between damaged and undamaged DNA (Wang and Grossman, 1993). Footprinting studies on different types of damage (e.g. a pyrimidine dimer or a cisplatin adduct) have indicated that UvrA protects a 37 to 38 bp region (Moolenaar *et al.*, 1994) (Visse *et al.*, 1992).

The UvrA-UvrB complex is able to distinguish undamaged from damaged DNA 10^3-fold more efficiently than UvrA alone (DellaVecchia *et al.*, 2004). Upon addition of UvrB to UvrA and DNA a 19 to 23 bp footprint is detected compared to the 37 to 38 bp UvrA footprint (Moolenaar *et al.*, 1994) (Van Houten *et al.*, 1987) (Visse *et al.*, 1991) (Snowden and Van Houten, 1991). Experiments revealed that both the UvrA-UvrB and the UvrB footprints were of a similar size (Moolenaar *et al.*, 1994). AFM data indicated that upon addition of UvrB to a mixture of UvrA and damaged DNA the contour length of the DNA shortened by a length equivalent to approximately 72 bp (Verhoeven *et al.*, 2001). The authors predicted that the shortening was due to wrapping of the DNA around the UvrB molecule. Further studies indicated that only the DNA 3′ of the lesion (with respect to the damaged strand) was involved in this wrapping (Verhoeven *et al.*, 2001).

When damage is located UvrA loads UvrB onto the damaged DNA. One proposed mechanism for damage recognition and UvrB loading is the padlock model (Theis *et al.*, 2000). In the padlock model UvrA is proposed to cause the movement of the β-hairpin of UvrB away from domain 1b (Theis *et al.*, 2000). This UvrA-UvrB conformation can translocate for short distances along the undamaged strand. During this process consecutive nucleotides are flipped out of the DNA helix into a conserved pocket behind the UvrB β-hairpin (Truglio *et al.*, 2006). If no damage is encountered the complex

dissociates. However if damage is encountered UvrA dissociates (Orren *et al.*, 1992). The dissociation of UvrA triggers UvrB to return to its original conformation trapping the undamaged strand between the β-hairpin and domain 1b (Theis *et al.*, 2000). UvrB loading and damage recognition is dependent on the β-hairpin without which the DNA could not become trapped (Skorvaga *et al.*, 2004). Mutations within this hairpin ($UvrB_{Y095}$ or $UvrB_{Y096}$) prevent UvrB from loading onto DNA (Moolenaar *et al.*, 2001).

Formation of an incision complex

The next step in NER is the formation of the incision complex that consists of UvrB, UvrC and the DNA. UvrC can recognise and bind the stable UvrB-DNA complex (Moolenaar *et al.*, 1995) (Moolenaar *et al.*, 2000). It has been proposed that the homologous region of UvrB (domain 4) and UvrC (amino acids 201 to 240) interact via salt bridges between $UvrB_{E653}$ and $UvrC_{R230}$ and also between $UvrB_{R659}$ and $UvrC_{E224}$ (Sohi *et al.*, 2000) (Goosen and Moolenaar, 2001). Mutations within these homologous regions ($UvrB_{FL652}$ and $UvrC_{FL223}$) prevented the formation of a stable incision complex (Moolenaar *et al.*, 1997). C-terminal truncations of UvrB in which the UvrC homology region was removed are also unable to interact with UvrC, indicating the requirement for domain 4 of UvrB in the formation of the UvrC complex (Moolenaar *et al.*, 1995) (Moolenaar *et al.*, 1998a).

The incision reactions

Once UvrC has recognised and bound the UvrB-DNA complex the incision reactions can take place. UvrC is directly responsible for both incision reactions (Verhoeven *et al.*, 2000). The first incision reaction takes place three to five phosphodiester bonds 3′ from the lesion. The precise 3′ site for incision seems to depend on the lesion involved. UvrC incises the DNA four phosphodiester bonds 3′ of pyrimidine dimers (Sancar and Rupp, 1983), (Yeung *et al.*, 1983) and five phosphodiester bonds 3′ of psoralen adducts (Sancar and Rupp, 1983). The second incision reaction takes place eight phosphodiester bonds 5′ of the lesion on all damage substrates tested to date (Sancar and Rupp, 1983) (Yeung *et al.*, 1983) (Moolenaar *et al.*, 1997).

Different regions of UvrC are proposed to be involved in the individual incision reactions. The 3′ incision requires the N-teminal half of the UvrC protein that contains the UvrB homology region (Moolenaar *et al.*, 1997) (Verhoeven *et al.*, 2000). The interaction between the homologous region of UvrB and UvrC is important for the 3′ incision. This

was shown by mutating UvrB or UvrC within this region ($UvrB_{FL652}$ and $UvrC_{FL223}$). The 3′ incision activity in experiments containing these mutants was only 50% of the wild-type activity. However 5′ incision activity remained as wild-type on damaged DNA with pre-nicked 3′ cleavage. These mutants are deficient in forming stable UvrB-UvrC-DNA complexes indicating the necessity for a stable complex for 3′ but not 5′ incision (Moolenaar *et al.*, 1997). $UvrC_{RA042}$, a mutant within the GIY-YIG region, is also deficient in 3′ incision but is able to form a stable UvrB-UvrC-DNA complex (Verhoeven *et al.*, 2000). This mutant may therefore be directly involved in the incision reaction.

For 5′ incision the C-terminal domain (CTD) of UvrC is required (Lin and Sancar, 1992). At the C-terminal end of UvrC there are two helix-hairpin-helix motifs that are important for DNA binding. A C-terminal truncation of UvrC ($UvrC_{1\text{-}554}$) in which these two motifs are absent is able to incise the DNA 3′ of the lesion as normal but its 5′ incision activity is much reduced (Moolenaar *et al.*, 1998b). It is postulated that conformational changes occur within UvrC after the 3′ incision has been made. These changes are stabilized by the interactions UvrC makes with the DNA through the two helix-hairpin-helix motifs (Moolenaar *et al.*, 1998b). In the C-terminal truncation the complex does not have these motifs and thus becomes unstable and probably dissociates before 5′ incision can occur. Such protein-DNA interactions were shown to be important for 5′ incision as removal of the undamaged strand 5′ of the lesion (with respect to the damaged strand) causes 50% loss of 5′ cleavage (Moolenaar *et al.*, 2000). Further residues within the C-terminal half of UvrC ($UvrC_{D399}$, $UvrC_{D438}$, $UvrC_{D466}$, $UvrC_{H538}$) have been identified through mutation studies as being important for the 5′ incision but have no effect on the 3′ incision activity (Lin and Sancar, 1992).

Excision, polymerisation and ligation

On completion of incision UvrB and UvrC remain bound to the DNA (Husain *et al.*, 1985) (Orren *et al.*, 1992). UvrB is believed to be bound to the undamaged strand whilst UvrC is believed to be bound to the damaged strand (Orren *et al.*, 1992). UvrD is a helicase which unwinds the short section of DNA containing the damaged oligonucleotide. This process causes the displacement of UvrC (Caron *et al.*, 1985) (Orren *et al.*, 1992). UvrB is only removed from the DNA when the polymerisation step occurs. This step requires both DNA polymerase and dNTPs. In the absence of dNTPs there is no DNA synthesis and UvrB remains bound indicating that it is the actual process of polymerization that is important

for UvrB displacement (Caron *et al.*, 1985) (Husain *et al.*, 1985) (Orren *et al.*, 1992). The polymerization process uses the 3′ end of the DNA as a primer and the undamaged strand as a template to synthesis the correct DNA sequence. Finally DNA ligase will seal the nick between the 3′ end of the newly synthesised section and the 5′ end of the original DNA to generate an undamaged DNA molecule.

Transcription-coupled repair in *Escherichia coli*

The main characteristic of TCR is its increased repair rate over NER (Mellon and Hanawalt, 1989). TCR only takes place in transcribed regions of the genome (Mellon and Hanawalt, 1989). Failure to repair lesions in these areas can result in severe consequences including the loss of protein expression and the cell becoming unviable. It is therefore an advantage to the cell to repair lesions located in these transcribed regions before lesions located within untranscribed regions of the genome.

In vitro TCR has been detected with the combined action of the six *E. coli* NER proteins and two additional *E. coli* proteins: RNAP and Mfd the TRCF (Selby and Sancar, 1993).

Mfd

Mfd is a 1148 amino acid, 130 kDa protein. Mfd from *E. coli* has recently been crystallised in its entirety with eight domains being identified: 1a, 1b and 2 through 7 (Figure 1.9 and Figure 1.11) (Deaconescu *et al.*, 2006). A separate paper reports the structure of the isolated N-terminal region (domains 1a, 1b and 2) of Mfd also from *E. coli* (Assenmacher *et al.*, 2006). Primary sequence analysis indicated that Mfd shares a region of homology with UvrB (Selby and Sancar, 1993). Structural analysis indicated that this homology region extends to cover domains 1a, 1b and 2 of UvrB and Mfd (Figure 1.12) (Assenmacher *et al.*, 2006) (Deaconescu *et al.*, 2006). Primary sequence analysis also indicated that Mfd shares a region of homology, including the superfamily 2 helicase motifs, to RecG, a protein involved in processing stalled replication forks, (Selby and Sancar, 1993). In structural analysis of this region the two Mfd translocation domains (domains 5 and 6) are similar to the equivalent domains in RecG (domains TD1 and TD2) (Deaconescu *et al.*, 2006; Singleton *et al.*, 2001). However the relative orientation of domain 5 towards domain 6 differs from the equivalent RecG domains (Singleton *et al.*, 2001) (Deaconescu *et al.*, 2006). This difference in orientation is believed to be due to the

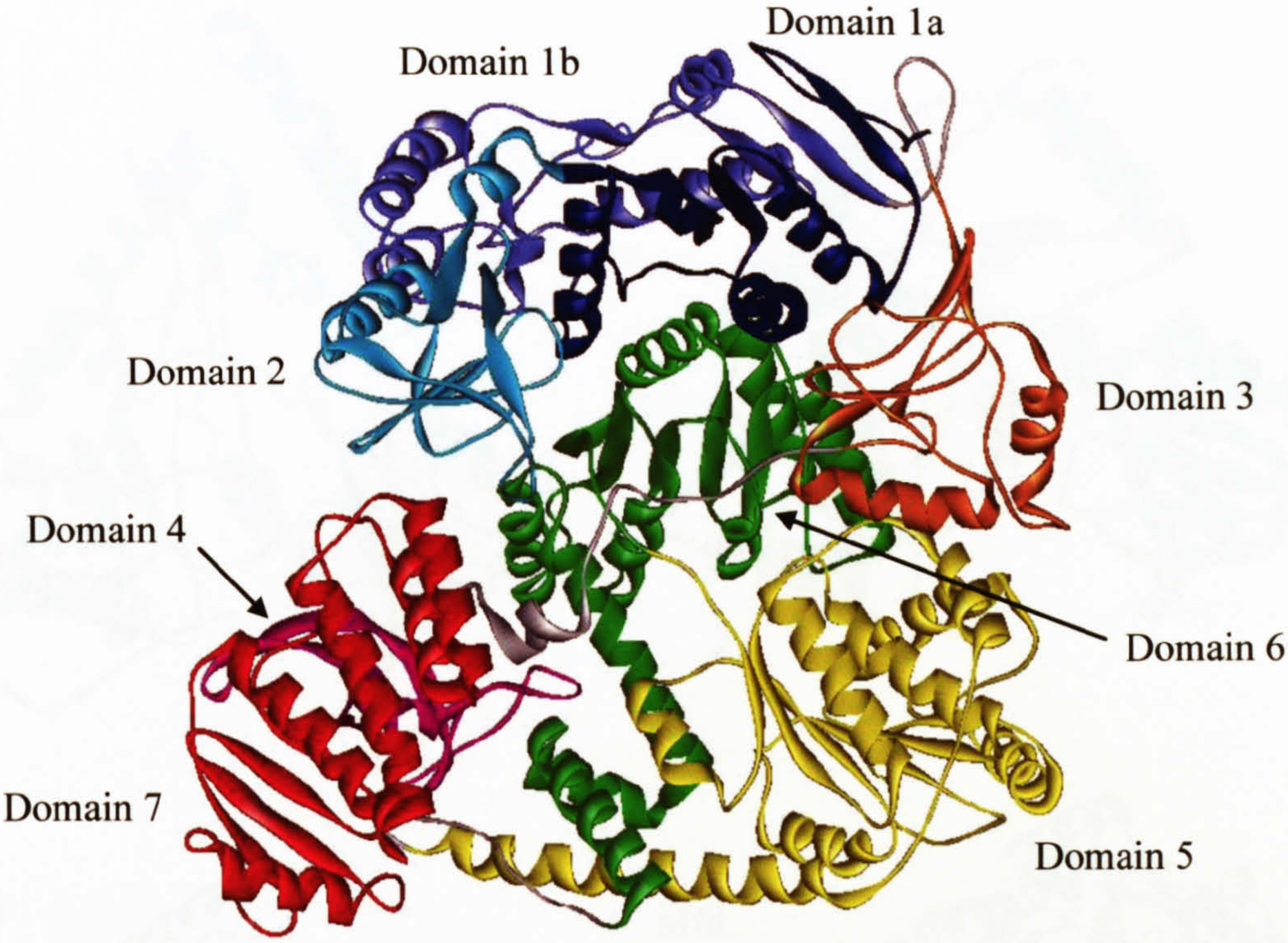

Figure 1.11 Crystal structure of Mfd.

The crystal structure of *E. coli* Mfd is shown (protein data bank number, 2EYQ). The domains are coloured as follows: dark blue, domain 1a; purple, domain 1b; aqua, domain 2; orange, domain 3; pink, domain 4; yellow, domain 5; green, domain 6; red, domain 7; and grey indicates flexible linkers. The diagram is adapted from (Deaconescu *et al.*, 2006).

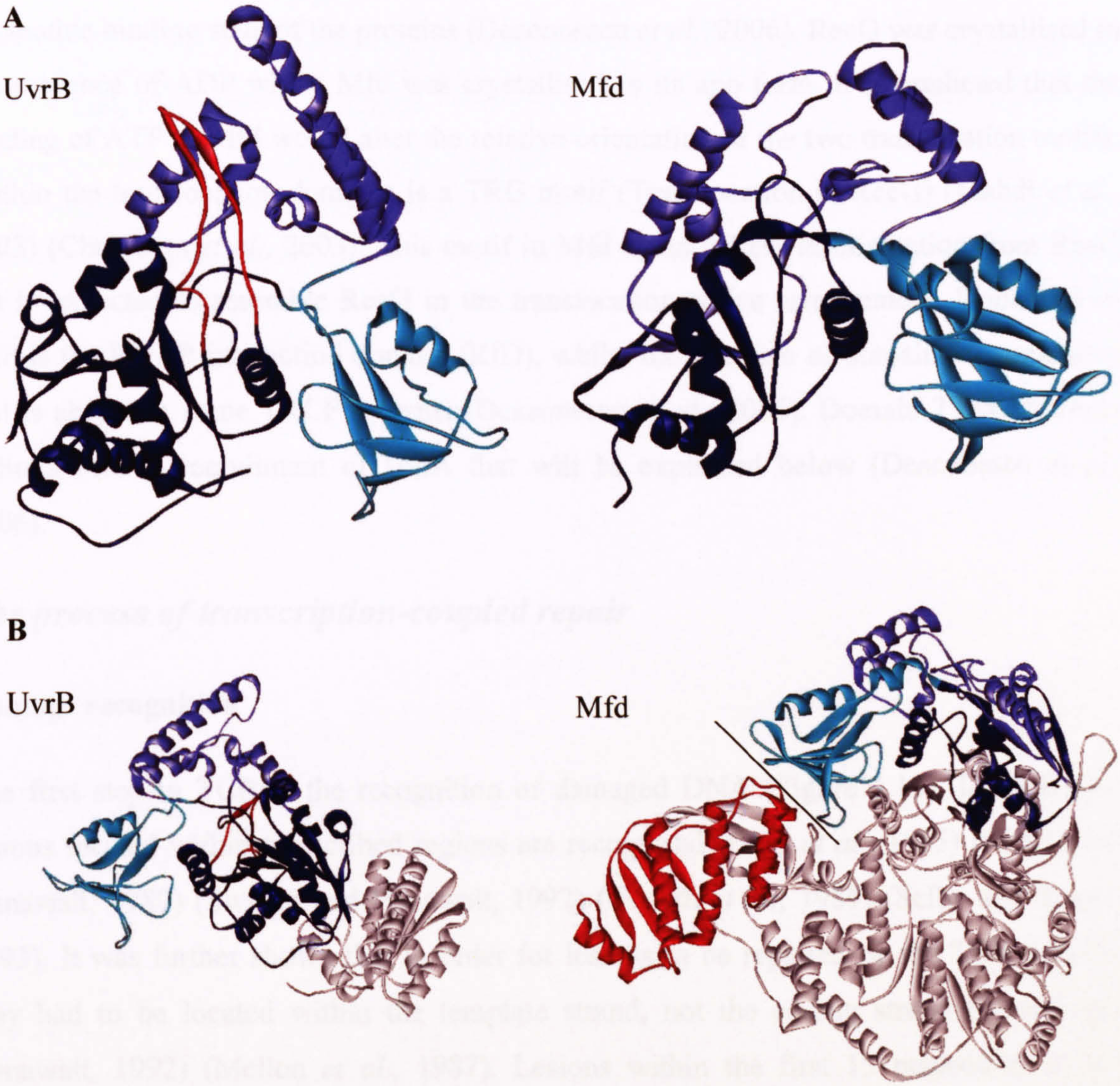

Figure 1.12 The UvrA interaction domain of UvrB and Mfd.

(**A**) The region of structural homology between UvrB and Mfd is shown (domains 1a, 1b and 2). (**B**) The UvrA interaction domain of UvrB is available for binding to UvrA but the UvrA interaction domain of Mfd is blocked (indicated by the black line) by domain 7. The domains are coloured as follows: dark blue, domain 1a; purple, domain 1b; aqua, domain 2; red, domain 7 in Mfd or the β-hairpin in UvrB; and grey indicates the remainder of the protein.

nucleotide binding state of the proteins (Deaconescu *et al.*, 2006). RecG was crystallised in the presence of ADP whilst Mfd was crystallised in its apo form. It is predicted that the binding of ATP to Mfd would alter the relative orientation of the two translocation motifs. Within the translocation domains is a TRG motif (Translocation in RecG) (Mahdi *et al.*, 2003) (Chambers *et al.*, 2003). This motif in Mfd again differs in orientation from RecG but is expected to resemble RecG in the translocation active arrangement. Domain 4 of Mfd is the RNAP interaction domain (RID), whilst the function of domain 3 is unknown and is absent in some TRCF proteins (Deaconescu *et al.*, 2006). Domain 7 may have an indirect role in recruitment of UvrA that will be explained below (Deaconescu *et al.*, 2006).

The process of transcription-coupled repair

Damage recognition

The first step in TCR is the recognition of damaged DNA (Figure 1.13). In TCR only lesions located within transcribed regions are recognised (Bohr *et al.*, 1985) (Mellon and Hanawalt, 1989) (Sweder and Hanawalt, 1992) (Terleth *et al.*, 1989) (Selby and Sancar, 1993). It was further shown that in order for lesions to be repaired by the TCR pathway they had to be located within the template strand, not the coding strand (Sweder and Hanawalt, 1992) (Mellon *et al.*, 1987). Lesions within the first 15 nucleotides of the transcription unit were not subjected to this increased repair rate (Selby and Sancar, 1995b). Repair of lesions in promoter regions were actually inhibited compared with global NER rates (Selby and Sancar, 1995b). DNA up and downstream of the lesion was also required for successful TCR. At least 87 bp of DNA downstream (untranscibed region) of the lesion (Selby and Sancar, 1995b) and at least 25 bp of DNA upstream (transcribed region) of the RNAP complex (Park *et al.*, 2002) was required to detect the increased repair rate.

Transcription starts with RNAP bound at a promoter in the form of an initiation complex ($\alpha_2\beta\beta'\sigma$). The initiation complex generally goes through several cycles of abortive initiation producing short RNA transcripts up to 15 nucleotides in length (reviewed in (Record Jr *et al.*, 1996)). At some stage the initiation complex enters into its elongation form (with the loss of the σ factor). This elongation complex travels along the DNA locally

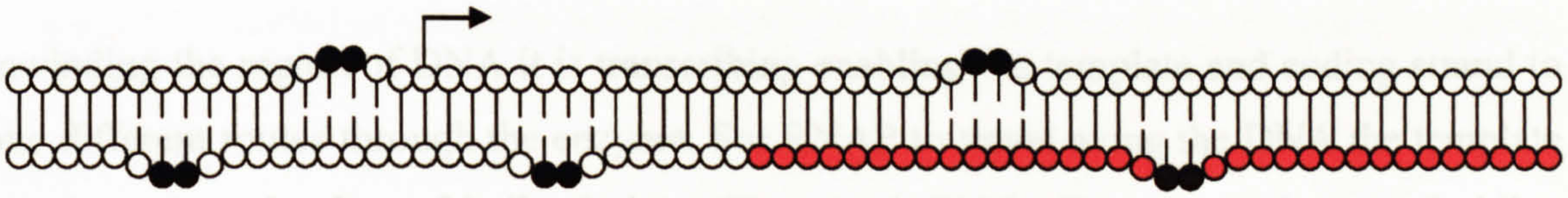

Figure 1.13 Transcription-coupled repair regions.

DNA lesions were subjected to transcription-coupled NER instead of global NER if they were present either at or 5′ of +15 in the template strand of a gene that was currently being transcribed (Selby and Sancar, 1995b). Lesions located elsewhere were repaired by standard NER. The red circles indicate the region in which lesions can be repaired by TCR.

unwinding the region of DNA it is transcribing enabling the template and coding strand to take different routes through the enzyme. For RNAP to travel along the DNA the template strand needs to be free of bulky lesions (Tornaletti, 2005). Damage such as pyrimidine dimers located in the coding strand do not effect transcription (Selby and Sancar, 1990). If a pyrimidine dimer is encountered in the template strand RNAP will stall (Selby and Sancar, 1990). A stalled elongation complex indicates that there is a problem that needs to be addressed before transcription can pass this point. *In vitro* the stalled elongation complex actually inhibits NER presumably because it blocks the lesion from the NER proteins (Selby and Sancar, 1990). For the increased rate of repair associated with lesions located within the template strand two things must therefore happen: RNAP must dissociate; and repair enzymes must be recruited. Both of these events are believed to be controlled by Mfd.

Recruitment of Mfd

Stalled elongation complexes can be recognised and bound by Mfd (Selby and Sancar, 1995a). Truncation studies indicated that $Mfd_{379\text{-}571}$ (encompassing all of domain 4 and some of domains 3 and 5) was able to interact with the B1 domain of the β-subunit of stalled RNAP complexes (Park *et al.*, 2002). The region of RNAP that Mfd interacts with is close to where the upstream DNA exits (Borukhov *et al.*, 2005) (Smith and Savery, 2005). Residues within this region of RNAPβ have been mutated and are deficient in RNAP displacement, the first evidence of TCR mutants that are not within a TRCF (Smith and Savery, 2005).

Mfd also interacts with the DNA upstream of the RNAP complex (Park *et al.*, 2002) probably through interactions with domains 5 and 6. In the absence of RNAP Mfd can bind DNA non-specifically on its own but requires ATP to be bound (Selby and Sancar, 1995b).

Displacement of RNAP

Having recognised and bound a stalled RNAP complex Mfd must then displace it. Mfd displaces RNAP in an ATP-dependent manner (Selby and Sancar, 1993) (Selby and Sancar, 1995a). Mfd uses the energy generated by ATP hydrolysis to translocate forward, pushing the RNAP complex forward (Park *et al.*, 2002). During transcription RNAP can

often become stalled at naturally occurring stall sites and become backtracked (Tornaletti, 2005). The motion of Mfd will enable RNAP to continue transcribing past this point. However if RNAP has stalled at a lesion the force generated by Mfd will cause the dissociation of RNAP from the DNA probably by indirectly causing the collapse of the transcription bubble (Park *et al.*, 2002) (Park and Roberts, 2006). The TRG motif is important for RNAP dissociation as Mfd TRG mutants are unable to displace RNAP from DNA (Chambers *et al.*, 2003). Interestingly Mfd can only displace stalled elongation complexes (Selby and Sancar, 1995a). It has no effect on initiation complexes which contain a sigma factor (Selby and Sancar, 1995a). The sigma factor prevents Mfd from binding RNAP (Park *et al.*, 2002). If Mfd can not bind the initiation complex it explains why TCR is not detected within the first 15 nucleotides of a transcription unit. It also explains why lesions within promoter regions are protected from repair as once RNAP is bound it can not be displaced from the site by Mfd.

Recruitment of UvrA and UvrB

The increased repair rate associated with lesions repaired by the TCR pathway over lesions repaired by the global NER pathway is believed to be due to an increase in the recruitment of the NER proteins. This implies that the recruitment of UvrA to a lesion within a transcription unit is faster than the rate at which UvrA would normally detect a lesion. The repair of the lesion will enable a different molecule of RNAP to transcribe along the DNA to produce the desired transcript enabling the cell to function correctly. Mfd is responsible for recruiting the NER proteins to the lesion. There are many questions to be answered about the NER recruitment process including whether UvrA is only recruited once RNAP has dissociated or whether it binds to either RNAP or Mfd before TCR has started.

A weak interaction between the β subunit of RNAP and UvrA has been observed during cross-linking studies on damaged and undamaged DNA (Ahn and Grossman, 1996) (Lin *et al.*, 1998). If such a reaction is physiologically relevant UvrA could be brought to the vicinity of the lesion during the natural transcription process. However it would need to dissociate from RNAP when RNAP is displaced in order to bind and recognise the lesion.

An alternative theory is that UvrA is bound to Mfd before Mfd has been recruited to a stalled RNAP complex. A third theory is that UvrA is recruited by Mfd at some point during RNAP displacement. A direct interaction between $Mfd_{1\text{-}378}$ (comprising domains

1a, 1b, 2 and some of domain 3) and UvrA has been observed in pull-down assays (Selby and Sancar, 1995a). As mentioned previously domains 1a, 1b and 2 of Mfd share structural similarity to the UvrA binding region of UvrB (Assenmacher *et al.*, 2006) (Selby and Sancar, 1993) (Deaconescu *et al.*, 2006). It is therefore likely that this region of Mfd is involved in UvrA binding. However in the Mfd crystal structure domain 7 is blocking the surface of domain 2 which is believed to be specifically responsible for the interaction with UvrA (Figure 1.12). Domain 7 is thought to be moved through a series of conformational changes. These changes are proposed to be triggered either by ATP binding or by the interaction Mfd makes with RNAP (Deaconescu *et al.*, 2006). The repositioning of domain 7 would enable UvrA to access and bind domain 2. How UvrA is then loaded onto the DNA, or whether this step is actually necessary, has yet to be determined. The binding of UvrA to Mfd will cause an increase in the local concentration of UvrA in the vicinity of the lesion which may be sufficient to explain the enhanced repair rate. It is believed that UvrA must then go on to recruit UvrB as there is no evidence that UvrB is recruited by Mfd and there is some evidence to suggest that UvrB and Mfd do not interact (Selby and Sancar, 1993). Following the recruitment of UvrA and UvrB the process of NER continues as in the global NER pathway with the recruitment of UvrC, UvrD, DNA polymerase and DNA ligase.

To further understand the recruitment of the NER enzymes in TCR it is important to increase our understanding of the UvrA-UvrB and the UvrA-Mfd interactions. Currently there is no evidence to suggest that UvrB and Mfd can interact with UvrA simultaneously and some evidence to suggest that they can not (Selby and Sancar, 1993). This had led to the suggestion that both proteins bind to, and compete for, the same region of UvrA. This hypothesis is supported by structural data in which UvrB and Mfd share a region of homology that has been linked to the UvrA interaction (Assenmacher *et al.*, 2006) (Deaconescu *et al.*, 2006). However there is currently no genetic data to support this theory.

Aims

The overall aim of this work was to characterise the UvrA-UvrB and the UvrA-Mfd interaction by analysing the residues within UvrA that are essential for these interactions. To do this there were several sub-aims. The first aim was to develop a system that would enable the UvrA-UvrB and also the UvrA-Mfd interaction to be identified. The system

needed to enable a genetic screen to be used that would allow the key region of UvrA to be mutagenised and key amino acid residues to be identified. A second screen was also used that would enable the identification of a wide variety of UvrA residues that would be deficient in a variety of UvrA functions, including its interaction with UvrB and Mfd.

Wild-type and mutant proteins all needed to be characterised *in vitro* and therefore protein expression and purification protocols were developed to enable the purification of a large number of proteins. Any mutants that were identified would be characterised both *in vivo* and *in vitro* to understand the role of the residues that had been mutagenised. *In vitro* analysis would include nucleotide hydrolysis, DNA binding and UvrB binding assays as well as an overall NER incision assay.

As part of the *in vitro* characterisation analysis it was important that a suitable incision assay could be used to check the overall effect of the mutation on the NER process. As the TCR process has strict template requirements with regards to DNA flanking the lesion on both sides an assay was developed that would enable the introduction of a single lesion into a defined position within an intact plasmid. This would enable the DNA to be used in future TCR studies.

CHAPTER 2

MATERIALS AND METHODS

Chemicals were supplied by Sigma or BDH unless stated otherwise.

Agars and broths

LB broth (per litre)	10 g	tryptone
	5 g	yeast extract
	10 g	NaCl
	pH 7.25 to 7.50	
LB agar (per litre)	10 g	tryptone
	5 g	yeast extract
	10 g	NaCl
	1.6%	Bacto Agar
	pH 7.25 to 7.50	
M9 broth (per litre)	6 g	Na_2HPO_4
	3 g	KH_2PO_4
	1 g	NH_4Cl
	0.5 g	NaCl
2 x YT (per litre)	16 g	tryptone
	10 g	yeast extract
	5 g	NaCl

Agar and broth supplements

Ampicillin	100 μg/ml working concentration
Chloramphenicol	25 μg/ml working concentration
IPTG (Apollo Scientific Ltd.)	1 mM working concentration
Kanamycin	50 μg/ml working concentration
Tetracycline	25 μg/ml working concentration
X-gal (Apollo Scientific Ltd.)	80 μg/ml working concentration

Solutions

Standard buffers

5 x TBE	446 mM	Tris-HCl
	445 mM	Orthoboric acid
	10 mM	EDTA (pH 8.0)
50 x TAE	2 M	Tris-HCl
	5.71% v/v	Glacial acetic acid
	50 mM	EDTA (pH 8.0)
TE buffer	10 mM	Tris-HCl (pH 8.0)
	1 mM	EDTA (pH 8.0)

Loading dyes

6 x DNA loading dye	30% v/v	Glycerol
	1 x	TBE
	373 µM	Bromophenol blue (Pharmacia Biotech)
	464 µM	Xylene cyanol (Bio-Rad)
	(50 ng/µl	RNase (Sigma) was added for alkaline lysis minipreped DNA)
STEB stop buffer	0.1 M	Tris-HCl (pH 8.0)
	0.1 M	EDTA (pH 8.0)
	1.17 M	Sucrose
	597 µM	Bromophenol blue
Formamide stop solution	95% v/v	Formamide
	20 mM	EDTA
	746 µM	Bromophenol blue
	928 µM	Xylene cyanol

Protein sample buffer	115 mM	Tris-HCl (pH 6.8)
	69.4 mM	SDS
	20% v/v	Glycerol
	746 μM	Bromophenol blue
	1.24 M	β-mercaptoethanol added just before use

Protein gel buffers

2 x resolving gel buffer	0.75 M	Tris-HCl (pH 8.3)
10 x stacking gel buffer	1.25 M	Tris-HCl (pH 6.8)
10 x Tris glycine buffer	248 mM	Tris-HCl
	2 M	Glycine (Severn Biotech)
SDS PAGE running buffer	34.7 mM	SDS
	1 x	Tris glycine buffer
Coomassie stain	50% v/v	Methanol
	10% v/v	Acetic acid
	2.42 mM	Coomassie brilliant blue (Bio-Rad)
Fast destain	40% v/v	Methanol
	10% v/v	Acetic acid
Slow destain	10% v/v	Methanol
	10% v/v	Acetic acid

Gel composition

Agarose gels

1% agarose	1% w/v	Agarose (Helena)
	1 x	TAE
	1.27 μM	Ethidium bromide

Acrylamide gels

DNA and electrophoretic mobility shift assay (EMSA) gels

6% and 7.5% acrylamide	6/7.5% v/v	Acrylamide (30% w/v acrylamide 37.5:1 Bis Acrylamide) (Severn Biotech Ltd.)
	1 x	TBE
4% acrylamide	4% v/v	Acrylamide (30% w/v acrylamide 37.5:1 Bis Acrylamide)
	0.5 x	TBE
	10 mM	$MgCl_2$
Denaturing 6% acrylamide	7 M	Urea (Fisher)
	1 x	TBE
	6% v/v	Acrylamide (40% w/v acrylamide 19:1 Bis Acrylamide) (Severn Biotech Ltd.)

SDS PAGE gel

10% resolving protein	1 x	resolving gel buffer
	10% v/v	Acrylamide (30% w/v acrylamide 37.5:1 Bis Acrylamide)
	3.47 mM	SDS
6% stacking protein	1 x	Stacking gel buffer
	6% v/v	Acrylamide (30% w/v acrylamide 37.5:1 Bis Acrylamide)
	3.47 mM	SDS

Acrylamide gel supplements

Polymerization of acrylamide gels was achieved by the addition of:

4.38 mM	APS (final concentration)
861 µM	TEMED (final concentration)

Plasmid DNA extraction buffers

Solution I	50 mM	Glucose
	10 mM	EDTA
	25 mM	Tris-HCl (pH 8.0)
Solution II	0.2 M	NaOH (Riedel-detlaen)
	34.7 mM	SDS
Solution III	3 M	KAc (pH 4.8)

Buffers for western blots

Transfer buffer	10% v/v	Methanol
	1 x	Tris glycine
1 x PBS	170 mM	NaCl
	3 mM	KCl
	1 mM	Na_2HPO_4
	1.8 mM	KH_2PO_4 (pH 7.4)
PBS tween	0.05% v/v	Tween
	1 x	PBS
Blocking buffer	10% w/v	Milk powder (Somerfield)
	1 x	PBS

Buffers for the purification of histidine-tagged proteins

Wash buffer	50 mM	NaH_2PO_4
	300 mM	NaCl
	20 mM	Imidazole
	pH to 8.0 using NaOH	
Elution buffer	50 mM	NaH_2PO_4
	300 mM	NaCl
	500 mM	Imidazole
	pH to 8.0 using NaOH	

Dialysis buffer	20 mM	Tris-HCl (pH 8.0)
	2 mM	EDTA
	400 mM	KCl
	4 mM	DTT (Melford) added just before use
Storage buffer	10 mM	Tris-HCl (pH 8.0)
	1 mM	EDTA
	200 mM	KCl
	50% v/v	Glycerol
	2 mM	DTT added just before use

Reaction buffers

1 x repair buffer	40 mM	Hepes (Apollo scientific) (pH 7.8)
(Selby and Sancar, 1995b)	100 mM	KCl
	8 mM	$MgCl_2$
	4% v/v	Glycerol
	100 µg/ml	BSA (NEB)
	5 mM	DTT
1 x transcription buffer	40 mM	Tris-Ac (pH 7.9)
(Savery *et al.*, 1998)	100 mM	KCl
	10 mM	$MgCl_2$
	5 mM	DTT
Z buffer	10 mM	KCl
(Miller, 1972)	1 mM	$MgSO_4$
	60 mM	Na_2HPO_4
	30 mM	NaH_2PO_4
	104 µM	SDS
	38.6 mM	β-mercaptoethanol added just before use

Methods

Centrifugation

The six centrifuges used in this work are listed in Table 2.1.

Gel electrophoresis

Agarose gels

Agarose gels were run at 100 V for one to two hours in 1 x TAE buffer containing 0.5 μg/ml ethidium bromide. DNA bands were visualised using a UV transilluminator (UVP).

Non-denaturing acrylamide gels for analysis of DNA

The 7.5% acrylamide gel solution and the acrylamide gel supplements were mixed and poured between gel plates 1.5 mm apart (part of the Bio-Rad mini protean 3 system). The gels were run at 100 V for approximately one hour in 1 x TBE. Gels were stained in 1.27 μM ethidium bromide for 30 minutes (unless SYBR Green had been added to the DNA samples). The DNA bands were visualised using a UV transillumintor and the amount of DNA quantified using Kodak imaging software.

EMSA gels

The 6% acrylamide gel solution or the 4% acrylamide gel solution (containing 10 mM $MgCl_2$) were mixed with the acrylamide gel supplements and poured between gel plates 1.0 mm apart (part of the Bio-Rad protean II xi system). The gels were pre-run (in buffer containing the same concentration of TBE and $MgCl_2$ as the gel) at 40 mA (max 200 V) at 4°C for 30 minutes before being loaded and run under the same conditions for three hours. The gels were dried and placed on phosphor screens overnight. ^{32}P labelled DNA was detected using a Typhoon phosphoimager (Amersham) and visualised using ImageQuant software.

Denaturing acrylamide gels

10 ml urea sequencing gel solution and the acrylamide gel supplements were mixed and syringed between gel plates 0.4 mm apart (part of the BRL S2 system) to form a seal at the bottom. Once the seal had set the remaining space was filled by the addition of 50 ml urea

Centrifuge	Rotor	Max. speed (g)	Use
Eppendorf 5415D	Standard	16110	Bench top work at room temperature
Eppendorf 5415DR	Standard	16110	Bench top work at 4 °C
Eppendorf 5804	A-4-44	4500	Used for centrifugation of samples between 3 and 100 ml (100 ml in two 50 ml aliquots)
Sorvall RC6	SS34	50228	High speed centrifugation
Sorvall RC3B	H-6000A	7200	Centrifugation of cultures greater than 100 ml
Sorvall UltraPro 80	65V13	602644	High speed CsCl maxiprep centrifugation step

Table 2.1 Centrifuges.

The centrifuges and rotors used in this thesis are listed against their main use.

sequencing gel solution mixed with the acrylamide gel supplements. The gel was pre run until it reached 55°C (approximately one hour) (2000 V, 200 mA, 200 W max.) in 1 x TBE buffer. Gels were immediately loaded and run at 55°C under the same conditions. Gels were fixed in slow destain for two times two minutes and then dried and placed on phosphor screens overnight. ^{32}P containing bands were detected using the Typhoon phosphoimager and visualised using ImageQuant software.

SDS PAGE gels

The 10% resolving gel solution and the acrylamide gel supplements were mixed and poured to a depth of 5 cm between gel plates 0.75 mm apart (part of the Bio-Rad mini protean 3 system). Isopropanol was gently placed over the top to create a smooth surface. Once the resolving gel was set the isopropanol was washed away with water and replaced by the 6% stacking gel solution containing the acrylamide gel supplements. Gels were run in SDS PAGE running buffer at 200 V for approximately one hour. Protein bands were visualised by staining the gel in coomassie stain for one hour and then destaining in fast destain for 30 minutes and slow destain overnight. Alternatively bands were visualised using the bio-safe coomassie stain (Bio-Rad) following the manufactures protocol.

Microbiological techniques

Bacterial strains

E. coli strains used in this thesis are listed in Table 2.2. Either XL1-Blue, TOP10 or RLG221 were used for standard cloning procedures. KS1 and MG1655Δ*uvrA* were used to screen for mutants in the bacterial two-hybrid and UV sensitivity screens respectively.

Conjugation – generation of Escherichia coli strain MG1655ΔuvrA

Conjugation was used to transfer the F′ episome (encoding $lacI^q$) from XL1-Blue cells into FB21635, the Δ*uvrA* strain (essentially as described in (Miller, 1972)). Overnight cultures of XL1-Blue and FB21635 cells were diluted 100-fold in LB broth containing tetracycline or kanamycin respectively. The cultures were incubated at 37°C for three hours. 1 ml of each culture was combined (or kept separate as controls) and incubated at 37°C for one hour without shaking. A sample of cells were then plated onto LB agar plates containing IPTG, X-gal and either tetracycline, kanamycin or both. Colonies that appeared blue on

Strain	Derivative of	Genotype	Antibiotic resistance[1]	Source
FB21635	MG1655	*uvrA::Tn5*(Kan^R)	Kan	*E. coli* genome project, University of Wisconsin
KS1	MC1000	*plac*O$_R$2-62 [F' *lacI*^{q}]	Kan	(Dove *et al.*, 1997)
MC1000		*araD139*([]), *DE(araA-leu)7697*, *DE(codB-lacI)3*, *galK16*, *galE15(GalS)*, *LAM-*, *e14-*, *relA1*, *rpsL150(strR)*, *spoT1*, *mcrB1*		(Casadaban and Cohen, 1980)
MG1655		F-, lambda-, *ilvG-*, *rfb*-50, *rph*-1		(Blattner *et al.*, 1997)
MG1655 Δ*uvrA*	FB21635	F' *proAB*, *lacI*^{q}ZΔ*M15*, Tn*10*, (Tet^r)	Kan, Tet	This Work
RLG221		*recA56*, *araD139*, (*ara-leu)7697*, *lacX74*, *galU*, *galK*, *hsdR*, *strA*		(Barnard *et al.*, 2003)
TOP10		F- *mcrA*, Δ(*mrr-hsdRMS-mcrBC*), Φ80*lacZ*ΔM15, Δ*lacX*74, *recA*1, *araD*139, Δ(*ara-leu*)7697, *galU*, *galK*, *rpsL*, (Str^R), *endA*1, *nupG*		Invitrogen
XL1-Blue		*endA1*, *gyrA96*, *hsdR17*, *lac*, *recA1*, *relA1*, *supE44*, *thi-1*, [F' *proAB*, *lacI*^{q}Z*ΔM15*, Tn*10*, (Tet^r)]	Tet	Stratagene

Table 2.2 *Escherichia coli* strains.

The *E. coli* strains used in this thesis are listed with their genotype. The antibiotic that can be used for their selection and the source of the strain are also listed. [1] The abbreviations used are: Kan, kanamycin; Tet, tetracycline.

LB agar plates containing IPTG, X-gal, tetracycline and kanamycin were streaked, incubated overnight and single colonies used to inoculate LB broth containing the above antibiotics. The cultures were incubated at 37°C for eight hours and then mixed with equal quantities of 50% glycerol, frozen in liquid nitrogen and stored at -80°C. The strain was named MG1655Δ*uvrA*.

Competent cell preparation

Chemically competent Escherichia coli

Chemically competent cells were prepared essentially as described by Sambrook and Russell (Sambrook and Russell, 2001). LB broth (50 ml) containing the appropriate antibiotics were inoculated with 0.5 ml of an overnight culture. The cultures were incubated at 37°C to an A_{600} of 0.5 and then placed on ice for 10 minutes. The cells were centrifuged at 2770 g at 4°C for 10 minutes, the pellet suspended in 20 ml ice cold 0.1 M $CaCl_2$ (Fisher) and incubated on ice for a further 20 minutes. The cells were centrifuged at 2770 g at 4°C for 10 minutes and the pellet suspended in 5 ml ice cold 0.1 M $CaCl_2$ and 20% glycerol. The cells were incubated on ice for at least 30 minutes before use and were stored at -80°C if not used that day.

Electrocompetent Escherichia coli

Electrocompetent cells were prepared essentially as described by Sambrook and Russell (Sambrook and Russell, 2001). LB broth (50 ml) containing the appropriate antibiotics were inoculated with 0.5 ml of an overnight culture. The cultures were incubated at 37°C to an A_{600} of 0.5 and then placed on ice for 20 minutes. The cells were subjected to four cycles of centrifugation, suspension and incubation. Centrifugation was at 2770g at 4°C for 10 minutes. Suspension was in 50 ml (cycle 1), 25 ml (cycle 2), 2 ml (cycle 3) or 0.2 ml (cycle 4) of ice cold 10% glycerol and the incubations were on ice for 10 minutes. The cells were incubated on ice for at least a further 30 minutes and used that day.

Transformations

Transformation of chemically competent Escherichia coli

Chemically competent *E. coli* were transformed essentially as described by Sambrook and Russell (Sambrook and Russell, 2001). Chilled chemically competent *E. coli* cells (100 µl) were transformed with 10 ng plasmid DNA or 10 µl ligation mix by premixing and incubating on ice for 30 minutes, incubating at 42°C for two minutes, incubating on ice for two minutes, adding 400 µl LB broth and incubating at 37°C for 30 minutes. Transformation mixtures were then centrifuged at 16110 g for one minute, 450 µl of supernatant discarded and the cells suspended in the remaining LB broth. The cells were spread onto agar plates containing the appropriate antibiotics and supplements and incubated overnight at 30°C or 37°C.

Transformation of electrocompetent Escherichia coli

Electrocompetent *E. coli* were transformed essentially as described by Sambrook and Russell (Sambrook and Russell, 2001). Chilled electrocompetent *E. coli* cells (40 µl) were transformed with 1 ng plasmid DNA or 2 µl ligation mix by mixing and placing in a 0.1 cm MicroPulser cuvette (Bio-Rad), electroporating at 1.8 kV for four to six ms (using the bacterial setting on a micropulser electroporator (Bio-Rad)), adding 1 ml 2 x YT and incubating at 37 °C for 30 minutes. Transformation mixtures were then centrifuged at 16110 g for one minute and the pellet suspended in 50 µl M9 media. The cells were spread onto agar plates containing the appropriate antibiotics and supplements and incubated overnight at 30°C or 37°C.

DNA manipulation

DNA purification

DNA purification from agarose gels and enzymatic reactions

DNA was extracted from agarose gels using either the QIAquick gel extraction kit (Qiagen) or the GeneCleanIII kit (Q-Biogene). DNA was extracted from enzymatic reactions such as PCR and digests using the QIAquick PCR purification kit (Qiagen), the QIAquick nucleotide removal kit (Qiagen) or the GeneCleanIII kit. The manufacturers protocol was followed for these kits.

DNA purification by phenol chloroform extraction and ethanol precipitation

The DNA solution to be extracted was made up to at least 200 µl by the addition of TE buffer. An equal volume of phenol: chloroform: isoamyl alcohol (25:24:1) was added and the solution vortexed for 15 seconds and centrifuged at 16110 g for five minutes. The upper layer was kept and 20 µg of glycogen (Fermentus Life Sciences), 0.1 volume of 3 M NaAc (pH 5.2) and 2 volumes of ethanol added before placing at -20°C for at least 30 minutes. The solution was centrifuged at 16110 g for 15 minutes, the pellet washed in 1 ml 70% ethanol and air-dried before suspending in 5 to 50 µl TE buffer.

Plasmid DNA extraction from culture

Plasmid DNA was extracted from up to 5 ml of bacterial culture using the QIAprep spin miniprep kit (Qiagen) or by alkaline lysis (see below). Plasmid DNA was extracted from large cultures by the HiSpeed plasmid midi kit (Qiagen), the plasmid midi kit (Qiagen) or by CsCl maxiprep (see below).

Alkaline lysis minipreps

Plasmid DNA was extracted by the alkaline lysis technique essentially as described by Sambrook and Russell (Sambrook and Russell, 2001). 3 ml of overnight cultures were centrifuged at 16110 g for one minute. The pellet was suspended in 100 µl solution I and incubated at room temperature for five minutes. 200 µl of solution II was added and the tube gently inverted five times before incubating on ice for five minutes. 150 µl solution III was added and the tube gently inverted five times before incubating on ice for five minutes. The solution was centrifuged at 16110 g for five minutes and the supernatant transferred to a fresh tube. 300 µl phenol: chloroform: isoamyl alcohol (25:24:1) was added, the solution vortexed for 15 seconds and centrifuged at 16110 g for two minutes. The upper 300 µl was kept, 600 µl ice cold ethanol (Fisher) added and the solution centrifuged at 16110 g for five minutes. The pellet was washed with 1 ml of 70% ethanol, air-dried and suspended in 50 µl TE buffer.

CsCl Maxipreps

Plasmid DNA was extracted by the CsCl technique essentially as described by Sambrook and Russell (Sambrook and Russell, 2001). 400 ml of LB broth containing the appropriate

antibiotics was inoculated with 4 ml of overnight culture and incubated at 37°C until an A_{600} of 1.2 was reached. Chloramphenicol was added to a final concentration of 170 µg/ml and the culture incubated at 37°C overnight. The culture was centrifuged at 4657 g at 4°C for 15 minutes, the pellet suspended in 5 ml solution I containing 5 mg lysozyme and incubated on ice for five minutes. 10 ml of solution II was added and the tube gently inverted five times before incubating on ice for five minutes. 7.5 ml of Solution III was added and the tube gently inverted five times before incubating on ice for 5 minutes. The solution was centrifuged at 26892 g at 4°C for 15 minutes, the supernatant added to 13 ml isopropanol and the tube inverted five times before incubating on ice for 15 minutes. The solution was centrifuged at 26892 g at 20°C for 15 minutes, the pellet washed with 5 ml 70% ethanol, air-dried and suspended in 8 ml TE buffer. 8.2 g of CsCl (Melford) was added and the tube was incubated at 30°C until the CsCl dissolved. 200 µl 10 mg/ml ethidium bromide was added and the solution centrifuged at 7649 g at 20°C for 10 minutes. The supernatant was transferred to a 13.5 ml ultracentrifuge tube and the remainder of the tube filled up with paraffin. The solution was centrifuged at 192037 g at 15°C for 16 hours. To prevent the introduction of DNA damage the DNA bands were visualised using a dark reader (Clare Chemicals). The lower band (containing the supercoiled DNA) was transferred to a fresh tube. The ethidium bromide was removed by six extractions with equal volumes of water saturated butanol. The DNA was dialysed twice in 12-14 kDa MWCO dialysis tubing (Visking) in 500 ml TE buffer at 4°C. The DNA was then extracted and purified by phenol chloroform extraction and ethanol precipitation following the standard protocol except that centrifugal speeds were 2988 g and 26892 g respectively and the DNA was dissolved in 1 ml TE buffer. (Sambrook and Russell, 2001).

PCR

Standard PCR using Pfu DNA polymerase

PCR (50 µl) contained 10 ng DNA (or all the DNA generated by error-prone PCR (see below)), 200 µM dNTPs (Roche), 1 µM forward primer, 1 µM reverse primer and 1.25 U Pfu DNA polymerase (Promega) in the supplied buffer. The reactions were placed at 95°C for two minutes followed by 30 cycles of: 95°C for 30 seconds, 60°C for 30 seconds and 72°C for two minutes (unless otherwise indicated in the plasmid section of this chapter). The reactions were completed by a 10 minute incubation at 72°C.

Standard PCR using Phu DNA polymerase

PCR (50 µl) contained 10 ng DNA, 200 µM dNTPs, 0.5 µM forward primer, 0.5 µM reverse primer and 1 U Phu DNA polymerase (Finnzymes) in the supplied Phusion HF buffer. The reactions were placed at 98°C for two minutes followed by 35 cycles of: 98°C for 10 seconds, 63.9°C for 30 seconds and 72°C for a specified time (indicated in the plasmid section of this chapter). The reaction was completed by a 10 minute incubation at 72°C. This method was only used in generating pQE30UvrB$_{RE183}$ and pQE30UvrB$_{RA213}$.

Error-prone PCR

The error-prone PCR protocol described by Greene was essentially followed (Greene, 2002). Error-prone PCR (50 µl) contained 25 ng template DNA, 1 mM dCTP (Roche), 1 mM dTTP (Roche), 0.2 mM dATP (Roche), 0.2 mM dGTP (Roche), 2 µM forward primer, 2 µM reverse primer, 10 mM Tris-HCl (pH 8.3), 50 mM KCl, 7 mM $MgCl_2$, 0.5 mM $MnCl_2$ and 2.5 U Taq DNA polymerase (Promega). The reactions were placed at 94°C for five minutes followed by one to five cycles of: 94°C for 30 seconds, 60°C for 30 seconds and 72°C for two minutes. The DNA was purified by phenol chloroform extraction and ethanol precipitation and amplified further following the standard PCR protocol.

Site-directed mutagenesis

Site-directed mutagenesis was carried out as shown in Figure 2.1 using the standard PCR protocol for each individual PCR (Sambrook and Russell, 2001). PCR-A and PCR-B each contain one mutagenic primer and one outer primer (that can contain a restriction site to aid cloning of the final product). PCR-C was subsequently set up using both outer primers and equal amounts (normally 5 µl) of the initial PCR products.

Annealing oligonucleotides

An annealing reaction was used to generate a short DNA insert that contained restriction sites for cloning (see pBRcIωXK). The annealing reaction (40 µl) contained 50 µM PL01 and 50 µM PL02. It was incubated at 100°C for two minutes and cooled to room temperature overnight.

Annealing reactions were also used to generate short fragments for EMSA. These annealing reactions (90 µl) contained 50 µM RA0003-ann and 10 µM of either [γ^{32}P]

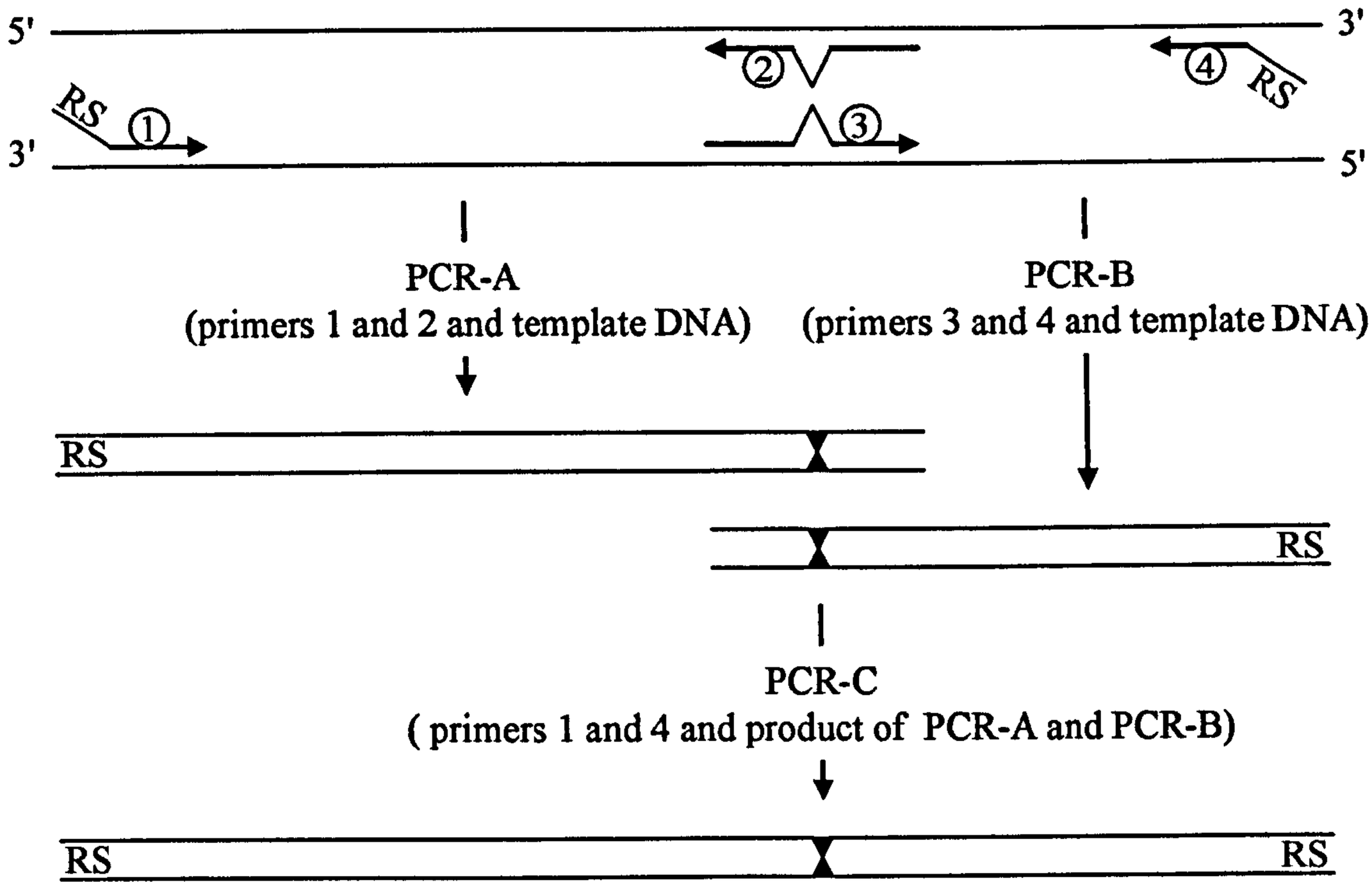

Figure 2.1 Site-directed mutagenesis.

Site-directed mutagenesis that generates a single point mutation requires two initial PCRs to generate products PCR-A and PCR-B. These products and the outer primers (1 and 4) are used in a final PCR to generate the full-length mutant that can be cloned into the desired vector using the restriction sites (RS) generated by primers 1 and 4.

RA0004-FldT or [γ^{32}P] RA0005-con. They were incubated at 37°C for five minutes and then cooled to 4°C at a rate of 0.1°C every second.

DNA digestion, dephosphorylation and generation of blunt ends

Analytical digests (10 µl) were incubated at 37°C for one hour and contained 100 to 200 ng DNA and 10 U restriction enzyme (each) in the supplied buffer. Preparative digests (50 µl) were incubated at 37°C for three hours and contained 1 to 2 µg DNA and 10 to 25 U restriction enzyme (each) in the supplied buffer.

Following preparative digests (50 µl reaction volumes) the DNA could be blunt ended and/or dephosphorylated. To generate blunt ends from 5′ overhangs 4 µl of 0.25 mM dNTPs and 0.5 µl 2 U/µl Klenow fragment (Roche) were added and the reaction incubated at 37°C for 30 minutes and then 70°C for 15 minutes. DNA was dephosphorylated at 37°C by the addition of 1 µl of 1 U/µl calf intestinal alkaline phosphatase (CIAP) (Promega) at the start of two consecutive 30 minute periods.

Phosphorylation of DNA ([γ^{32}P] labelling)

Phosphorylation reactions (20 to 50 µl) were incubated at 37°C for 30 minutes then 70°C for 20 minutes and contained 3 to 100 nM DNA (1 µM for a primer), 20 µCi [γ^{32}P] ATP (Amersham) or 1 mM ATP (Roche) and 10 to 20 U polynucleotide kinase (Roche) in the supplied buffer. Reactions that contained [γ^{32}P] ATP were passed through a micro Bio-Spin 6 column (Bio-Rad) following the manufactures protocol to remove unbound nucleotides whilst standard reactions were purified by phenol chloroform extraction and ethanol precipitation.

Ligations

Ligations (20 µl) were incubated on thawing ice overnight and contained approximately 1 µl vector, approximately 3 µl insert and 1 U T4 DNA ligase (Fermentus Life Sciences) in the supplied buffer.

Plasmids

The plasmids used and generated in this thesis are listed in Table 2.3. Selected plasmid maps are shown in Figure 2.2. All plasmids constructed were sequenced either by MWG

Plasmid[1] (size (bp) and antibiotic resistance)	**Description**	**Source**
pACYC184 (4245, chl and tet)	Standard cloning vector containing the *cat* gene.	NEB
pBRcIω (4803, amp)	Contains the λ *cI* gene upstream of *rpoZ*.	(Dove and Hochschild, 1998)
pBRcIωXK (4554, amp)	Derivative of pBRcIω. Contains the λ *cI* gene upstream of an XbaI and KpnI site.	This work
pBSII (pBluescript®IIKS-) (2961, amp)	Standard cloning vector containing a multiple cloning site (MCS).	Stratagene
pBSIIUvrA (5758, amp)	Derivative of pBSII. The *uvrA* gene amplified from MG1655 cells was cloned in on a BamHI/HindIII fragment.	Dr. N. Savery
pBSIIUvrAΔKpnI (5758, amp)	Derivative of pBSIIUvrA. The KpnI site within the *uvrA* gene has been silently mutated.	This work
pBSIIUvrB (4957, amp)	Derivative of pBSII. The *uvrB* gene amplified from MG1655 cells was cloned in on a BamHI/HindIII fragment.	Dr. N. Savery
pBSIIUvrC$_{23\text{-}610}$ (4703, amp)	Derivative of pBSII. The DNA sequence coding for UvrC$_{23\text{-}610}$ amplified from MG1655 cells was cloned in on a BamHI/HindIII fragment.	Dr. N. Savery
pBSIIUvrC (4769, amp)	Derivative of pBSIIUvrC$_{23\text{-}610}$. The 5′ region of the *uvrC* gene amplified from MG1655 cells was cloned in on a BamHI/SphI fragment to generate the full-length *uvrC* gene.	This work
pETMfd (9686, amp)	Contains the *mfd* gene downstream of its promoter.	(Chambers *et al.*, 2003)
pKD46 (amp)	Plasmid used to generate the Δ*uvrA* genotype of FB21635 cells.	*E. coli* genome project, University of Wisconsin
pQE30 (3461, amp)	Standard expression vector containing a MCS downstream of a sequence that encodes a hexa-histidine tag enabling histidine-tagged proteins to be expressed.	Qiagen
pQE30UvrA (and derivatives) (6246, amp)	Derivative of pQE30. The *uvrA* gene has been cloned into the MCS on a BamHI/HindIII fragment enabling histidine-tagged UvrA to be expressed.	This work
pQE30UvrB (and derivatives) (5445, amp)	Derivative of pQE30. The *uvrB* gene has been cloned into the MCS on a BamHI/HindIII fragment enabling histidine-tagged UvrB to be expressed.	This work

Plasmid[1] (size (bp) and antibiotic resistance)	**Description**	**Source**
pQE30UvrC (5257, amp)	Derivative of pQE30. The *uvrC* gene has been cloned into the MCS on a BamHI/HindIII fragment enabling histidine-tagged UvrC to be expressed.	This work
pRA02 (3601, amp)	Derivative of pSRlacUV5$_{203}$. The lacUV5$_{203}$ fragment was replaced with the promoter and 5′ region of *rpoA*. At the 3′ end of the *rpoA* gene there are XbaI and KpnI sites that enable genes to be cloned in enabling $\alpha_{1\text{-}248}$ fusion proteins to be expressed.	This work
pRA02UvrA$_{1\text{-}252.mutations}$ (4357, amp)	Derivative of pRA02UvrA$_{1\text{-}252}$ containing the coding sequence for the indicated UvrA$_{1\text{-}252}$ mutation.	This work
pRA02UvrA$_{1\text{-}n}$ (Various[2], amp)	Derivative of pRA02 containing the coding sequence for the indicated UvrA truncation in frame with the *rpoA* gene enabling $\alpha_{1\text{-}248}$-UvrA$_{1\text{-}n}$ fusion protein to be expressed.	This work
pRA03 (4371, chl)	Derivative of pACYC184. The λ *cI* gene upstream of XbaI and KpnI sites has been inserted as an EcoRI/SalI fragment. This allows λcI fusion proteins to be expressed from a chloramphenicol resistant plasmid.	This work
pRA03UvrB$_{35\text{-}252}$ (5022, chl)	Derivative of pRA03 containing the coding sequence for UvrB$_{35\text{-}252}$ cloned in frame with λ *cI* enabling λcI-UvrB$_{35\text{-}252}$ fusion protein to be expressed.	This work
pRA03UvrB$_{35\text{-}252.mutations}$ (5022, chl)	Derivative of pRA03UvrB$_{35\text{-}252}$ containing the coding sequence of the indicated UvrB mutation.	This work
pRA03Mfd$_{1\text{-}219}$ (5025, chl)	Derivative of pRA03 containing the coding sequence of Mfd$_{1\text{-}219}$ cloned in frame with λ *cI* enabling λcI-Mfd$_{1\text{-}219}$ fusion protein to be expressed.	This work
pREIIα (amp)	Contains the *rpoA* gene downstream of a *lac*UV5 promoter.	(Blatter *et al.*, 1994)
pREIIαΔXbaI (amp)	Derivative of pREIIα in which the XbaI site between the promoter and the *rpoA* gene is destroyed.	This work
pSRlacUV5$_{203}$ (2646, amp)	Contains the *lac*UV5$_{203}$ promoter upstream of a terminator sequence.	pSR/*lacUV5*(-140/63) (Savery *et al.*, 2002)

Plasmid[1] (size (bp) and antibiotic resistance)	Description	Source
pSRT7A1 (2568, amp)	Derivative of pSRlacUV5$_{203}$. The EcoRI/HindIII *lac*UV5$_{203}$ promoter containing fragment was replaced with the T7A1 (-91 to +28) promoter fragment. The fragment contains (starting at position +26) a BseCI recognition sequence overlapping a Dam recognition sequence that will enable a single modification to be introduced.	Dr. N. Savery
pUT18 (3023, amp)	Vector for use in the adenylate cyclase bacterial two-hybrid screen. Contains a MCS upstream of the sequence coding for the T18 domain of adenylate cyclase enabling fusion proteins to be expressed.	(Karimova *et al.*, 2001)
pUT18Mfd$_{1-219}$ (3674, amp)	Derivative of pUT18 containing the coding sequence for Mfd$_{1-219}$ on a XbaI/KpnI fragment.	This work
pUT18UvrA$_{1-n}$ (Various[2], amp)	Derivative of pUT18 containing the coding sequence for the indicated region of UvrA on a XbaI/KpnI fragment.	This work
pUT18UvrB$_{35-252}$ (3671, amp)	Derivative of pUT18 containing the coding sequence for UvrB$_{35-252}$ on a XbaI/KpnI fragment.	This work

Table 2.3 Plasmids.

The plasmids used and generated in this thesis are listed. [1]Numbers in subscript in this column refer to amino acid residues (except for pSRlacUV5$_{203}$). [2]The size of these plasmids depends on the size of the *uvrA* truncation inserted.

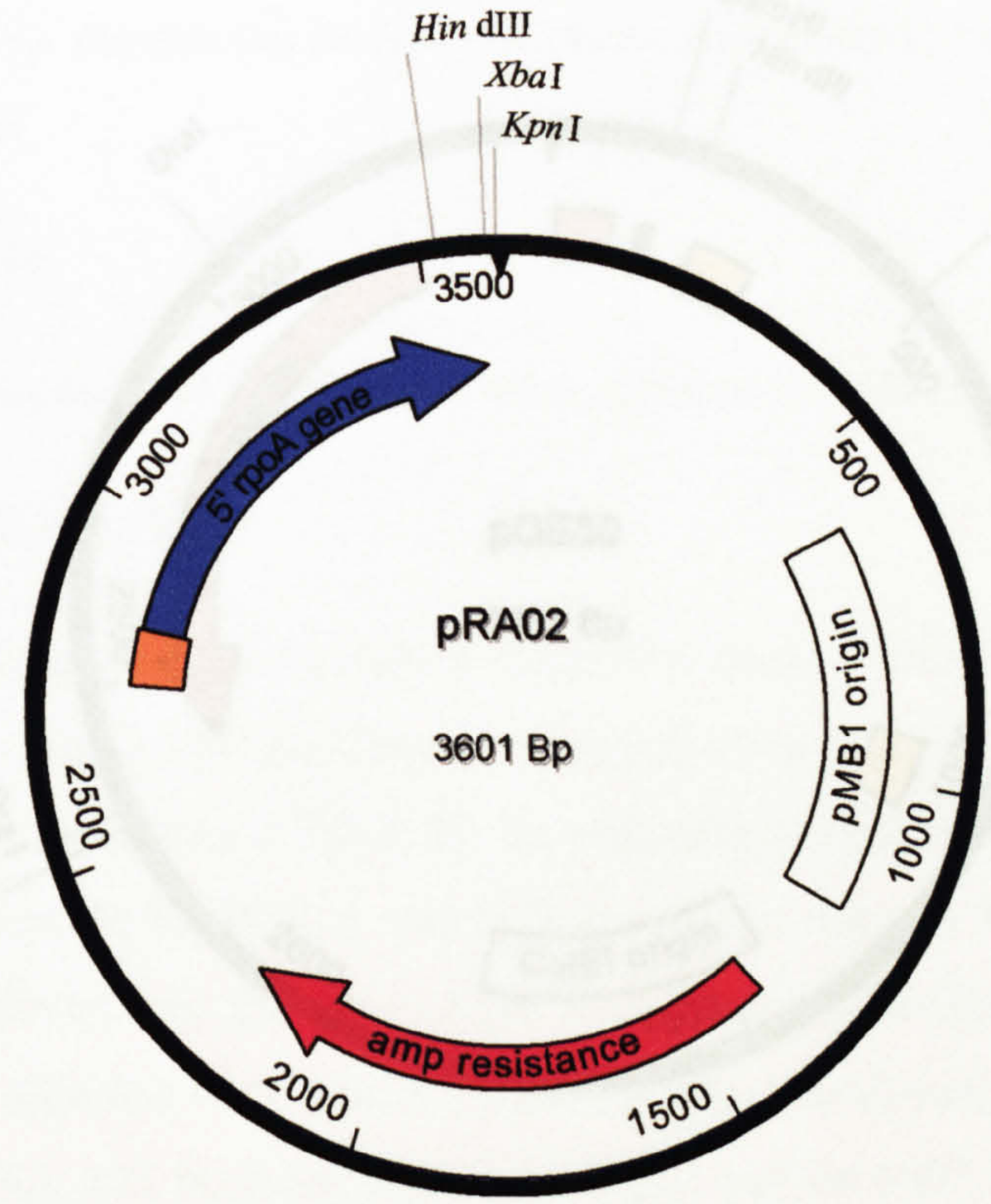

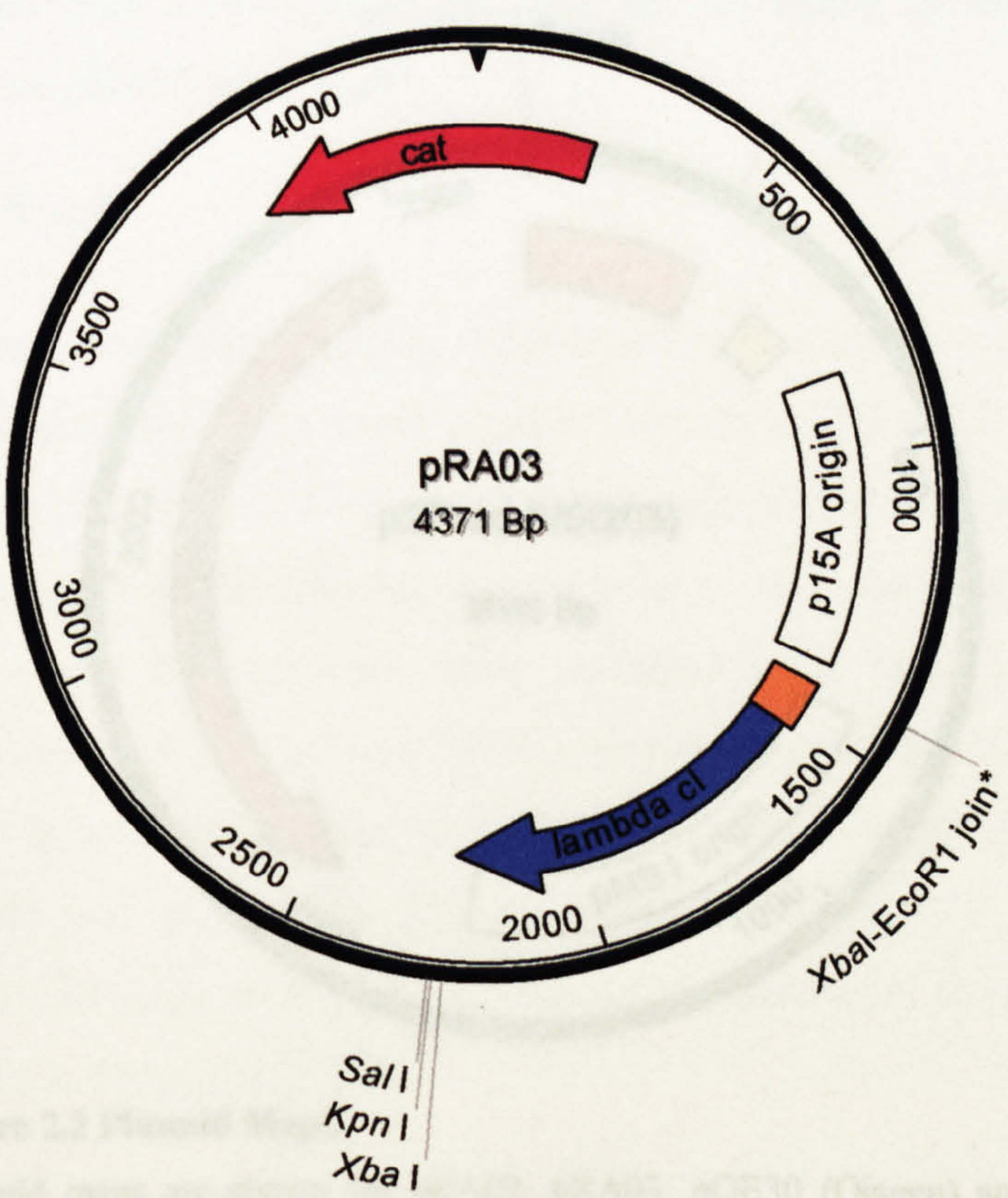

Figure 2.2 Page 1 of 2

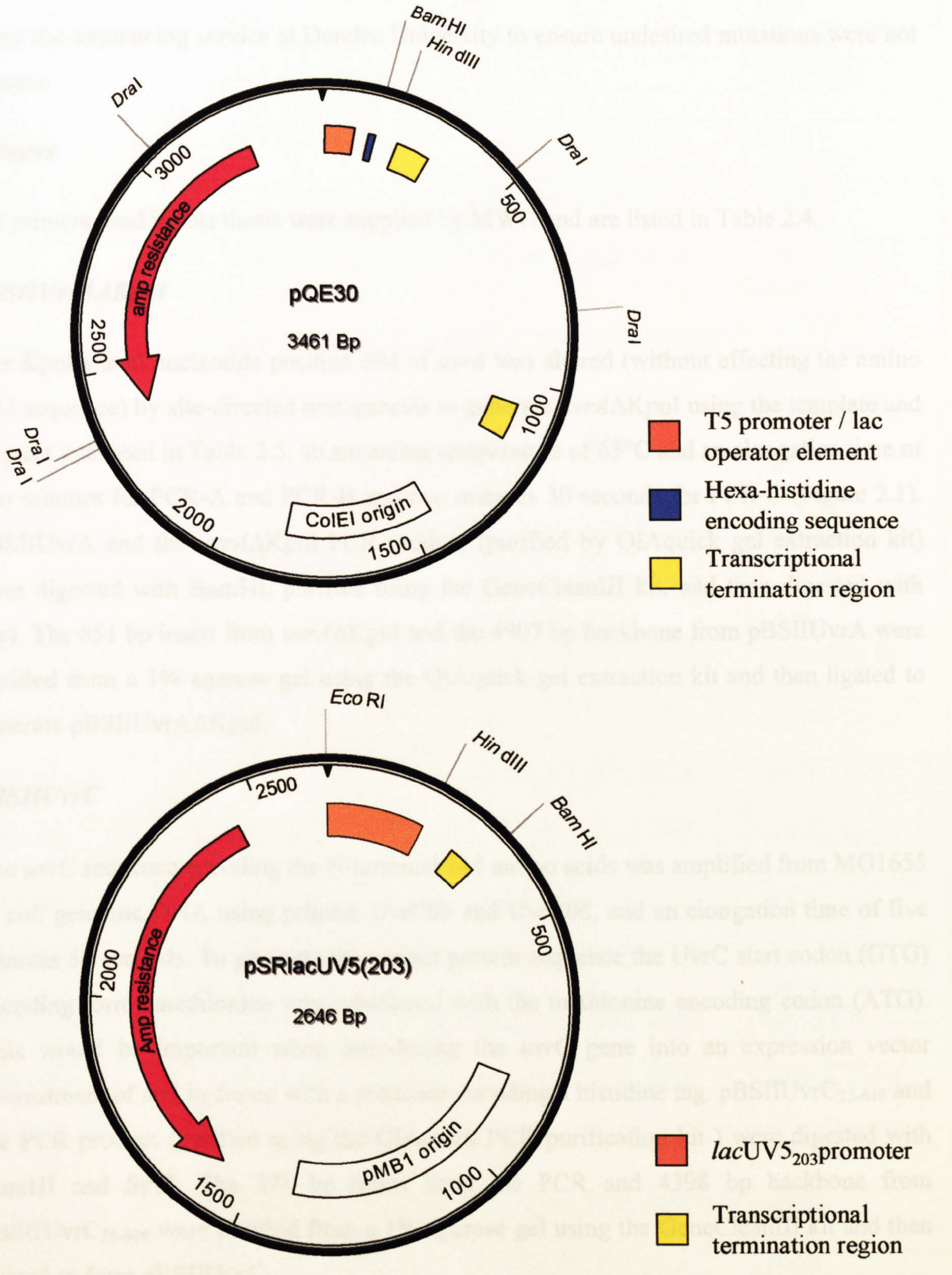

Figure 2.2 Plasmid Maps.

Plasmid maps are shown for pRA02, pRA03, pQE30 (Qiagen) and pSRlacUV5$_{203}$. These plasmids and derivatives of these plasmids are described in the text and Table 2.3. The pSRT7A1 plasmid map can be derived from the pSRlacUV5$_{203}$ plasmid map by exchanging the *lac*UV5$_{203}$ promoter with the T7A1 promoter.

or by the sequencing service at Dundee University to ensure undesired mutations were not present.

Primers

All primers used in this thesis were supplied by MWG and are listed in Table 2.4.

pBSIIUvrAΔKpnI

The KpnI site at nucleotide position 694 of *uvrA* was altered (without effecting the amino acid sequence) by site-directed mutagenesis to generate *uvrA*ΔKpnI using the template and primers indicated in Table 2.5, an annealing temperature of 63°C and an elongation time of two minutes for PCR-A and PCR-B and two minutes 30 seconds for PCR-C (Figure 2.1). pBSIIUvrA and the *uvrA*ΔKpnI PCR product (purified by QIAquick gel extraction kit) were digested with BamHI, purified using the GeneCleanIII kit, and then digested with StyI. The 851 bp insert from *uvrA*ΔKpnI and the 4907 bp backbone from pBSIIUvrA were purified from a 1% agarose gel using the QIAquick gel extraction kit and then ligated to generate pBSIIUvrAΔKpnI.

pBSIIUvrC

The *uvrC* sequence encoding the N-terminal 144 amino acids was amplified from MG1655 *E. coli* genomic DNA using primers UvrC05 and UvrC06, and an elongation time of five minutes 50 seconds. To generate the correct protein sequence the UvrC start codon (GTG) encoding formylmethionine was substituted with the methionine encoding codon (ATG). This would be important when introducing the *uvrC* gene into an expression vector downstream of and in-frame with a sequence encoding a histidine tag. pBSIIUvrC$_{23\text{-}610}$ and the PCR product (purified using the QIAquick PCR purification kit) were digested with BamHI and SphI. The 371 bp insert from the PCR and 4398 bp backbone from pBSIIUvrC$_{23\text{-}610}$ were purified from a 1% agarose gel using the GeneCleanIII kit and then ligated to form pBSIIUvrC.

pQE30UvrA, pQE30UvrB and pQE30UvrC

pQE30, pBSIIUvrA, pBSIIUvrB, and pBSIIUvrC, were digested with BamHI and HindIII. At the same time pBSIIUvrA was also digested with DraI (that cleaved the pBSII

Primer	Sequence	Use[1]
Bluescript1	TGA CCA TGA TTA CGC CAA GC	oSDM
Bluescript2	GCG CGT AAT ACG ACT CAC TA	EP, oSDM
D5431	ACC TGA CGT CTA AGA AAC C	PE
Mfd001F	GCC GCT CTA GAC ATG CCT GAA CAA TAT CGT	sPCR
Mfd219R	TTA TCG GTA CCT CGG TCG GAA ATT CGT GCG	sPCR
PL01	GGC CGC TCT AGA GTC CCG GGT ACC GTA AG	Annealing for plasmid construction
PL02	TCG ACT TAC GGT ACC CGG GAC TCT AGA GC	Annealing for plasmid construction
Prom2	TAG GCG TAT CAC GAG GCC CTT TGG	sPCR
pSRlacUV5_ BamHI	GAT CCC CGA CGA CGA CAT GG	PE, SL
RA0003-ann	CTC ATA CGA CGC TGT CGA TCC AGT CAC TGT CAT GCG CTA TCC GAT CCT AG	Annealing for EMSA
RA0004-FldT	CTA GGA TCG GAT AGC GCA TGA CAG TGA CTG GAT CGA CAG CGT CGT ATG AG	Annealing for EMSA
RA0005-con	CTA GGA TCG GAT AGC GCA TGA CAG TGA CTG GAT CGA CAG CGT CGT ATG AG	Annealing for EMSA
rpoA248R	CTA GGG TAC CTA GTC TAG AGC CTC TGG TTT CTC TTC TTT CAC	sPCR
UvrA001F	GCC GCT CTA GAT ATG GAT AAG ATC GAA GTT	sPCR
UvrA01	CGG GAT CCA TGG ATA AGA TCG AAG TTC GGG GC	oSDM, sPCR
UvrA06	TTA TCG GTA CCC AAC CAC CGG AAA GCT CCA G	sPCR,
UvrA07	TTA TCG GTA CCC AGG CGA AGT TGG CGG AGA A	EP, oSDM, sPCR
UvrA08	TTA TCG GTA CCC AGC AGG TCG GGC AGG CCC C	EP, sPCR
UvrA09	TTA TCG GTA CCC AAC CGT ACA ACA CCA CTT T	oSDM, sPCR
UvrA10	TTA TCG GTA CCC AAA ACT TGG CTA ATT CTT C	sPCR,
UvrA11	TTA TCG GTA CCC ACG CAC CAA TCT GGC TCG C	sPCR,
UvrA12	TTA TCG GTA CCC ACT CCA GCC CCT GAA TAT C	sPCR,
UvrA13	TTA TCG GTA CCC ACA GCA TCG GCT TAA GGA A	sPCR,
UvrA14	GGA GCT TTC CGG TGG TAC GGC GGT AGT GGC GG	SDM-UvrAΔKpnI
UvrA15	CCG CCA CTA CCG CCG TAC CAC CGG AAA GCT CC	SDM-UvrAΔKpnI

Primer	Sequence	Use[1]
UvrA17	GCC GCT CTA GAT ATG GAT AAG ATC GAA GTT C	EP, oSDM
UvrA18	GCT GTC GCA GCC GGT TGG CAA GCG TCT GAT G	SDM-$UvrA_{EV144}$
UvrA19	CAT CAG ACG CTT GCC AAC CGG CTG CGA CAG C	SDM-$UvrA_{EV144}$
UvrA20	GTC TGA TGC TAC ATG CGC CAA TCA TTA AAG	SDM-$UvrA_{LH151}$
UvrA21	CTT TAA TGA TTG GCG CAT GTA GCA TCA GAC	SDM-$UvrA_{LH151}$
UvrA22	CCG CCA CTA CCG CGG TAC CAC CGG AAA GCT CC	sPCR
UvrA23	CCC GCG ACA AGC TAT TTG TCG TGA CCG GGC	SDM-$UvrA_{IF027}$
UvrA24	GCC CGG TCA CGA CAA ATA GCT TGT CGC GGG	SDM-$UvrA_{IF027}$
UvrA25	CCT GGC AAG CCA GGA TTA CAT CCG TGC TCG	SDM-$UvrA_{GD173}$
UvrA26	CGA GCA CGG ATG TAA TCC TGG CTT GCC AGG	SDM-$UvrA_{GD173}$
UvrA27	GGC AAG CCA GGG CTG TAT CCG TGC TCG TAT TG	SDM-$UvrA_{YC174}$
UvrA28	CAA TAC GAG CAC GGA TAC AGC CCT GGC TTG CC	SDM-$UvrA_{YC174}$
UvrA29	GAA ACA TAC CAT TGT CGT GGT GGT TGA TCG	SDM-$UvrA_{EV201}$
UvrA30	CGA TCA ACC ACC ACG ACA ATG GTA TGT TTC	SDM-$UvrA_{EV201}$
UvrB035F	GCC GCT CTA GAA CAG ACG TTA CTT GGC GTG	oSDM, sPCR
UvrB08	GAC ATT GCA CTT GCC GTG GAA CTG TTT GAC	SDM-$UvrB_{RA213}$
UvrB09	GTC AAA CAG TTC CAC GGC AAG TGC AAT GTC	SDM-$UvrB_{RA213}$
UvrB10	GAGCTGCAATACGCTGAGAATGATCAAGCATTC	SDM-$UvrB_{RE183}$
UvrB11	GAATGCTTGATCATTCTCAGCGTATTGCAGCTC	SDM-$UvrB_{RE183}$
UvrB252R	TTA TCG GTA CCC GCG GTG TGA CGT AGT GC	oSDM, sPCR
UvrC05	AGT AGC GCC AGT GTT TCA CG	sPCR
UvrC06	CGG GAT CCA TGA GTG ATC AGT TTG AC	sPCR

Table 2.4 Primers.

The primers used in this thesis are listed. [1] Key for column is: EP, primer for error-prone PCR; oSDM, outer primer for site-directed mutagenesis; PE, primer for primer extension; SDM-, mutagenic primer for site-directed mutagenesis (with mutant indicated); SL, primer for sequencing ladders; sPCR, primer for standard PCR. [2] The bold T indicates that a fluorescein molecule is attached.

Mutation	Template	Primer 1	Primer 2	Primer 3	Primer 4
*uvrA*ΔKpnI[1]	pBSIIUvrA	UvrA01	UvrA15	UvrA14	UvrA09
$UvrA_{IF027}$[2]	pBSIIUvrAΔKpnI	UvrA17	UvrA24	UvrA23	UvrA07
$UvrA_{EV144}$[2]	pBSIIUvrAΔKpnI	UvrA17	UvrA19	UvrA18	UvrA07
$UvrA_{LH151}$[2]	pBSIIUvrAΔKpnI	UvrA17	UvrA21	UvrA20	UvrA07
$UvrA_{GD173}$[2]	pBSIIUvrAΔKpnI	UvrA17	UvrA26	UvrA25	UvrA07
$UvrA_{YC174}$[2]	pBSIIUvrAΔKpnI	UvrA17	UvrA28	UvrA27	UvrA07
$UvrA_{EV201}$[2]	pBSIIUvrAΔKpnI	UvrA17	UvrA30	UvrA29	UvrA07
$UvrB_{RE183}$[3]	pBSIIUvrB	Bluescript2	UvrB11	UvrB10	Bluescript1
$UvrB_{RE183}$[4]	pBSIIUvrB	UvrB035F	UvrB11	UvrB10	UvrB252R
$UvrB_{RA213}$[3]	pBSIIUvrB	Bluescript2	UvrB09	UvrB08	Bluescript1
$UvrB_{RA213}$[5]	$pUT18UvrB_{35\text{-}252}$	UvrB035F	UvrB09	UvrB08	UvrB252R

Table 2.5 Templates and primers used for site-directed mutagenesis.

Site-directed mutagenesis requires four primers to generate the mutant of interest as shown in Figure 2.1. Primers 2 and 3 are the mutagenic primers and 1 and 4 are the outer primers. PCR-A is carried out using primers 1 and 2 and PCR-B using primers 3 and 4. PCR-C uses primers 1 and 4 and the products of PCR-A and PCR-B to generate a full-length mutagenic PCR product. [1], [2], [3], [4] and [5] indicate that these mutants were generated to be cloned into pBSIIUvrA, $pRA02UvrA_{1\text{-}252}$, pQE30UvrB, $pRA03UvrB_{35\text{-}252}$ and $pUT18UvrB_{35\text{-}252}$ respectively.

backbone that was a similar size to the *uvrA* fragment). The 2827 bp insert from pBSIIUvrA, the 2026 bp insert from pBSIIUvrB, the 1838 bp insert from pBSIIUvrC and the 3419 bp backbone from pQE30 were purified from a 1% agarose gel using the GeneCleanIII kit and then ligated to form pQE30UvrA, pQE30UvrB and pQE30UvrC.

pUT18UvrA$_{1-n}$, pUT18UvrB$_{35-252}$ and pUT18Mfd$_{1-219}$

PCR was used to introduce restriction sites at the ends of various truncations of *uvrA*, *uvrB* and *mfd* using the conditions indicated in Table 2.6. pUT18 and the purified PCR products (purified using the GeneCleanIII kit) were digested with XbaI, purified using the GeneCleanIII kit and then digested with KpnI. pUT18 was then dephosphorylated. The 3008 bp backbone from pUT18 and the various inserts (sizes indicated in Table 2.6) were purified from a 1% agarose gel using the GeneCleanIII kit and then ligated to form pUT18UvrA$_{1-n}$, pUT18UvrB$_{35-252}$ and pUT18Mfd$_{1-219}$.

pREIIαΔXbaI

pREIIα was digested with XbaI, the 5′ overhangs blunt ended and then ligated to form pREIIαΔXbaI.

pRA02

The promoter and 5′ region of *rpoA* was amplified from pREIIαΔXbaI using primers Prom2 and rpoA248R and an elongation time of seven minutes. The PCR product was purified using the GeneCleanIII kit and then phosphorylated. pSRlacUV5$_{203}$ was digested with EcoRI and HindIII, the 5′ overhangs blunt ended and then dephosphorylated. The 2547 bp backbone from pSRlacUV5$_{203}$ and the 1146 bp insert from the PCR were purified from a 1% agarose gel using the GeneCleanIII kit and then ligated to generate pRA02.

pBRcIωXK

Primers PL01 and PL02 were annealed forming double stranded DNA containing internal XbaI and KpnI sites with ends complementary to NotI and SalI digested DNA. pBRcIω was digested with NotI and SalI and the 4524 bp backbone purified from a 1% agarose gel using the QIAquick gel extraction kit. The backbone and the annealed primers were ligated to form pBRcIωXK.

Protein	Amino acid residues	Template	Forward primer	Reverse primer	Annealing temp (°C)	Extension time	Insert size (bp)[1]	Plasmid size (bp)[2]
UvrA	1-230	pBSIIUvrA	UvrA001F	UvrA06	60	2 min 26 sec	699	3707
UvrA	1-252	pBSIIUvrAΔKpnI	UvrA001F	UvrA07	60	4 min 52 sec	765	3773
UvrA	1-280	pBSIIUvrAΔKpnI	UvrA001F	UvrA08	60	4 min 52 sec	849	3857
UvrA	1-350	pBSIIUvrAΔKpnI	UvrA001F	UvrA09	60	4 min 52 sec	1059	4067
UvrA	1-400	pBSIIUvrAΔKpnI	UvrA001F	UvrA10	55	5 min 41 sec	1209	4217
UvrA	1-503	pBSIIUvrAΔKpnI	UvrA001F	UvrA11	60	11 min 23 sec	1518	4526
UvrA	1-680	pBSIIUvrAΔKpnI	UvrA001F	UvrA12	55	5 min 41 sec	2049	5057
UvrA	1-940	pBSIIUvrAΔKpnI	UvrA001F	UvrA13	55	5 min 41 sec	2829	5837
UvrB	35-252	pBSIIUvrB	UvrB035F	UvrB252R	60	2 min	663	3671
Mfd	1-219	pETMfd	Mfd001F	Mfd219R	60	2 min	666	3674

Table 2.6 Information for construction of pUT18 derivatives.
The PCR conditions to generate *uvrA*, *uvrB* and *mfd* truncations are indicated. [1] The insert size is the size of the PCR product once digested with XbaI and KpnI. [2] The plasmid size is given for pUT18 with the coding sequence for the region of UvrA, UvrB or Mfd (indicated at the left) inserted.

pRA03

pBRcIωXK and pACYC184 were digested with EcoRI and XbaI respectively. The 5′ overhangs were blunt ended, the DNA purified using the GeneCleanIII kit and then digested with SalI. The 3527 bp backbone from pACYC184 and the 844 bp insert from pBRcIωXK were purified from a 1% agarose gel using the QIAquick gel extraction kit and then ligated to form pRA03. Sequence analysis indicated that the generation of pACYC184 blunt ends did not go to completion with the final G of the TCTAG sequence not being present, thus instead of TCTAGAATTC the sequence TCTAAATTC is present at the XbaI/EcoRI join.

pRA02UvrA$_{1-n}$

pRA02 and pUT18UvrA$_{1-n}$ were digested with XbaI, the DNA was purified using the GeneCleanIII kit and then digested with KpnI. The 3592 bp backbone from pRA02 and inserts from pUT18UvrA$_{1-n}$ (see Table 2.6 for sizes) were purified from a 1% agarose gel using the QIAquick gel extraction kit and then ligated to form pRA02UvrA$_{1-n}$.

pRA03UvrB$_{35-252}$ and pRA03Mfd$_{1-219}$

pRA03, pUT18UvrB$_{35-252}$ and pUT18Mfd$_{1-219}$ were digested with XbaI, the DNA was purified using the GeneCleanIII kit and then digested with KpnI. The 4359 bp backbone from pRA03 and inserts from pUT18UvrB$_{35-252}$ and pUT18Mfd$_{1-219}$ (see Table 2.6 for sizes) were purified from a 1% agarose gel using the QIAquick gel extraction kit and then ligated to form pRA03UvrB$_{35-252}$ and pRA03Mfd$_{1-219}$.

pRA02UvrA$_{1-252.mutants}$

Error-prone PCR was carried out to amplify and randomly mutate the first 756 nucleotides of *uvrA* (corresponding to the N-terminal 252 amino acids), using pBSIIUvrAΔKpnI as template and UvrA17 and UvrA07 as primers. Alternatively specific mutants were generated by site-directed mutagenesis using the template and primers indicated in Table 2.5. pRA02UvrA$_{1-252}$ and the PCR products (purified using the GeneCleanIII kit) were digested with XbaI, the DNA purified using the GeneCleanIII kit and then digested with KpnI. pRA02UvrA$_{1-252}$ was then dephosphorylated. The 3592 bp backbone from pRA02UvrA$_{1-252}$ and the 765 bp insert from the PCR products were purified from a 1%

agarose gel using the QIAquick gel extraction kit and then ligated to create pRA02UvrA$_{1\text{-}252.mutations}$. Single UvrA mutants VE202 and DG205, and double UvrA mutants indicated in chapter 3 were generated by error-prone PCR. Single UvrA mutants IF027, EV144, LH151, GD173, YC174 and DG205 were generated by site-directed mutagenesis.

pUT18UvrB$_{35\text{-}252.RA213}$

The sequence coding for UvrB$_{35\text{-}252.RA213}$ was generated by site-directed mutagenesis using the template and primers indicated in Table 2.5. pUT18UvrB$_{35\text{-}252}$ and the PCR product (purified using the GeneCleanIII kit) were digested with XbaI, the DNA purified using the GeneCleanIII kit and digested with KpnI. pUT18UvrB$_{35\text{-}252}$ was then dephosphorylated. The 3008 bp backbone from pUT18UvrB$_{35\text{-}252}$ and the 663 bp insert from the PCR were purified from a 1% agarose gel using the QIAquick gel extraction kit and then ligated to create pUT18UvrB$_{35\text{-}252.RA213}$.

pRA03UvrB$_{35\text{-}252.RE183}$ and pRA03UvrB$_{35\text{-}252.RA213}$

The sequence coding for UvrB$_{35\text{-}252.RE183}$ was generated by site-directed mutagenesis using the template and primers indicated in Table 2.5. pRA03UvrB$_{35\text{-}252}$, the PCR product (purified using the GeneCleanIII kit) and pUT18UvrB$_{35\text{-}252.RA213}$ were digested with XbaI, the DNA purified using the GeneCleanIII kit and digested with KpnI. pRA03UvrB$_{35\text{-}252}$ was then dephosphorylated. The 4359 bp backbone from pRA03UvrB$_{35\text{-}252}$ and the 663 bp insert from both the PCR and pUT18UvrB$_{35\text{-}252.RA213}$ were purified from a 1% agarose gel using the QIAquick gel extraction kit and then ligated to form pRA03UvrB$_{35\text{-}252.RE183}$ and pRA03UvrB$_{35\text{-}252.RA213}$.

pQE30UvrA$_{mutants}$

Error-prone PCR was carried out to amplify and randomly mutate the first 690 nucleotides of *uvrA* (corresponding to the N-terminal 230 amino acids), using pBSIIUvrA as template, Bluescript2 and UvrA08 as primers and an annealing temperature of 55°C. Alternatively standard PCR was carried out using pRA02UvrA$_{1\text{-}252}$ that contained the desired mutation, UvrA01 and UvrA22 as primers and an annealing temperature of 55°C. pQE30UvrA and the PCR products (purified using the QIAquick PCR purification kit) were digested with BamHI, the DNA purified using the QIAquick PCR purification kit and digested with

KpnI. pQE30UvrA was then dephosphorylated. The 5553 bp backbone from pQE30UvrA and the 693 bp inserts from the PCR products were purified from a 1% agarose gel using the QIAquick gel extraction kit and ligated to form pQE30UvrA$_{mutants}$. Single UvrA mutants RL023, GS034, SA038, SP038, FI064, FS064. LQ065, VD073, SY080, QL087, GR099, CR120, LP151 and KE159 were generated by error-prone PCR and LH151, GD173, YC174, EV201, VE202 and DG205 were generated by standard PCR.

pQE30UvrB$_{RE183}$ and pQE30UvrB$_{RA213}$

UvrB single mutants were generated by site-directed mutagenesis using the template and primers indicated in Table 2.5 and the Phu DNA polymerase PCR protocol with an elongation time of 25 seconds for PCR-A and PCR-B and 35 seconds for PCR-C (Figure 2.1). pQE30UvrB and the PCR product (purified using the QIAquick PCR purification kit) were digested with BamHI and HindIII. pQE30UvrB was then dephosphorylated. The 3419 bp backbone from pQE30UvrB and the 2026 bp insert from the PCR products were purified from a 1% agarose gel using the QIAquick gel extraction kit and then ligated to form pQE30UvrB$_{mutations}$. Single UvrB mutants RE183 and RA213 were generated in this way.

Preparation of DNA fragments for incision assays

pSRlacUV5$_{203}$ EcoRI/BamHI fragment to be ^{32}P labelled at the 5' BamHI end

The 347 bp pSRlacUV5$_{203}$ EcoRI/BamHI fragment to be ^{32}P labelled at the 5′ BamHI end was generated from a CsCl maxiprep preparation of pSRlacUV5$_{203}$. A preparative 100 µl digest contained 25 µg of pSRlacUV5$_{203}$ and 25 U BamHI in the supplied buffer. The digested DNA was dephosphorylated, purified by phenol chloroform extraction and ethanol precipitation and digested with 25 U EcoRI in a 50 µl preparative digestion reaction. 6 x DNA loading dye and 100 x SYBR green were added to a final concentration of 1 x and 10 x respectively. The DNA was run on a 7.5% acrylamide gel, visualised on a dark reader and the 347 bp fragment excised. The gel slice was placed in 12-14 kDa MWCO dialysis tubing and the DNA extracted by electroelution at 40 mA for 45 minutes in 0.1 x TBE buffer. The DNA was purified by phenol chloroform extraction and ethanol precipitation. Samples of fragment and DNA ladders of known concentrations were run on a 7.5% acrylamide gel and the DNA concentration quantified using Kodak imaging software. The fragment was subsequently ready for ^{32}P labelling at the 5′ BamHI end.

pSRT7A1 EcoRI/BamHI fragment to be ^{32}P labelled at the 5' BamHI end

The 268 bp pSRT7A1 EcoRI/BamHI fragment to be ^{32}P labelled at the 5′ BamHI end was generated from a Qiagen maxiprep preparation of pSRT7A1 purified by Dr. N. Savery from the *dam*$^{+}$ *E. coli* strain XL1-Blue. A preparative BamHI digest was carried out and the DNA purified by phenol chloroform ethanol precipitation before some was internally biotinylated by a member of the Prof. E. Weinhold laboratory (Pljevaljcic *et al.*, 2004). The biotinylated and unmodified DNA were dephosphorylated, purified by phenol chloroform extraction and ethanol precipitation, digested with EcoRI and purified by phenol chloroform extraction and ethanol precipitation. The DNA was subsequently ready for ^{32}P labelling at the 5′ BamHI end of both the 268 bp and the 2300 bp fragments.

^{32}P DNA ladders

^{32}P DNA ladders for urea sequencing gels were generated using a T7 sequencing kit (USB). Template DNA was denatured as follows: 2 µg of DNA was suspended in 30 µl TE buffer, 3 µl 2 M NaOH was added, the reaction incubated at room temperature for 15 minutes, 3 µl 5 M NH_4Ac (pH 4.8) and 75 µl ethanol were added and the reaction incubated at -20°C for 15 minutes. The DNA was centrifuged at 16110 g, 4°C for 15 minutes and the pellet washed in 1 ml 70% ethanol. The pellet was air-dried and suspended in 10 µl H_2O. The annealing, labelling and termination reactions were carried out according to the manufacturer's protocol using the components of the T7 sequencing kit and [$\alpha^{32}P$] dATP (Amersham). Ladders of pSRT7A1 and pSRlacUV5$_{203}$ were generated in this way using primer pSRlacUV5_BamHI.

Screening protocols

Bacterial two-hybrid screening procedures to identify UvrA mutants

One-step screen

pRA02UvrA$_{1\text{-}252.mutants}$ were generated as described above using five cycles of error-prone PCR. Electrocompetent KS1 cells that contained either pRA03UvrB$_{35\text{-}252}$ or pRA03Mfd$_{1\text{-}219}$ were transformed with the ligation mixtures. The transformation mixtures were spread onto LB indicator plates (LB agar supplemented with 100 µg/ml ampicillin, 50 µg/ml kanamycin, 25 µg/ml chloramphenicol, 1 mM IPTG and 80 µg/ml X-gal) and

incubated at 30°C for 20 hours and then at room temperature for 24 hours. Colonies that appeared white were streaked to single colonies on LB X-gal indicator plates. From this plate a single white colony was used to inoculate 5 ml LB broth containing the above antibiotics. The cells were incubated at 37°C overnight and then the plasmid DNA extracted. The section of plasmid that had originally been amplified by error-prone PCR was sequenced.

Modification to one-step screen

The one-step screen protocol was used but this time one, two, three, four, or five cycles of error-prone PCR was used. KS1 cells that contained pRA03Mfd$_{1\text{-}219}$ were then transformed with the subsequent ligations.

Two-step screen

The two-step screening protocol started in the same way as the modified one-step screen except that only one or two cycles of error-prone PCR were used. In this protocol the 5 ml overnight cultures (of white colonies) were pooled in groups of 10. DNA was extracted from 3 ml of the pooled culture and then digested with NheI to cleave the pRA03Mfd$_{1\text{-}219}$ plasmid. KS1 cells that contained pRA03UvrB$_{35\text{-}252}$ were then transformed with the DNA mix. Colonies that appeared blue were streaked to single colonies on LB X-gal indicator plates. From this place a single blue colony was then used to inoculate 5 ml LB broth containing the above antibiotics. The cells were incubated at 37°C overnight and then the plasmid DNA extracted. The DNA was digested with NheI to destroy pRA03UvrB$_{35\text{-}252}$. KS1 cells containing pRA03UvrB$_{35\text{-}252}$ or pRA03Mfd$_{1\text{-}219}$ were then transformed with the DNA mix to confirm phenotype. If the phenotype was correct (i.e. KS1 colonies expressing λcIMfd$_{1\text{-}219}$ and the α fusion protein were white and KS1 colonies expressing λcIUvrB$_{35\text{-}252}$ and the α fusion protein were blue) the section of plasmid that had originally been amplified by error-prone PCR was sequenced.

Isolation of pRA02UvrA derivatives from the bacterial two-hybrid screen

From the screening procedures DNA preparations contained two plasmids. One was pRA02UvrA$_{1\text{-}252.mutant}$ and the other was either pRA03UvrB$_{35\text{-}252}$ or pRA03Mfd$_{1\text{-}219}$. The DNA was treated with NheI to cleave derivatives of pRA03. XL1-Blue cells were transformed with the DNA and spread onto LB agar plates supplemented with ampicillin

and tetracycline. Single colonies were used to inoculate 5 ml of LB broth containing the above antibiotics which were incubated at 37°C overnight. The DNA was extracted generating a pure pRA02UvrA$_{1\text{-}252.mutant}$ preparation.

UV sensitivity screen

Libraries of pQE30UvrA$_{mutants}$ were generated using error-prone PCR as described above. Electrocompetent MG1655Δ*uvrA* cells were transformed with the ligation mix and spread onto LB agar plates supplemented with ampicillin, kanamycin and tetracycline. The plates were incubated at 30°C for approximately 16 hours. Type 1 filter paper (two sheets 70 mm and two sheets 110 mm diameter) (Whatman) covering a replica plater was used to transfer colonies from the overnight plates onto two fresh LB plates containing the same antibiotics. The first replica plate was irradiated for 10 seconds at 2 J/m^2/s using a UVLS-28 254 nm lamp (UVP) to give a final dose of 20 J/m^2 254 nm UV light. The second replica was left unirradiated. Both replica plates were incubated at 30°C for 16 hours. Colonies from the unirradiated control plate that had not grown on the irradiated plate were streaked onto LB agar plates containing the above antibiotics and incubated at 30°C for approximately 16 hours. Single colonies were used to inoculate 10 ml LB broth containing the above antibiotics which were then incubated overnight at 37°C. A sample was centrifuged (equivalent to 100 / A_{600} µl) and the pellet suspended in 20 µl SDS PAGE loading dye and heated to 95°C for five minutes. Samples (5 µl) were resolved on 10% SDS PAGE gels alongside cells containing pQE30UvrA and pQE30 that would and would not express full-length UvrA. 3 ml of each overnight culture that expressed full-length UvrA protein was harvested and the plasmid DNA extracted.

To confirm the UV sensitivity phenotype a UV sensitivity assay was used. LB broth (5 ml) containing 100 µg/ml ampicillin and 50 µg/ml kanamycin was inoculated with MG1655Δ*uvrA* cells transformed with the purified pQE30UvrA derivative (or pQE30 and pQE30UvrA as controls). The cells were incubated at 37°C for 16 to 18 hours and then diluted to an A_{600} of 0.0625 in LB broth (10 ml) containing the above antibiotics. The cells were incubated at 37°C until an A_{600} of at least 0.4 was reached and then placed on ice. Cells (2.5 / A_{600} ml) were centrifuged at 2770 g at 4°C for 10 minutes and the pellet suspended in 5 ml M9 buffer to give approximately 5 x 10^8 *E. coli* cells/ml. A 1 ml sample of each culture was placed in one well of a six well plate and irradiated for 30 seconds at 2 J/m^2/s to give a final dose of 60 J/m^2 254 nM UV light. The cells (irradiated and

unirradiated) were subjected to five 10-fold serial dilutions in M9 broth. 2 µl samples of each diluted irradiated and unirradiated culture were spotted onto LB agar plates containing the above antibiotics and incubated at 30°C overnight. If the UV sensitivity phenotype was confirmed the plasmid DNA was sequenced.

Protein purification and protein detection

UvrA, UvrB and UvrC protein purification

Wild-type and mutant UvrA proteins (A) were purified from MG1655Δ*uvrA* cells transformed with the appropriate pQE30UvrA derivative. Wild-type and mutant UvrB proteins (B) were purified from XL1-Blue cells transformed with the appropriate pQE30UvrB derivative. UvrC (C) was purified from XL1-Blue cells transformed with pQE30UvrC. 100 ml of LB broth was supplemented with 100 µg/ml ampicillin (A, B, C) and 50 µg/ml kanamycin (A) or 25 µg/ml tetracycline (B, C) and was inoculated with a single colony and incubated at 37°C for 16 hours. The cells were harvested by centrifugation at 2770 g (A, B) or 4657 g (C) at 4°C for 10 minutes, the pellet suspended in 20 ml of wash buffer containing 10 mg of lysozyme and then incubated on ice for 30 minutes. The cells were lysed on ice by three 15 second bursts of sonication. 15 ml of wash buffer was added and the cells centrifuged at 38724 g at 4°C for 30 minutes. The supernatant was passed through a 0.45 µm filter (Millipore) and wash buffer was added to a total volume of 50 ml. The protein of interest was purified from the lysate using a 1 ml, $NiSO_4$ charged, HiTrap chelating column (Amersham) on an ÄKTA FPLC (Amersham). The protein was eluted from the column using a 20 to 500 mM imidazole gradient generated from the wash and elution buffers. Fractions containing only the protein of interest were dialysed at 4°C overnight in 1 L of dialysis buffer and then for four hours in 1 L of storage buffer.

Mfd protein purification

Mfd was a gift from Dr. A. Smith who purified it as described by Chambers *et al.* (Chambers *et al.*, 2003).

Protein concentration

The concentration of UvrA, UvrB, UvrC and Mfd was determined using the Bio-Rad protein assay following the manufactures microassay protocol. BSA (0, 1, 2, 4, 6 and 8 μg) (Pierce) was used as a standard. Proteins were analysed on a 10% SDS PAGE gel to confirm relative concentration and purity.

Western blotting

Proteins from cell lysates of the bacterial two-hybrid samples of interest were resolved on a 10% SDS PAGE gel. The stacking gel was removed and the resolving gel was soaked in transfer buffer for 15 minutes. Immobilon-P PVDF membrane (Millipore) was soaked in methanol for 30 seconds, water for two minutes and transfer buffer for five minutes. The blotting apparatus (mini trans-blot cell) were assembled according to the manufactures instructions (Bio-Rad). The transfer took place at 100 V (250 mA) for one hour. The membrane was placed in methanol then dried on filter paper for 15 minutes. The membrane was placed in blocking buffer overnight and then washed in 1 x PBS for two 15 minutes periods. The membrane was rewetted in methanol and was probed with a rabbit polyclonal anti-RNAPα subunit primary antibody (a gift from Prof. A. Ishihama) in 10 ml of blocking buffer for two hours and then five washes of five minutes in PBS tween took place. The membrane was probed with 5 μl HRP conjugated anti-rabbit IgG secondary antibody (Santa Cruz) in 10 ml of blocking buffer for one hour. The membrane was washed for five times five minutes in PBS tween followed by a final five minute wash in 1 x PBS. The membrane was then developed using the POD chemilluminescence system (Roche) following the manufactures protocol and the film exposed in the Curix60 (AGFA) machine.

In vivo assays

β-galactosidase assays

β-galactosidase assays were carried out essentially as described by Miller (Miller, 1972). LB broth (10 ml) containing 50 μg/ml kanamycin, 100 μg/ml ampicillin and 25 μg/ml chloramphenicol was inoculated with KSI cells transformed with a pRA02 derivative and a pRA03 derivative. The cultures were incubated at 30°C for 16 to 18 hours and then diluted to an A_{600} of 0.007 in fresh LB broth (10 ml) containing the above antibiotics and 1 mM

IPTG. The cultures were incubated at 30°C until they reached an A_{600} of approximately 0.35 and then placed on ice. 100 µl of each culture were transferred into two tubes containing 900 µl Z buffer and 30 µl chloroform (Fisher) (as a control 100 µl Z buffer was added instead of culture). The tubes were vortexed for 10 seconds and incubated for 15 minutes at 30°C before 200 µl of 4 mg/ml ONPG in Z buffer was added to each tube. The reactions were incubated for two hours at 30°C and stopped by the addition of 500 µl 1 M Na_2CO_3 (Fisher) and vortexed for five seconds. The A_{420} and A_{550} were measured and specific β-galactosidase activity determined using the formula: Activity (Miller Units) = $1000 \times ((A_{420} - (1.75 \times A_{550})) / (12 \times A_{600}))$. Assays were carried out in triplicate and averages and standard deviations calculated.

UV survival assay

LB broth (5 ml) containing 100 µg/ml ampicillin and 50 µg/ml kanamycin was inoculated with MG1655Δ*uvrA* cells transformed with a pQE30UvrA derivative (or pQE30 as a control). The cells were incubated at 30°C for 16 to 18 hours and then 200 µl transferred into 10 ml LB broth containing the above antibiotics. The cells were incubated at 37°C until an A_{600} of at least 0.5 was reached and then placed on ice. Cells ($0.5/A_{600}$ ml) were centrifuged at 16110 g for one minute and the pellet suspended in 1 ml M9 broth. The cells were 10-fold serial diluted five times in M9 broth. 2 µl of each diluted culture were spotted onto 21 LB agar plates containing the above antibiotics. The 21 plates were split into seven groups of three. The seven groups were irradiated for 0, 10, 20, 30, 40, 50 and 60 seconds at 0.4 $J/m^2/s$ to give a final dose of 0, 4, 8, 12, 16, 20 and 24 J/m^2 254 nm UV light respectively. The plates were incubated at 30°C for 16 hours. UV survival was calculated by counting the number of colonies within the most diluted viable spot and multiplying this number by its dilution factor. The three values within each group were then averaged. The assays were carried out in triplicate with an average of averages taken and standard deviation calculated.

In vitro assays

Nucleotide hydrolysis assays

Nucleotide hydrolysis assays were carried out in a final volume of 200 µl. A 170 µl cocktail of phosphoenolpyruvate (PEP), nicotinamide adenine dinucleotide (NADH),

pyruvate kinase / lactate dehydrogenase (PK/LDH) and repair buffer was prepared. A 20 µl cocktail of UvrA, UvrB, and Mfd in 1 x storage buffer was added. Reactions were incubated at 37°C for five minutes before 10 µl ATP or GTP was added. The final component concentrations were 500 µM PEP, 400 µM NADH, 4.2 U PK, 4.8 U LDH, 1 x repair buffer, 0.1 x storage buffer and the indicated concentrations of UvrA, UvrB, Mfd, ATP and GTP (see chapter 5). Reactions were incubated at 37°C in a 96 well plate spectrometer (Versamax) and A_{340} readings taken every 15 seconds for one hour. Reaction rates were determined by taking the steepest gradient, generally over 120 data points (30 minutes) after the first five minutes of the reaction using SOFTmax PRO software. The reactions were carried out in triplicate. A plot of the average rates against NTP concentration allowed V_{max} and K_m values to be determined using GraFit software.

EMSAs

DNA binding by UvrA

EMSAs to determine DNA binding by $UvrA_{(mutants)}$ were carried out in a final volume of 10 µl. An 8 µl cocktail of $\gamma^{32}P$ labelled DNA, ATPγS and repair buffer was prepared and incubated at 37°C for five minutes before 2 µl $UvrA_{(mutant)}$ in 1 x storage buffer was added. The final component concentrations were 1 nM $\gamma^{32}P$ labelled DNA, 1 mM ATPγS, 0.8 x repair buffer, 0.2 x storage buffer and the indicated concentration of UvrA (see chapter 5). Reactions were incubated at 37°C for 30 minutes and then 8 µl loaded onto a 6% acrylamide gel. Each assay was performed at least twice.

DNA binding by UvrA and UvrB

EMSAs to determine DNA binding by a mixture of $UvrA_{(mutants)}$ and UvrB were carried out in a final volume of 10 µl. A 7 µl cocktail contained ATPγS and repair buffer. 1 µl of $UvrA_{(mutant)}$ and 1 µl of UvrB were added and the reaction incubated at 37°C for 15 minutes. 1 µl of $\gamma^{32}P$ labelled DNA was then added. The final component concentrations were 1 mM ATPγS, 0.8 x repair buffer, 0.2 x storage buffer, 1 nM $\gamma^{32}P$ labelled DNA and the indicated concentration of UvrA and UvrB (see chapter 5). Reactions were incubated at 37°C for 15 minutes and then 8 µl loaded onto a 6% acrylamide gel. Each assay was performed at least twice.

Biotin modified DNA binding by streptavidin

EMSAs to confirm the biotinylation of DNA were carried out in a final volume of 10 µl. A 9 µl cocktail contained biotinylated DNA, BSA and transcription buffer. The reactions were preincubated at 37°C for two minutes before the addition of 1 µl of streptavidin in transcription buffer (a gift from Dr. M. Dillingham). The final component concentrations were 0.25 nM biotinylated DNA, 0.1 mg/ml BSA, 1 x transcription buffer and the indicated concentration of streptavidin tetramer (see chapter 4). The reactions were incubated at 37°C for 10 minutes before 2 µl of 6 x loading dye was added. The reactions were loaded onto a 6% acrylamide gel.

DNA irradiation

For DNA irradiation 100 nM pSRlacUV5$_{203}$ was placed in 10 µl spots and irradiated for 75 seconds at 0.4 J/m^2/s to give a final dose of 30 J/m^2 254 nm UV light. Alternatively 8 nM of the pSRlacUV5$_{203}$ BamHI/EcoRI fragment was placed in 10 µl spots and irradiated for 75 seconds at 4 J/m^2/s to give a final dose of 300 J/m^2 254 nm UV light.

Incision assays

Incision of UV damaged plasmid DNA

Incision assays were carried out in a final volume of 10 µl. A 6 µl cocktail contained pSRlacUV5$_{203}$ (that had or had not been irradiated) and repair buffer. A 3 µl cocktail of UvrA, UvrB and UvrC in storage buffer was added and the reactions incubated at 37°C for five minutes before the addition of 1 µl ATP. The final component concentrations were 5.73 nM pSRlacUV5$_{203}$, 1 x repair buffer, 0.3 x storage buffer, 100 nM UvrA, 100 nM UvrB, 200 nM UvrC and 1 mM ATP. The reactions were incubated at 37°C for 30 minutes before the addition of 5 µl of STEB stop buffer and a further incubation at 67°C for 20 minutes. The samples were resolved on a 1% agarose gel. As a control a 10 µl reaction containing 2 U of T4EV (Epicentre), 5.73 nM pSRlacUV5$_{203}$ and 1 x repair buffer was incubated at 37°C for 30 minutes before the addition of STEB stop buffer.

Assay to determine UvrABC 5' incision activity

To determine the specific UvrABC 5′ incision site in relation to a biotin adduct a different incision assay was used. These incision assays were carried out in a final volume of 10 µl.

The reaction contained 0.25 nM γ^{32}P labelled DNA, 0.8 x repair buffer, 0.3 x storage buffer, 100 nM $UvrA_{(mutant)}$, 100 nM $UvrB_{(mutant)}$, 200 nM UvrC and 1 mM ATP where present. As a control the DNA was digested with HindIII or mock treated without enzymes and/or ATP. The reactions were incubated at 37°C for 30 minutes. The DNA was purified by phenol chloroform extraction and ethanol precipitation and suspended in 5 µl of water and 5 µl formamide stop solution, incubated at 95°C for five minutes, centrifuged briefly and loaded onto a denaturing 6% acrylamide gel.

Assay to determine UvrABC 3' incision activity

To determine the specific UvrABC 3′ incision site in relation to a biotin adduct the DNA was first incubated with UvrABC and then used as the template for primer extension reactions. Nicking reactions were carried out in a final volume of 10 µl and contained 1.025 nM DNA, 0.8 x repair buffer, 0.2 x storage buffer, 100 nM UvrA, 100 nM UvrB, 200 nM UvrC and 1 mM ATP. The reaction was incubated at 37°C for 15 minutes before an additional 1 µl of 10 mM ATP was added (making the reaction 11 µl) for a further 15 minute incubation. As a control the DNA was digested with HindIII or mock treated without enzymes. The DNA was purified by phenol chloroform extraction and ethanol precipitation and suspended in 8.2 µl of water to make a final DNA concentration of 1.25 nM.

Primer extension reactions were carried out in a final volume of 20 µl and contained 0.25 nM DNA (4 µl of the above DNA), 0.5 mM dNTPs, 1.5 mM $MgCl_2$, 5 µM ^{32}P labelled primer and 2.5 U Taq DNA polymerase in the supplied buffer. The reactions were incubated at 95°C for five minutes, 55°C for 30 seconds and 72°C for 10 minutes. The DNA was then purified by phenol chloroform extraction and ethanol precipitation and suspended in 5 µl H_2O and 5 µl formamide stop solution, incubated at 95°C for five minutes, centrifuged briefly and loaded onto a denaturing 6% acrylamide gel.

CHAPTER 3

IDENTIFICATION OF UvrA MUTANT PROTEINS

Introduction

In NER UvrA acts as a molecular matchmaker, scanning the DNA for damage and then loading UvrB directly onto the damaged DNA (Sancar and Hearst, 1993). In TCR UvrA is proposed to be recruited to the damage site through interactions it makes with Mfd (Selby and Sancar, 1995a). UvrA then loads UvrB onto the DNA as part of the NER process. At the start of this work there was very little information available about how UvrA interacts with UvrB and Mfd. No amino acid residues had been identified that were specifically involved in either the UvrA-UvrB or the UvrA-Mfd interaction. It was therefore of interest to identify residues of UvrA that are important for the UvrA-UvrB and the UvrA-Mfd interaction.

Two approaches were taken to identify amino acid residues of UvrA that are involved in interacting with UvrB and/or Mfd. The first approach was based on a bacterial two-hybrid system. This system was used to specifically identify mutants of UvrA that were unable to interact with UvrB or Mfd within the bacterial two-hybrid context. The second approach was based on the UV sensitivity phenotype of Δ*uvrA* cells. This system would identify a variety of physiologically relevant UvrA mutants. However the mutants could be deficient in any property of UvrA that was essential for the UV resistant phenotype of *uvrA*$^{+}$ cells.

Lambda cI RNAP bacterial two-hybrid screen

The main aim of this work was to identify UvrA residues that are important for the interaction of UvrA with UvrB and Mfd. A bacterial two-hybrid system in which truncated versions of the wild-type proteins interacted to show a detectable phenotype was used to screen libraries of UvrA mutants to identify these residues. The system required protein-protein contact between the proteins of interest in order to give enhanced transcriptional activation of a reporter gene (Figure 3.1) (Dove *et al.*, 1997). The system was designed to enhance transcription of an artificially introduced chromosomal copy of *lacZ* on protein-protein contact (Dove *et al.*, 1997). Upstream of *lacZ* in KS1 cells there is a *plac*O_R2-62 promoter that is a derivative of the *lac* promoter with a λcI operator site (O_R2) centred at position -62 from the transcriptional start site (Figure 3.1A) (Dove *et al.*, 1997). As with the yeast two-hybrid system (Fields and Song, 1989) there were two partners: λcI and the NTD (residues 1-248) of the RNAP α subunit (that will be referred to

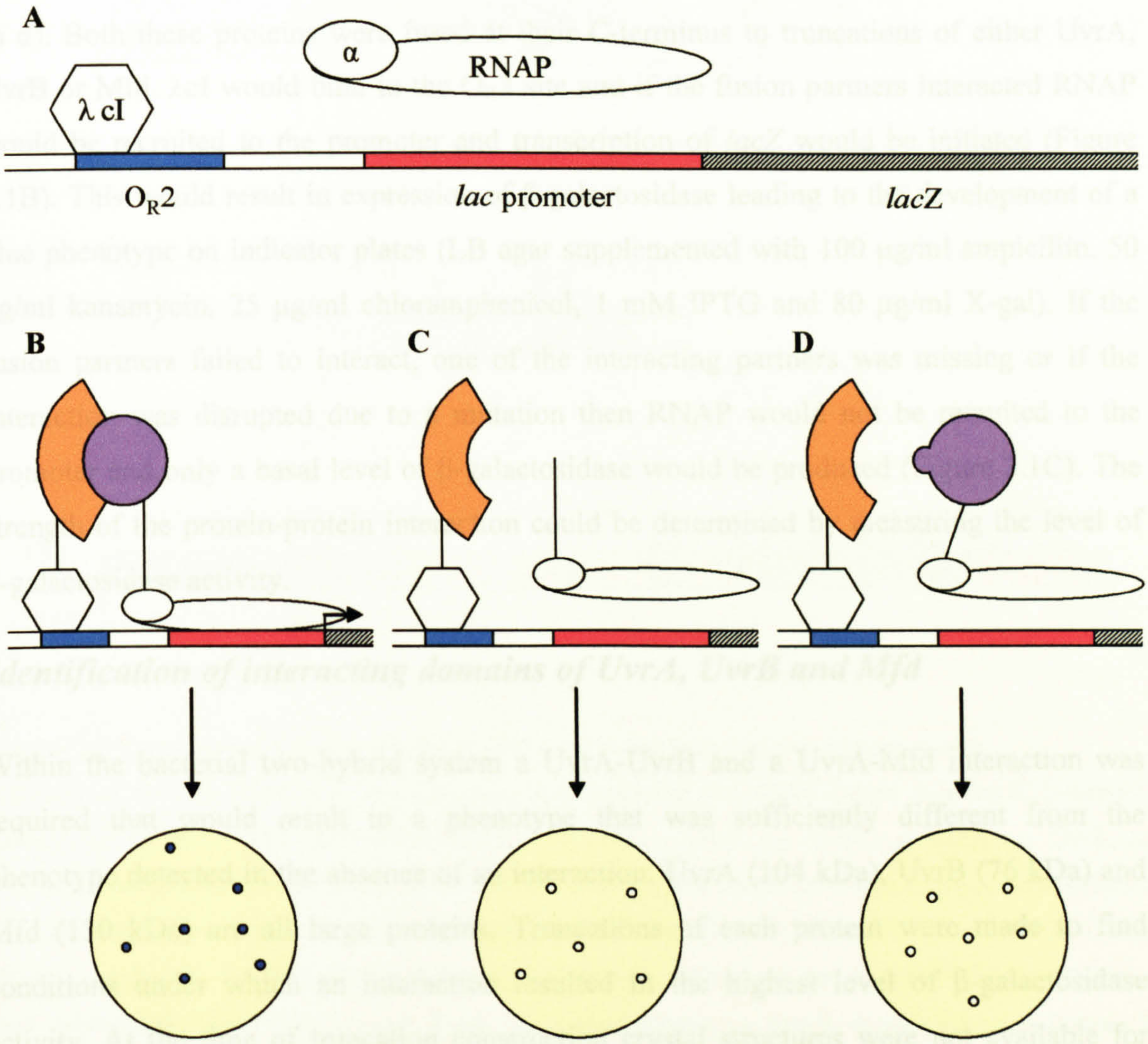

Figure 3.1 Bacterial two-hybrid β-galactosidase reporter screen.

(**A**) KS1 cells contain a chromosomal copy of *lacZ* with a *plac*O_R2-62 promoter upstream. KS1 cells were transformed with two plasmids; one coded for a λcI fusion protein and the other a $\alpha_{1\text{-}248}$ fusion protein. (**B**) Interacting partners that were fused to λcI and α brought RNAP to the promoter. RNAP then transcribed *lacZ* leading to the expression of β-galactosidase. The presence of β-galactosidase in a cell was detected as a blue colony phenotype on indicator plates (LB agar supplemented with the appropriate antibiotics, 1 mM IPTG and 80 μg/ml X-gal). (**C**) When one (or both) interacting partner was missing or (**D**) one of the interacting partners had a mutation in disrupting the interaction, RNAP was not recruited to the promoter and a white colony phenotype was observed on indicator plates.

as α). Both these proteins were fused at their C-terminus to truncations of either UvrA, UvrB or Mfd. λcI would bind to the O_R2 site and if the fusion partners interacted RNAP would be recruited to the promoter and transcription of *lacZ* would be initiated (Figure 3.1B). This would result in expression of β-galactosidase leading to the development of a blue phenotype on indicator plates (LB agar supplemented with 100 μg/ml ampicillin, 50 μg/ml kanamycin, 25 μg/ml chloramphenicol, 1 mM IPTG and 80 μg/ml X-gal). If the fusion partners failed to interact, one of the interacting partners was missing or if the interaction was disrupted due to a mutation then RNAP would not be recruited to the promoter and only a basal level of β-galactosidase would be produced (Figure 3.1C). The strength of the protein-protein interaction could be determined by measuring the level of β-galactosidase activity.

Identification of interacting domains of UvrA, UvrB and Mfd

Within the bacterial two-hybrid system a UvrA-UvrB and a UvrA-Mfd interaction was required that would result in a phenotype that was sufficiently different from the phenotype detected in the absence of an interaction. UvrA (104 kDa), UvrB (76 kDa) and Mfd (130 kDa) are all large proteins. Truncations of each protein were made to find conditions under which an interaction resulted in the highest level of β-galactosidase activity. At the time of truncation construction crystal structures were not available for UvrA and Mfd, and the crystal structures that were available for UvrB lacked domain 2 which is believed to contain the UvrA binding region (Theis *et al.*, 1999) (Machius *et al.*, 1999). Therefore the truncations were based on secondary structure predictions (PSIPRED and NNPREDICT) and available truncation data (Figure 3.2) (Claassen and Grossman, 1991) (Selby and Sancar, 1993). $UvrB_{114-251}$ and Mfd_{82-219} are homologous (Selby and Sancar, 1993) and $UvrB_{115-250}$ was shown to interact with UvrA (Hsu *et al.*, 1995). This homology region was therefore present in the region of UvrB (amino acids 35 to 252) and Mfd (amino acids 1 to 219) used.

UvrB can stimulate the ATPase activity of $UvrA_{1-230}$ and full-length UvrA to the same extent (Claassen and Grossman, 1991). Claassen and Grossman concluded that the N-terminal 230 amino acids of UvrA are important for the UvrA-UvrB interaction (Claassen and Grossman, 1991). There was little additional information available on the UvrB binding domain of UvrA and no information available on the Mfd binding domain of

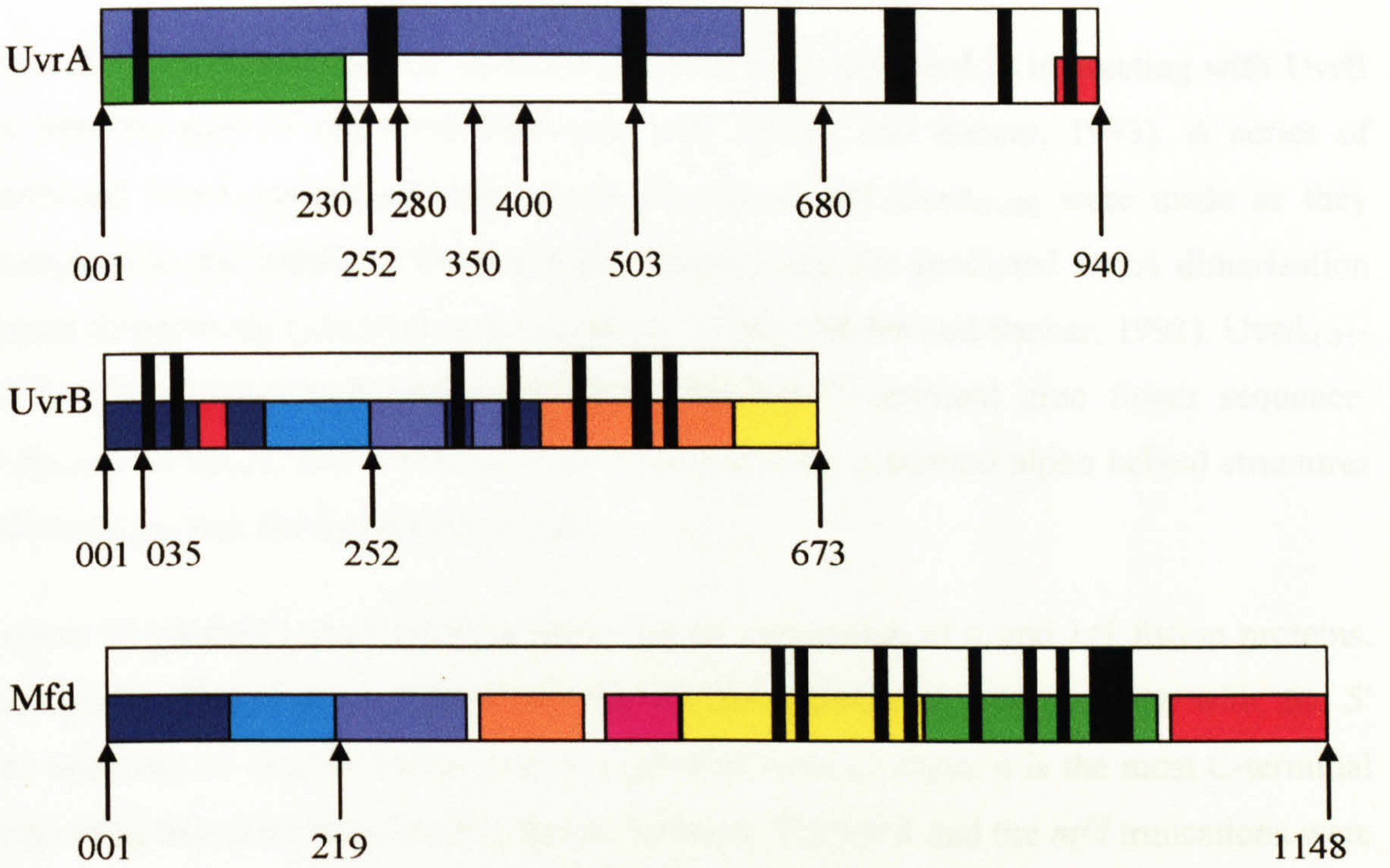

Figure 3.2 Truncations of UvrA, UvrB and Mfd used in the bacterial two-hybrid system.

Truncations of UvrA, UvrB and Mfd were used in the bacterial two hybrid system. A series of C-terminal truncations of UvrA were constructed: $UvrA_{1\text{-}230}$, $UvrA_{1\text{-}252}$, $UvrA_{1\text{-}280}$, $UvrA_{1\text{-}350}$, $UvrA_{1\text{-}400}$, $UvrA_{1\text{-}503}$, $UvrA_{1\text{-}680}$ and $UvrA_{1\text{-}940}$ (full-length). UvrB and Mfd each had one truncation made: $UvrB_{35\text{-}252}$ and $Mfd_{1\text{-}219}$. The coloured boxes indicate the following domains. **UvrA** - green, the predicted UvrB interaction domain ($UvrA_{1\text{-}230}$); purple, the predicted UvrA dimerization domain ($UvrA_{1\text{-}680}$); and red, the damage recognition and stabilisation domain ($UvrA_{900\text{-}940}$). **UvrB** - dark blue, domain 1a; purple, domain 1b; aqua, domain 2; orange, domain 3; yellow, domain 4; and red the β-hairpin (Theis *et al.*, 1999). **Mfd** - dark blue, domain 1a; purple, domain 1b; aqua, domain 2; orange, domain 3; pink, domain 4; yellow, domain 5; green, domain 6; and red, domain 7 (Deaconescu *et al.*, 2006). See Figure 1.9 for descriptions of the motifs (thick black lines).

UvrA. It was assumed that the same area of UvrA was involved in interacting with UvrB and Mfd because of the UvrB-Mfd homology (Selby and Sancar, 1993). A series of C-terminal UvrA truncations were made. $UvrA_{1-230}$ and $UvrA_{1-680}$ were made as they correspond to the predicted UvrB binding domain and the predicted UvrA dimerization domain respectively (Claassen and Grossman, 1991), (Myles and Sancar, 1991). $UvrA_{1-252}$ and $UvrA_{1-280}$ were truncated before and after the N-terminal zinc finger sequence. $UvrA_{1-350}$, $UvrA_{1-400}$ and $UvrA_{1-503}$ were truncated after predicted alpha helical structures and $UvrA_{1-940}$ was the full-length protein.

A series of plasmids were constructed to enable expression of α and λcI fusion proteins. Truncations of *uvrA* were cloned into pRA02 downstream of, and in-frame with, the 5′ gene sequence of *rpoA* to create plasmids $pRA02UvrA_{1-n}$ (where n is the most C-terminal amino acid) that code for $\alpha UvrA_{1-n}$ fusion proteins. The *uvrB* and the *mfd* truncations were cloned into pRA03 downstream of, and in-frame with, the λ *cI* gene to create plasmids $pRA03UvrB_{35-252}$ and $pRA03Mfd_{1-219}$ that code for $\lambda cIUvrB_{35-252}$ and $\lambda cIMfd_{1-219}$ respectively.

To identify which truncation of UvrA gave the strongest interaction with $UvrB_{35-252}$ and which gave the strongest interaction with Mfd_{1-219}, KS1 cells containing *plac*O_R2-62 upstream of *lacZ* were first transformed with pRA03, $pRA03UvrB_{35-252}$ or $pRA03Mfd_{1-219}$ They were then each transformed with pRA02 or $pRA02UvrA_{1-n}$. β-galactosidase activity was determined from subsequent cultures. KS1 cells that contained $pRA02UvrA_{1-940}$ failed to grow after subculture as did KS1 cells that contained $pRA02UvrA_{1-680}$ in combination with $pRA03Mfd_{1-219}$. β-galactosidase activity was determined for those combinations that did grow (Figure 3.3). When one or both interacting partners were absent a basal level of β-galactosidase activity was detected. When $\alpha UvrA_{1-230}$ and either $\lambda cIUvrB_{35-252}$ or $\lambda cIMfd_{1-219}$ were present the β-galactosidase activity remained near this basal level. When any of the other $\alpha UvrA_{1-n}$ fusion proteins were present in combination with $\lambda cIUvrB_{35-252}$ or $\lambda cIMfd_{1-219}$ an elevated level of β-galactosidase activity was detected. The level of β-galactosidase activity altered with the different $\alpha UvrA_{1-n}$ fusion proteins but the same trend was seen when either $\lambda cIUvrB_{35-252}$ or $\lambda cIMfd_{1-219}$ were present. The greatest β-galactosidase activity detected with $\lambda cIUvrB_{35-252}$ or $\lambda cIMfd_{1-219}$ was when $\alpha UvrA_{1-252}$ was present.

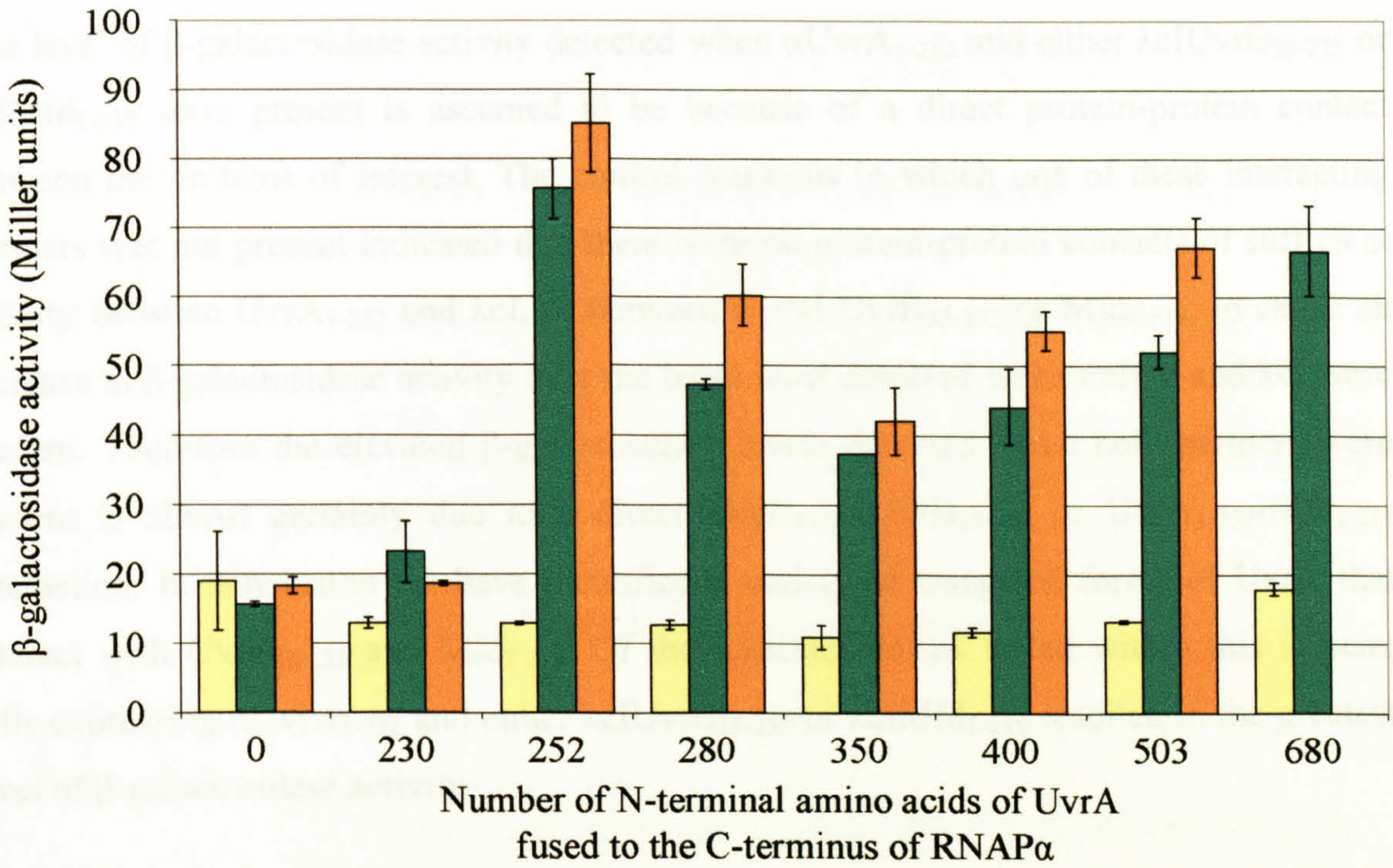

Figure 3.3 Effect of UvrA truncations in β-galactosidase reporter screen.

KS1 cells were transformed with pRA02 and pRA03 derivatives encoding α and λcI fusion proteins respectively. Cultures were grown to an A_{600} of 0.35 to 0.4 and specific β-galactosidase activity was determined. Yellow, green and orange bars indicate cells expressing λcI, λcIUvrB$_{35\text{-}252}$ and λcIMfd$_{1\text{-}219}$ respectively. Assays were carried out in triplicate (with the exception of λcIUvrB-αUvrA$_{1\text{-}350}$ which was assayed only once due to poor growth) and results averaged. Error bars shown are standard deviations.

The level of β-galactosidase activity detected when $\alpha UvrA_{1\text{-}252}$ and either $\lambda cIUvrB_{35\text{-}252}$ or $\lambda cIMfd_{1\text{-}219}$ were present is assumed to be because of a direct protein-protein contact between the proteins of interest. The control reactions in which one of these interacting partners was not present indicated that there were no protein-protein contacts of sufficient affinity between $UvrA_{1\text{-}252}$ and λcI, or between α and $UvrB_{35\text{-}252}$ or $Mfd_{1\text{-}219}$, to cause an increase in β-galactosidase activity over the basal level detected when only α and λcI were present. Therefore the elevated β-galactosidase levels detected when both partners were present is almost certainly due to a direct $UvrA_{1\text{-}252}$-$UvrB_{35\text{-}252}$ or $UvrA_{1\text{-}252}$-$Mfd_{1\text{-}219}$ interaction. In conclusion we have identified a variety of truncated forms of UvrA that interact with $UvrB_{35\text{-}252}$ and $Mfd_{1\text{-}219}$. Of the truncated forms tested within this system, cells expressing $\alpha UvrA_{1\text{-}252}$ and either $\lambda cIUvrB_{35\text{-}252}$ or $\lambda cIMfd_{1\text{-}219}$ resulted in the greatest level of β-galactosidase activity.

Identification of UvrA mutants – one-step screen

The phenotype resulting from the interaction between $UvrA_{1\text{-}252}$ and $UvrB_{35\text{-}252}$ or $Mfd_{1\text{-}219}$ was used to identify residues within UvrA that affected these interactions. Colonies of KS1 cells that expressed $\alpha UvrA_{1\text{-}252}$ and either $\lambda cIUvrB_{35\text{-}252}$ or $\lambda cIMfd_{1\text{-}219}$ showed a blue phenotype (light blue with a dark blue centre) on X-gal indicator plates. Colonies that lacked one or other of the interacting partners appeared white. The two phenotypes were distinguishable and therefore cells that expressed mutant proteins which disrupted the interaction were expected to be detectable as white colonies on indicator plates.

Random mutants of $UvrA_{1\text{-}252}$ were generated using error-prone PCR (Figure 3.4). Initially five error-prone PCR cycles were followed by 30 standard PCR cycles. The PCR products were cloned into pRA02$UvrA_{1\text{-}252}$ on a XbaI/KpnI fragment to generate a library of *uvrA* mutant plasmids. KS1 cells that already contained either pRA03$UvrB_{35\text{-}252}$ or pRA03$Mfd_{1\text{-}219}$ were then transformed with the *uvrA* mutant library. The transformation mixtures were spread onto LB indicator plates and incubated. There were a significant proportion of white colonies on the indicator plates. Single white colonies were grown in LB broth containing the appropriate antibiotics and the plasmid DNA extracted and sequenced. Of eight clones sequenced seven contained a frameshift or a stop codon. The remaining candidate, which had been selected from KS1 cells expressing $\lambda cIUvrB_{35\text{-}252}$, encoded $\alpha UvrA_{1\text{-}252.EV144+LH151}$.

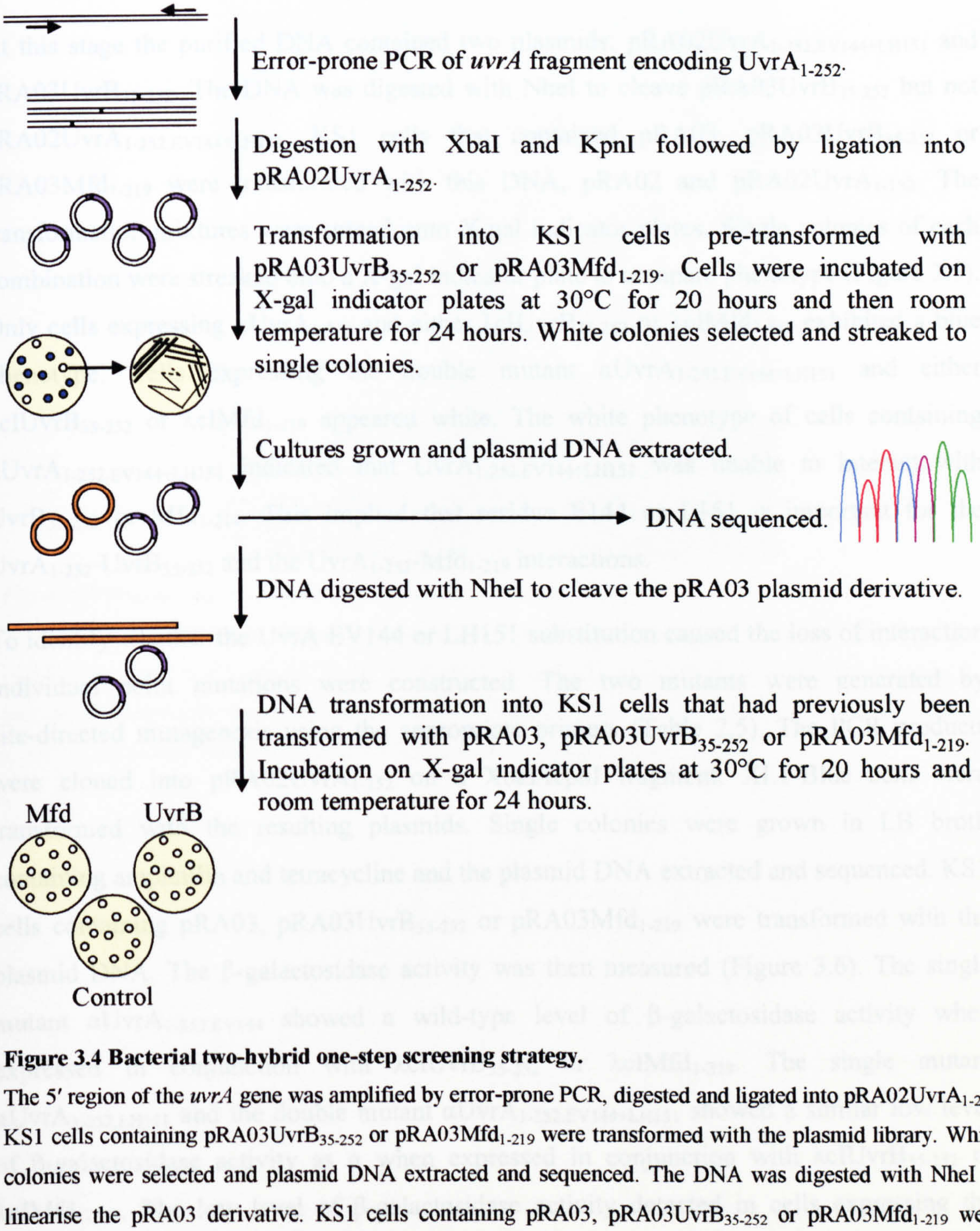

Figure 3.4 Bacterial two-hybrid one-step screening strategy.

The 5′ region of the *uvrA* gene was amplified by error-prone PCR, digested and ligated into $pRA02UvrA_{1-252}$. KS1 cells containing $pRA03UvrB_{35-252}$ or $pRA03Mfd_{1-219}$ were transformed with the plasmid library. White colonies were selected and plasmid DNA extracted and sequenced. The DNA was digested with NheI to linearise the pRA03 derivative. KS1 cells containing pRA03, $pRA03UvrB_{35-252}$ or $pRA03Mfd_{1-219}$ were transformed with the DNA for use in β-galactosidase assays.

At this stage the purified DNA contained two plasmids: pRA02UvrA$_{1\text{-}252.EV144+LH151}$ and pRA03UvrB$_{35\text{-}252}$. The DNA was digested with NheI to cleave pRA03UvrB$_{35\text{-}252}$ but not pRA02UvrA$_{1\text{-}252.EV144+LH151}$. KS1 cells that contained pRA03, pRA03UvrB$_{35\text{-}252}$ or pRA03Mfd$_{1\text{-}219}$ were transformed with this DNA, pRA02 and pRA02UvrA$_{1\text{-}252}$. The transformation mixtures were spread onto X-gal indicator plates. Single colonies of each combination were streaked onto a X-gal indicator plate to compare phenotype (Figure 3.5). Only cells expressing αUvrA$_{1\text{-}252}$ and either λcIUvrB$_{35\text{-}252}$ or λcIMfd$_{1\text{-}219}$ exhibited a blue phenotype. Cells expressing the double mutant αUvrA$_{1\text{-}252.EV144+LH151}$ and either λcIUvrB$_{35\text{-}252}$ or λcIMfd$_{1\text{-}219}$ appeared white. The white phenotype of cells containing αUvrA$_{1\text{-}252.EV144+LH151}$ indicated that UvrA$_{1\text{-}252.EV144+LH151}$ was unable to interact with UvrB$_{35\text{-}252}$ or Mfd$_{1\text{-}219}$. This implied that residue E144 or L151 is important for the UvrA$_{1\text{-}252}$-UvrB$_{35\text{-}252}$ and the UvrA$_{1\text{-}252}$-Mfd$_{1\text{-}219}$ interactions.

To identify whether the UvrA EV144 or LH151 substitution caused the loss of interaction individual point mutations were constructed. The two mutants were generated by site-directed mutagenesis using the appropriate primers (Table 2.5). The PCR products were cloned into pRA02UvrA$_{1\text{-}252}$ on a XbaI/KpnI fragment. XL1-Blue cells were transformed with the resulting plasmids. Single colonies were grown in LB broth containing ampicillin and tetracycline and the plasmid DNA extracted and sequenced. KS1 cells containing pRA03, pRA03UvrB$_{35\text{-}252}$ or pRA03Mfd$_{1\text{-}219}$ were transformed with the plasmid DNA. The β-galactosidase activity was then measured (Figure 3.6). The single mutant αUvrA$_{1\text{-}252.EV144}$ showed a wild-type level of β-galactosidase activity when expressed in conjunction with λcIUvrB$_{35\text{-}252}$ or λcIMfd$_{1\text{-}219}$. The single mutant αUvrA$_{1\text{-}252.LH151}$ and the double mutant αUvrA$_{1\text{-}252.EV144+LH151}$ showed a similar low level of β-galactosidase activity as α when expressed in conjunction with λcIUvrB$_{35\text{-}252}$ or λcIMfd$_{1\text{-}219}$. The low level of β-galactosidase activity detected in cells expressing the αUvrA$_{1\text{-}252.LH151}$ mutant indicates that residue L151 is important for protein-protein contact. The wild-type β-galactosidase activity seen in cells expressing αUvrA$_{1\text{-}252.EV144}$ indicates that residue E144 has no direct role in the protein-protein interaction detected in this screen.

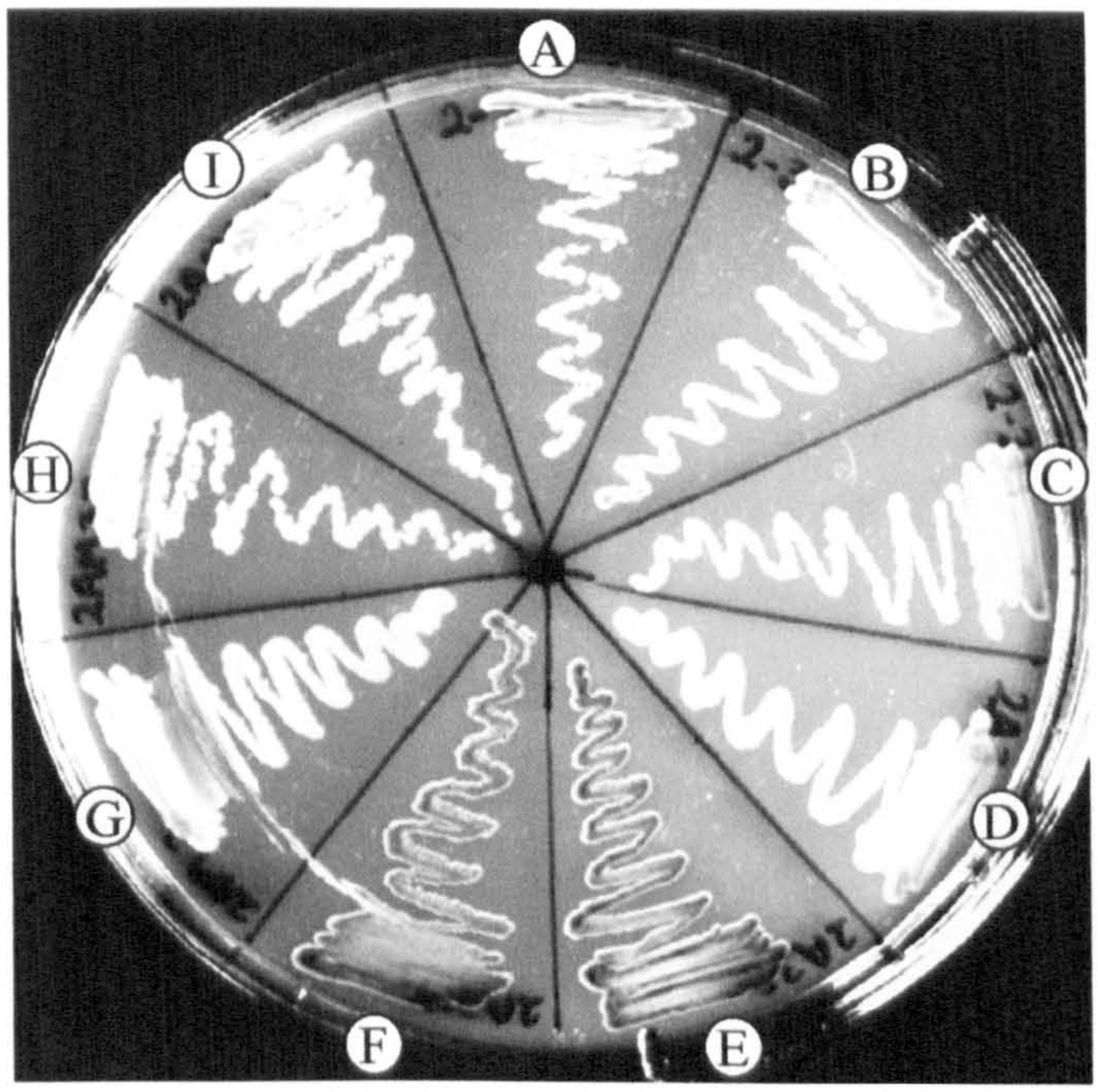

Figure 3.5 Phenotypes from the β-galactosidase reporter screen.

The phenotypes of KS1 cells expressing either λcI (A, D and G), λcIUvrB$_{35\text{-}252}$ (B, E, H) or λcIMfd$_{1\text{-}219}$ (C, F, I) and either α (A, B, C), αUvrA$_{1\text{-}252}$ (D, E, F) or αUvrA$_{1\text{-}252.EV144+LH151}$ (G, H, I) on an indicator plate (LB agar supplemented with the appropriate antibiotics, 1 mM IPTG and 80 μg/ml X-gal). Blue colonies indicate a positive interaction whilst white colonies indicate that no interaction was detected.

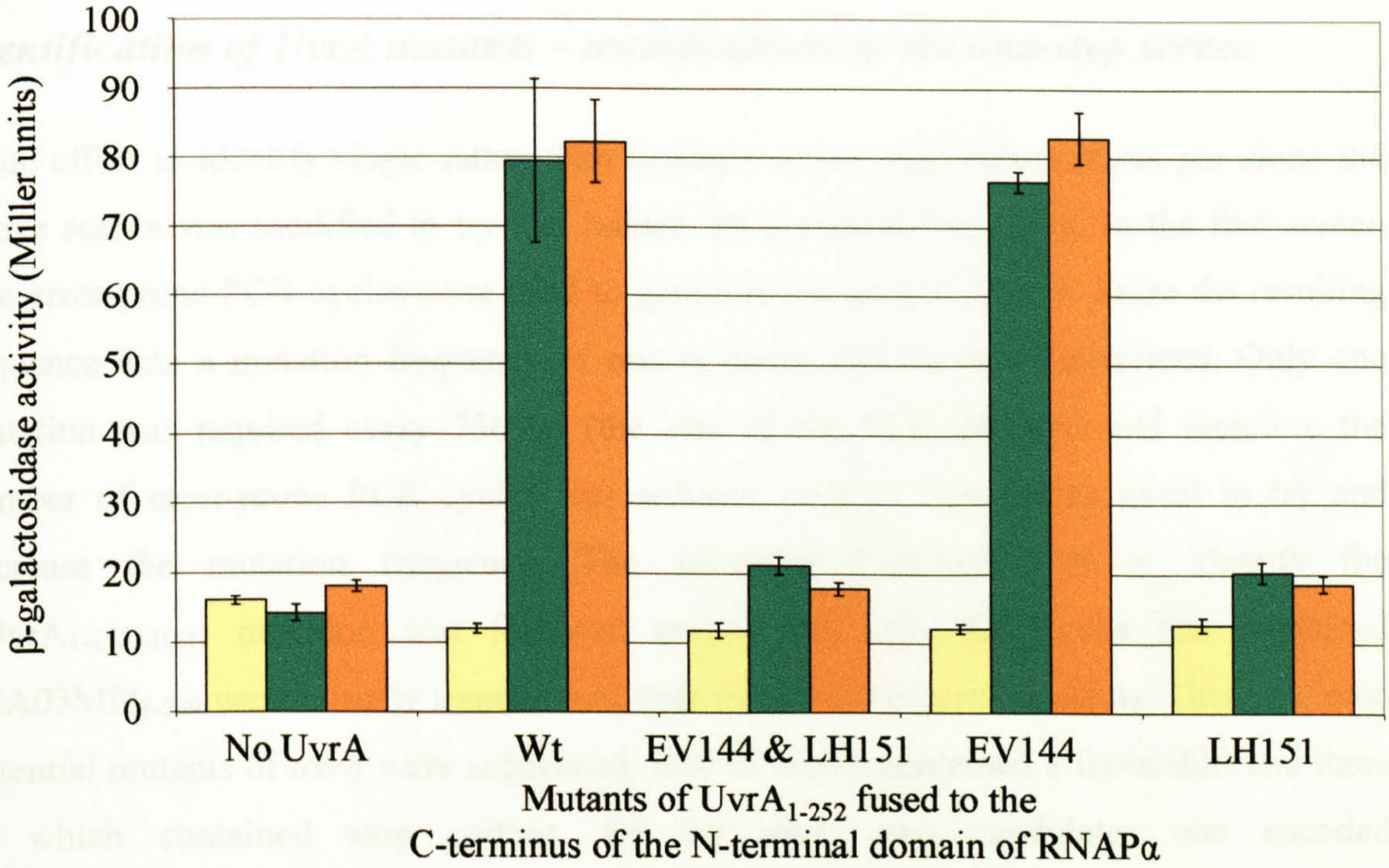

Figure 3.6 Effect of UvrA mutants EV144 and LH151 on β-galactosidase activity.

β-galactosidase activity was determined on KS1 cells transformed with a pRA02 and a pRA03 derivative which enable expression of α and λcI fusion proteins respectively. Yellow, green and orange bars indicate cells expressing λcI, λcIUvrB$_{35-252}$ and λcIMfd$_{1-219}$ respectively. Assays were carried out in triplicate and results averaged. Error bars shown are standard deviations.

Identification of UvrA mutants – modifications to the one-step screen

In an effort to identify single rather than multiple amino acid substitutions per clone the above screen was modified to try and reduce the mutation frequency. In the first screen five error-prone PCR cycles were used to generate the mutant library. From the resulting sequence data a mutation frequency of one in every 230 bp was determined. Only one mutation was required every 756 bp (the size of the PCR product) and therefore the number of error-prone PCR cycles was reduced (one to five cycles used) to try and decrease the mutation frequency. The screening protocol used to identify the $\alpha UvrA_{1\text{-}252.LH151}$ mutation was followed except that only KS1 cells that contained $pRA03Mfd_{1\text{-}219}$ were initially transformed with the library of *uvrA* mutants. This time nine potential mutants of *uvrA* were sequenced, four of which contained a frameshift and three of which contained stop codons. Of the other two candidates one encoded $\alpha UvrA_{1\text{-}252.IF027+GD173}$ and the other encoded $\alpha UvrA_{1\text{-}252.VE202}$. Site-directed mutagenesis was used to generate the DNA sequence from which the single mutants $\alpha UvrA_{1\text{-}252.IF027}$ and $\alpha UvrA_{1\text{-}252.GD173}$ could be expressed (Table 2.5). KS1 cells containing pRA03, $pRA03UvrB_{35\text{-}252}$ or $pRA03Mfd_{1\text{-}219}$ were transformed with $pRA02UvrA_{1\text{-}252.IF027}$, $pRA02UvrA_{1\text{-}252.GD173}$ or $pRA02UvrA_{1\text{-}252.VE202}$ and the subsequent β-galactosidase activity measured. Cells expressing the mutant protein $\alpha UvrA_{1\text{-}252.IF027}$ had similar levels of β-galactosidase activity to wild-type (data not shown). Cells expressing $\alpha UvrA_{1\text{-}252.GD173}$ or $\alpha UvrA_{1\text{-}252.VE202}$ only had a low level of β-galactosidase activity when expressed in conjunction with $\lambda cIUvrB_{35\text{-}252}$ or $\lambda cIMfd_{1\text{-}219}$ (Figure 3.7). The low level of β-galactosidase seen with $\alpha UvrA_{1\text{-}252.GD173}$ and $\alpha UvrA_{1\text{-}252.VE202}$ indicates that G173 and V202 are important for the protein-protein contacts detected in this system.

Identification of UvrA mutants – two-step screen

It is possible that some residues of UvrA are involved solely in either the UvrA-UvrB or the UvrA-Mfd interaction. Modifications to the one-step screen were made to identify residues of UvrA that are important for interacting with Mfd but are not required to interact with UvrB (Figure 3.8). The *uvrA* mutant plasmid libraries were produced from one and two cycles of error-prone PCR (followed by 30 standard PCR cycles). KS1 cells containing $pRA03Mfd_{1\text{-}219}$ were transformed with the *uvrA* mutant plasmid library. Colonies expressing a white phenotype (indicating the absence of a UvrA-Mfd interaction)

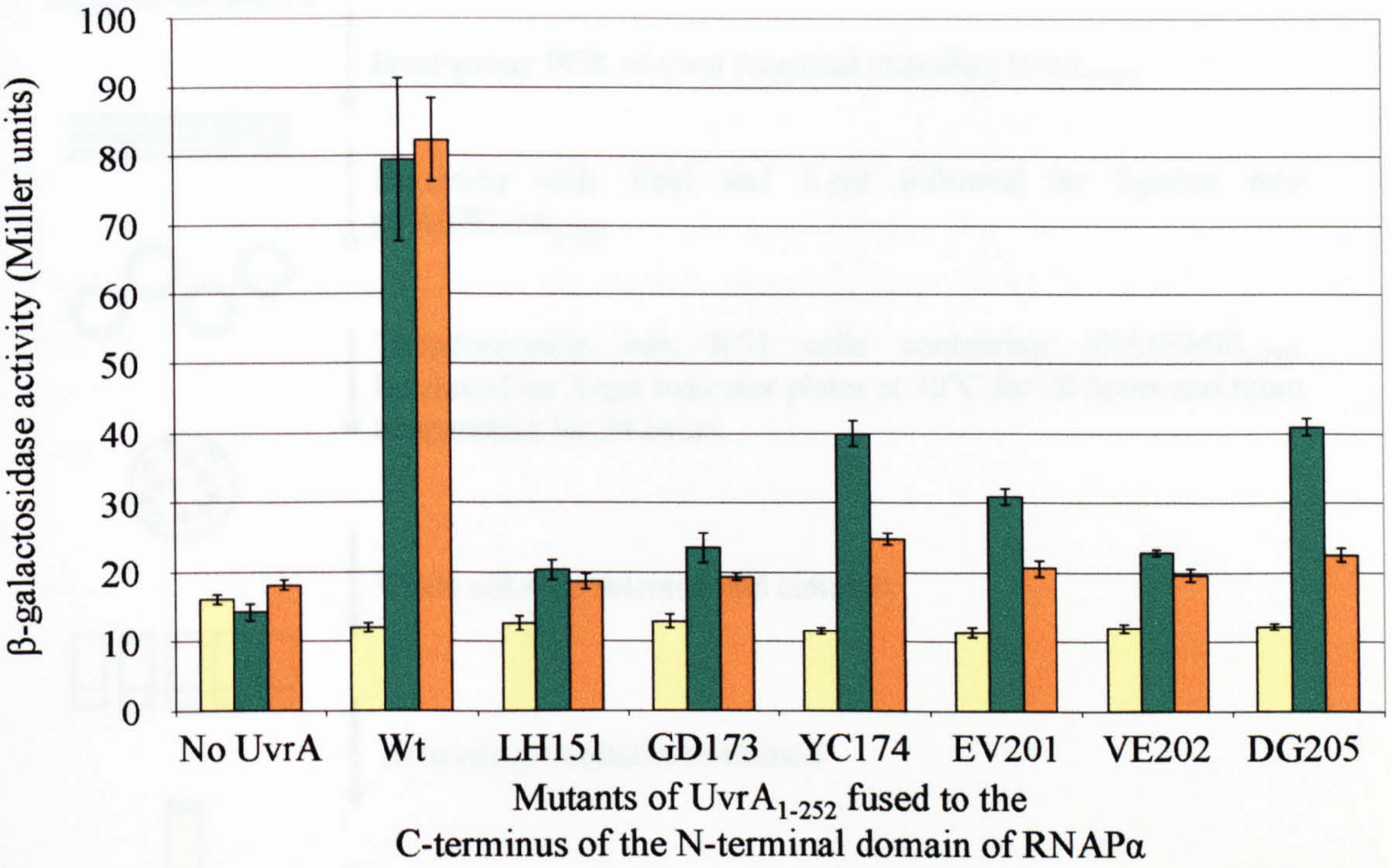

Figure 3.7 Effect of UvrA mutants in the β-galactosidase reporter screen.

β-galactosidase activity was determined on KS1 cells transformed with a pRA02 and a pRA03 derivative which enable expression of α and λcI fusion proteins respectively. Yellow, green and orange bars indicate cells expressing λcI, λcIUvrB$_{35-252}$ and λcIMfd$_{1-219}$ respectively. Assays were carried out in triplicate and results averaged. Error bars shown are standard deviations. The data for No UvrA, Wt UvrA and UvrA$_{LH151}$ is the same as in Figure 3.6.

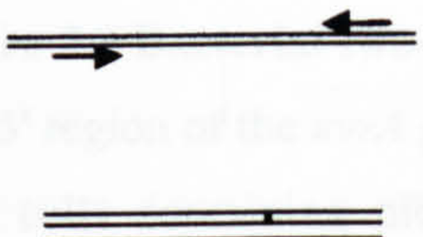

Error-prone PCR of *uvrA* fragment encoding $UvrA_{1-252}$.

Digestion with XbaI and KpnI followed by ligation into $pRA02UvrA_{1-252}$.

Transformation into KS1 cells containing $pRA03Mfd_{1-219}$. Incubated on X-gal indicator plates at 30°C for 20 hours and room temperature for 24 hours.

White colonies selected and cultured.

10 overnight cultures combined.

Plasmid DNA extracted.

DNA digested with NheI to cleave $pRA03Mfd_{1-219}$ plasmid.

DNA transformation into KS1 cells containing $pRA03UvrB_{35-252}$. Incubation on X-gal indicator plates at 30°C for 20 hours and room temperature for 24 hours. Blue colonies streaked.

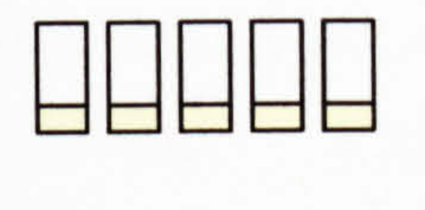

Overnight cultures grown and plasmid DNA extracted.

DNA sequenced.

DNA digested with NheI to cleave UvrB plasmid.

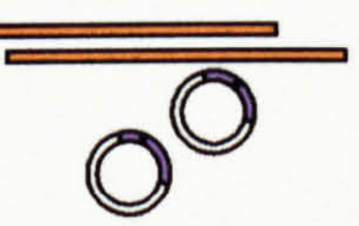

DNA transformation into KS1 cells that contained $pRA03UvrB_{35-252}$ or $pRA03Mfd_{1-219}$. Incubation on X-gal indicator plates at 30°C for 20 hours and room temperature for 24 hours.

Figure 3.8 Bacterial two-hybrid two-step screening strategy.

The 5′ region of the *uvrA* gene was amplified by error-prone PCR, digested and ligated into pRA02UvrA$_{1\text{-}252}$. KS1 cells containing pRA03Mfd$_{1\text{-}219}$ were transformed with the plasmid library. White colonies were selected and cultured. 10 cultures were pooled and the plasmid DNA extracted. The DNA was digested with NheI to linearise the pRA03Mfd$_{1\text{-}219}$ plasmid. KS1 cells containing pRA03UvrB$_{35\text{-}252}$ were then transformed with DNA. Blue colonies were selected and cultured and the DNA extracted and digested with NheI to linearise the pRA03UvrB$_{35\text{-}252}$ plasmid. Phenotype was confirmed by transforming KS1 cells that contained pRA03Mfd$_{1\text{-}219}$ or pRA03UvrB$_{35\text{-}252}$ with the DNA. The DNA was sequenced once the phenotype had been confirmed.

were used to inoculate 5 ml LB broth containing ampicillin, kanamycin and chloramphenicol that were then incubated at 37°C overnight. 10 cultures were pooled and their plasmid DNA extracted. At this stage the DNA samples contained pRA03Mfd$_{1\text{-}219}$ and 10 potentially different pRA02UvrA$_{1\text{-}252}$ mutant plasmids. The DNA mix was digested with NheI to cleave the chloramphenicol resistant plasmid pRA03Mfd$_{1\text{-}219}$. KS1 cells containing the chloramphenicol resistant plasmid, pRA03UvrB$_{35\text{-}252}$, were transformed with the digested DNA mix. Colonies expressing a blue phenotype (indicating the presence of a UvrA-UvrB interaction) were streaked to single colonies. The single colonies were incubated overnight in LB broth containing ampicillin, kanamycin and chloramphenicol and then their plasmid DNA extracted. The DNA was digested with NheI to cleave pRA03UvrB$_{35\text{-}252}$. KS1 cells containing either pRA03UvrB$_{35\text{-}252}$ or pRA03Mfd$_{1\text{-}219}$ were again transformed with the DNA to confirm phenotype. Seven clones were identified that failed to interact with Mfd (white phenotype) but still interacted with UvrB (blue phenotype). These clones were sequenced. One contained a frameshift, four contained double mutations (coding for αUvrA$_{1\text{-}252.IF021+YC174}$, αUvrA$_{1\text{-}252.ND138+EV201}$, αUvrA$_{1\text{-}252.AT009+DG205}$ and αUvrA$_{1\text{-}252.QH130+DG205}$) and two contained single mutations (both coding for αUvrA$_{1\text{-}252.DG205}$). The two double mutants in which the UvrA$_{DG205}$ substitution was present were not taken further forward.

The results from the modified one-step screen indicated that UvrA residues G173 and V202 are important for the UvrA$_{1\text{-}252}$-UvrB$_{35\text{-}252}$ and the UvrA$_{1\text{-}252}$-Mfd$_{1\text{-}219}$ interaction. UvrA mutants YC174 and EV201 from the double mutants were adjacent to G173 and V202 respectively. It was therefore predicted that YC174 and EV201 were responsible for the change in phenotype and therefore these single mutants (not IF021 or ND138) were generated by site-directed mutagenesis (Table 2.5). KS1 cells that contained pRA03, pRA03UvrB$_{35\text{-}252}$, or pRA03Mfd$_{1\text{-}219}$ were transformed with pRA02UvrA$_{1\text{-}252.YC174}$, pRA02UvrA$_{1\text{-}252.EV201}$ and pRA02UvrA$_{1\text{-}252.DG205}$. β-galactosidase activity was then measured (Figure 3.7). When αUvrA$_{1\text{-}252.YC174}$, αUvrA$_{1\text{-}252.EV201}$ or αUvrA$_{1\text{-}252.DG205}$ was expressed in KS1 cells expressing λcIMfd$_{1\text{-}219}$ only a low level of β-galactosidase activity was detected. When they were expressed in KS1 cells expressing λcIUvrB$_{35\text{-}252}$ the level of β-galactosidase activity measured was lower than when αUvrA$_{1\text{-}252}$ was expressed but was still greater than the basal level seen when α was present. Therefore residues Y174, E201 and D205 are important for the UvrA$_{1\text{-}252}$-Mfd$_{1\text{-}219}$ interaction but are not as important for

the $UvrA_{1-252}$-$UvrB_{35-252}$ interaction. The different effect of these mutants on the $UvrA_{1-252}$-$UvrB_{35-252}$ and the $UvrA_{1-252}$-Mfd_{1-219} interaction is interesting. At least some of the UvrA residues involved in the $UvrA_{1-252}$-Mfd_{1-219} and the $UvrA_{1-252}$-$UvrB_{35-252}$ interaction are the same whilst other residues have a greater role in the $UvrA_{1-252}$-Mfd_{1-219} interaction than in the $UvrA_{1-252}$-$UvrB_{35-252}$ interaction.

Expression levels of UvrA mutants under bacterial two-hybrid conditions

Six UvrA mutants have been identified that appear to affect the $UvrA_{1-252}$-$UvrB_{35-252}$ and the $UvrA_{1-252}$-Mfd_{1-219} interaction that is detected in this bacterial two-hybrid screen. One possible reason for a reduction in β-galactosidase activity is that the mutant proteins are not expressed or are unstable and degrade faster than the wild-type fusion protein. To confirm protein levels KS1 cells containing pRA03 and a pRA02 derivative were analysed by western blot. The membrane was probed with an anti-α antibody. Cultures containing all six of the mutant plasmids expressed the correct size fusion protein with the same intensity as the wild-type fusion protein (Figure 3.9). The level of endogenous RNAPα was detected at the same intensity in all lanes. Therefore the six UvrA amino acid substitutions: LH151, GD173, YC174, EV201, VE202 and DG205, did not significantly affect the fusion protein concentration within the cell.

Mutations in UvrB

Interactions detected in bacterial two-hybrid screens are not always physiologically relevant. A mutant known to disrupt the UvrA-UvrB or the UvrA-Mfd interaction would be a good control to check that the correct interaction was being detected in this screen. At the time of establishing the screen no mutants of UvrA, UvrB or Mfd had been identified that were specifically defective in these protein-protein interactions. Sequence alignments revealed only one fully conserved residue within the homology region of all UvrB and Mfd proteins sequenced to date. This residue within the *E. coli* UvrB protein was R213 and seemed a reasonable candidate to be involved in the interaction with UvrA. In 2004, after the identification of the six UvrA mutants from this bacterial two-hybrid screen, a mutant that affected the *B. caldotenax* (*Bca*) UvrA-UvrB interaction was identified (Truglio *et al.*, 2004). EMSA and pull-down assays indicated that the ^{Bca}UvrA-$^{Bca}UvrB_{RE183}$ interaction was much weaker than the ^{Bca}UvrA-^{Bca}UvrB interaction (Truglio *et al.*, 2004). Truglio *et al.* also published the $^{Bca}UvrB_{YA096}$ crystal structure with

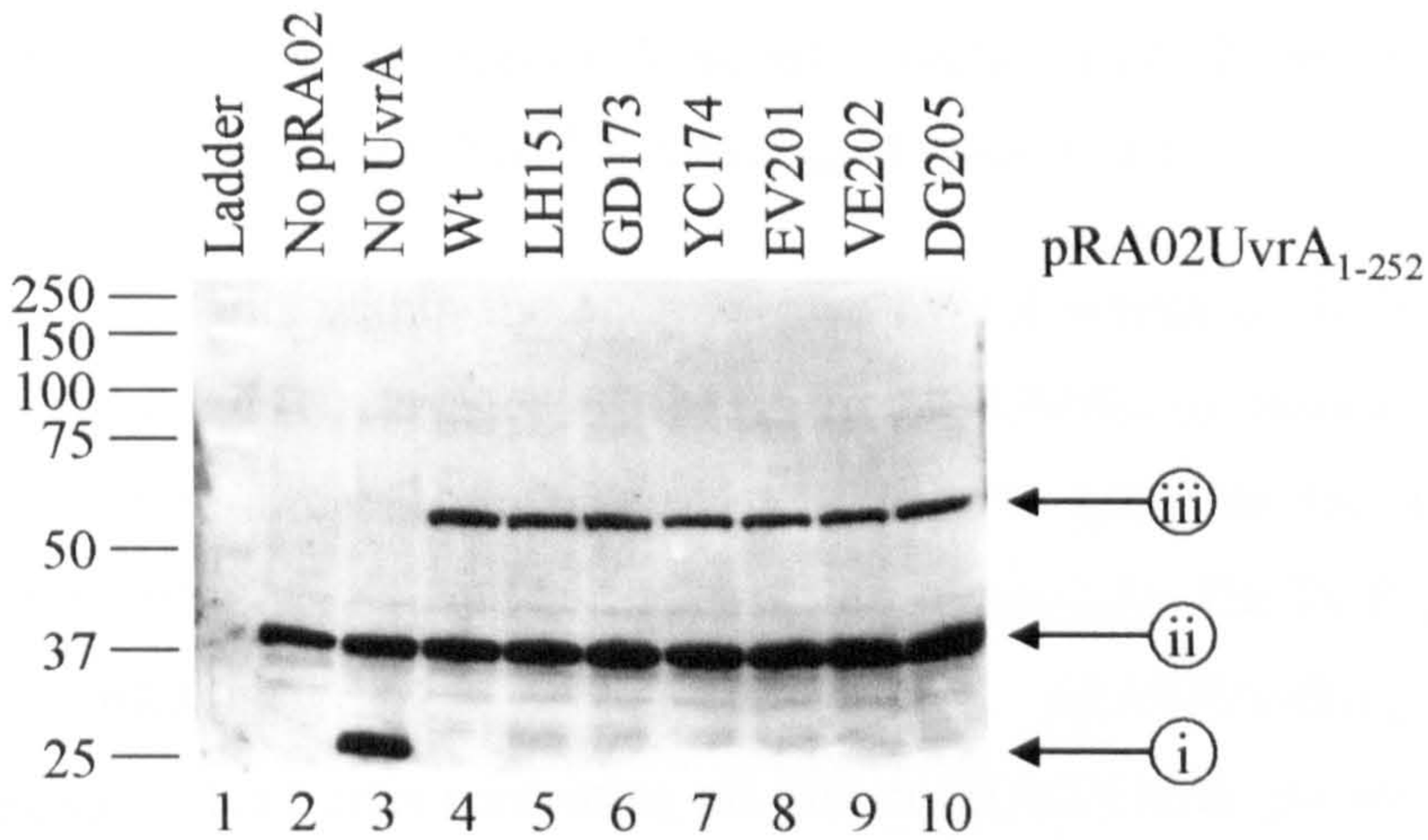

Figure 3.9 Expression levels of αUvrA$_{1-252}$ mutants in the β-galactosidase activity assay.

A sample of KS1 cells containing plasmid pRA03 and either no additional plasmid, pRA02 or pRA02UvrA$_{1-252}$ (encoding the indicated mutant) were harvested at an A_{600} between 0.35 and 0.45. The samples were run on a 10% SDS PAGE gel and transferred onto a membrane. The membrane was probed with a polyclonal anti-α primary antibody and then an HRP anti-rabbit IgG secondary antibody. i, indicates the NTD of the RNAPα subunit expressed from plasmid pRA02; ii, indicates the endogenous RNAPα subunit in the cell; iii, indicates the NTD of the RNAPα subunit fused at its C-terminus to the NTD of UvrA (either Wt or mutant). The ladder (kDa) is Preincision Plus protein standard (BioRad).

an intact domain 2 (the UvrA interaction domain) (Truglio *et al.*, 2004). Both R183 and R213 are on the surface of domain 2 of $^{Bca}UvrB_{YA096}$ (Figure 3.10).

The effect of these mutants within the bacterial two-hybrid screen could be measured to determine the physiological relevance of the $UvrA_{1\text{-}252}$-$UvrB_{35\text{-}252}$ interaction identified within this system. Site-directed mutagenesis was used to generate the gene sequence coding for *E. coli* $UvrB_{35\text{-}252.RE183}$ and $UvrB_{35\text{-}252.RA213}$ (Table 2.5). The PCR products were cloned into $pRA03UvrB_{35\text{-}252}$ to generate $pRA03UvrB_{35\text{-}252.RE183}$ and $pRA03UvrB_{35\text{-}252.RA213}$. KS1 cells containing pRA02 or $pRA02UvrA_{1\text{-}252}$ were transformed with these plasmids and β-galactosidase activity measured (Figure 3.11). The level of β-galactosidase activity in KS1 cells expressing $\alpha UvrA_{1\text{-}252}$ and $\lambda cIUvrB_{35\text{-}252}$, $\lambda cIUvrB_{35\text{-}252.RE183}$ or $\lambda cIUvrB_{35\text{-}252.RA213}$ was very similar. The interaction detected in the bacterial two-hybrid screen is therefore not affected by mutating $UvrB_{35\text{-}252}$ at residue R183 or R213.

UV sensitivity screen

In a complementary approach a second screen was established to identify UvrA mutants. This *in vivo* screen was based on the observation that Δ*uvrA* cells are UV sensitive (Howard-Flanders *et al.*, 1966). On exposure to UV light the DNA within cells would be damaged (Figure 3.12). In Δ*uvrA* cells where there is no functional UvrA the damaged DNA would remain as the cells would have no functional NER pathway (Figure 3.12A). DNA damage that was not repaired would result in a decrease in cell viability. Therefore Δ*uvrA* cells would exhibit a UV sensitive phenotype. If a plasmid based copy of *uvrA* was introduced into Δ*uvrA* cells the cells would be able to express UvrA. When UvrA was present the damaged DNA could be repaired by the NER pathway (Figure 3.12B). Therefore $uvrA^+$ cells would be UV resistant. If a mutated copy of *uvrA* was introduced into the cells instead of wild-type *uvrA* a UvrA mutant would be expressed. The damaged DNA would not be repaired if the residue that was mutated was essential for one of the NER properties of UvrA (Figure 3.12C). These cells would therefore be UV sensitive.

The bacterial two-hybrid system was designed to specifically identify protein-protein contact mutants. The UV sensitivity screen would identify physiologically relevant UvrA mutants that were defective in any essential UvrA property important for the NER

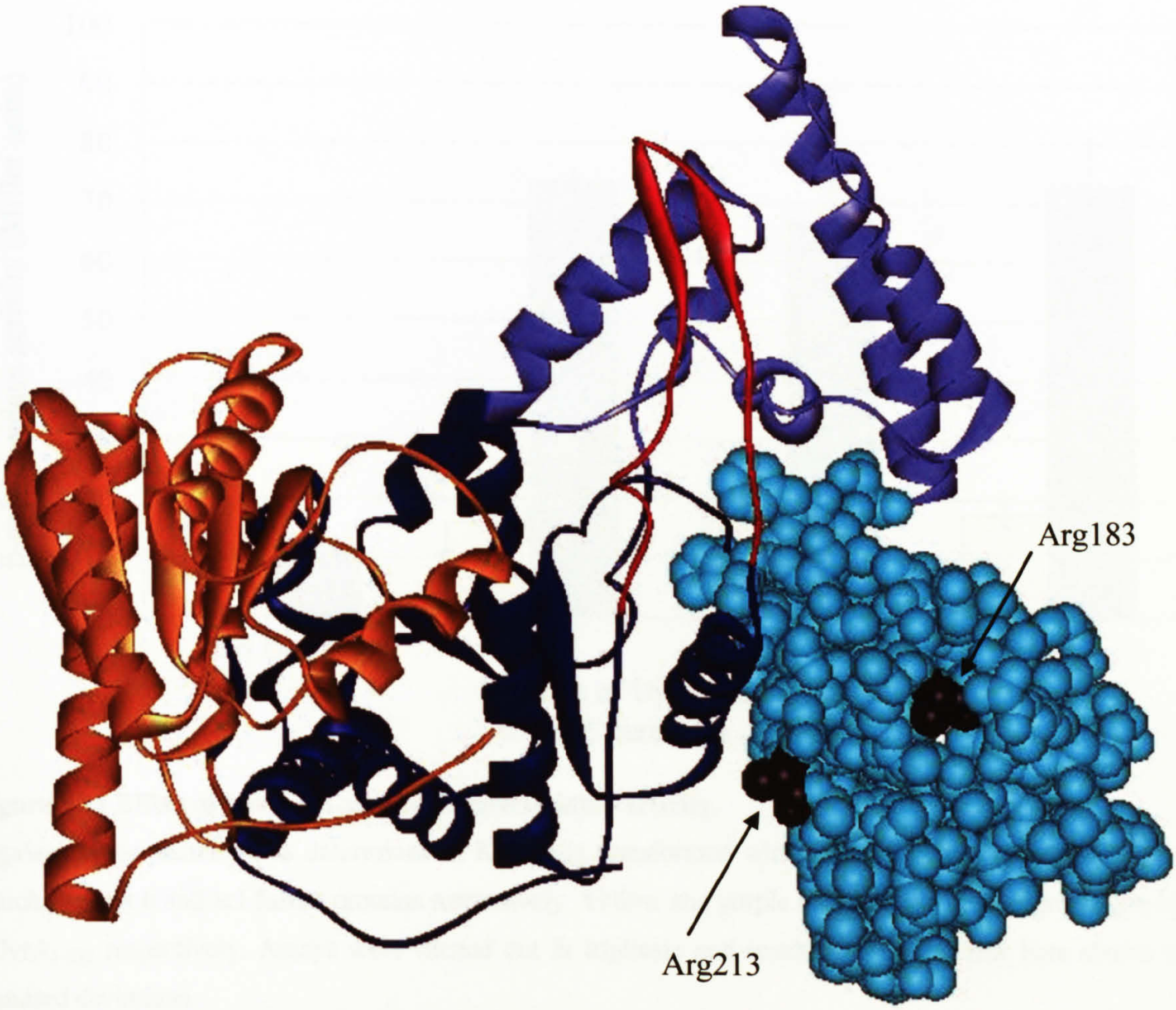

Figure 3.10 Crystal structure of UvrB.

The crystal structure of $UvrB_{YA096}$ from *B caldotenax* (PDB code 1D9X) (Truglio *et al.*, 2004). Domain 2, the proposed UvrA interaction domain is shown as a molecular surface. Two residues, R183 and R213, whose corresponding *E. coli* resides are also R183 and R213 and have been mutated in this work, are indicated in black. The domains are coloured as follows: dark blue, domain 1a; purple, domain 1b; aqua, domain 2; orange, domain 3; and red, β-hairpin.

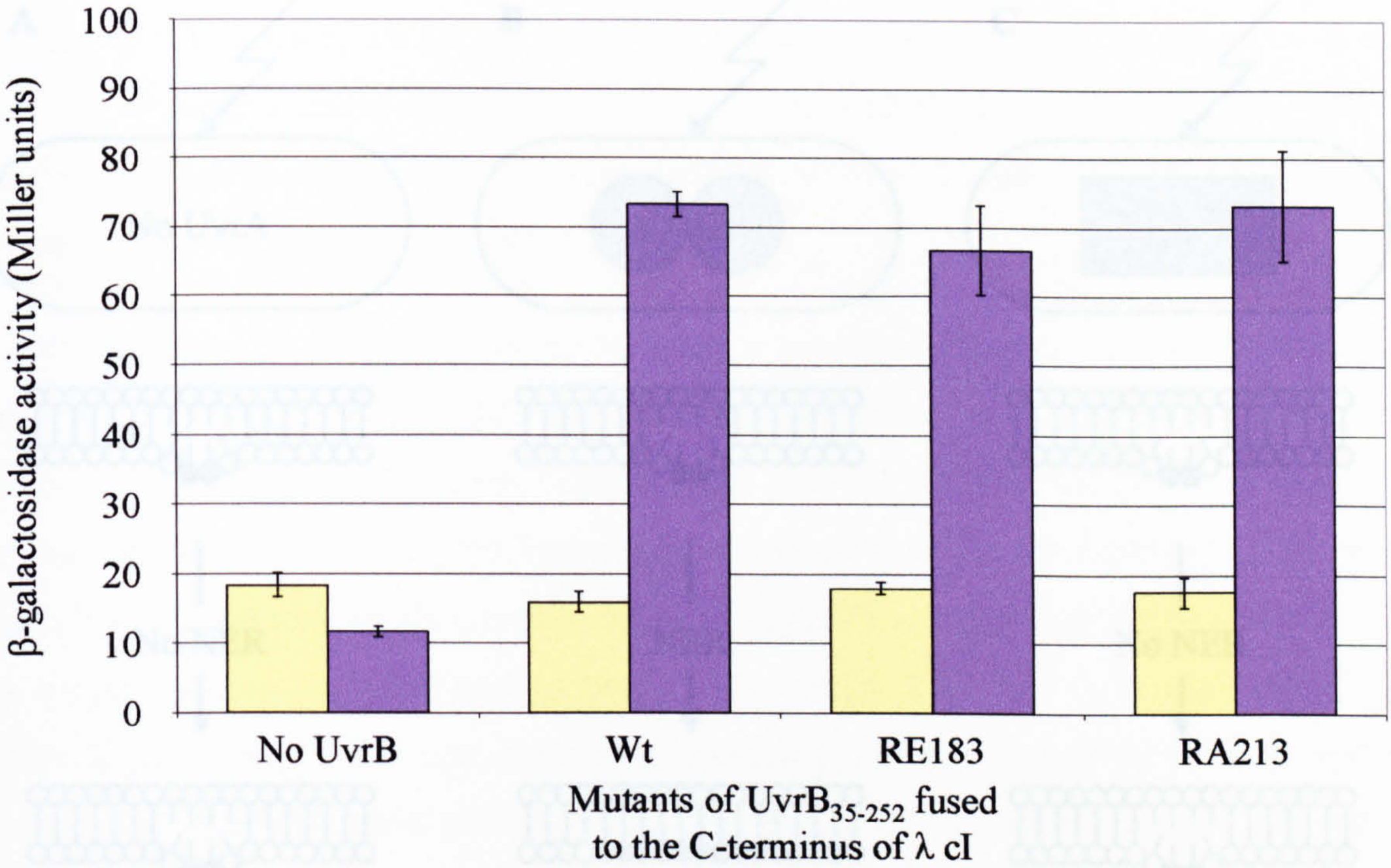

Figure 3.11 Effect of UvrB mutants on β-galactosidase activity.

β-galactosidase activity was determined in KS1 cells transformed with a pRA02 and a pRA03 derivative which express α and λcI fusion proteins respectively. Yellow and purple bars indicate cells expressing α and $\alpha UvrA_{1-252}$ respectively. Assays were carried out in triplicate and results averaged. Error bars shown are standard deviations.

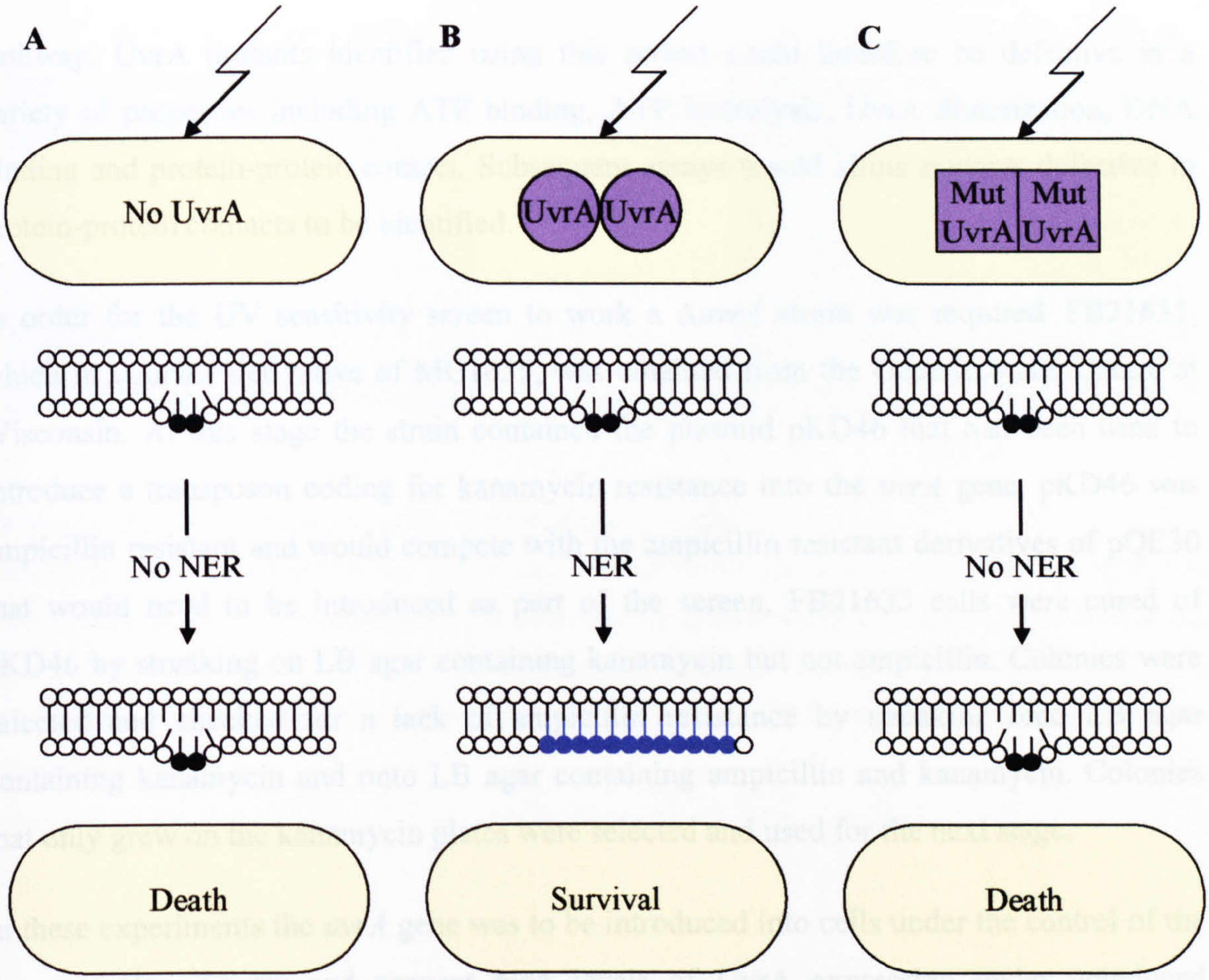

Figure 3.12 Principle behind the UV sensitivity screen.

(**A**) DNA damage introduced by UV irradiation can not be repaired by Δ*uvrA* cells. Therefore the cells die (UV sensitive phenotype). (**B**) DNA damage introduced by UV irradiation can be repaired by $uvrA^{+}$ cells. Therefore the cells survive (UV resistant phenotype). (**C**) DNA damage introduced by UV irradiation is not repaired in cells expressing UvrA mutants deficient in any essential UvrA property. Therefore the cells die (UV sensitive phenotype).

pathway. UvrA mutants identified using this screen could therefore be defective in a variety of properties including ATP binding, ATP hydrolysis, UvrA dimerization, DNA binding and protein-protein contact. Subsequent assays would allow mutants defective in protein-protein contacts to be identified.

In order for the UV sensitivity screen to work a Δ*uvrA* strain was required. FB21635, which is a Δ*uvrA* derivative of MG1655, was obtained from the Genetic Stock Centre at Wisconsin. At this stage the strain contained the plasmid pKD46 that had been used to introduce a transposon coding for kanamycin resistance into the *uvrA* gene. pKD46 was ampicillin resistant and would compete with the ampicillin resistant derivatives of pQE30 that would need to be introduced as part of the screen. FB21635 cells were cured of pKD46 by streaking on LB agar containing kanamycin but not ampicillin. Colonies were selected and checked for a lack of ampicillin resistance by streaking onto LB agar containing kanamycin and onto LB agar containing ampicillin and kanamycin. Colonies that only grew on the kanamycin plates were selected and used for the next stage.

In these experiments the *uvrA* gene was to be introduced into cells under the control of the *lac* promoter. To try and prevent high levels of UvrA expression under uninduced conditions a high concentration of the lac repressor was required. The lac repressor should bind to the *lac* promoter preventing RNAP from binding and thus prevent transcription of *uvrA*. To achieve this the F′ episome from XL1-Blue that contains $lacI^q$ that encodes for large quantities of Lac repressor was introduced into FB21635 cells (that had been cured of pKD46) by conjugation. These cells were named MG1655Δ*uvrA*. MG1655 cells have a functional *uvrA* gene and are not resistant to any antibiotics. *MG1655ΔuvrA* cells have a kanamycin resistant cassette within the *uvrA* gene (making it Δ*uvrA*) and also contain the F′ episome from XL1-Blue cells.

The UV phenotype of cells that contained *uvrA* (MG1655) and cells that did not (MG1655Δ*uvrA* and FB21635) was determined using a survival assay protocol that involves cell irradiation then dilution. 1 ml of each cell type was irradiated with 60 J/m^2 254 nm UV light whilst the remaining cells were not irradiated. The irradiated and unirradiated cells were subject to 10-fold serial dilutions, spotted onto LB agar plates and incubated at 30°C for 16 hours. Approximately 10% of MG1655 cells ($uvrA^+$) survived irradiation (Figure 3.13) whilst all FB21635 (Δ*uvrA*) cells died. MG1655Δ*uvrA* cells that

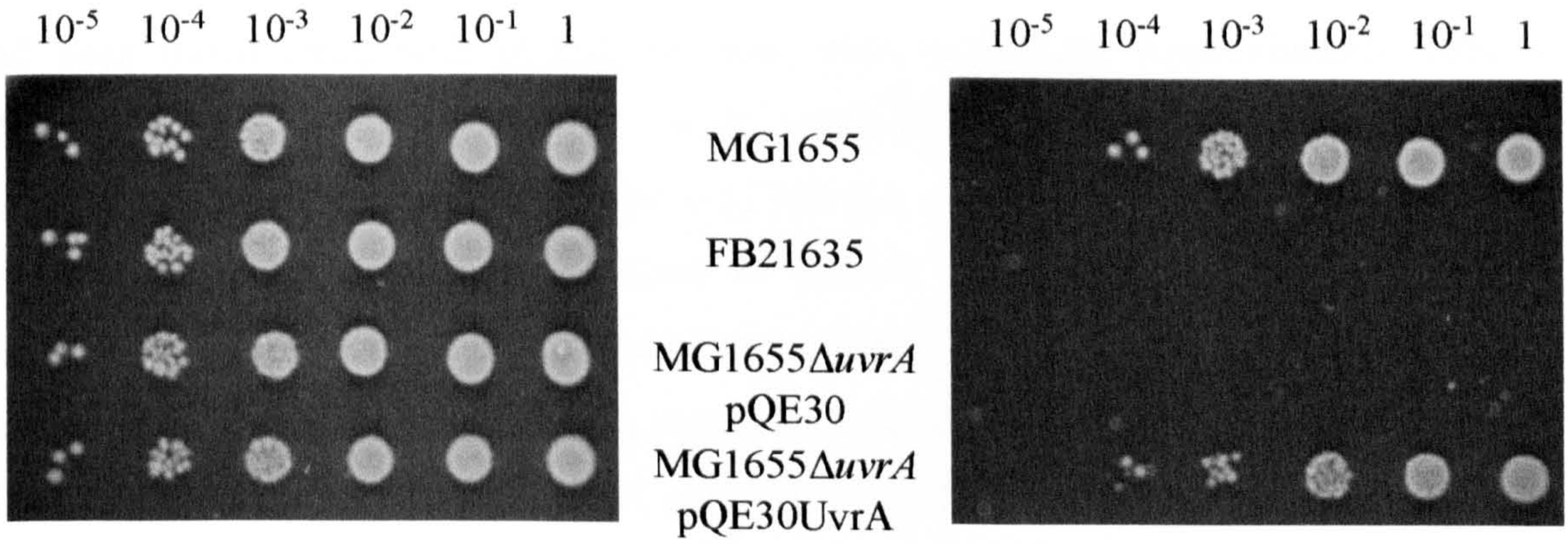

Figure 3.13 UV irradiation phenotype of *Escherichia coli* cells.

MG1655, FB21635, MG1655Δ*uvrA* pQE30 and MG1655Δ*uvrA* pQE30UvrA were grown at 37°C from culture until an A_{600} of 0.4 was obtained. The cells were harvested and suspended in M9 media. 1 ml of each culture was irradiated at 60 J/m^2 254 nm UV light and 10-fold serial dilutions of both the irradiated and the unirradiated cells were made. The serial dilutions were spotted (2 µl) on two LB agar plates and incubated overnight at 37°C.

had been transformed with pQE30 all died when irradiated. Approximately 10% of MG1655Δ*uvrA* cells transformed with pQE30UvrA survived irradiation. The MG1655Δ*uvrA* cells transformed with pQE30UvrA survived despite the absence of an inducer that should have been required to remove the Lac repressor. There was no significant difference detected between MG1655 and MG1655Δ*uvrA* pQE30UvrA cells indicating that histidine-tagged UvrA was able to substitute for wild-type UvrA. The UV resistant phenotype of MG1655Δ*uvrA* pQE30UvrA cells is due to the introduction of the plasmid copy of *uvrA*. The UV resistance was not because of the F′ episome or the backbone of pQE30. The difference in UV phenotype between MG1655Δ*uvrA* transformed with pQE30 or pQE30UvrA is sufficient to enable screening of UvrA mutants that are unable to complement the UV sensitive phenotype of Δ*uvrA* cells.

Identification of UvrA mutants

MG1655Δ*uvrA* cells were used as a basis to screen for mutants of UvrA that were unable to complement the cells UV sensitive phenotype. Two cycles of error-prone PCR were carried out on the 5′ region of *uvrA* that coded for the N-terminal 230 amino acids. These were cloned into pQE30UvrA on a BamHI/KpnI fragment to generate a library of mutant plasmids. Electrocompetent MG1655Δ*uvrA* cells were subsequently transformed with the mutant plasmids. The transformation mix was spread onto LB agar plates containing ampicillin and kanamycin and incubated overnight at 30°C. Two replica plates were made of which the first was irradiated with 20 J/m^2 254 nm UV light. Both the irradiated and the unirradiated plates were incubated overnight at 30°C. A total of approximately 2500 colonies grew on unirradiated plates of which 199 failed to grow on the irradiated plate (Figure 3.14). The 199 colonies that failed to grow on the irradiated plates contained pQE30UvrA plasmid derivatives that were unable to complement the MG1655Δ*uvrA* phenotype. Therefore it was assumed that the pQE30UvrA plasmids within these 199 colonies did not code for fully functional UvrA proteins. These 199 colonies were analysed further.

The next step was to identify which of the 199 colonies expressed full-length UvrA protein. A reason for the colonies being UV sensitive was if expression of full-length UvrA did not take place. During the error-prone PCR protocol mutations could have been introduced that would code for a stop codon or a frameshift within the 5′ region of UvrA.

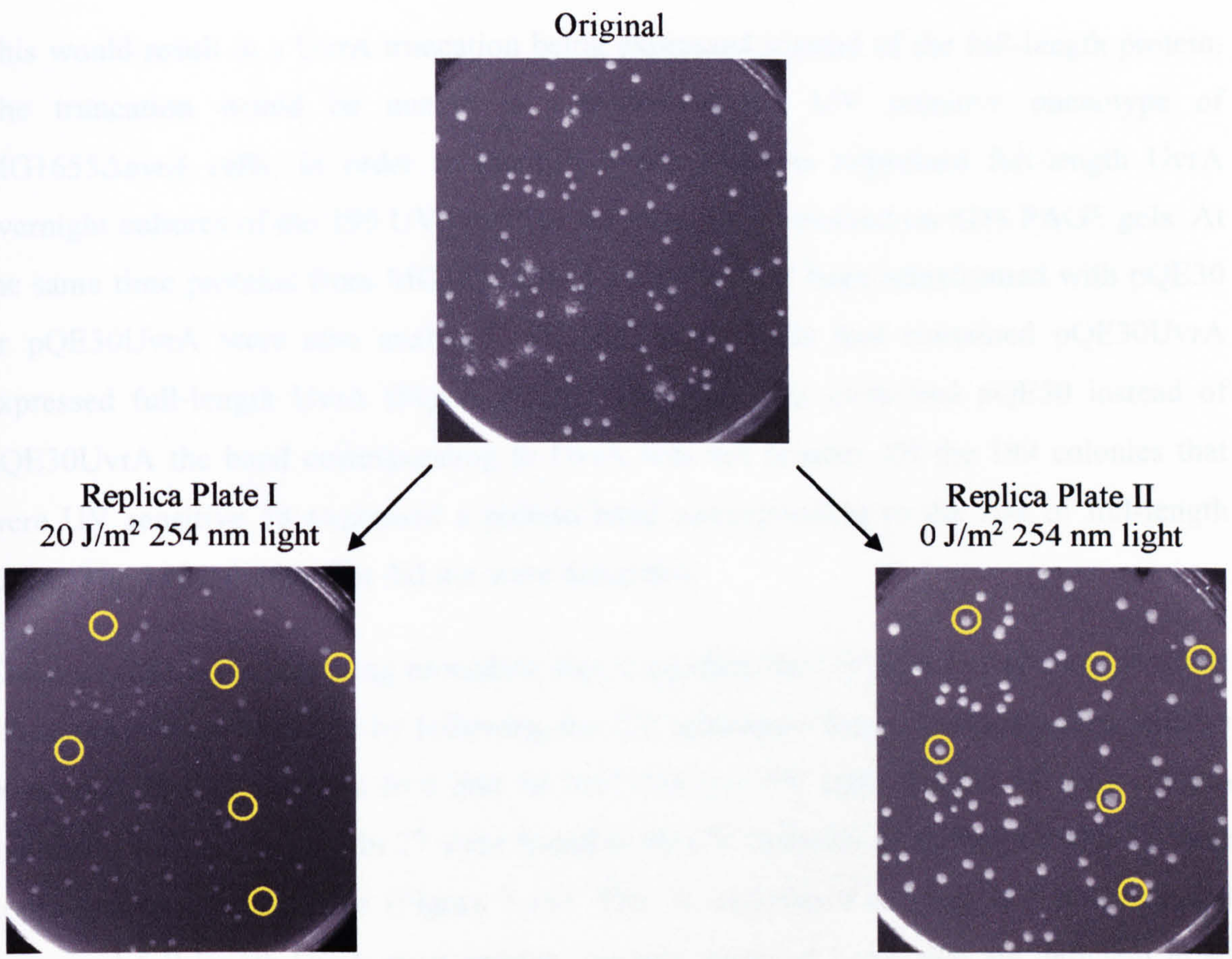

Figure 3.14 Screening for UV sensitive colonies.

MG1655Δ*uvrA* cells were transformed with a *uvrA* mutant library cloned into pQE30UvrA and incubated overnight at 37°C (original). Two replica plates of the overnight plate were produced. The first of these replicas was exposed to 20 J/m^2 254 nm UV light. Both plates were incubated at 30°C for 16 hours. Yellow circles indicate replica colonies that are present on replica plate II but are absent on the irradiated replica plate I indicating that they are UV sensitive.

This would result in a UvrA truncation being expressed instead of the full-length protein. The truncation would be unable to complement the UV sensitive phenotype of MG1655Δ*uvrA* cells. In order to identify which colonies expressed full-length UvrA overnight cultures of the 199 UV sensitive colonies were resolved on SDS PAGE gels. At the same time proteins from MG1655Δ*uvrA* cells that had been transformed with pQE30 or pQE30UvrA were also analysed. MG1655Δ*uvrA* cells that contained pQE30UvrA expressed full-length UvrA (Figure 3.15). When the cells contained pQE30 instead of pQE30UvrA the band corresponding to UvrA was not present. Of the 199 colonies that were UV sensitive 58 expressed a protein band corresponding to the size of full-length UvrA. The 141 colonies that did not were discarded.

The next step in the screening procedure was to confirm the UV sensitive phenotype of the 58 mutants. This was done by following the UV sensitivity assay irradiation then dilution protocol exposing the cells to 0 and 60 J/m^2 254 nm UV light. Of the 58 colonies that expressed full-length protein 27 were found to be UV resistant on reanalysis and 31 were confirmed as UV sensitive (Figure 3.16). The 31 colonies that were UV sensitive and expressed full-length UvrA must express mutated forms of UvrA that are deficient in an essential UvrA property. From an initial 2500 colonies 31 (1.2%) expressed a full-length copy of UvrA and were UV sensitive (Table 3.1). The plasmid DNA from the 31 clones was sequenced. Of the 31 clones 14 contained single point mutations, eight contained double point mutations seven contained multiple (>2) point mutations and two failed to sequence. The 14 single UvrA mutants encoded amino acid substitutions: RL023, GS034, SA038, SP038, FI064, FS064, LQ065, VD073, SY080, QL087, GR099, CR120, LP151 and KE159.

In vivo properties of UvrA mutants

As a result of the two screening procedures 20 single mutants of UvrA had been identified and required further characterisation. An UV survival assay was used to quantify the affect of each mutation on the UV resistant phenotype of MG1655Δ*uvrA* cells transformed with pQE30UvrA. In this assay the irradiation was applied after the cells had been diluted and spotted onto LB agar plates. A variety of irradiation doses were used in this assay instead of 60 J/m^2 that had been used in the screening procedures. Initially MG1655Δ*uvrA* cells were transformed with pQE30 or pQE30UvrA. The number of cells surviving different UV

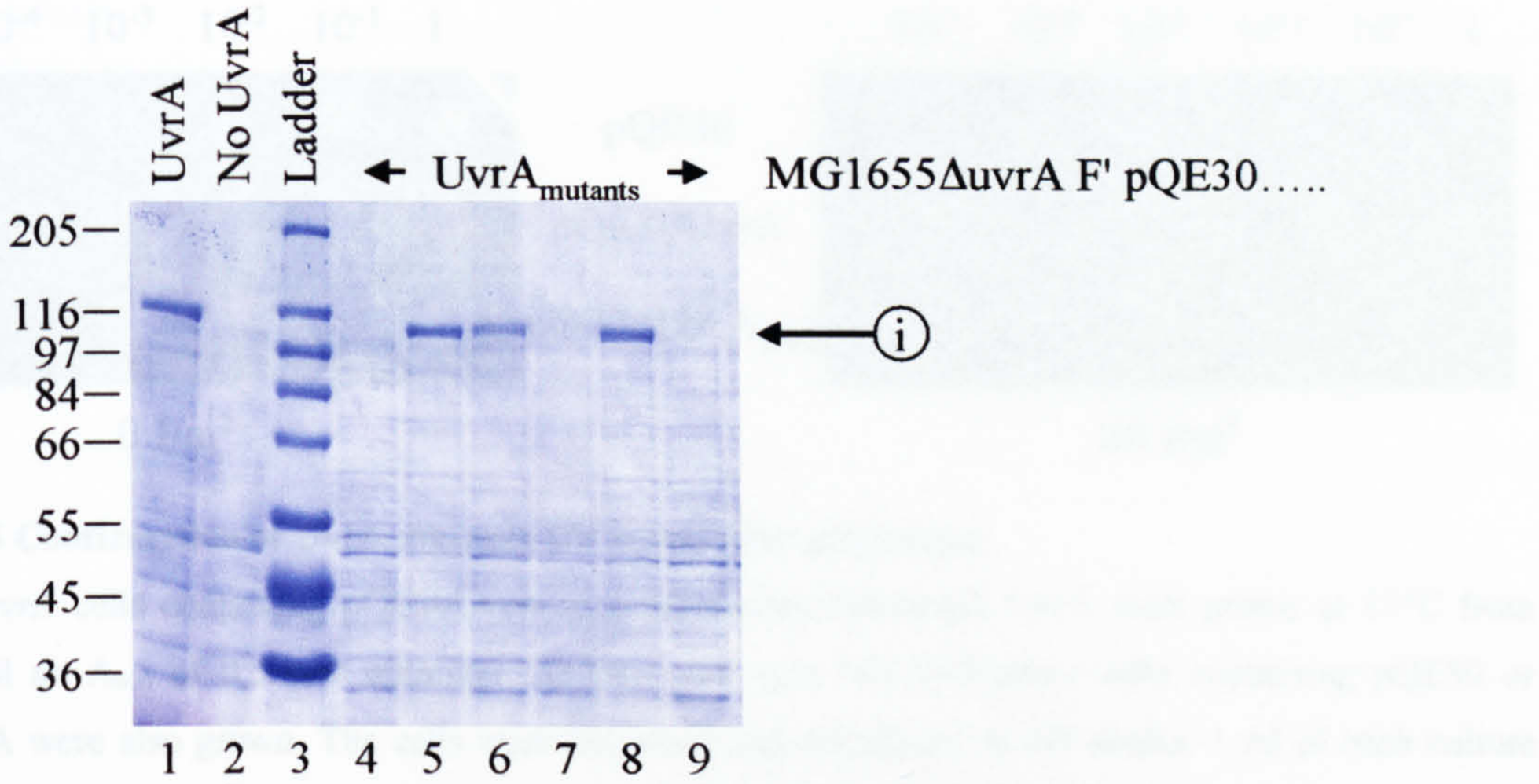

Figure 3.15 Protein expression of UV sensitive colonies.

MG1655Δ*uvrA* pQE30UvrA$_{mutants}$ that were identified as being UV sensitive were analysed for protein expression. Samples of overnight cultures were harvested, SDS PAGE loading dye added and heated to 95°C for five minutes. The samples were loaded onto a 10% SDS PAGE gel. MG1655Δ*uvrA* cells containing pQE30 or pQE30UvrA that do and do not express full-length UvrA were also loaded onto the gel. i, indicates the band corresponding to full-length UvrA. The ladder (kDa) is SigmaMarker.

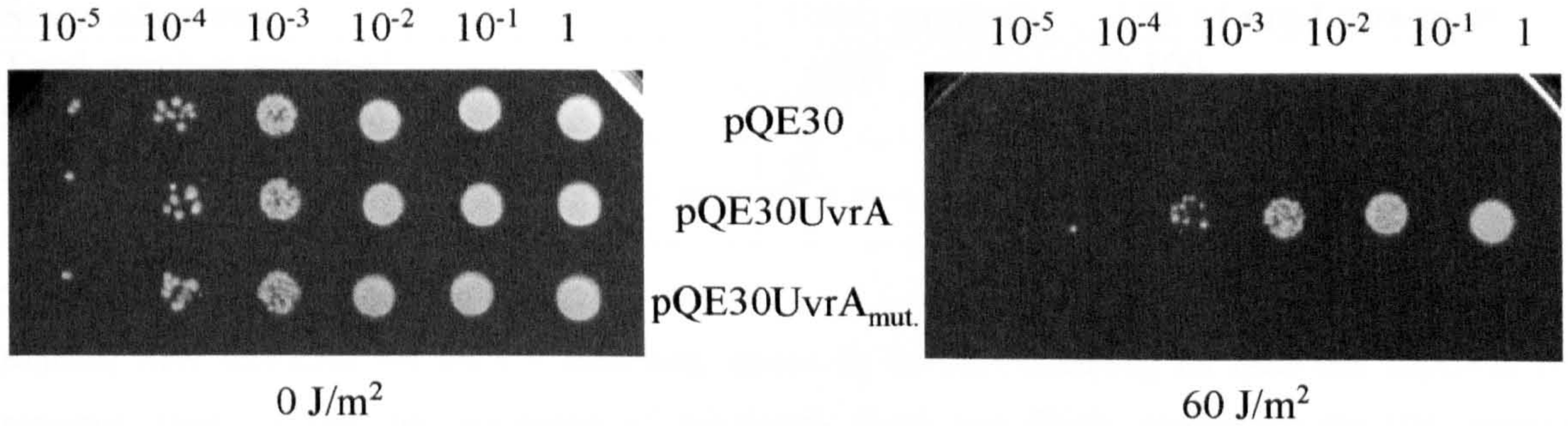

Figure 3.16 Confirmation of UvrA mutants UV irradiation phenotype.

MG1655Δ*uvrA* cells containing pQE30UvrA$_{mutants}$ expressing full-length UvrA were grown at 37°C from culture until an A_{600} of 0.5 was obtained. At the same time MG1655Δ*uvrA* cells containing pQE30 or pQE30UvrA were also grown. The cells were harvested and suspended in M9 media. 1 ml of each culture was irradiated at 60 J/m^2 254 nm UV light and 10-fold serial dilutions of both the irradiated and the unirradiated cells were made. The serial dilutions were spotted (2 µl) on two LB agar plates containing the appropriate antibiotics and incubated overnight at 30°C. Example plates are shown.

Stage of screen	Total number	% of total screened
Total number screened	~2500	100
Step 1 UV sensitive	199	8.0
Step 2 Full-length UvrA expressed	58	2.3
Step 3 UV sensitivity assay	31	1.2

Table 3.1 UV sensitivity screen statistics.

Mutants were identified via the UV sensitivity screen by initially screening for cells that appeared UV sensitive, then checking for expression of full-length UvrA and finally confirming the UV sensitive phenotype.

dosages was recorded, averaged and plotted on a log graph (Figure 3.17). MG1655Δ*uvrA* cells transformed with pQE30 struggled to survive UV irradiation greater than 4 J/m^2. MG1655Δ*uvrA* cells transformed with pQE30UvrA were able to survive UV irradiation. A dose of 24 J/m^2 saw a 100-fold reduction in survival.

Before the UV phenotype of cells expressing the UvrA mutants could be analysed the UvrA mutations identified from the bacterial two-hybrid screen needed to be transferred to the full-length gene. The region of *uvrA* encoding the identified mutation was amplified by PCR, cloned into pQE30UvrA on a BamHI/KpnI fragment and sequenced.

The UV irradiation phenotype of all mutants from both the bacterial two-hybrid and UV sensitivity screen were analysed quantitatively. MG1655Δ*uvrA* cells were transformed with the pQE30UvrA mutant plasmids or the control plasmids pQE30 and pQE30UvrA and UV survival assays carried out as above. The cells were exposed to seven different dosages of UV ranging from 0 to 24 J/m^2 and incubated overnight at 30°C. The cells were counted and plotted on log graphs (Figure 3.18) (the results from cells that did and did not express wild-type UvrA are as shown in Figure 3.17). The mutants fall into three categories. The six mutants identified from the bacterial two-hybrid assay ($UvrA_{LH151}$, $UvrA_{GD173}$, $UvrA_{YC174}$, $UvrA_{EV201}$, $UvrA_{VE202}$ and $UvrA_{DG205}$) conferred UV resistance to the cells (*uvrA*$^+$). $UvrA_{SP038}$ and $UvrA_{GR099}$ (isolated on the basis of their UV sensitivity) were unable to confer any UV resistance to the cells (Δ*uvrA*). Cells that expressed either $UvrA_{RL023}$, $UvrA_{GS034}$, $UvrA_{SA038}$, $UvrA_{FI064}$, $UvrA_{FS064}$, $UvrA_{LQ065}$, $UvrA_{VD073}$, $UvrA_{SY080}$, $UvrA_{QL087}$, $UvrA_{CR120}$, $UvrA_{LP151}$ or $UvrA_{KE159}$ (all isolated on the basis of UV sensitivity) were 10 to 1000-fold more sensitive than cells expressing wild-type UvrA but did confer some UV resistance to the cells.

Discussion

A total of 17 UvrA residues have been identified that are important for UvrA function. Of these five were uniquely identified from the bacterial two-hybrid screen, 11 were uniquely identified from the UV sensitivity screen and one residue (L151) was identified from both screens.

The bacterial two-hybrid screen was designed to identify a UvrA-UvrB interaction and a UvrA-Mfd interaction. Several truncations of UvrA were tested within the system.

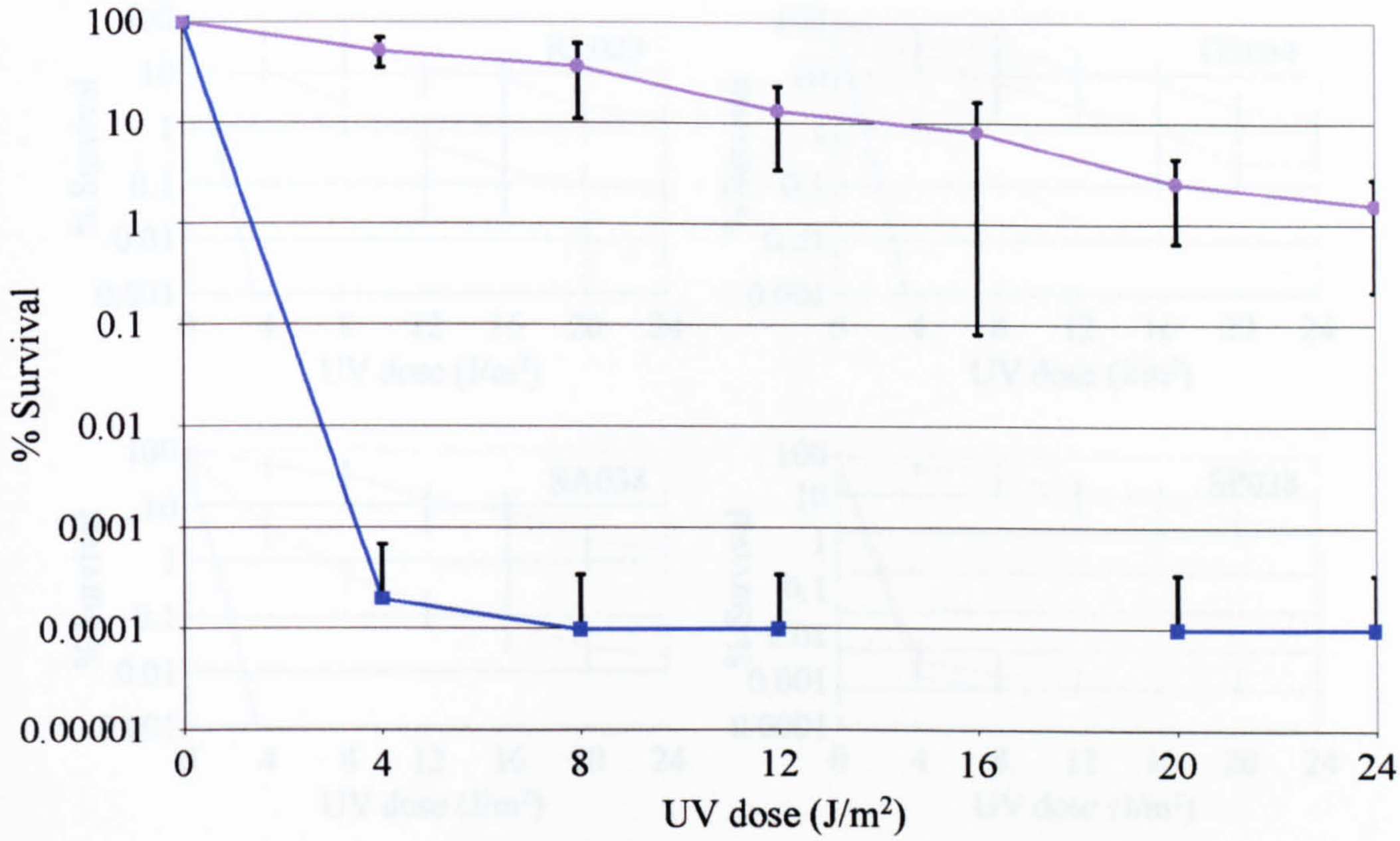

Figure 3.17 UV sensitivity.

UV irradiation phenotype of MG1655Δ*uvrA* cells transformed with pQE30 (blue) or pQE30UvrA (purple). Spot assays were used in which cells were 10-fold serial diluted, spotted onto 21 LB agar plates containing kanamycin and ampicillin and then exposed to UV irradiation for differing times (three plates for each time period). The number of colonies in the most diluted viable spots were counted. Each individual assay result was an average of three spots (one spot from each plate) and each assay was carried out five times. A survival of 0.0001% would correspond to one individual colony present in the undiluted spot. No colonies were present for MG1655Δ*uvrA* cells transformed with pQE30 and irradiated at 16 J/m^2.

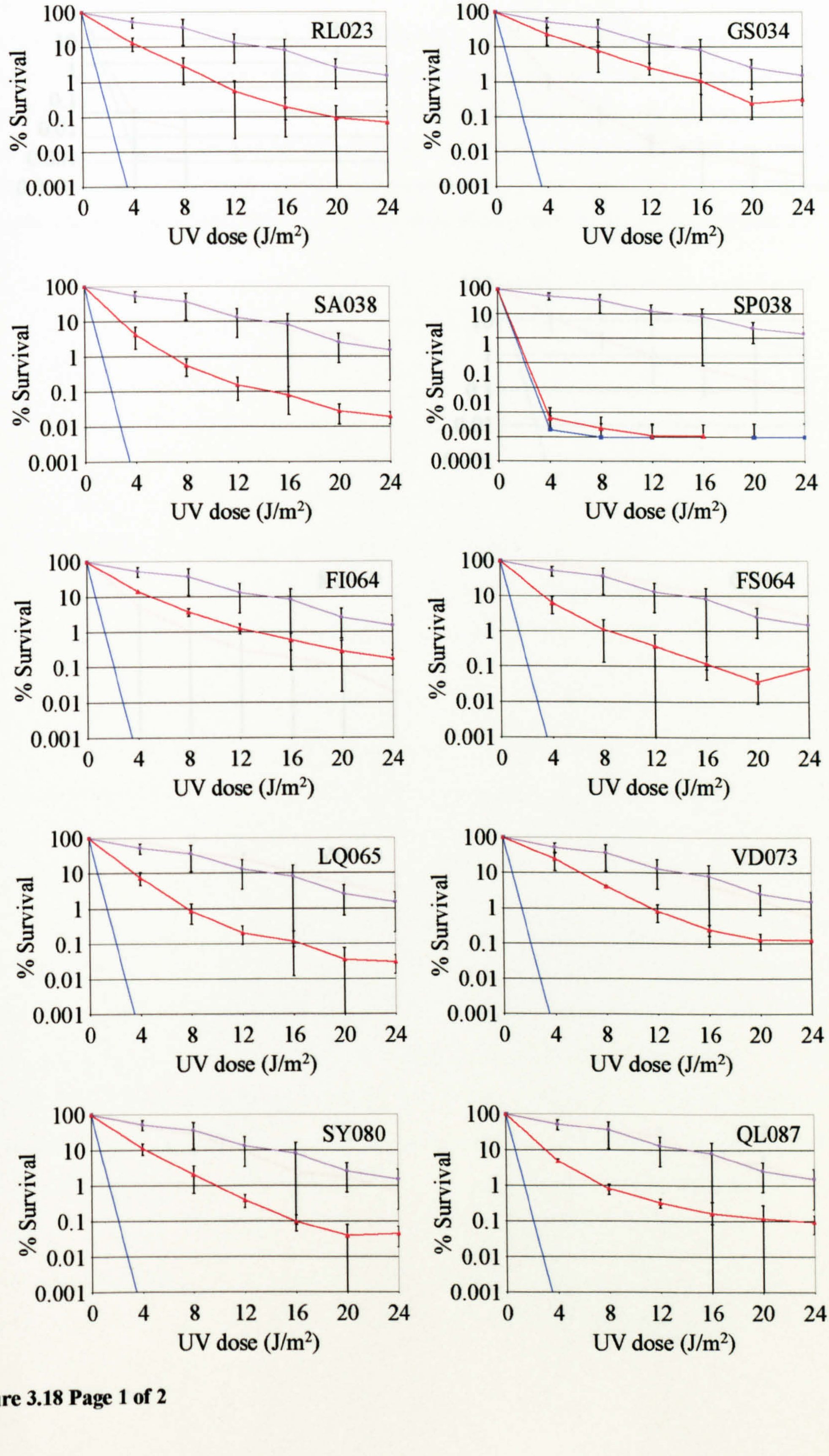

Figure 3.18 Page 1 of 2

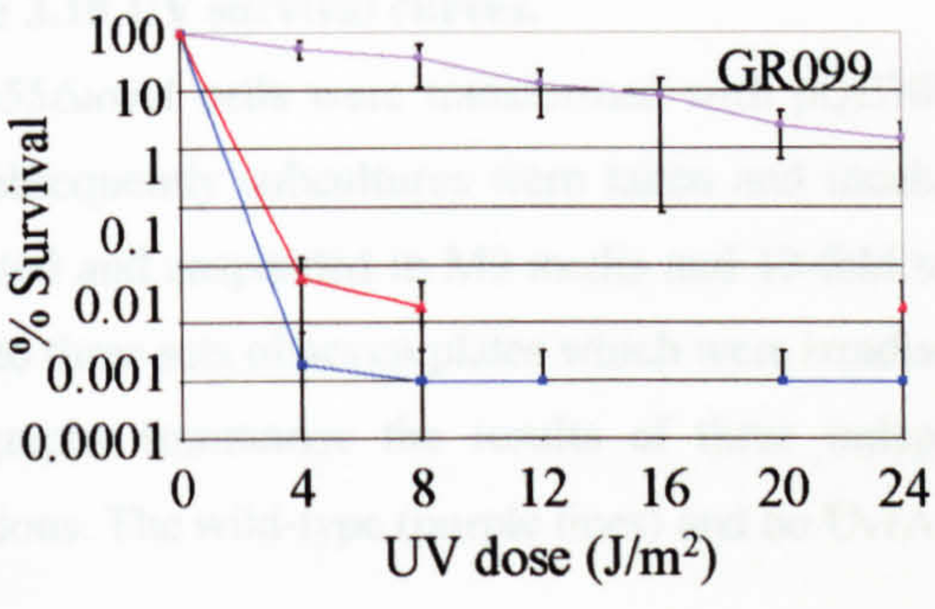

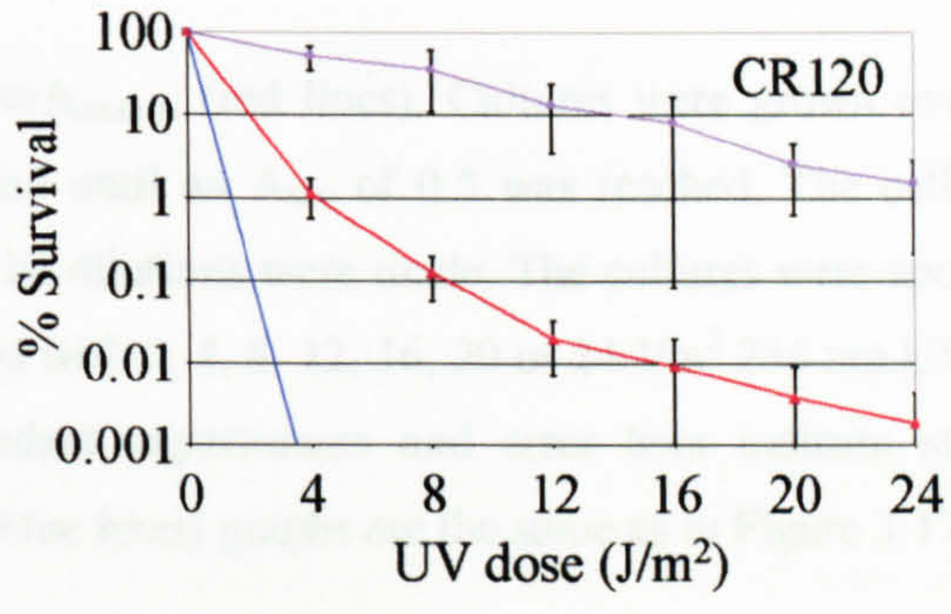

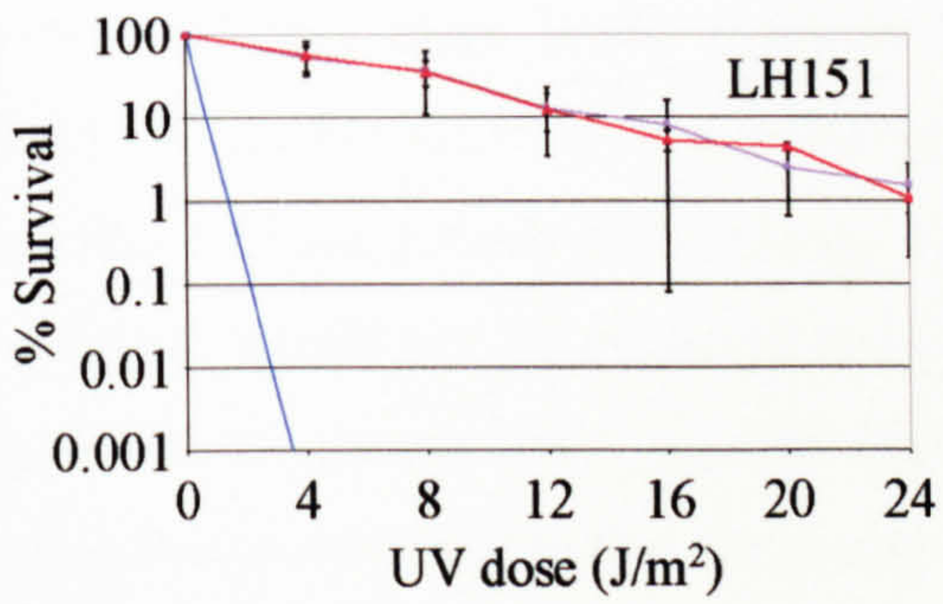

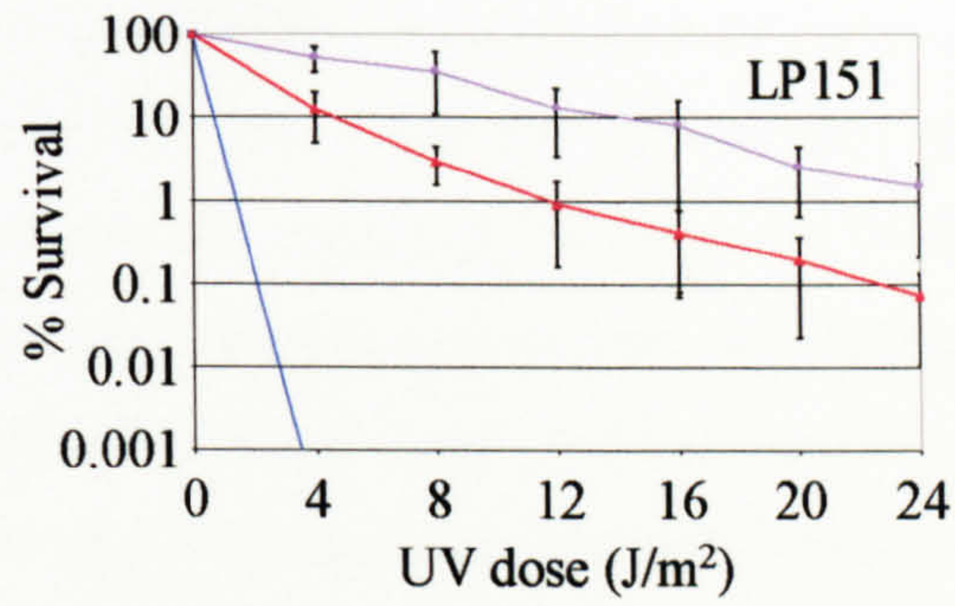

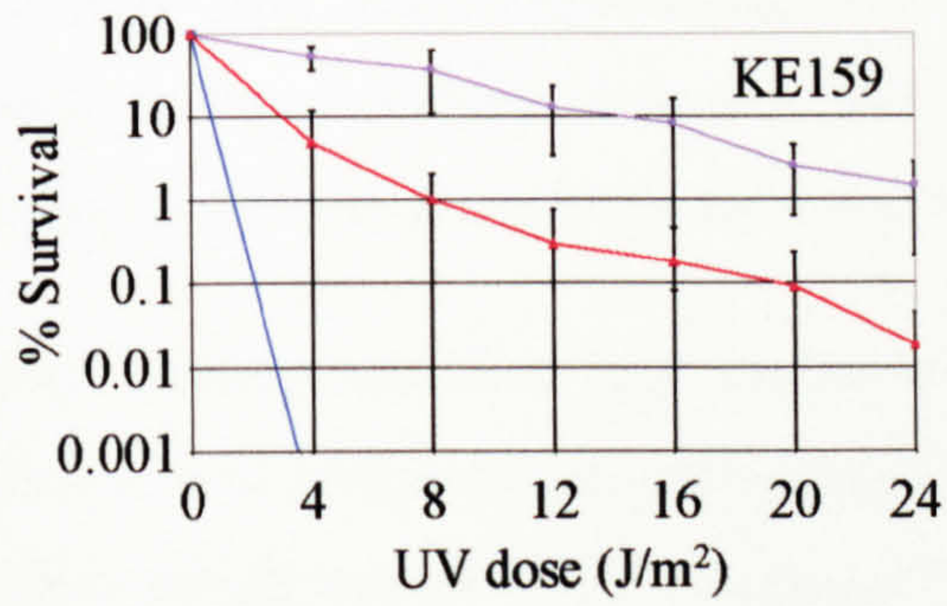

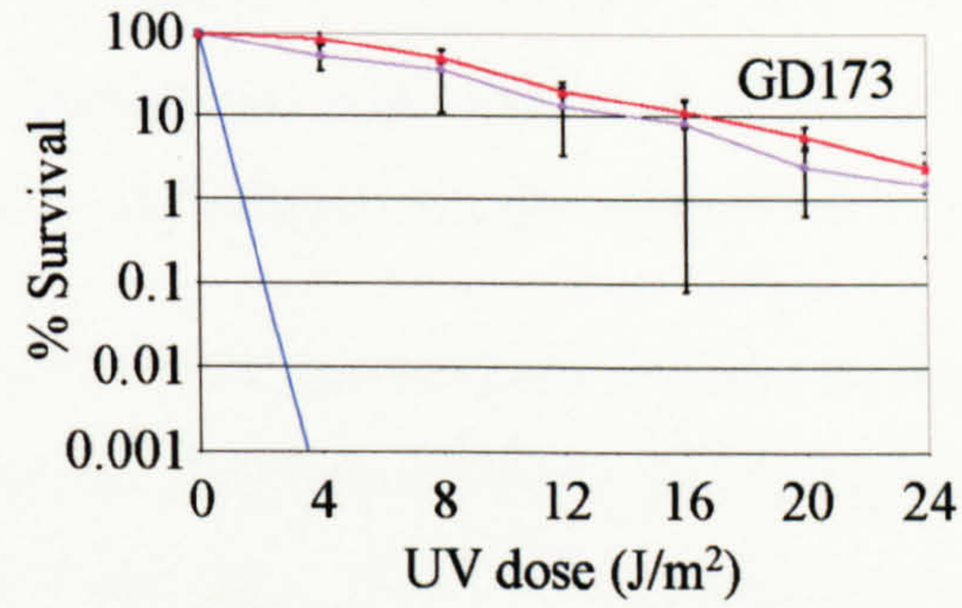

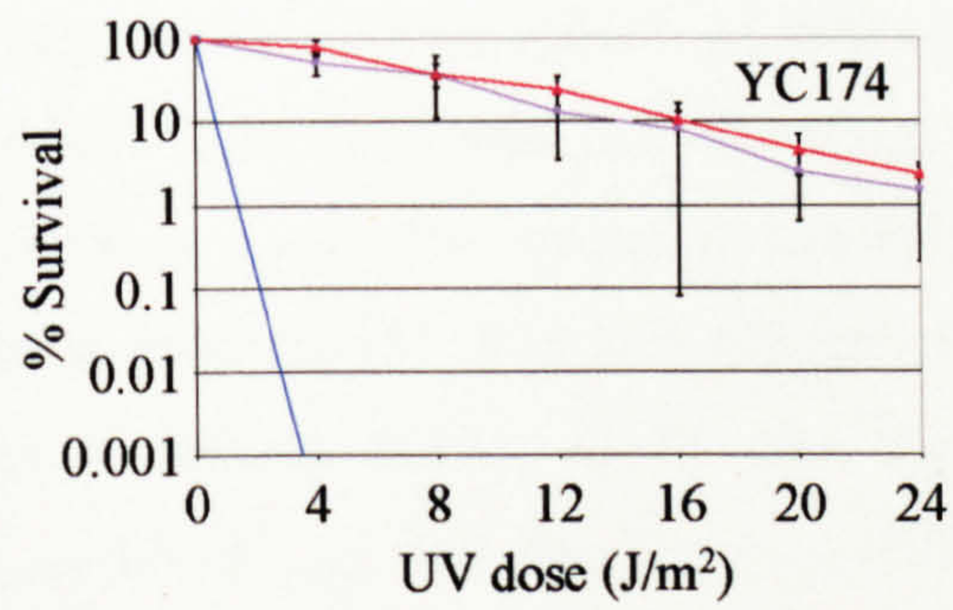

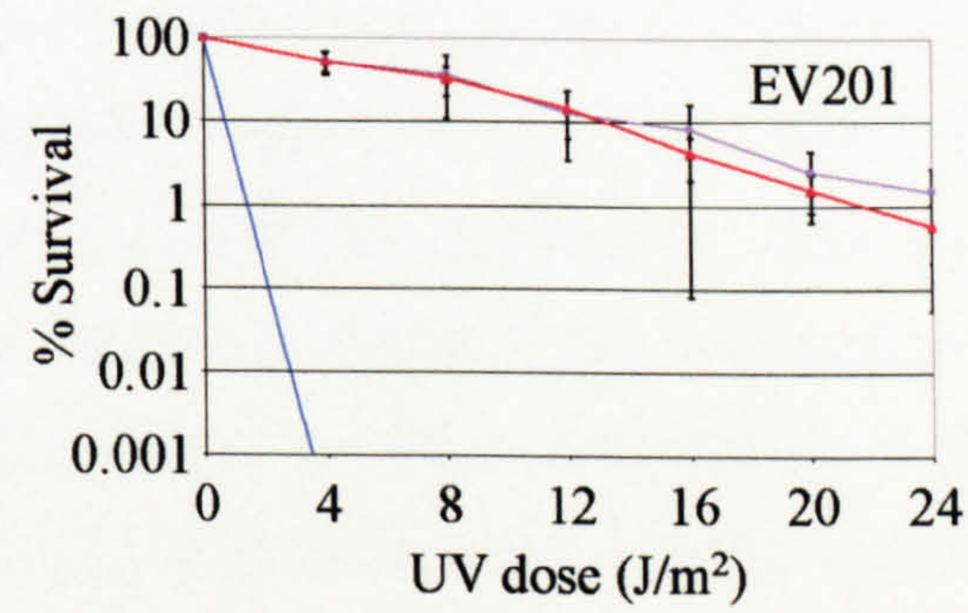

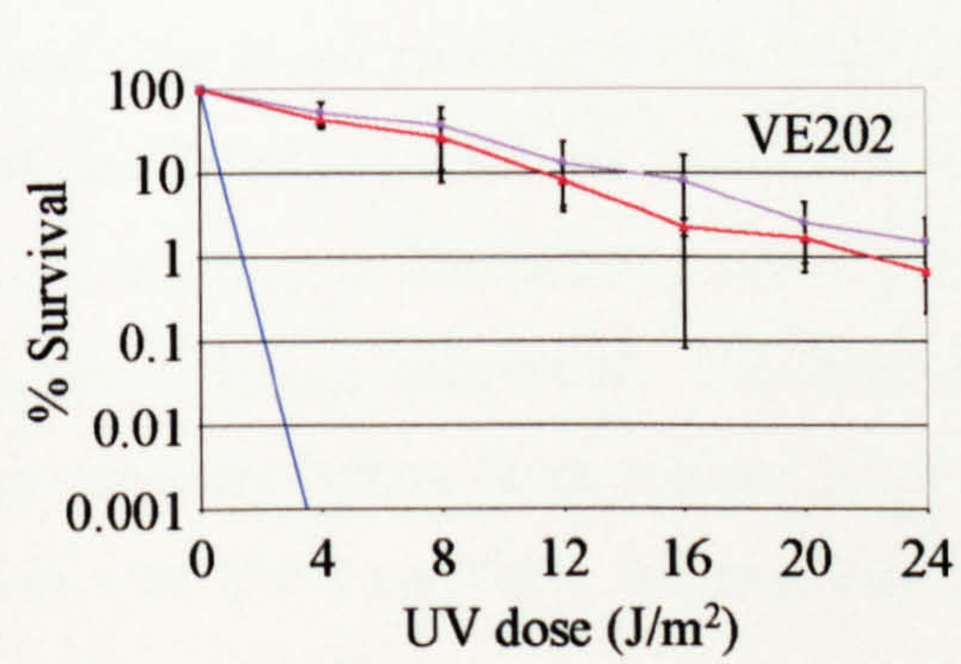

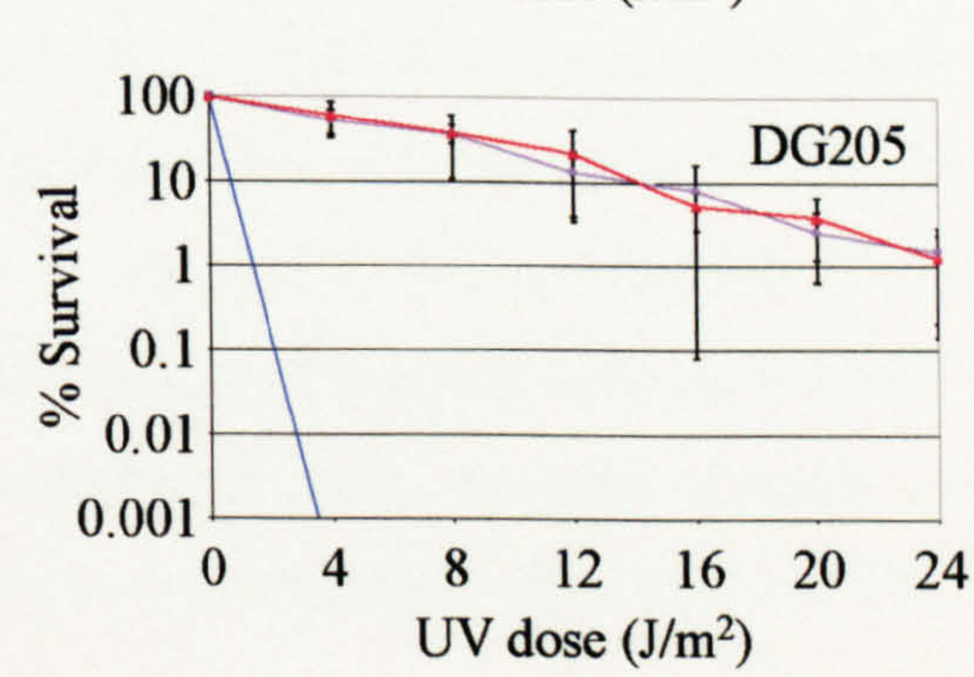

Figure 3.18 Page 2 of 2

Figure 3.18 UV survival curves.

MG1655Δ*uvrA* cells were transformed with pQE30UvrA$_{mutants}$ (red lines). Cultures were grown overnight and subsequently subcultures were taken and incubated until an A_{600} of 0.5 was reached. The cells were harvested and suspended in M9 media and 10-fold serial dilutions were made. The cultures were spotted (2 µl) onto three sets of seven plates which were irradiated with 0, 4, 8, 12, 16, 20 or 24 J/m^2 254 nm UV light. The graphs summarise the results of three independent experiments and error bars indicate standard deviations. The wild-type (purple lines) and no UvrA (blue lines) graphs are the same as in Figure 3.17.

$UvrA_{1-252}$ was able to interact with the truncation of UvrB and the truncation of Mfd to give a detectable phenotype. Thus this region of UvrA was taken as the basis for the bacterial two-hybrid screen. Interestingly the region of UvrA that had previously been proposed to interact with UvrB ($UvrA_{1-230}$) was unable to interact with either truncation of UvrB or Mfd to give a detectable phenotype (Claassen and Grossman, 1991). The evidence to suggest that $UvrA_{1-230}$ is involved in the UvrA-UvrB interaction was based on the results of an ATPase assay. In this assay an ATPase deficient mutant of UvrB ($UvrB_{KA045}$) stimulated the activity of wild-type full-length UvrA. This UvrB mutant was also able to stimulate the ATPase activity of $UvrA_{1-230}$. However this region of UvrA lacks a Walker B motif and thus would not be expected to hydrolyse ATP with or without the presence of $UvrB_{KA045}$. In this assay $UvrA_{1-230}$ had been purified from *uvrA*$^+$ cells (Claassen *et al.*, 1991). It is therefore possible that the low level of ATPase activity detected in the absence of $UvrB_{KA045}$ was due to contamination by full-length UvrA. If this is true then the increased ATPase activity detected when $UvrB_{KA045}$ was added to the $UvrA_{1-230}$ preparation is actually more likely to be due to the stimulation of full-length UvrA.

The UvrA mutants identified from the bacterial two-hybrid screen fall into two categories: those that almost completely disrupted the $UvrA_{1-252}$-$UvrB_{35-252}$ and the $UvrA_{1-252}$-Mfd_{1-219} interaction which include $UvrA_{1-252.LH151}$, $UvrA_{1-252.GD173}$ and $UvrA_{1-252.VE202}$; and those that disrupted the $UvrA_{1-252}$-Mfd_{1-219} interaction but were still capable to some degree of forming the $UvrA_{1-252}$-$UvrB_{35-252}$ interaction which include $UvrA_{1-252.YC174}$, $UvrA_{1-252.EV201}$ and $UvrA_{1-252.DG205}$. The bacterial two-hybrid mutants are clustered in three patches centred at residues 151, 173 and 203 (purple residues in Figure 3.19). All three patches contain a residue (L151, G173 and V202) whose mutation resulted in both the $UvrA_{1-252}$-$UvrB_{35-252}$ and the $UvrA_{1-252}$-Mfd_{1-219} interactions being almost completely disrupted. The UvrA residues Y174, E201 and D205, which when mutated resulted in the loss of the $UvrA_{1-252}$-Mfd_{1-219} interaction but were still able to partially maintain the $UvrA_{1-252}$-$UvrB_{35-252}$ interaction, could play a supportive but unessential role in the $UvrA_{1-252}$-$UvrB_{35-252}$ interaction. The three different patches could indicate that the UvrA tertiary structure brings these regions close together to form one patch through which it interacts with UvrB and Mfd. Alternatively UvrA could interact with UvrB and Mfd via a variety of structurally separated sites.

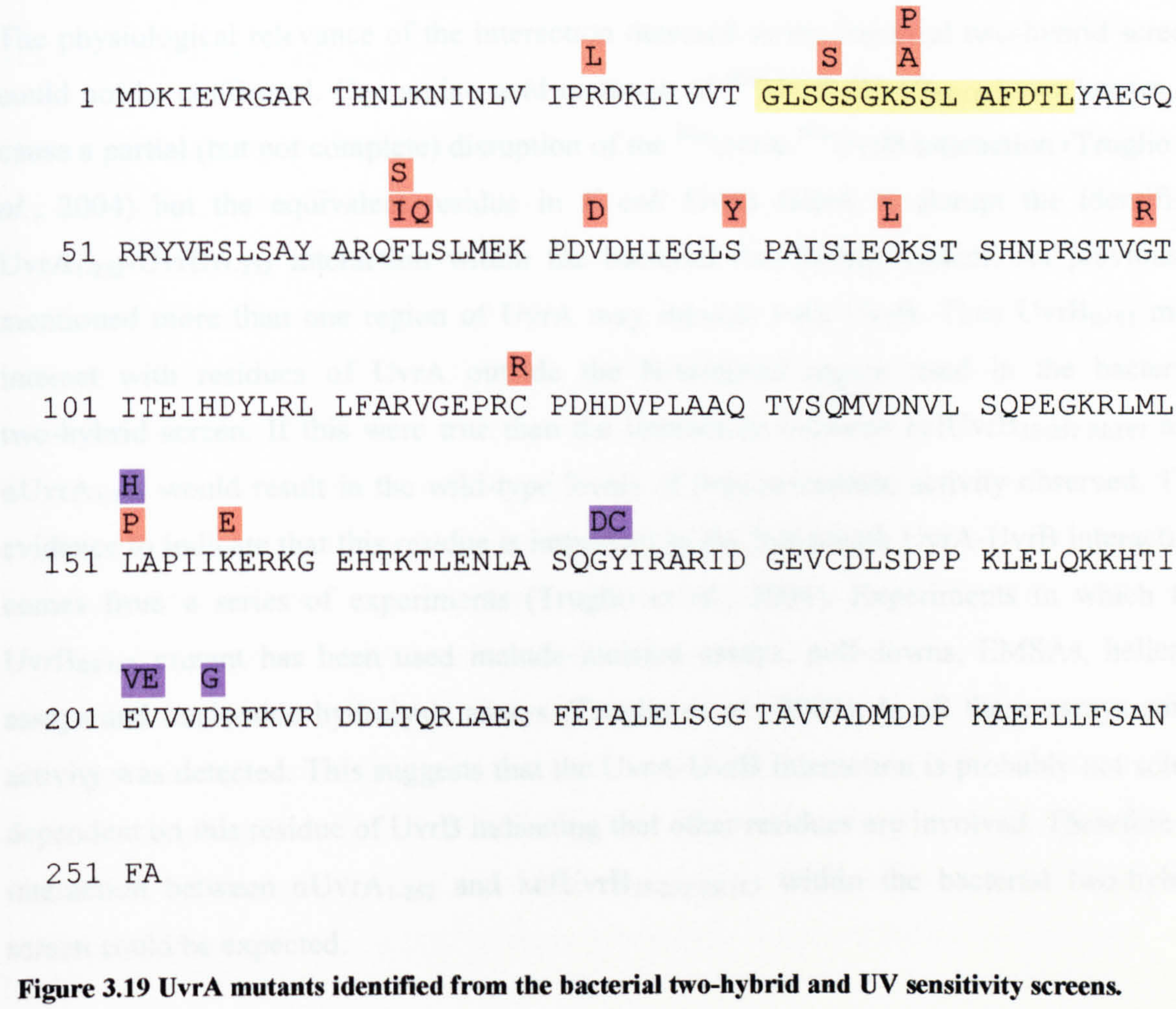

Figure 3.19 UvrA mutants identified from the bacterial two-hybrid and UV sensitivity screens.

The amino acid sequence of the NTD of UvrA, which was subjected to random mutagenesis, is indicated. Purple boxes above the sequence indicate the UvrA mutations identified from the bacterial two-hybrid screen. Orange boxes above the protein sequence indicate the UvrA mutations identified from the UV sensitivity screen. The yellow box corresponds to the Walker A motif.

The physiological relevance of the interaction detected in the bacterial two-hybrid screen could not be confirmed. One amino acid mutation of ^{Bca}UvrB ($UvrB_{RE183}$) was known to cause a partial (but not complete) disruption of the ^{Bca}UvrA-^{Bca}UvrB interaction (Truglio *et al.*, 2004) but the equivalent residue in *E. coli* UvrB failed to disrupt the identified $UvrA_{1-252}$-$UvrB_{35-252}$ interaction within the bacterial two-hybrid system. As previously mentioned more than one region of UvrA may interact with UvrB. Thus $UvrB_{R183}$ may interact with residues of UvrA outside the N-terminal region used in the bacterial two-hybrid screen. If this were true then the interaction between $\lambda cIUvrB_{35-252.RE183}$ and $\alpha UvrA_{1-252}$ would result in the wild-type levels of β-galactosidase activity observed. The evidence to indicate that this residue is important in the full-length UvrA-UvrB interaction comes from a series of experiments (Truglio *et al.*, 2004). Experiments in which the $UvrB_{RE183}$ mutant has been used include incision assays, pull-downs, EMSAs, helicase assays and nucleotide hydrolysis assays (Truglio *et al.*, 2004). In all these assays some activity was detected. This suggests that the UvrA-UvrB interaction is probably not solely dependent on this residue of UvrB indicating that other residues are involved. Therefore an interaction between $\alpha UvrA_{1-252}$ and $\lambda cIUvrB_{35-252.RE183}$ within the bacterial two-hybrid screen could be expected.

The inability of $UvrB_{RA213}$ to interrupt the bacterial two-hybrid interaction was expected as a double mutant within *B. caldotenax* UvrB (in which the equivalent residue was mutated) ($UvrB_{RA213+EA215}$) had little effect on the UvrA-UvrB interaction detected by EMSAs (Truglio *et al.*, 2004).

When the six substitutions identified from the bacterial two-hybrid screen were transferred into full-length UvrA they are all are able to confer UV resistance to Δ*uvrA* cells. An explanation for this is that the UvrA mutants are overexpressed compared to the expression of chromosomal wild-type UvrA (in $uvrA^+$ cells). The high expression levels could compensate for an interaction affinity defect associated with these mutants. Alternatively, the UV resistant phenotype could indicate that other regions of each protein interact *in vivo* and that these interactions are sufficient to enable wild-type levels of NER to take place. A further region of UvrB (domain 4) has been implicated in binding full-length UvrA (Hsu *et al.*, 1995). It is possible that further regions of UvrA are also involved in the UvrA-UvrB interaction. Additional interactions between the proteins may help to stabilise the

interaction detected in the bacterial two-hybrid screen, eliminating the effect of the mutations within the full-length protein.

The region encoding the N-terminal 230 amino acids of UvrA was randomly mutagenized as part of the UV sensitivity screen. However all 12 single amino acid mutants that were identified in this screen were between residue 23 and 159 with nine of the 12 in the N-terminal 100 amino acids (orange residues in Figure 3.19). Two UvrA residues, S38 and F64, were each identified by two different single point mutants. As expected some (three) mutations were present within the Walker A region. Mutations within the Walker A region would be expected to have low or no ATPase activity and therefore would be unable to support NER, essential for a UV resistant phenotype. The identification of the Walker A mutants confirmed that the screen was working as expected and was identifying mutants that altered essential properties of UvrA. Interestingly there was very little overlap between the residues identified in the UV sensitivity screen and the residues identified from the bacterial two-hybrid screen. However residue L151 was identified from both screens indicating that the bacterial two-hybrid screen may be physiologically relevant. The mutants identified from the UV sensitivity screen could be deficient in any number of different functions. The properties of these mutants are discussed further in chapter 5.

CHAPTER 4

PROTEIN PURIFICATION AND ASSAY DEVELOPMENT

Introduction

In vitro assays are useful tools in understanding the biochemical nature of protein-protein interactions. Therefore the UvrA mutant proteins identified in the previous chapter were characterised *in vitro*. Bulky DNA damage can be incised *in vitro* by the combined action of UvrA, UvrB and UvrC in the presence of Mg^{2+} and ATP (Seeberg *et al.*, 1976) (Sancar and Rupp, 1983) (Yeung *et al.*, 1983). UvrA, UvrB and UvrC have each been purified to homogeneity by other groups (Seeberg and Steinum, 1982) (Thomas *et al.*, 1985) (Yeung *et al.*, 1986b). It was important to develop a simple and reproducible purification protocol for UvrA, UvrB and UvrC that could also be used to purify the mutant proteins. One of the simplest ways to achieve this would be to introduce a tag. The addition of extra amino acids could potentially alter the structure and function of the protein of interest. Therefore it would be important that tagged proteins were assayed for their expected functions. Many tagged proteins function normally (Yin and Proteau, 2003) and thus tagging the NER proteins is a potential way of establishing quick and simple purification procedures. In the previous chapter, results of *in vivo* experiments indicated that histidine-tagged UvrA could complement Δ*uvrA* cells.

The combined action of UvrA, UvrB and UvrC should result in incision of DNA both 3′ and 5′ of bulky damage (Sancar and Rupp, 1983). *In vitro* the UvrABC protein complex has previously been shown to incise DNA containing a variety of bulky lesions including CPDs (Sancar and Rupp, 1983), cholesterol (Moolenaar *et al.*, 1998a) and fluorescein (Skorvaga *et al.*, 2004). To study NER and TCR it would be ideal to have one modification in all DNA molecules at a specified site. Irradiating DNA with UV light is one way of introducing damage. However the type, position and number of damage sites will vary between the DNA molecules within the same experiment. This can make the interpretation of results difficult. A second way to introduce damage is to use direct chemical methods to synthesise oligonucleotides to contain specific lesions such as cholesterol and fluorescein. This method results in the molecules being identical but the DNA fragment size is restricted. The modified oligonucleotides can be used to generate longer fragments using PCR. This will enable extension 3′ of the lesion but the length of the DNA 5′ to the lesion is still restricted. These methods were therefore not ideal to introduce a single site of damage within a transcriptional unit to study the process of TCR. To study NER and TCR identical modified large DNA fragments were required. The modification had to be

recognised as a site of damage by the NER proteins and also had to act as a substrate for TCR assays by causing RNAP to stall. In a novel method sequence-specific methyltransferase induced labelling (SMILing), that can be used to introduce modifications at specific DNA sequences, was used to introduce a modification to a single specified base within a plasmid.

Purification of UvrA, UvrB and UvrC

For *in vitro* NER based assays UvrA, UvrB and UvrC were required. Therefore the genes were cloned in-frame downstream of a sequence encoding a hexa-histidine tag. The expressed UvrA, UvrB and UvrC proteins would consequently have a N-terminal hexa-histidine label. This hexa-histidine tag would enable simple purification over one FPLC column using the strong binding affinity histidine residues have for metal ions such as Ni^{2+}.

Cloning of uvrA, uvrB, and uvrC

To enable expression and purification of UvrA, UvrB and UvrC, *uvrA*, *uvrB* and *uvrC* were cloned into plasmids. The plasmids pBSIIUvrA, pBSIIUvrB and pBSIIUvr$C_{23\text{-}610}$ contained the gene sequences for *uvrA*, *uvrB* and all but the 5′ 56 nucleotides of *uvrC* that had each been amplified by PCR from the genomic DNA of *E. coli* strain MG1655. The 5′ region of the *uvrC* gene from the genomic DNA of *E. coli* strain MG1655 was amplified and cloned into pBSIIUvr$C_{23\text{-}610}$ to generate pBSIIUvrC as described in chapter 2. The PCR amplified complete *uvrA*, *uvrB* and *uvrC* genes were sequenced within the pBSII plasmids. The genes were then cloned into the commercially available expression vector pQE30 on a BamHI/HindIII fragment. The genes were cloned so that they were in-frame and downstream of the hexa-histidine coding sequence present within the plasmid. Upstream of the hexa-histidine coding sequence there was a T5 promoter that could be recognised and bound by *E. coli* RNAP. Overlapping the T5 promoter was a *lac* operator site enabling transcription of the gene of interest to be controlled. Therefore plasmids had been generated that would allow the controlled expression of N-terminal hexa-histidine labelled UvrA, UvrB and UvrC.

Expression of histidine-tagged UvrA, UvrB and UvrC

It was necessary to determine the conditions required for protein expression of UvrA, UvrB and UvrC. XL1-Blue cells, which carry the *lacI*^{q} gene on a F′ episome, were transformed with plasmids pQE30UvrA or pQE30UvrB. Cultures were incubated overnight and then duplicate subcultures were set up, one of which contained 1 mM IPTG. The cultures were incubated at 37°C overnight and then expression levels of UvrA and UvrB were analysed on SDS PAGE gels (data not shown). Expression of UvrA and UvrB was detected but interestingly these proteins were only seen when the cultures had not been induced.

The expression of UvrA and UvrB seen in the uninduced XL1-Blue cultures was unexpected. The system was designed so that transcription of the gene would be repressed without the addition of the inducer, IPTG. In principle the Lac repressor protein should have been abundant due to *lacI*^{q}. The Lac repressor should have bound to the operator site preventing RNAP from binding and transcribing the genes of interest. For expression to be detected in the uninduced system RNAP must have been able to transcribe the gene. Therefore the Lac repressor can not have been tightly bound to the operator site if it was bound at all. This could indicate that an inducer such as lactose was present.

It was also unexpected to see lower or no expression of UvrA and UvrB in the induced cultures than the uninduced cultures. Addition of IPTG should have resulted in the release of Lac repressor from the operator site allowing RNAP to transcribe the genes of interest. An explanation for the reduced protein expression seen in the induced cultures could be due to the Uvr proteins being toxic to the cells in amounts greater than their uninduced levels.

Further analysis of the XL1-Blue cultures containing pQE30UvrA or pQE30UvrB revealed that the highest level of protein expression was seen in cultures that had been incubated from a single colony for 16 hours at 37°C without induction. Figure 4.1 indicates typical levels of UvrA, UvrB and UvrC expression from cultures of XL1-Blue cells containing pQE30UvrA, pQE30UvrB and pQE30UvrC respectively after a 16 hour incubation at 37°C. Bands corresponding to the correct MW for each protein (UvrA 104 kDa, UvrB 76 kDa, UvrC 70 kDa) were easily detected. UvrA and UvrB were expressed at

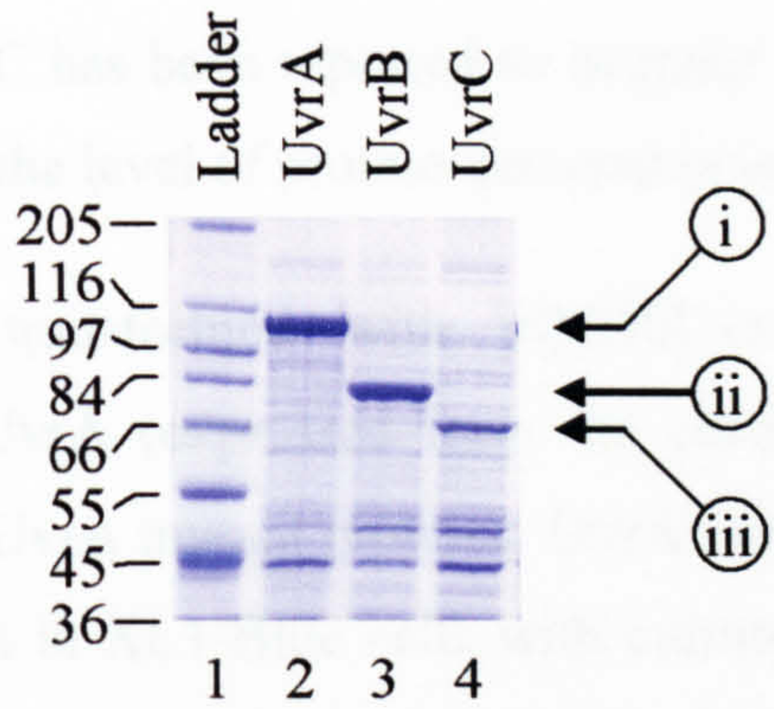

Figure 4.1 UvrA, UvrB and UvrC expression levels.

A single colony of XL1-Blue *E. coli* cells that had been transformed with plasmid pQE30UvrA, pQE30UvrB or pQE30UvrC was incubated at 37°C for 16 hours in 100 ml LB broth supplemented with ampicillin and tetracycline. A small sample ($1000/A_{600}$ µl) was harvested. The pellet was suspended in 100 µl protein sample buffer and incubated at 95°C for five minutes. The samples (5 µl) were resolved on a 10% SDS PAGE gel. i, ii, and iii correspond to the expected size for UvrA, UvrB and UvrC respectively. The ladder (kDa) used was SigmaMarker.

a higher level than UvrC. UvrC has been reported to degrade faster than UvrA and UvrB and thus it is unsurprising that the level of protein detected is lower (Thomas *et al.*, 1985).

MG1655Δ*uvrA* cells were transformed with pQE30UvrA. This was to prevent contamination by wild-type UvrA (expressed from the chromosome), which would be important when purifying the UvrA mutant proteins. UvrA expression was achieved in the same way as UvrA expression in XL1-Blue cells with cultures incubated at 37°C for 16 hours. Similar levels of expression were seen for the wild-type UvrA protein in both XL1-Blue and MG1655Δ*uvrA* cells (data not shown). The expression level of all three proteins was sufficient to attempt protein purification.

Purification of UvrA, UvrB and UvrC

UvrA was purified from 100 ml MG1655Δ*uvrA* cells transformed with pQE30UvrA. UvrB and UvrC were purified from 100 ml XL1-Blue cells transformed with pQE30UvrB and pQE30UvrC respectively. The expressed UvrA, UvrB and UvrC each had a hexa-histidine tag at their N-terminus. Histidine binds strongly to metal ions such as nickel and consequently this property was used in the purification process. Single colonies were used to inoculate 100 ml LB broth and incubated according to the protocol described in chapter 2. The hexa-histidine tagged proteins were purified by passing the cells over a HiTrap chelating column that had been charged with Ni^{2+} which would bind the hexa-histidine tagged proteins. The bound protein was washed and then eluted using imidazole to compete with the hexa-histidine tag for the metal ions. UvrA, UvrB and UvrC were eluted from the column when the imidazole concentration had reached approximately 120 mM, 100 mM and 140 mM respectively (Figure 4.2). A single peak was observed for both UvrA and UvrB and samples of these fractions contained a single protein corresponding to the expected size. The trace for UvrC contained a shouldered peak of which the main peak contained the band of the correct size. Fractions of each sample that contained pure protein were dialysed into dialysis buffer and then into storage buffer. Protein concentration was determined. From 100 ml of culture approximately 8 mg of UvrA, 15 mg of UvrB and 0.25 mg of UvrC were purified in a final volume of approximately 500 µl. 1 µg of each purified wild-type protein was resolved on a SDS PAGE gel to confirm relative concentration and purity (Figure 4.3). Each protein was purified more than once during this work. UvrA and

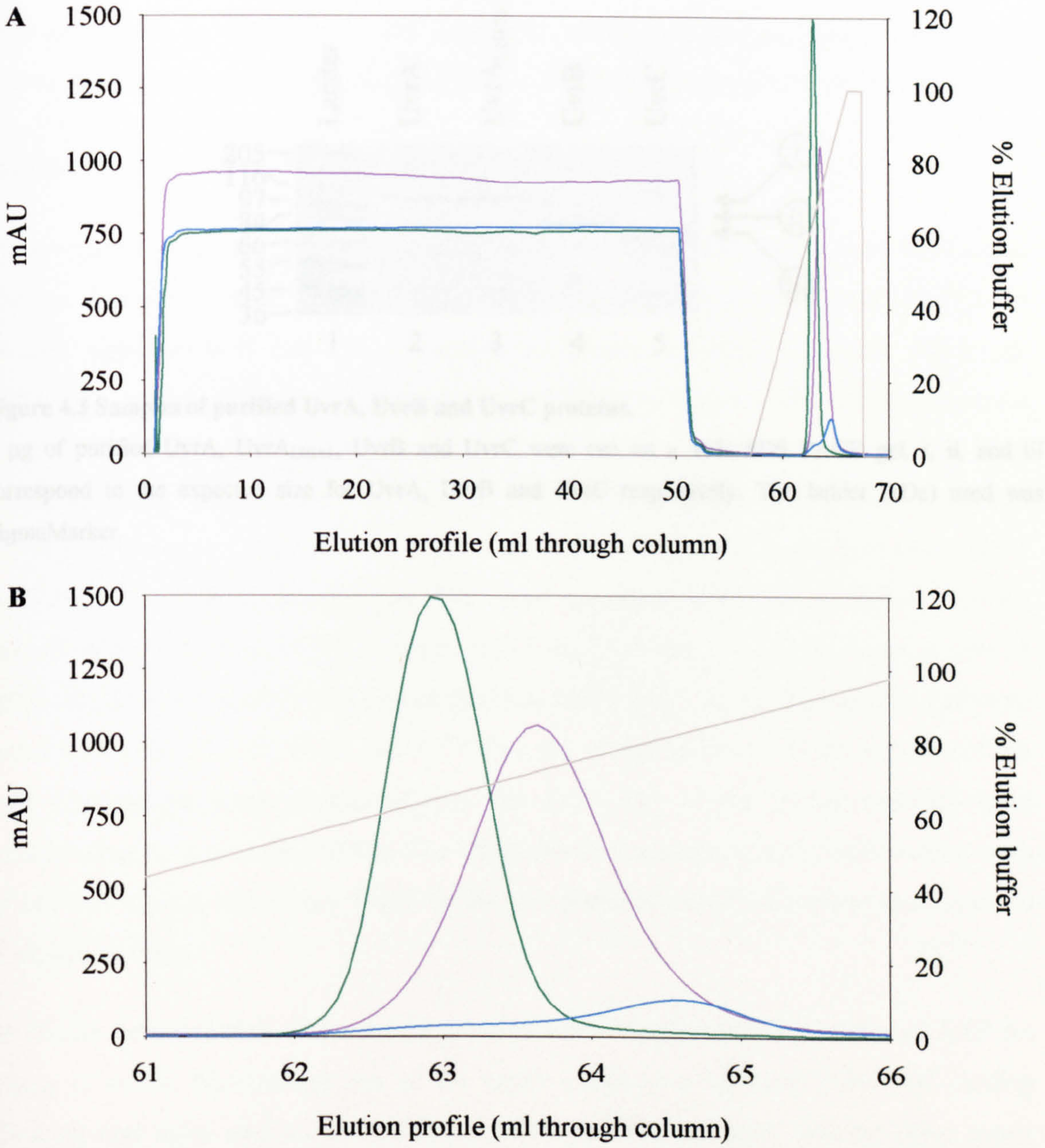

Figure 4.2 UvrA, UvrB and UvrC protein purification profiles.

UvrA was purified from 100 ml MG1655Δ*uvrA* cells that contained pQE30UvrA. UvrB and UvrC were purified from 100 ml XL1-Blue cells that contained pQE30UvrB and pQE30UvrC respectively. The cells were sonicated, centrifuged and the soluble fraction purified over a 1 ml chelating column that had been charged with Ni^{2+} using a FPLC. The A_{280} elution profiles are shown: the purple line corresponds to UvrA, the green line to UvrB, the light blue line to UvrC and the grey line to the percentage of elution buffer (0 to 100%). Panel A represents a typical purification profile and panel B is a close up of the elution profile of panel A.

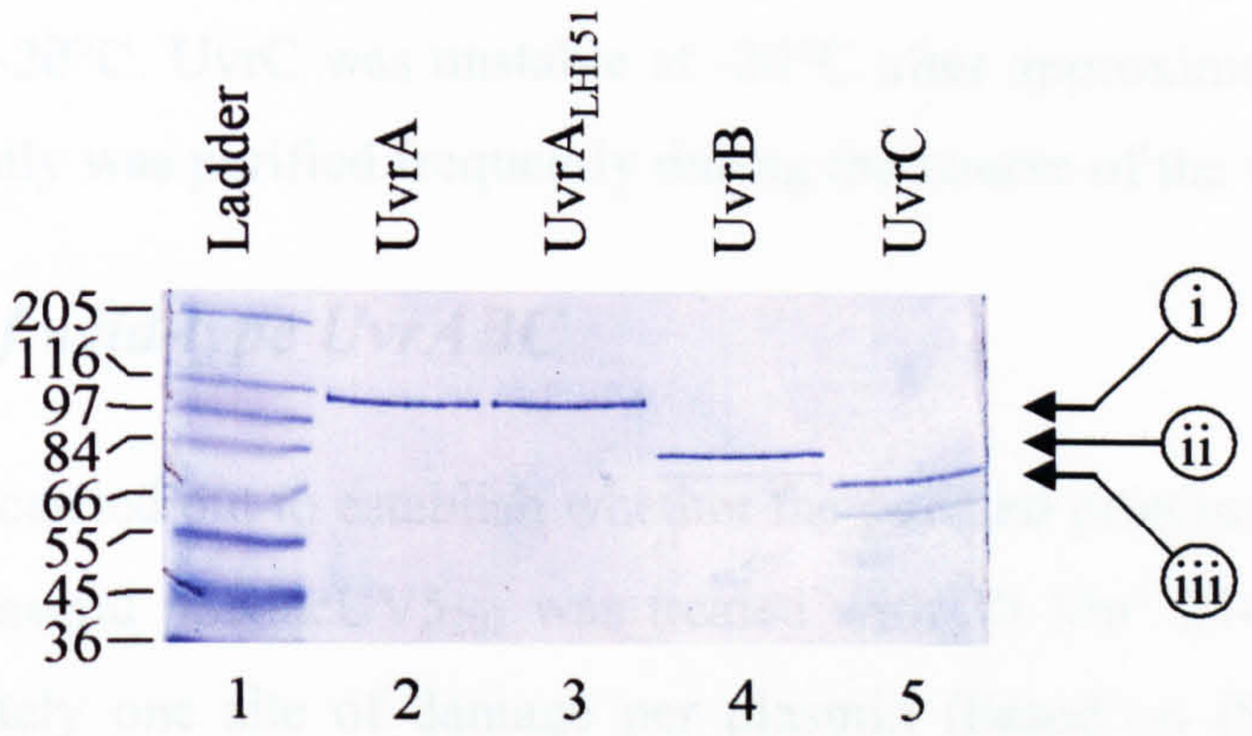

Figure 4.3 Samples of purified UvrA, UvrB and UvrC proteins.

1 μg of purified UvrA, UvrA$_{LH151}$, UvrB and UvrC were run on a 10% SDS PAGE gel. i, ii, and iii correspond to the expected size for UvrA, UvrB and UvrC respectively. The ladder (kDa) used was SigmaMarker.

UvrB were stable at -20°C. UvrC was unstable at -20°C after approximately four to eight weeks and consequently was purified frequently during the course of the work.

Incision activity of wild-type UvrABC

Incision assays were carried out to establish whether the purified proteins were working as expected. Initially plasmid pSRlacUV5$_{203}$ was treated with 30 J/m^2 254 nM UV light to introduce approximately one site of damage per plasmid (based on (Sancar and Rupp, 1983)). This would introduce UV photoproducts that would act as a substrate for the repair proteins. Combinations of UvrA, UvrB, UvrC and ATP were added (Figure 4.4). As a control the DNA was treated with the enzyme T4EV that specifically recognises and cleaves CPDs, a type of UV photoproduct. Supercoiled DNA runs faster than linear DNA which runs faster than nicked DNA. Untreated damaged DNA ran at the supercoiled position. When the damaged DNA was treated with T4EV the DNA was nicked at sites of pyrimidine dimers and ran at the nicked position on the gel. Damaged DNA that had been treated with UvrA, UvrB, UvrC and ATP also ran at this position. If one or more of the repair components were eliminated then the DNA ran at the higher mobility band corresponding to supercoiled DNA. The DNA that had not specifically been treated with UV but was treated with either T4EV or the Uvr proteins ran at both the supercoiled and the nicked position.

The results indicated that all the repair proteins were required in the presence of ATP for nicking to occur. Eliminating one of the repair enzymes completely prevented nicking indicating that there was no contamination of the purified proteins with the other repair proteins. The reaction was dependent on ATP being present which is consistent with the published data indicating that the repair proteins require ATP for function (Yeung *et al.*, 1983). The DNA appeared to be damaged to some extent before the irradiation took place as some nicked DNA was detected when the unirradiated DNA was treated with either T4EV or the NER proteins (Figure 4.4 lane 15 and 16 respectively). In conclusion the repair proteins and ATP are sufficient to nick UV damaged DNA.

To check that the 5′ incision reaction was occurring eight phosphodiester bonds 5′ of the damaged site further incision assays were carried out. This time the 5′ ^{32}P labelled pSRlacUV5$_{203}$ EcoRI/BamHI fragment was irradiated with 300 J/m^2 UV light to introduce

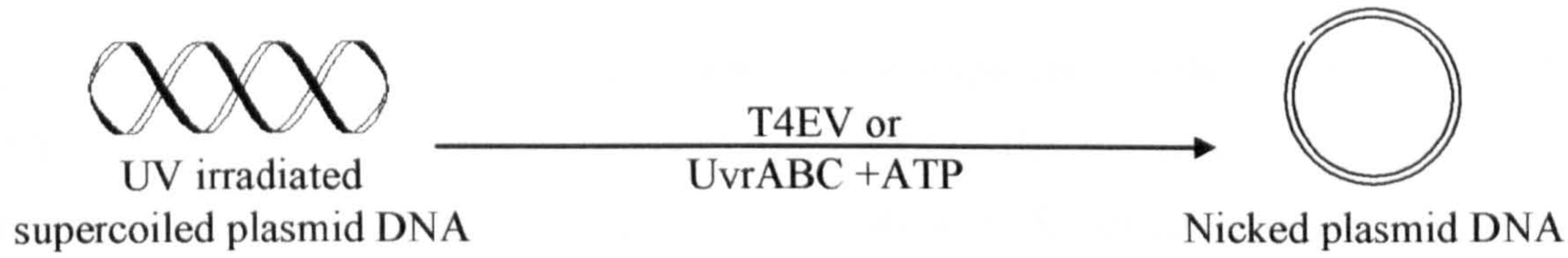

Figure 4.4 Incision assay on pSRlacUV5$_{203}$.

pSRlacUV5$_{203}$ was exposed to 30 J/m^2 254 nm UV light where indicated. The DNA was then treated where indicated with 20 U T4EV, 40 nM UvrA, 100 nM UvrB, 70 nM UvrC and 2 mM ATP. The reactions were incubated at 37°C for 30 minutes and then run on a 1% agarose gel. The ladder is GeneRuler (Fermentus Life Sciences). i, indicates the position of nicked pSRlacUV5$_{203}$; ii, indicates the position of supercoiled pSRlacUV5$_{203}$.

approximately one site of damage per fragment. The fragment was then treated with either T4EV, or the repair proteins UvrA, UvrB and UvrC in the presence of ATP. Reactions were incubated and run on sequencing gels to identify the exact position of cleavage (Figure 4.5). The DNA fragment was nicked in a variety of places with T4EV. Each incision occurred between two pyrimidine bases. The UvrABC cleavage in the presence of ATP was identical to the T4EV lane except that the detected bands had been shifted eight nucleotides in the 5′ direction. This data corresponds to published data which states that the NER proteins nick the DNA eight phosphodiester bonds 5′ to the site of damage (Sancar and Rupp, 1983). Therefore the histidine-tagged Uvr proteins are functioning as expected.

Development of a novel *in vitro* incision assay

The use of UV irradiation to introduce damage into DNA has advantages and disadvantages when studying NER and more specifically TCR. One disadvantage is that pyrimidine dimers and 6-4 photoproducts could be introduced at any pyrimidine-pyrimidine position on the DNA. This would lead to a variety of different DNA templates in one reaction. A second disadvantage is that whilst it is ideal to have one damage site per molecule the use of UV would result in some DNA molecules containing multiple damage sites whilst others would have none. For NER and TCR experiments it would be beneficial to have a substrate with a single modified site at a specific position particularly in the context of a transcription unit. Primers containing a single modification such as cholesterol, fluorescein or a thymine dimer at a specific site are now commercially available. These modified primers are synthesised within a short sequence of DNA and as such are unsuitable for TCR assays in which 90 bp of DNA is required 5′ of the lesion (Selby and Sancar, 1995b). Therefore to easily introduce a modification at a specific site in the middle of a long DNA fragment we utilised the relatively new method of SMILing DNA (Pljevaljcic *et al.*, 2004).

SMILing DNA utilises DNA methyltransferases (MTases) to modify the DNA. *In vivo* methyltransferases normally modify the DNA by transferring a methyl group from a cofactor such as S-adenosylmethionine (AdoMet) onto the DNA at a specific site (Cheng and Roberts, 2001). Each DNA methyltransferase (MTase) recognises a specific DNA sequence and transfers the methyl group from the cofactor onto a specific nucleotide

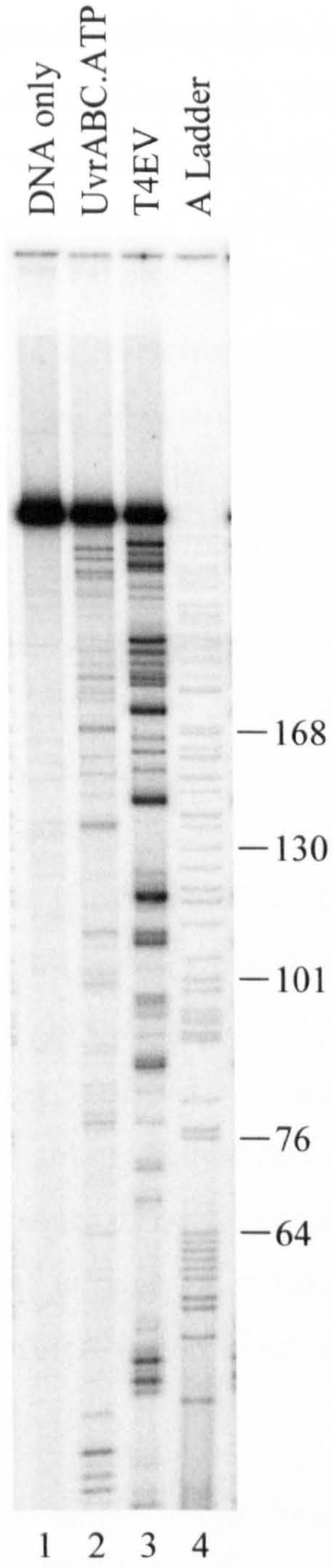

Figure 4.5 Incision assay on 5′ ^{32}P labelled pSRlacUV5$_{203}$ EcoRI/BamHI fragment.

The pSRlacUV5$_{203}$ EcoRI/BamHI 5′ ^{32}P labelled fragment was exposed to 300 J/m^2 254 nm UV light. The DNA was then mock treated (lane 1), treated with 100 nM UvrA, 100 nM UvrB and 200 nM UvrC with 1 mM ATP in repair buffer (lane 2) or treated with 2 U T4EV (lane 3). The reactions were incubated at 37°C for 30 minutes, purified using the Qiagen nucleotide removal kit and run on a 6% acrylamide 7 M urea sequencing gel. The 'A' sequencing ladder was generated using pSRlacUV5_BamHI as the primer and pSRlacUV5$_{203}$ as the template (lane 4). The gel is a typical representative of three independent experiments.

within that sequence at a specific position (Urig *et al.*, 2002). Two methyltransferases are important for the following discussion: Dam and M.BseCI. Dam is one of the most common DNA MTases in prokaryotes acting to protect the host DNA (Urig *et al.*, 2002). It specifically recognises the sequence GATC and transfers a methyl group onto each adenine base (one on each strand) at the N^6 position. M.BseCI also acts to transfer a methyl group onto the N^6 position of adenine but would only do so if the adenine residue was in the sequence $^{5'}ATCGAT^{3'}$ and then only the adenine at position 5 would be modified (Rina and Bouriotis, 1993). The ability of DNA MTases to recognise and modify different recognition sequences was utilised in the concept of SMILing DNA.

Methyl groups on DNA molecules are not recognised by NER as sites of damage presumably because they are small and do not cause helical distortions. Methylation also plays a role in protecting host DNA and as such it would be unbeneficial to the cell if the methyl groups acted as substrate for NER. As mentioned above MTases require cofactors from which the methyl group is transferred. AdoMet, a common methyl donor, has been chemically modified so that the entire cofactor becomes covalently linked to the DNA in the presence of certain MTases (Pljevaljcic *et al.*, 2004). This modified cofactor, N-adenosyl-aziridine, can be further modified to contain a label such as a fluorophore (Pljevaljcic *et al.*, 2003) or a biotin group (Pljevaljcic *et al.*, 2004). Thus when a MTase is added to a DNA solution in the presence of the biotin or fluorophore modified cofactor the DNA is modified in such a way as to have an internal modification. This labelling will occur at the usual methylation position within DNA sequences that were recognised by that specific MTase.

SMILing DNA therefore allows a single unique recognition sequence to be modified within a plasmid. However the modification will occur on both strands (depending on the methyltransferase used). The DNA base sequence can not be altered as this would result in the loss of recognition by the MTase. However the bases within the sequence can be modified by methylation. Figure 4.6 indicates an example of overlapping methylation sites for the MTases Dam and M.BseCI. If methylation of the Dam recognition sequence occurs then one of the adenine residues that would normally be methylated by M.BseCI would have already been methylated as it was also part of the Dam recognition sequence. If the Dam methylated DNA was then placed in a reaction with M.BseCI and a modified cofactor only one strand of the M.BseCI recognition sequence would be available for

A

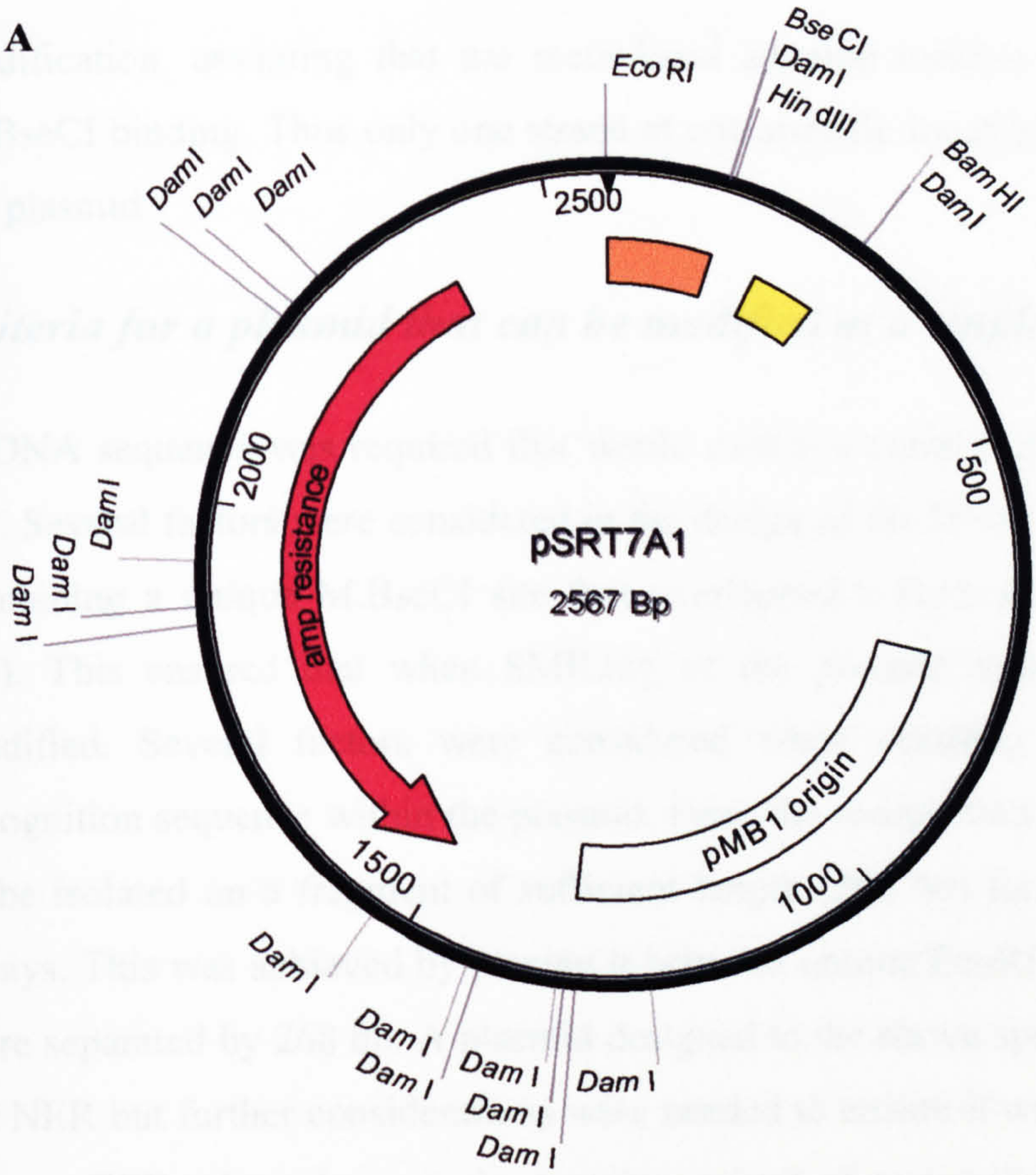

B

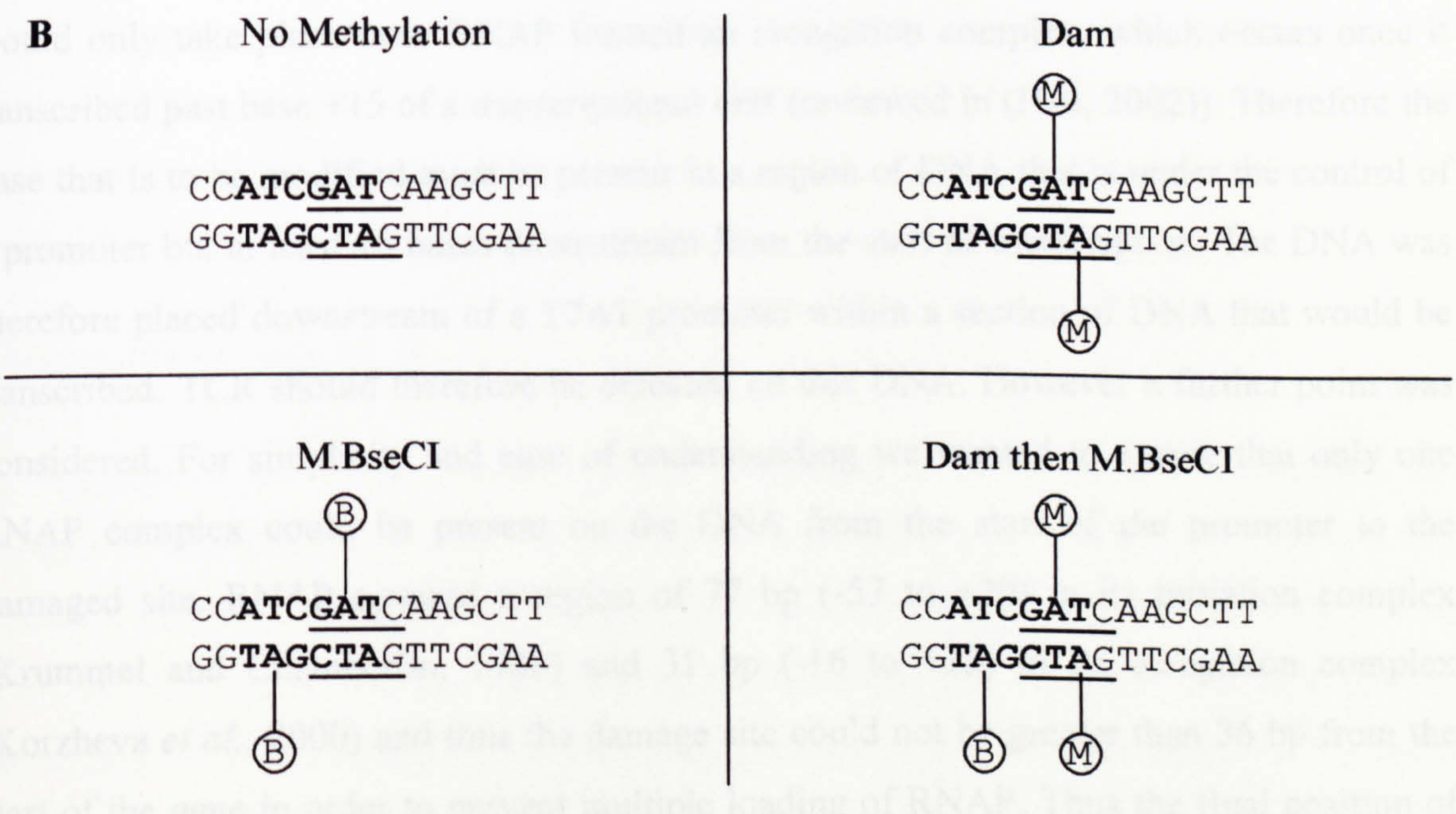

Figure 4.6 Methylation patterns.

(**A**) Plasmid map of pSRT7A1. (**B**) pSRT7A1 was used as the substrate for the SMILing DNA reaction. The relevant DNA sequence is shown. Bold type indicates the M.BseCI recognition sequence and underlined type indicates the Dam recognition sequence. M represents a methyl group that would be introduced in the presence of Dam and B represents a 6Baz group that would be introduced in the presence of M.BseCI and a modified cofactor.

modification, assuming that the methylated adenine residue did not interfere with the M.BseCI binding. Thus only one strand at one specific location would be modified within the plasmid.

Criteria for a plasmid that can be modified at a single specific position

A DNA sequence was required that would enable a variety of repair assays to be carried out. Several factors were considered in the design of the DNA. A plasmid was constructed containing a unique M.BseCI site that overlapped a Dam recognition sequence (Figure 4.6). This ensured that when SMILing of the plasmid took place only one site was modified. Several factors were considered when deciding the final position of the recognition sequence within the plasmid. First, the recognition sequence needed to be able to be isolated on a fragment of sufficient length (300 bp) for use in EMSA and nicking assays. This was achieved by placing it between unique EcoRI and BamHI sequences that were separated by 268 bp. A plasmid designed to the above specifications would be of use for NER but further considerations were needed to ensure it would also be useful for TCR assays. TCR takes place on the template strand of transcribed DNA. Furthermore TCR would only take place once RNAP formed an elongation complex, which occurs once it transcribed past base +15 of a transcriptional unit (reviewed in (Hsu, 2002)). Therefore the base that is to be modified must be present in a region of DNA that is under the control of a promoter but at least 15 bases downstream from the start of transcription. The DNA was therefore placed downstream of a T7A1 promoter within a section of DNA that would be transcribed. TCR should therefore be detected on this DNA. However a further point was considered. For simplicity and ease of understanding we wanted to ensure that only one RNAP complex could be present on the DNA from the start of the promoter to the damaged site. RNAP covered a region of 77 bp (-57 to +20) in its initiation complex (Krummel and Chamberlin, 1989) and 31 bp (-16 to +15) in its elongation complex (Korzheva *et al.*, 2000) and thus the damage site could not be greater than 36 bp from the start of the gene in order to prevent multiple loading of RNAP. Thus the final position of the base to be modified was at +27. With these criteria in mind plasmid pSRT7A1 was constructed by Dr. N. Savery.

Single site-specific modification of DNA

The plasmid, pSRT7A1, was designed and constructed to enable the addition of a single specific modification. The next step was to modify the plasmid to introduce the single specific modification. The plasmid needed to be modified first using Dam and then using M.BseCI. Methylation of the DNA by Dam was achieved by transforming the *E. coli* strain XL1-Blue, which is *dam*$^+$, with the plasmid. The plasmid was then purified from this strain and thus contained methyl groups at all adenine residues within GATC sequences. This would include the GATC sequence that overlapped with the M.BseCI sequence ATCGAT. It was not known if the topology of the DNA would affect the success of the modification (biotinylation) reaction and therefore a linear template was used. The Dam methylated pSRT7A1 plasmid was linearised by digestion with BamHI. The DNA was then biotinylated using the SMILing technique (E. Weinhold laboratory). They treated the DNA with M.BseCI to deliver the biotin containing cofactor 6Baz onto the DNA (Figure 4.7). They confirmed that the biotinylation had been successful by carrying out streptavidin binding assays at certain time points through the procedure. To do this they digested aliquots of DNA with EcoRI to produce a shorter fragment whose binding to streptavidin could be detected on an agarose gel. Only samples from mixes that contained M.BseCI and 6Baz were successfully shifted to a higher position. The DNA was successfully modified to completion as by the end of the incubation procedure the DNA fragment was all in the shifted lower mobility position (data not shown).

Fragment preparation

A fragment of the 6Baz modified DNA was generated for use in incision assays. The BamHI digested modified DNA, as well as the equivalent unmodified DNA (for use as a control), was dephosphorylated and then digested with EcoRI to generate two fragments: a 2300 bp unmodified fragment and a 268 bp modified fragment (Figure 4.8). The fragments were then 5′ ^{32}P end labelled. To confirm the presence of the 6Baz molecule a streptavidin EMSA was carried out (Figure 4.9). A high and a low mobility band were detected in the original mix corresponding to the short and the long fragment respectively. When Streptavidin was added an extra band at a lower mobility than the short fragment was detected. This extra band is presumably a streptavidin-biotinylated DNA complex as it was not detected in the lanes where the DNA was not biotinylated. The

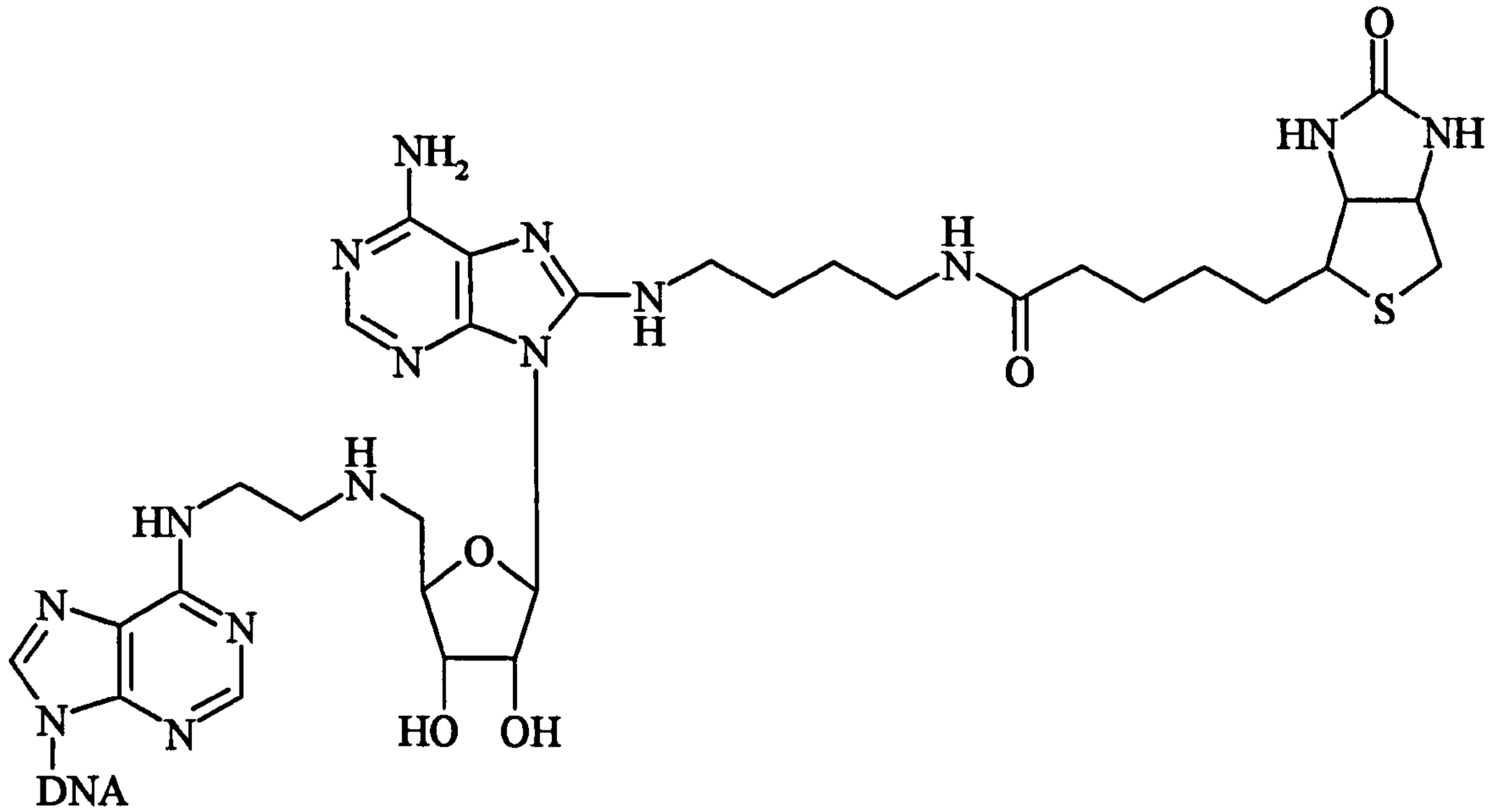

Figure 4.7 6Baz modified DNA.

The chemical structure of adenine covalently bound by the cofactor 6Baz (containing a biotin group). M.BseCI was used to catalyse the reaction.

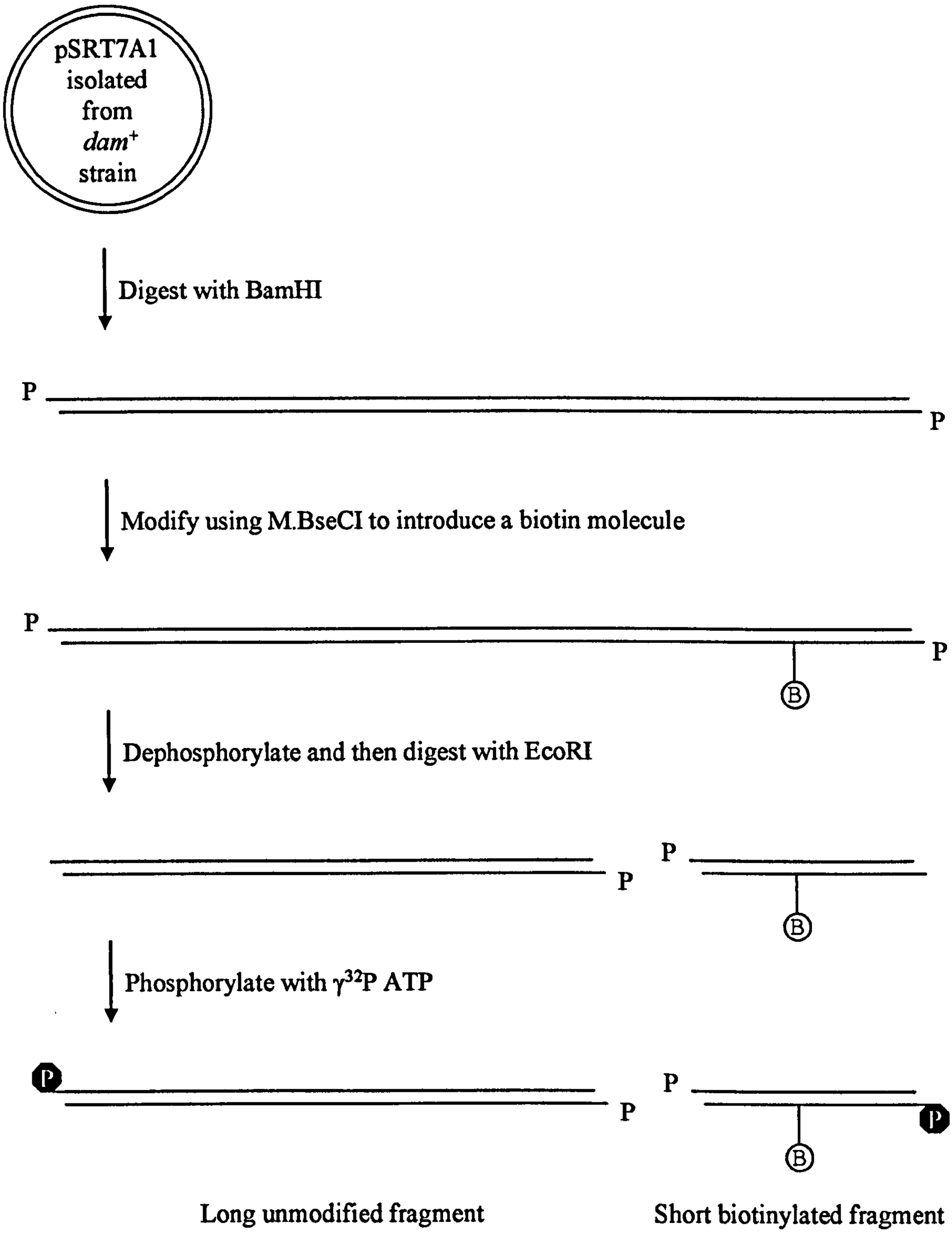

Figure 4.8 Preparation of SMILing DNA fragment.

Plasmid DNA purified from a *dam*$^+$ strain was: digested with BamHI, biotinylated by M.BseCI with the modified cofactor 6Baz, dephosphorylated and digested with EcoRI. A short biotinylated fragment and a long unmodified fragment are the end products that are 5′ labelled at their BamHI end. Methyl groups that would be present at all Dam recognition sites are not indicated for clarity.

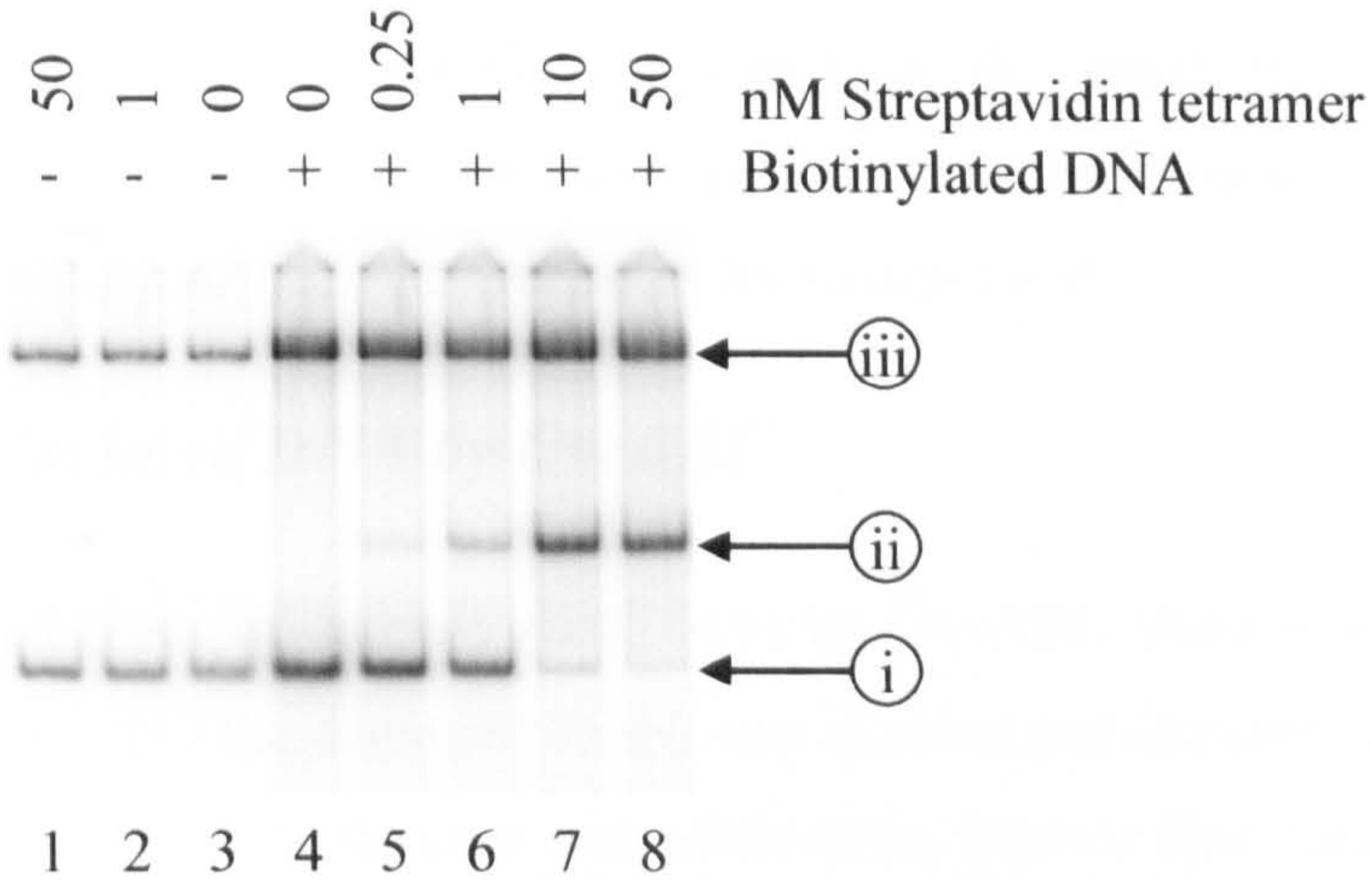

Figure 4.9 Streptavidin EMSA to confirm SMILing DNA.

The indicated concentration of Streptavidin tetramer was incubated at 37°C for 10 minutes with 0.25 nM 5′ labelled pSRT7A1 BamHI/EcoRI biotinylated (lanes 4 to 8) or unmodified (lanes 1 to 3) fragments. i, refers to the short fragment (268 bp); ii, to the streptavidin bound short fragment; iii, to the long fragment (2300 bp).

streptavidin-biotinylated DNA complex appeared as the short fragment disappeared indicating that the modification was present on the short fragment as expected. At least 96% of the DNA molecules had been successfully biotinylated.

Incision of biotinylated DNA by UvrABC

For all the reported types of damage recognised by UvrABC there is a clear pattern for cleavage. In all cases only the damaged strand was cleaved and the cleavage occurred eight phosphodiester bonds 5′ of the damage and either three, four or five phosphodiester bonds 3′ of the damage. At this stage it was unknown if the 6Baz modified DNA would be a substrate for NER. Therefore assays were carried out to determine if cleavage occurred and where the 5′ and 3′ cleavage sites were in relation to the modified base. Assays were also carried out to determine if the undamaged strand was cleaved. A sample of the DNA was also digested with HindIII. HindIII cleaves close to the modified lesion and would therefore act as a marker to enable the precise locations of UvrABC incision to be measured.

Incision 5′ to the biotinylated site

To determine if UvrABC recognised 6Baz as a site of damage an incision assay was used that was designed to detect the 5′ cleavage site furthest from the damaged site (Figure 4.10 lanes 1 to 8). In a separate reaction the DNA was digested with HindIII that should cleave the 11th phosphodiester bond 5′ of the biotinylated nucleotide. This would act as a marker to which the UvrABC cleavage could be compared. The DNA fragment on its own resolved as a single band corresponding to the initial size of the 268 bp fragment (lane 8). The expected 2300 bp fragment ran as a smear near the top of the gel. The DNA had been completely digested by HindIII (lane 7). A band that was three bases longer than the HindIII digested band was seen in the lane containing UvrABC and ATP (lane 2). This appears to confirm that the 6Baz molecule will act as a substrate for NER. The band corresponds to a cleavage position eight phosphodiester bonds 5′ of the damage, corresponding with previously published data of the 5′ cleavage by UvrABC proteins. Without ATP only a band corresponding to the full-length fragment was detected, indicating that ATP was required for the incision reaction to occur. A secondary band in the UvrABC incision reaction was detected 15 phosphodiester bonds 5′ of the modification

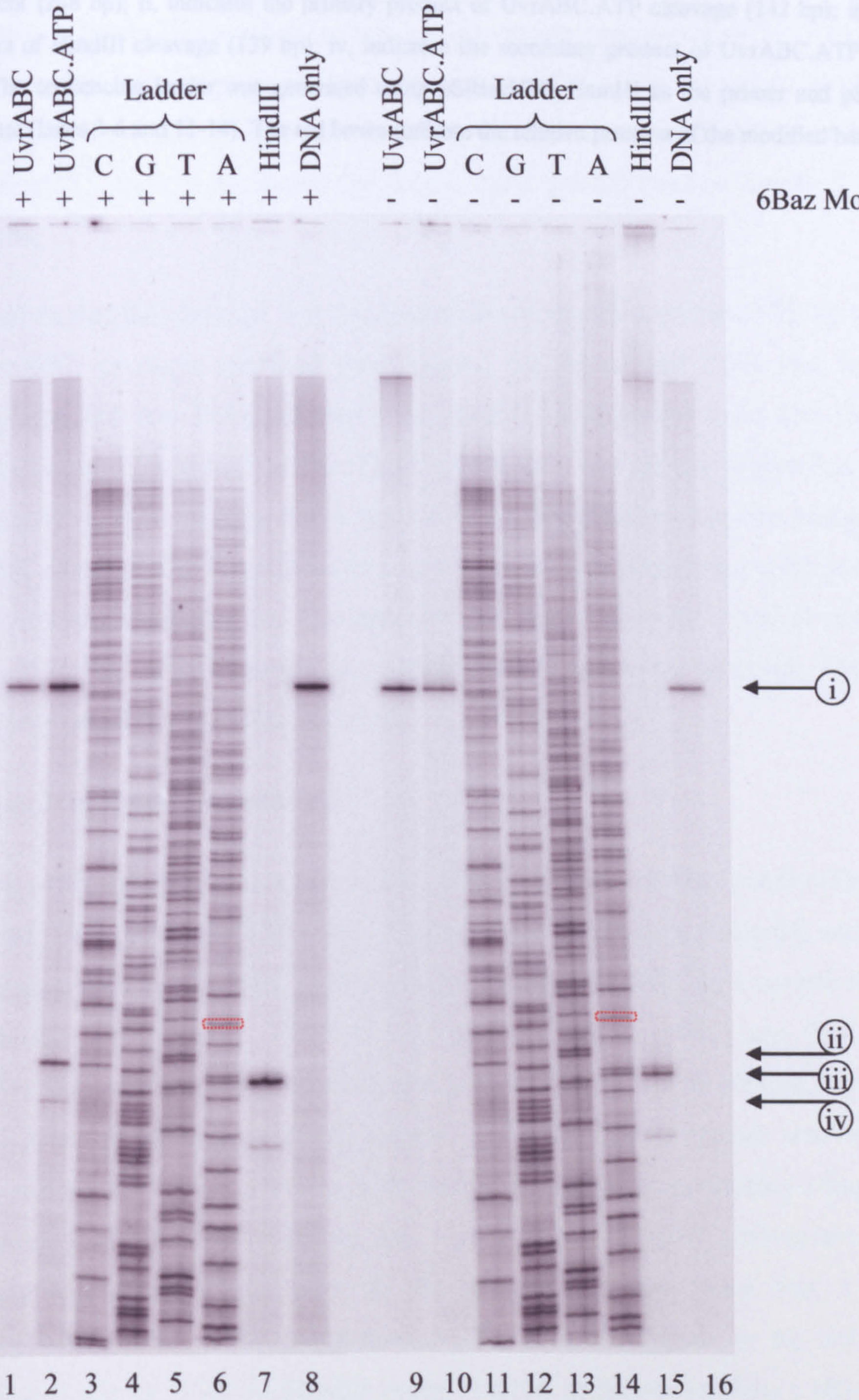

Figure 4.10 Incision assay on 5′ ^{32}P labelled pSRT7A1 EcoRI/BamHI SMILing DNA.

The pSRT7A1 EcoRI/BamHI fragment that had (lanes 1-8) or had not (lanes 9-16) been biotinylated by the SMILing reaction was 5′ ^{32}P labelled. The DNA (0.25 nM) was then mock treated (lanes 8 and 16), treated with 100 nM UvrA, 100 nM UvrB and 200 nM UvrC with (lanes 2 and 10) or without (lanes 1 and 9) 1 mM ATP in repair buffer or treated with 5 U HindIII (lanes 7 and 15). The reactions were incubated at 37°C for 30 minutes, purified and run on a 6% acrylamide 7 M urea sequencing gel. i, indicates the full-length short

fragment (268 bp); ii, indicates the primary product of UvrABC.ATP cleavage (142 bp); iii, indicates the product of HindIII cleavage (139 bp); iv, indicates the secondary product of UvrABC.ATP cleavage (135 bp). The sequencing ladder was generated using pSRlacUV5_BamHI as the primer and pSRT7A1 as the template (lanes 3-6 and 11-14). The red boxes indicate the relative position of the modified base.

(band iv). A band corresponding to this has previously been detected in UvrABC incision assays on other types of damage (Moolenaar *et al.*, 2000). The secondary band detected in the HindIII digest (lane 7) is at this stage unexplained. Thus in conclusion in can be stated that UvrABC appears to incise the DNA eight phosphodiester bonds 5′ of a 6Baz molecule.

To confirm that the cleavage was due to specific recognition of the SMILing modification by UvrABC the same reactions were carried out on control DNA that had not been biotinylated but had been digested with BamHI, dephosphorylated and digested with EcoRI (Figure 4.10 lanes 9 to 16). The UvrABC proteins did not cleave this DNA in the presence of ATP confirming that it was the 6Baz modification that was recognised by the UvrABC proteins. The HindIII digest again produced a primary band at the same site as on the biotinylated fragment and also produces the same secondary band 11 phosphodiester bonds 5′ to the main cleavage site indicating that this extra cleavage was not due to alterations caused by the 6Baz molecule.

Incision 3′ to the biotinylated site

Having established the 5′ cleavage site we wanted to know at what position the 3′ cleavage occurred. Unlabelled pSRT7A1 DNA that had been digested with BamHI and biotinylated was treated with the UvrABC proteins in the presence of ATP. As a control the DNA was also treated with HindIII. This time the reactions were purified and then used as the template for primer extension using the primer D5431 which anneals to the modified strand 3′ to the biotinylated site (Figure 4.11). If the DNA template was not nicked the DNA polymerase should continue to the end of the fragment generating a fragment of 358 nucleotides. If the DNA template was nicked then the DNA polymerase would only continue up to the nicked site. In the uncut DNA lane there was a single band corresponding to the DNA length from the 5′ end of the primer to the end of the DNA template (Lane 1). With the HindIII digested DNA acting as template a shorter band was observed corresponding to the position of HindIII cleavage with regard to the primer (Lane 7). Two bands were observed and it is thought that the longer one is due to Taq DNA polymerase adding an extra adenine once it reached the end (Friedberg *et al.*, 2006). Interestingly seven bands are observed in the lane containing the primer extension of the UvrABC and ATP digest. One of the bands corresponded in size to the DNA only lane and

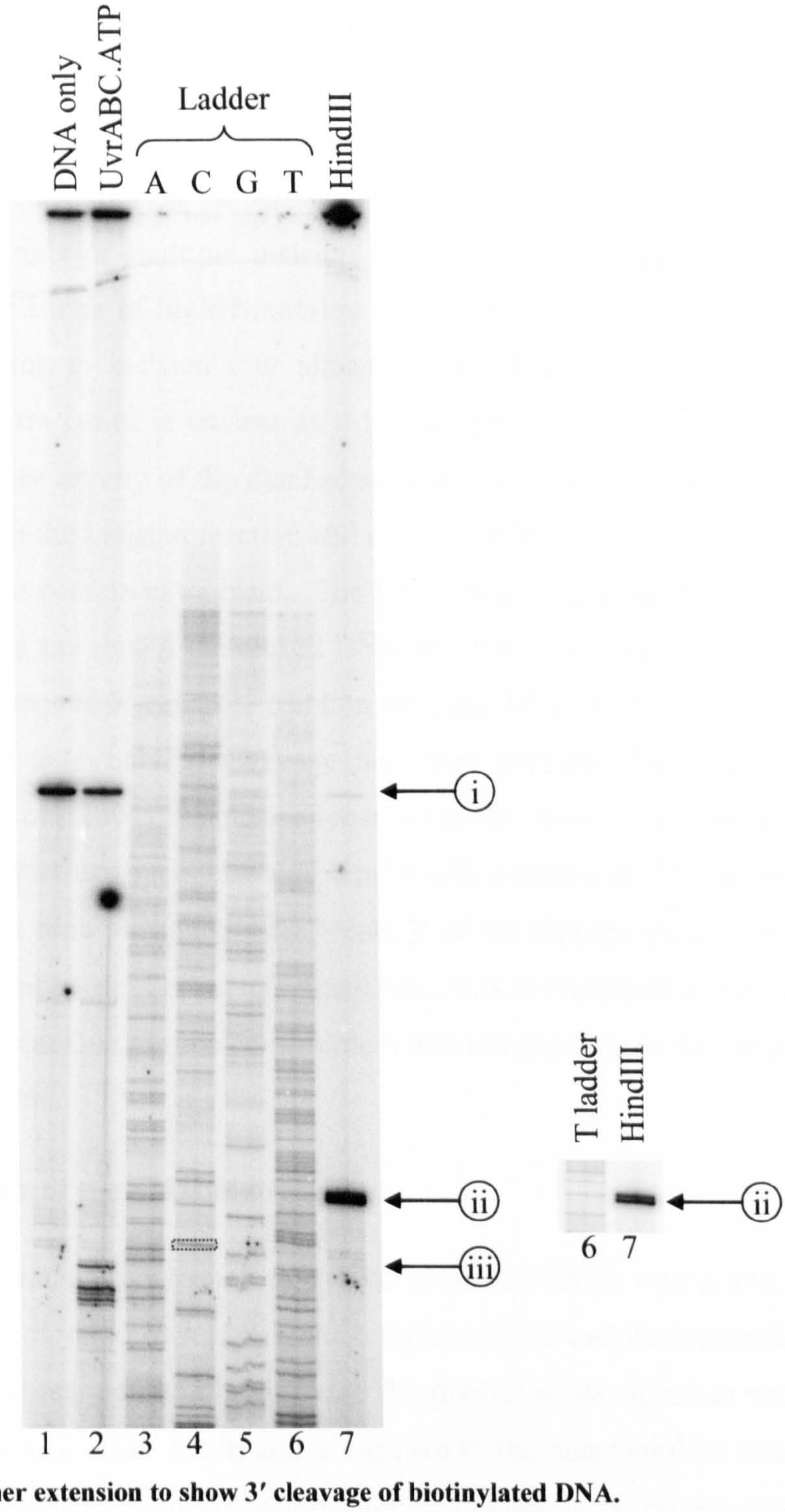

Figure 4.11 Primer extension to show 3′ cleavage of biotinylated DNA.

Nicking reactions were incubated at 37°C for a total of 30 minutes and contained 1.025 nM pSRT7A1 BamHI/BamHI biotinylated DNA and where indicated 100 nM UvrA, 100 nM UvrB, 200 nM UvrC, 1 mM ATP and 10 U HindIII. Additional ATP was added after the first 15 minutes to the reaction containing ATP. The DNA was purified from the reactions and primer extension was carried out using primer D5431. The ladder (lanes 3 to 6) was derived from pSRT7A1 using pSRlacUV5_BamHI as the primer. i, indicates the full-length primer extension product (358 bp); ii, indicates the length of primer extension on HindIII digested DNA; iii, indicates the length of primer extension on UvrABC.ATP cleaved DNA (212 bp). The red box indicates the relative position of the modified base.

thus indicated that the nicking reaction did not go to completion. There was then a group of bands around the area of expected 3′ cleavage. Of these the band of lowest mobility corresponded to a cleavage site four phosphodiester bonds 3′ of the biotinylated site which would fit the expected nicking properties of UvrABC. The bands of higher mobility could be a result of single or multiple incision reactions. The intensity of each band is not significant as the bands of higher mobility may or may not have been derived from the band corresponding to incision four phosphodiester bonds 3′ of the modification. The reason for the extra bands is unclear as it has not previously been reported that extra 3′ incisions take place on any of the damage substrates tested (Moolenaar *et al.*, 2000). It is likely to be due to the incision reaction and not a fault in the primer extension as the DNA only lane does not contain extra bands. The first of these extra bands was four bases away from the expected site thus if the nicked DNA acted as a substrate for NER then it would be feasible for a second 3′ cleavage reaction to occur. Nicked DNA does act as a substrate for NER but to date only 5′ cleavage has been assayed (Moolenaar *et al.*, 1998a) (DellaVecchia *et al.*, 2004). Another alternative is that there is a contamination by Cho, another enzyme that can recognise and bind UvrB complexes (Moolenaar *et al.*, 2002). Cho incises DNA nine phosphodiester bonds 3′ of the damage (Moolenaar *et al.*, 2002). However Cho, a much smaller protein than UvrC, was not detected on the SDS PAGE gels of my UvrC protein. Due to time constraints it was not possible to further investigation the 3′ cleavage reaction.

Strand specificity of the SMILing reaction

The above experiments confirmed that 6Baz modified DNA was a substrate for NER. However it was not yet known if only the template strand had been modified as predicted or if the SMILing reaction had biotinylated the non-template strand as well. The plasmid was extracted from a Dam^+ strain and subsequently the non-template strand should have been methylated and as such unavailable for biotinylation. A primer extension reaction was carried out on the digests used for the above reaction however this time the primer pSRlacUV5_BamHI which bound to the non-template strand was used. Multiple bands were seen in the vicinity of the modification but these bands were not specific to UvrABC cleavage as they were also visible in the DNA-only lane (Figure 4.12). This time the DNA could extend to the end of the 2568 bp plasmid although the extension reaction stopped short in the majority of instances (Figure 4.12 band ii). The HindIII digest, which should

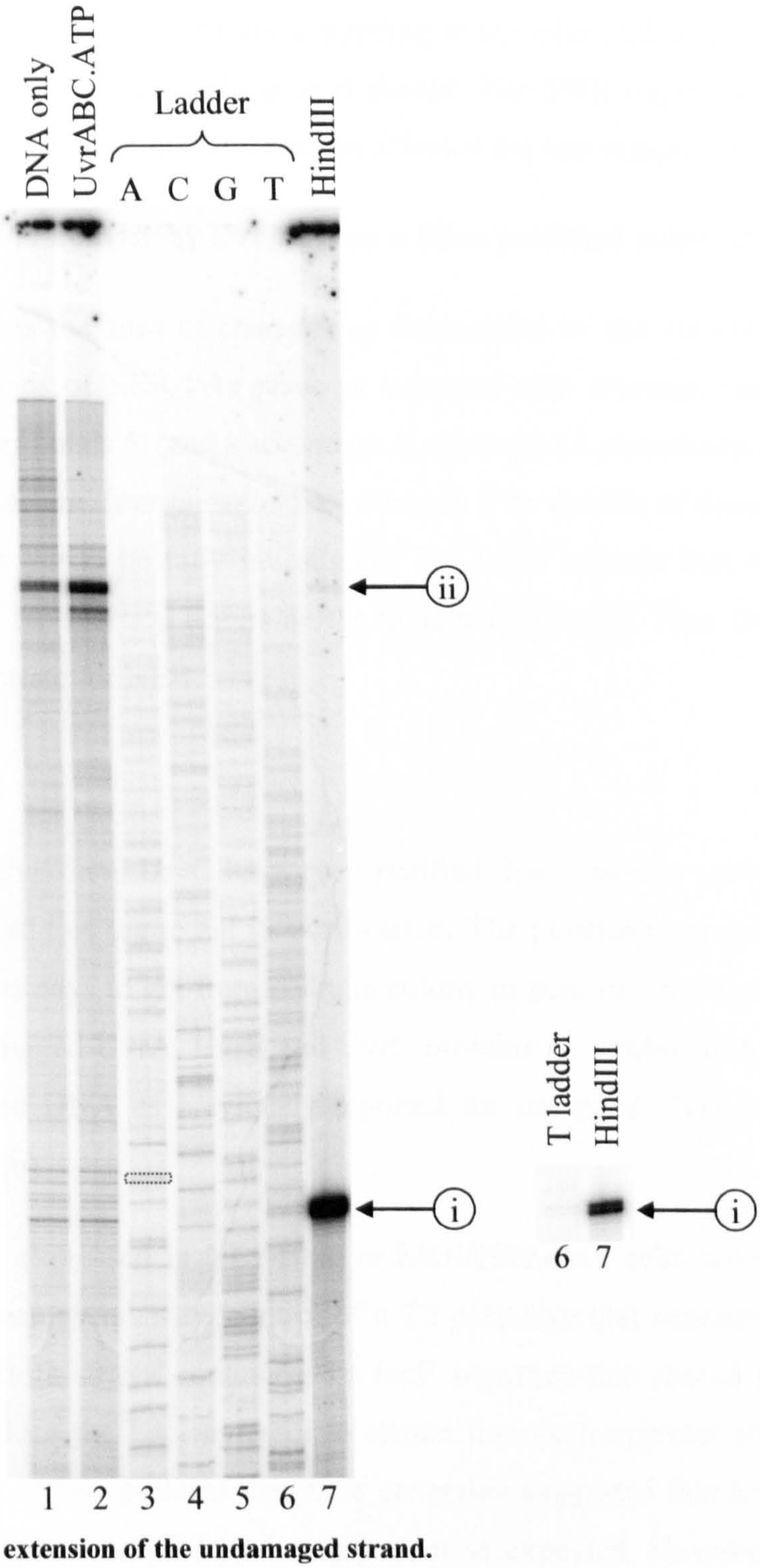

Figure 4.12 Primer extension of the undamaged strand.

Nicking reactions were incubated at 37°C for a total of 30 minutes and contained 1.025 nM pSRT7A1 BamHI/BamHI biotinylated DNA and where indicated 100 nM UvrA, 100 nM UvrB, 200 nM UvrC, 1 mM ATP and 10 U HindIII. Additional ATP was added after 15 minutes to the reaction containing ATP. The DNA was purified from the reactions and primer extension was carried out using primer pSRlacUV5_BamHI. The ladder (lanes 3 to 6) was derived from pSRT7A1 using pSRlacUV5_BamHI as the primer. i, indicates the length of primer extension on HindIII digested DNA (139 bp); ii, indicates a region of premature termination of the primer extension reaction. The red box indicates the relative position of the modified base.

nick both strands, produced a band corresponding to the expected size indicating that the primer extension reaction was working as it should. The SMILing reaction had therefore only modified the template strand and had not affected the non-template strand.

Summary of incision activity by UvrABC on a 6Baz modified substrate

Figure 4.13 indicates the sites of cleavage as determined by the various nicking assays. The incision reactions of NER take place as expected with cleavage reactions occurring eight phosphodiester bonds 5′ (and a secondary 5′ cleavage 15 phosphodiester bonds away) of the site of damage and four phosphodiester bonds 3′ to the site of damage. The extra 3′ cleavage sites have yet to be fully investigated but could indicate that nicked DNA is a substrate for NER. No incision occurs on the undamaged strand. Thus the 6Baz modified DNA acts as a substrate for NER.

Discussion

Wild-type UvrA, UvrB and UvrC have been purified. Each protein was expressed with a N-terminal hexa-histidine tag to aid its purification. The purification procedure was rapid, taking less than two days to get from a single colony to pure protein stored at -80°C. The purified histidine-tagged UvrA, UvrB and UvrC proteins in combination with ATP could incise UV damaged DNA as previously reported for untagged UvrA, UvrB and UvrC (Yeung *et al.*, 1986b).

The proteins were expressed in XL1-Blue or MG1655Δ*uvrA* cells without the need for induction despite being under the control of a T5 promoter that contained a *lac* operator site downstream. Both strains contained the *lacI*^{q} sequence that should have enabled the strains to overproduce the Lac repressor to ensure that each operator site was occupied. The large quantity of Uvr proteins that were generated suggested that a proportion of the operator sites were not occupied by Lac repressor as expected. However the addition of IPTG to the cells reduced rather than increased expression of the plasmid *uvr* gene within the cell. Expression of the protein in large quantities could harm the cell as it would be more likely that NER of undamaged sections of DNA would occur resulting in a high mutation frequency. As a result cells that were unable to produce the Uvr protein for any number of reasons including sequence or promoter mutations would be selected. The reason behind the reduction in expression was not investigated as the main aim was to

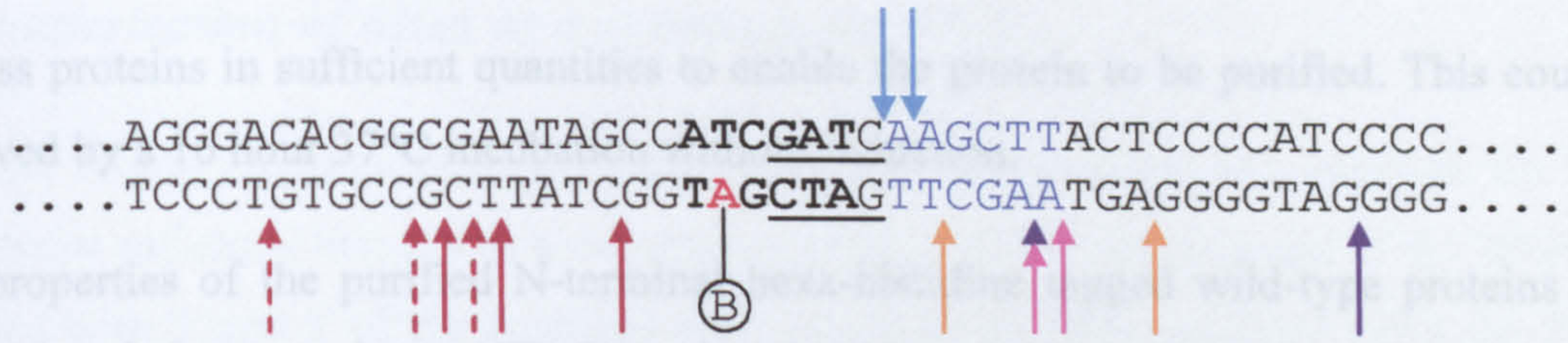

Figure 4.13 Position of cleavage.

Position of cleavage of modified SMILing DNA. The red arrows indicate 3′ cleavage by UvrABC as shown by primer extension (dashed arrows indicate a weak band which in some instances could be due to an adenine base added by Taq DNA polymerase during the primer extension reaction). Orange arrows indicate 5′ cleavage by UvrABC. Purple arrows indicate cleavage by HindIII under the conditions used for 5′ cleavage, pink arrows indicate cleavage by HindIII under the conditions used for primer extension reactions, and turquoise arrows indicate cleavage seen by HindIII on the undamaged strand under primer extension conditions. The red type indicates the 6Baz (B) modified residue, bold type indicates the M.BseCI recognition sequence, underlined type indicates the Dam methylation sequence, and blue type indicates the HindIII recognition sequence.

express proteins in sufficient quantities to enable the protein to be purified. This could be achieved by a 16 hour 37°C incubation without induction.

The properties of the purified N-terminal hexa-histidine tagged wild-type proteins were checked and shown to have ATP dependent incision activity when all were present. The purification procedure was quick, simple and reproducible, and the purified proteins worked within an NER incision assay.

SMILing DNA

Natural and manmade substrates for repair by NER are constantly being identified. However there was no simple way of introducing a single modification at a specific location within a long DNA molecule. A method for generating a single site of damage on a DNA molecule has been successfully established. The method relies on the activity of methyltransferases to introduce modifications within the DNA at their recognition sequences. This enabled the position of the damage to be controlled by simple cloning techniques. A single modified substrate was generated by: overlapping a Dam and a unique M.BseCI methyltransferase recognition sequence; Dam methylating the DNA; and then modifying the M.BseCI site using a modified cofactor. It is theoretically possible that any methyltransferases could be used providing that: the two recognition sequences overlapped and modified the same base in the same position; and the modified cofactor could be recognised by the MTase. In this way DNA can be modified at a wide variety of different sites within a molecule.

Currently the only type of modification that has been attached for use in this system is a biotin molecule. However there is no reason why any molecule cannot be attached in this manner providing it can be chemically attached to a modified cofactor and then accommodated by a MTase. Our collaborators in Germany have currently been able to introduce a number of different types of molecules onto different positions within DNA using cofactors that have been modified in a variety of ways and using different methyltransferases to carry out the modification procedure (Pljevaljcic *et al.*, 2004).

Characterisation of 6Baz as a substrate for NER

6Baz (or biotin) modified DNA had not previously been analysed as a substrate for NER. The results indicated that it was a suitable substrate for NER as cleavage of the DNA was detected both 5′ and 3′ of the modified base. For NER of 6Baz modified DNA the 5′ nick was in the classical position eight phosphodiester bonds away from the damage however there seems an abundance of 3′ nick sites. The reason behind the multiple 3′ nick sites has not yet been investigated but could be due to a variety of reasons. Firstly 6Baz has not been analysed within this system before and may interfere with the 3′ nicking activity. This however is unlikely as every NER substrate reported so far has consistently only had one site of cleavage at the 3′ side of damage and in these instances the cleavage is three to five phosphodiester bonds away from the damaged site. However, extra 5′ cleavage bands have been seen for various substrates (Moolenaar *et al.*, 2000). The 3′ site of cleavage is believed to be more controlled due to the nature of the protein DNA interaction with the positioning of the undamaged strand and damaged strand being separated by the β-hairpin of UvrB, locking it in position for UvrC to incise 3′ of the damage. A second possibility for the extra cleavage is that there is a contaminating nuclease within one of the purified protein preparations. Cho, the homologue of the NTD of UvrC, would causes incision of the DNA nine phosphodiester bonds 3′ of the damaged site (Moolenaar *et al.*, 2002). This could be responsible for the incision activity detected especially if it can recognise both nicked DNA and 6Baz modified DNA as damage substrates in collaboration with UvrB. Alternatively a different nuclease could be present. Thirdly the results could indicate that nicked DNA acts as a substrate for NER under the conditions used in this assay. At this stage the reason for the multiple incision sites is unclear but further analysis should be able to determine the reasons behind this.

Characterisation of 6Baz as a site of damage for TCR

Having established that a 6Baz adduct would be recognised and repaired by NER it would be useful to determine if it could be used as a tool for TCR. For TCR to occur the damage must stall the RNAP elongation complex enabling the recruitment of the NER apparatus. Initial experiments carried out by Dr. N. Savery (data not shown) indicated that RNAP was not stalled by the 6Baz modification and carried on transcribing until it reached a stop signal. The 6Baz molecule must therefore be small enough to pass through the DNA tract

of the RNAP molecule. Thus it would appear that although the 6Baz damaged molecule was a suitable substrate for NER experiments it was not of use for TCR.

Further work to develop a substrate for TCR experiments is ongoing. Two approaches are being taken. The first is to bind Streptavidin to the biotinylated DNA molecule to create a suitable blockade that will cause RNAP to stall. The second is to modify the DNA with larger molecules such as TexasRed in order to try and block RNAP.

At this stage we are confident that the SMILing method will be useful for developing a group of DNA molecules with the same modification at the same position for use in the TCR assay. Further work is required to identify a modification that will stall RNAP. Despite 6Baz not being a suitable roadblock for transcription it is still effective within NER and therefore useful for analysing *in vitro* NER activity.

CHAPTER 5

IN VITRO ANALYSIS OF UvrA MUTANT PROTEINS

Introduction

Within the process of NER UvrA forms homodimers, binds and hydrolyses ATP, binds to UvrB and DNA, and assists the loading of UvrB onto sites of DNA damage. Failure at any of these steps could reduce or even prevent successful NER, leading to a decrease in UV resistance of the cell.

The role of UvrA in the process of NER is complex with its nucleotide hydrolysis, DNA binding and UvrB binding activities all interlinked (Figure 5.1). UvrA initially forms homodimers in a reaction that can be stimulated by high UvrA concentration and/or ATP binding (Orren and Sancar, 1989) (Oh *et al.*, 1989). The UvrA dimer is then believed to bind UvrB (which is found in excess of UvrA *in vivo* (Crowley and Hanawalt, 1998)) to form a UvrA-UvrB complex which then goes on to bind DNA. However *in vitro* UvrA can first bind DNA and then recruit UvrB (Yeung *et al.*, 1986a). The formation of the UvrA-UvrB-DNA complex is dependent on ATP binding. Upon ATP hydrolysis within this complex UvrA loads UvrB onto the DNA (Orren and Sancar, 1989). The UvrA dimer is released and subsequently restarts the UvrA cycle to bind and load a different molecule of UvrB onto a different lesion within the DNA. The NER steps involving UvrA have been well characterised. However the specific regions and amino acid residues of UvrA involved in these individual steps have yet to be fully determined.

Within the process of TCR UvrA is proposed to be recruited to DNA damage through interactions with Mfd (Selby and Sancar, 1993). The Mfd-UvrA interaction has been suggested to involve the region of UvrA that interacts with UvrB, and the region of Mfd that shares sequence and structural similarity to UvrB (Selby and Sancar, 1993) (Assenmacher *et al.*, 2006) (Deaconescu *et al.*, 2006). Lesions are repaired 10-fold faster by TCR than by global NER (Bohr *et al.*, 1985). This is presumably due to a decrease in the time taken to form the UvrA-UvrB-DNA complex after the DNA has been damaged. This in turn is presumably due to the recruitment of UvrA to the lesion by Mfd. There is no evidence to suggest that Mfd can recruit UvrB to the lesion either directly by the formation of a UvrB-Mfd complex or indirectly by recruitment of a UvrA-UvrB complex through interactions made with UvrA.

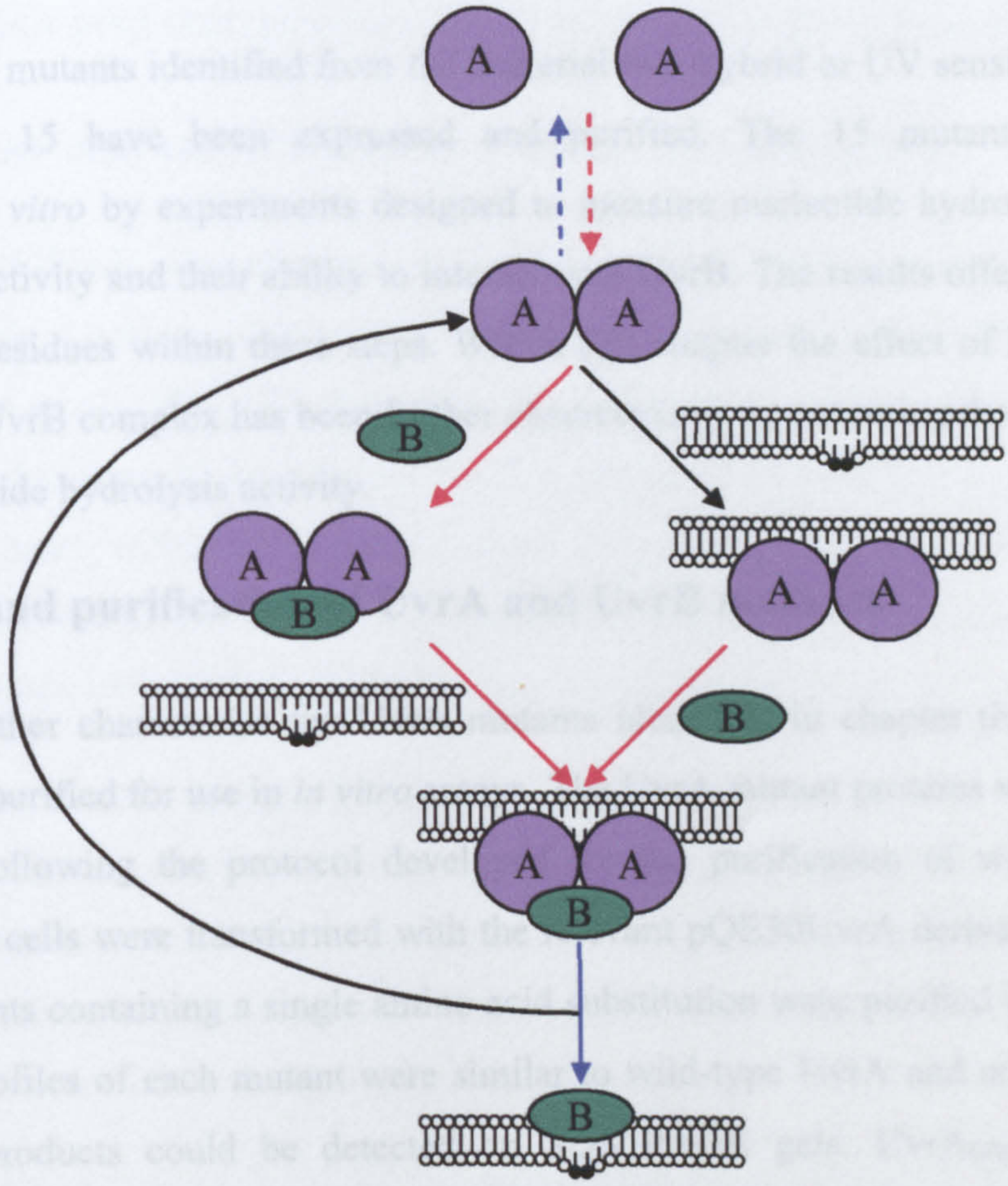

Figure 5.1 The role of UvrA in NER.

UvrA forms homodimers in a reaction that is stimulated by ATP binding and reversed by ATP hydrolysis. In a two-step reaction the UvrA dimer can first bind UvrB and then DNA or it can first bind DNA and then UvrB to form a UvrA-UvrB-DNA complex. The formation of the UvrA-UvrB-DNA complex requires ATP binding. Upon ATP hydrolysis UvrA loads UvrB onto the DNA and is then released. Solid red arrows indicate reactions requiring ATP to be bound whilst the solid blue arrow indicates a requirement for ATP hydrolysis. The dashed arrows indicate that these reactions are enhanced by but do not require ATP binding (red) or hydrolysis (blue).

Of the 20 UvrA mutants identified from the bacterial two-hybrid or UV sensitivity screens (chapter three) 15 have been expressed and purified. The 15 mutants have been characterised *in vitro* by experiments designed to measure nucleotide hydrolysis activity, DNA binding activity and their ability to interact with UvrB. The results offer insights into the key UvrA residues within these steps. Within this chapter the effect of Mfd on UvrA and the UvrA-UvrB complex has been further characterised, by assessing the effect of Mfd on their nucleotide hydrolysis activity.

Expression and purification of UvrA and UvrB mutants

In order to further characterise the UvrA mutants identified in chapter three they were expressed and purified for use in *in vitro* assays. The UvrA mutant proteins were expressed and purified following the protocol developed for the purification of wild-type UvrA except that the cells were transformed with the relevant pQE30UvrA derivative. 15 of the 20 UvrA mutants containing a single amino acid substitution were purified in this manner. The elution profiles of each mutant were similar to wild-type UvrA and no contaminants of the final products could be detected on SDS PAGE gels. $UvrA_{GS034}$, $UvrA_{SP038}$, $UvrA_{FI064}$, $UvrA_{GR099}$ and $UvrA_{CR120}$ were not purified.

$UvrB_{RE183}$ and $UvrB_{RA213}$ were also analysed *in vitro*. $UvrB_{RE183}$ would act as a negative control in UvrA-UvrB interaction assays as it had previously been shown to have a weak interaction with UvrA (Truglio *et al.*, 2004). $UvrB_{R213}$ was the only fully conserved residue within the proposed UvrA interaction domain of UvrB (Truglio *et al.*, 2004). $UvrB_{RE183}$ and $UvrB_{RA213}$ were expressed and purified following the protocol developed for the purification of wild-type UvrB except that the cells were transformed with the relevant pQE30UvrB derivative. The elution profiles were similar to wild-type UvrB and no contaminants of the final products could be detected on SDS PAGE gels. Therefore 15 UvrA mutants and two UvrB mutants had been successfully purified ready for *in vitro* analysis.

Effect of amino acid substitutions in UvrA and UvrB on incision activity

Effect of amino acid substitutions in UvrB on incision activity

Loss of the UvrA-UvrB interaction was expected to influence downstream NER processes including incision. $UvrB_{RE183}$ had previously been shown to have a reduced UvrA binding affinity (Truglio *et al.*, 2004). To determine if the incision activity detected on SMILing DNA (chapter four) would be affected by this known UvrA-UvrB interaction mutant, $UvrB_{RE183}$ was tested within the 5′ incision assay (Figure 5.2). At the same time the effect of $UvrB_{RA213}$ was also tested. The assay was carried out as described in chapter four except that the biotinylated DNA had not been digested with EcoRI (Figure 4.8).

When wild-type UvrB was present incision was detected eight and 15 phosphodiester bonds 5′ of the lesion as expected. $UvrB_{RA213}$ enabled incision of the DNA comparable to the incision level seen under wild-type conditions. When $UvrB_{RE183}$ was present only a small amount of cleavage was detected eight phosphodiester bonds 5′ from the biotin and no cleavage was detected 15 phosphodiester bonds away.

In this assay $UvrB_{RA213}$ was able to facilitate incision to wild-type levels which is consistent with published data in which this substitution had no detectable *in vitro* effect (Truglio *et al.*, 2004). The result of the known UvrA-UvrB interaction mutant, $UvrB_{RE183}$, indicated that a change in the UvrA-UvrB affinity has a detectable effect on cleavage under our assay conditions.

Effect of amino acid substitutions in UvrA on incision activity

The incision assay was repeated with the UvrA mutants to determine if any of the substitutions affected incision (Figure 5.3).

Most of the 15 UvrA mutants were able to facilitate incision activity although some were unable to support the secondary cleavage 15 phosphodiester bonds 5′ from the biotin site. $UvrA_{RL023}$, $UvrA_{VD073}$, $UvrA_{LP151}$ and $UvrA_{VE202}$ were unable to support incision activity.

The majority of the UvrA mutants were still able to fulfil their overall role in NER. However some were unable to do so and some behaved slightly differently than wild-type. At this stage it was not known if the UvrA mutants that failed to support incision of the

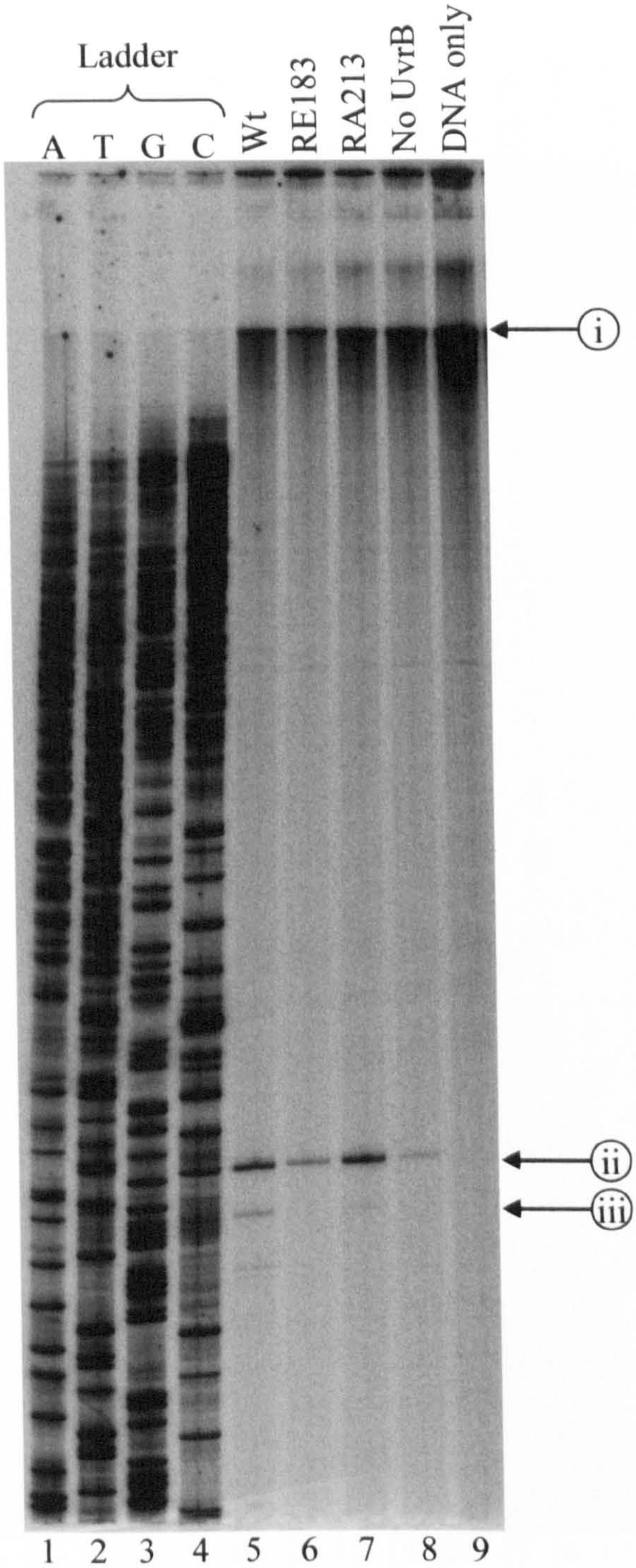

Figure 5.2 Effect of amino acid substitutions in UvrB on incision activity.

The pSRT7A1 BamHI/BamHI fragment that had been biotinylated by the SMILing reaction was 5′ ^{32}P labelled. The DNA (0.25 nM) was then treated with 100 nM UvrA, 100 nM UvrB mutant (as indicated), 200 nM UvrC and 1 mM ATP in repair buffer (lanes 5-7) or mock treated (lanes 8 and 9). The reactions were incubated at 37°C for 30 minutes, purified and run on a 6% acrylamide 7 M urea sequencing gel. The arrows indicate: i, the full-length fragment (2568 bp); ii, the cleavage product eight phosphodiester bonds 5′ from the biotin site (142 bp); iii, the cleavage product 15 phosphodiester bonds 5′ from the biotin site (135 bp). The sequencing ladder was generated using pSRlacUV5_BamHI as the primer and pSRT7A1 as the template (lanes 1-4). The unexpected incision product detected in lane 8 may be due to an experimental error.

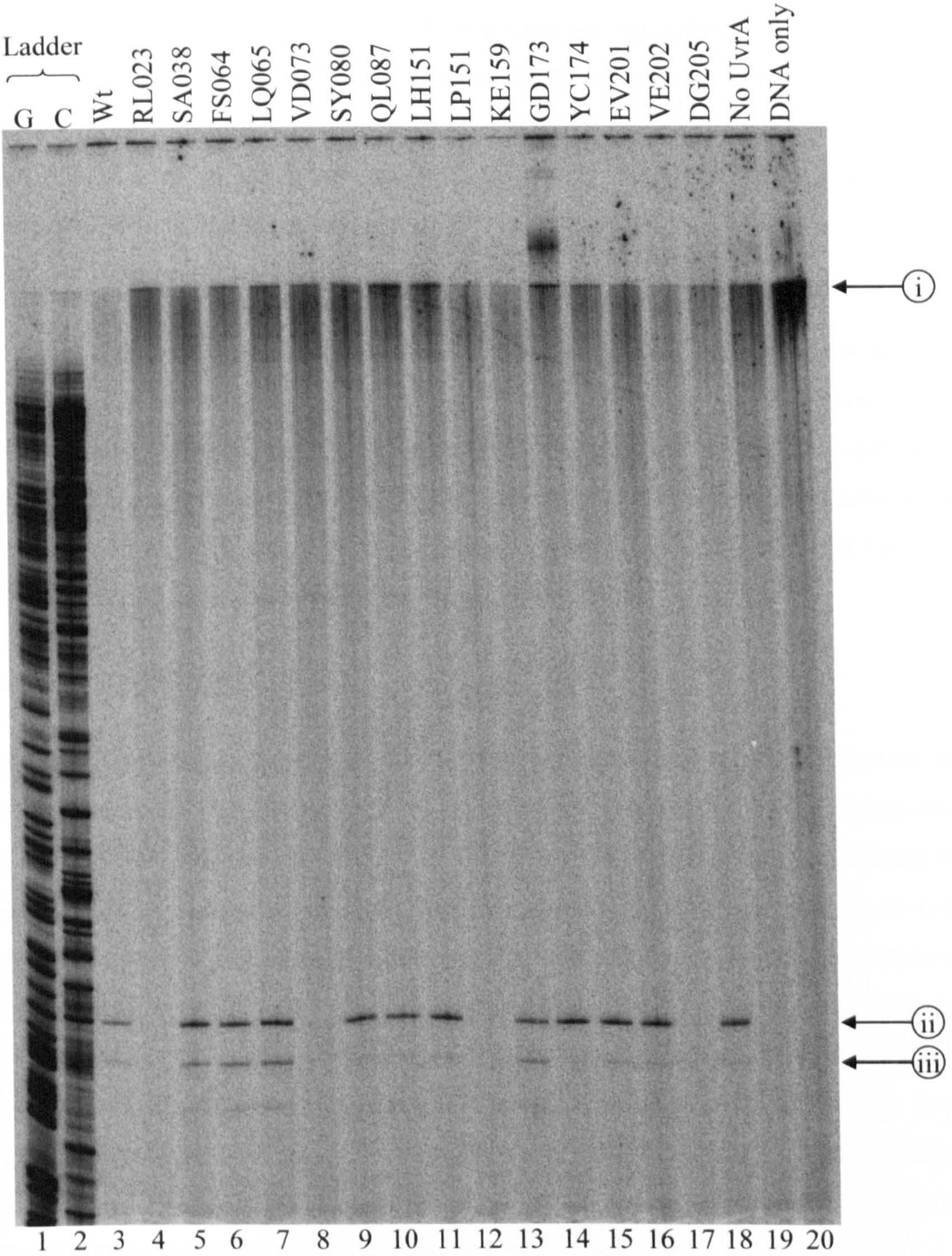

Figure 5.3 Effect of amino acid substitutions in UvrA on incision activity.

The pSRT7A1 BamHI/BamHI fragment that had been biotinylated by the SMILing reaction was 5′ ^{32}P labelled. The DNA (0.25 nM) was then treated with 100 nM of the indicated UvrA mutant, 100 nM UvrB, 200 nM UvrC and 1 mM ATP in repair buffer (lanes 3-18) or mock treated (lanes 19 and 20). The reactions were incubated at 37°C for 30 minutes, purified and run on a 6% acrylamide 7 M urea sequencing gel. The arrows indicate: i, the full-length fragment (2568 bp); ii, the cleavage product eight phosphodiester bonds 5′ from the biotin site (142 bp); iii, the cleavage product 15 phosphodiester bonds 5′ from the biotin site (135 bp). The sequencing ladder was generated using pSRlacUV5_BamHI as the primer and pSRT7A1 as the template (lanes 1-2).

DNA were functional in any aspect of NER. The band corresponding to incision 15 bases 5′ of the damage has previously been reported to be caused by a UvrA independent UvrB-UvrC incision reaction (Moolenaar *et al.*, 1998a). It would therefore be expected in all UvrA mutant lanes in which the original cleavage eight phosphodiester bonds 5′ form the biotin site had occurred. However, this was not observed and could indicate that this secondary incision reaction required UvrA.

Whilst this incision assay demonstrated that several of the mutant proteins facilitated NER the assay was not expected to detect mutants that only subtly affected individual steps of the NER process. When a defect was detected the nature of the defect could not be determined as many different UvrA functions were required to enable the incision reaction to occur. Therefore further *in vitro* assays were used to analyse the effect of the UvrA amino acid substitutions within the individual steps of NER.

Nucleotide hydrolysis activity

A high throughput (96 well) pyruvate kinase lactate dehydrogenase (PK/LDH) assay was utilised to monitor ATP hydrolysis rates by the UvrA protein (Figure 5.4) (Kiianitsa *et al.*, 2003). During nucleotide hydrolysis UvrA converts ATP to ADP and Pi (Seeberg and Steinum, 1982). A substrate level phosphorylation reaction in which PK transferred a phosphate group from phosphoenolpyruvate (PEP) onto ADP to form ATP and pyruvate enabled the level of ATP within the system to remain constant. The pyruvate was then reduced by NADH in a LDH catalysed reaction to form lactate and NAD. The loss of NADH from the reaction was monitored as a decrease in absorbance at 340 nm. Every time one molecule of ATP was converted to ADP one molecule of NADH reduced pyruvate and was thus lost. The loss of NADH from the system was plotted over time and the rate of ATP hydrolysis determined (Figure 5.5A).

Characterisation of nucleotide hydrolysis activity of wild-type UvrA

ATPase activity of wild-type UvrA

The ATPase activity of wild-type UvrA (purified as described in chapter four) was measured by nucleotide hydrolysis assays to confirm that its ATPase activity conformed to published data. Each nucleotide hydrolysis reaction consisted of 50 nM UvrA, between 0

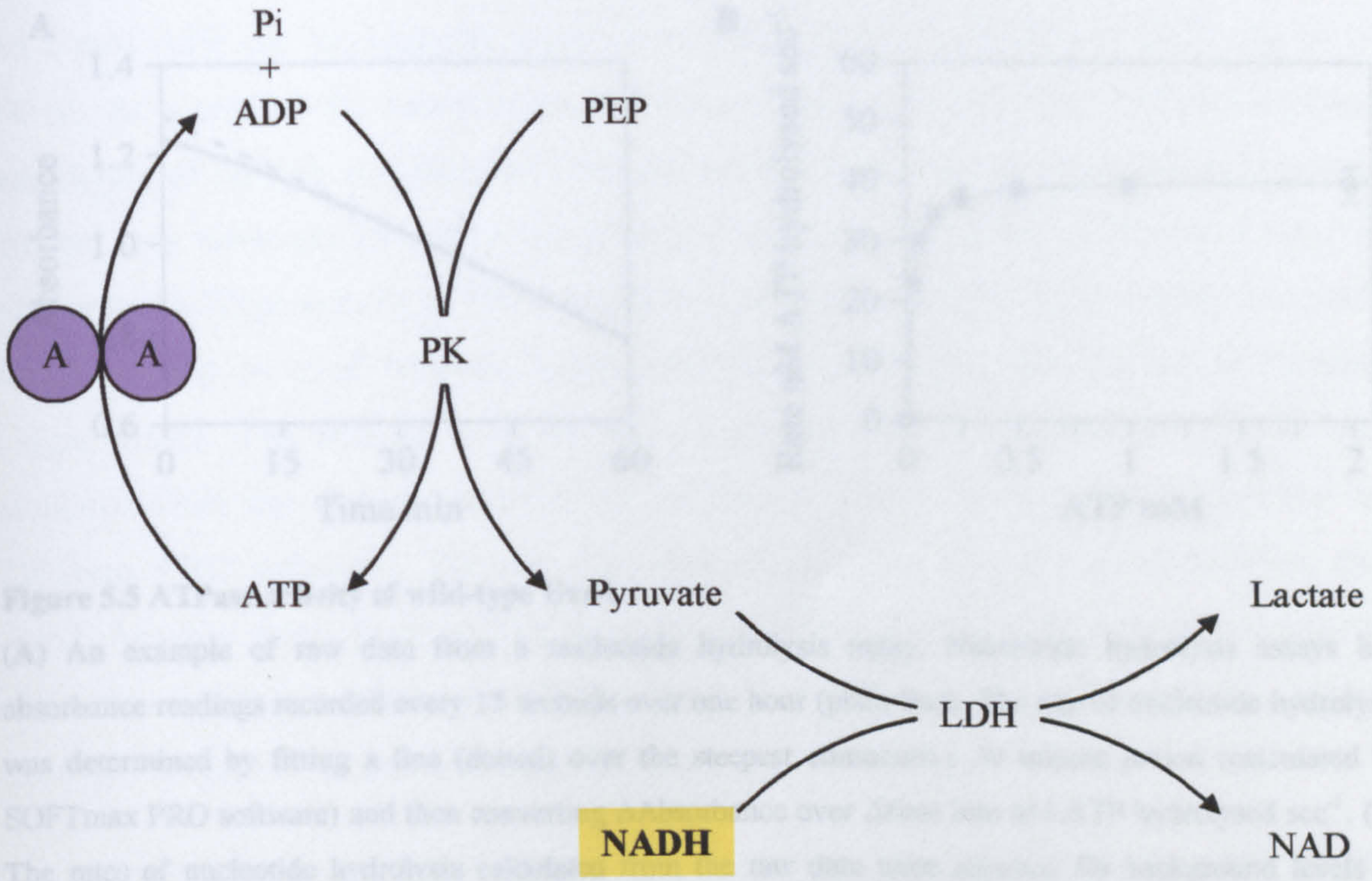

Figure 5.4 Principle of the PK/LDH nucleotide hydrolysis assay.

UvrA is an ATPase that hydrolyses ATP to ADP and free phosphate (Pi). In a substrate level phosphorylation reaction PK transfers a phosphate group from PEP onto ADP to generate ATP and pyruvate. Pyruvate is reduced by NADH in the LDH catalysed reaction resulting in the production of lactate and NAD. The amount of NADH present within a reaction can be detected in a spectrophotometer at a wavelength of 340 nm. For every one molecule of ATP that is hydrolysed one molecule of NADH is lost.

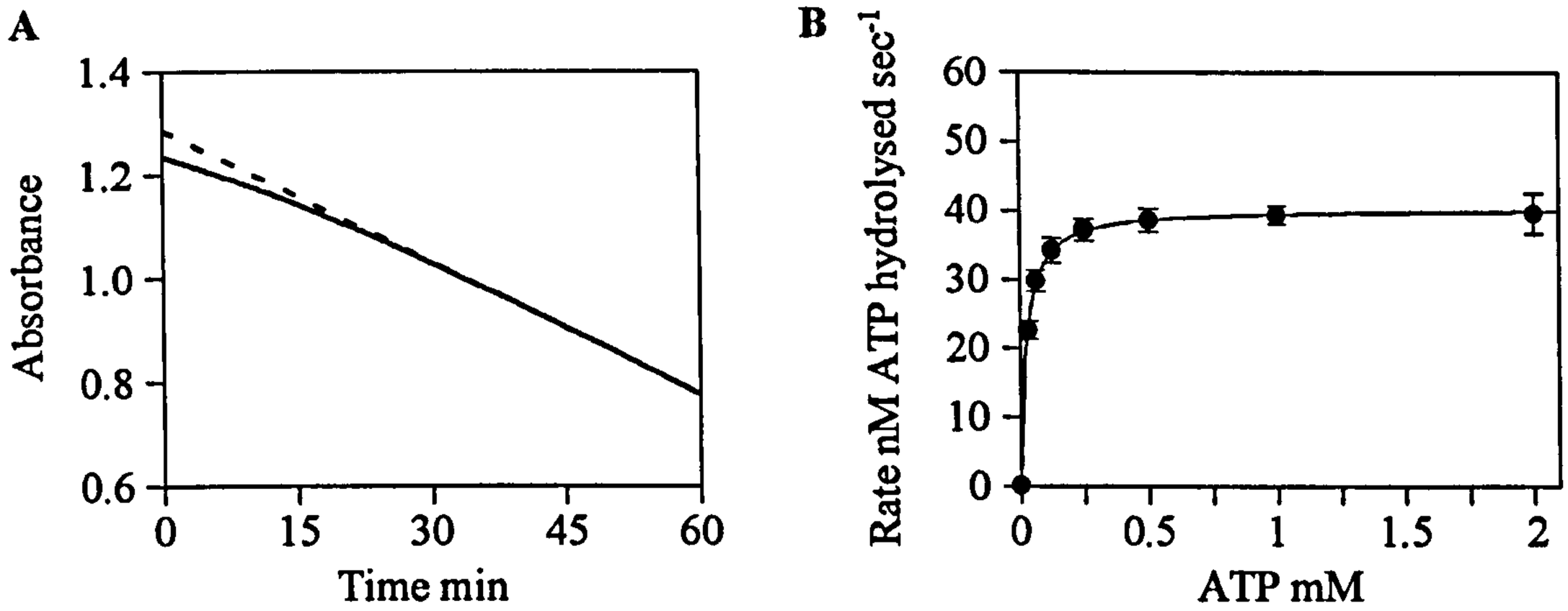

Figure 5.5 ATPase activity of wild-type UvrA.

(A) An example of raw data from a nucleotide hydrolysis assay. Nucleotide hydrolysis assays had absorbance readings recorded every 15 seconds over one hour (plain line). The rate of nucleotide hydrolysis was determined by fitting a line (dotted) over the steepest consecutive 30 minute period (calculated by SOFTmax PRO software) and then converting ΔAbsorbance over Δtime into nM ATP hydrolysed sec^{-1}. **(B)** The rates of nucleotide hydrolysis calculated from the raw data were adjusted for background levels of NADH degradation (no UvrA). The results were then averaged (at least three independent experiments) and plotted onto graphs with standard deviation. A Michaelis-Menten curve was fitted to the data using GraFit software.

and 2 mM ATP and the reagents required for the PK/LDH reaction in a final volume of 200 µl. As a control the reactions were repeated without UvrA. Very little background degradation of NADH was detected from the control reactions and what background was detected was subsequently subtracted from the UvrA assay results. Analysis of the raw data for the ATPase activity of UvrA revealed that the rate of hydrolysis slightly increased during the first 20 to 30 minutes before reaching a steady state for the last 30 minutes (Figure 5.5A). The rate of ATP hydrolysis for each ATP concentration tested was calculated from the steepest consecutive 30 minute period of the curve (identified by SOFTmax PRO software). The rate was then adjusted for background degradation (no UvrA). Average rates (from at least three independent experiments) were plotted against ATP concentration, a Michaelis-Menten curve fitted and the K_m, V_{max} and k_{cat} values calculated (Figure 5.5B and wild-type ATPase values in Table 5.1).

The ATPase K_m value of UvrA measured under these conditions (23.4 µM ATP) closely resembled that measured by Sancar's lab who reported a K_m value of 29.6 µM ATP (Myles and Sancar, 1991). However it differed from the range of K_m values (103 µM to 210 µM ATP) measured by Grossman's lab (Caron and Grossman, 1988) (Oh *et al.*, 1989) (Thiagalingam and Grossman, 1991) (Wang *et al.*, 1994). The ATPase k_{cat} value of UvrA measured under these conditions (48.5 min^{-1}) was similar to that measured by Sancar's lab (32.5 min^{-1}) and was close to the lower end of reported values from Grossman's lab (between 56 and 171 min^{-1}) (Myles and Sancar, 1991) (Caron and Grossman, 1988) (Oh *et al.*, 1989) (Thiagalingam and Grossman, 1991) (Wang *et al.*, 1994). The data confirmed that my purified histidine-tagged UvrA had similar ATPase activity to some previously published work.

Effect of UvrB on the nucleotide hydrolysis activity of UvrA

Under certain conditions the binding of UvrB to UvrA causes an effect on the overall nucleotide hydrolysis activity (Caron and Grossman, 1988). In the UvrA-UvrB complex there are five nucleotide hydrolysis regions. Of these, four are within UvrA. UvrA can hydrolyse ATP and can also hydrolyse GTP (Caron and Grossman, 1988). The fifth site is activated within UvrB upon binding to UvrA. This UvrB site will only hydrolyse ATP, it can not hydrolyse GTP (Caron and Grossman, 1988).

	ATPase properties of UvrA			GTPase properties of UvrA		
	K_m μM ATP	V_{max} nM ATP sec^{-1}	k_{cat} min^{-1}	K_m μM GTP	V_{max} nM GTP sec^{-1}	k_{cat} min^{-1}
Wild-type	23.4	40.4	48.5	33.5	58.5	70.2
RL023	288	10.7	12.8	737	10.2	12.2
SA038	106	5.62	6.75	48.6	2.70	3.24
FS064	18.6	54.2	65.0	28.7	64.5	77.4
LQ065	63.2	37.5	45.0	107	40.5	48.6
VD073	190	14.7	17.6	426	10.1	12.2
SY080	290	23.8	28.6	820	24.1	28.9
QL087	97.5	20.1	24.2	229	23.2	27.8
LH151	30.6	42.4	50.9	45.9	48.3	57.9
LP151	70.5	31.1	37.3	106	31.5	37.8
KE159	24.6	49.2	59.0	41.4	58.2	69.9
GD173	18.2	51.3	61.6	24.2	58.3	69.9
YC174	22.4	51.8	62.1	30.5	58.6	70.4
EV201	27.5	35.8	42.9	36.4	38.6	46.3
VE202	139	18.9	22.7	179	16.7	20.0
DG205	23.0	49.5	59.4	30.9	56.2	67.4

Table 5.1 ATPase and GTPase K_m, V_{max} and k_{cat} values for UvrA and UvrA mutants.

K_m, V_{max} and k_{cat} values were calculated from the data in Figure 5.5, Figure 5.6, Figure 5.10 and Figure 5.11.

The effect on overall ATPase activity when UvrB is mixed with UvrA depends on the conditions used. Under conditions in which the UvrA concentration was less than 5 nM and ATP was saturating the presence of 225 nM UvrB caused the stimulation of ATPase activity (Caron and Grossman, 1988). Under conditions in which UvrA concentration exceeded 5 nM the presence of UvrB inhibited ATPase activity (Caron and Grossman, 1988). The stimulation/inhibition effect on the ATPase activity of UvrA by UvrB would be complicated to interpret due to the activation of the UvrB ATPase activity upon the formation of the UvrA-UvrB complex (Caron and Grossman, 1988). Therefore ATP would not be a suitable substrate to analyses the effect of UvrB on the nucleotide hydrolysis activity of UvrA.

If GTP was used instead of ATP the interpretation of the effect of UvrB on the nucleotide hydrolysis activity of UvrA would be simplified. This is because UvrB (within the UvrA-UvrB complex) can not hydrolyse GTP whereas UvrA can (Caron and Grossman, 1988). Any change in GTPase activity upon addition of UvrB to UvrA would therefore be a direct result of a change in the UvrA GTPase activity. The effect of UvrB on UvrA can therefore be analysed by GTPase assays (Truglio *et al.*, 2004).

GTPase activity of wild-type UvrA

In order to analyse the effect of UvrB on the GTPase activity of UvrA it was important to establish the GTPase properties of my UvrA preparation. This was done using the ATPase assay conditions except that ATP had been substituted by GTP. The results from the GTPase assay were similar to the ATPase results (Figure 5.6 and wild-type GTPase data in Table 5.1). The GTPase K_m value (33.5 μM GTP) differed from the only previously reported value of 910 μM GTP (Caron and Grossman, 1988). The GTPase k_{cat} value (70.2 min^{-1}) was within two-fold of the 114 min^{-1} value previously reported (Caron and Grossman, 1988). My preparation of purified UvrA was confirmed to be a GTPase with a suitable level of activity for use in inhibition experiments.

Effect of UvrB on the GTPase activity of wild-type UvrA

The addition of UvrB to the UvrA GTPase assay described above should result in the measurable reduction of GTP hydrolysis (Claassen and Grossman, 1991). This would be a useful tool in characterisation studies of the UvrA mutant proteins. Therefore the effect of

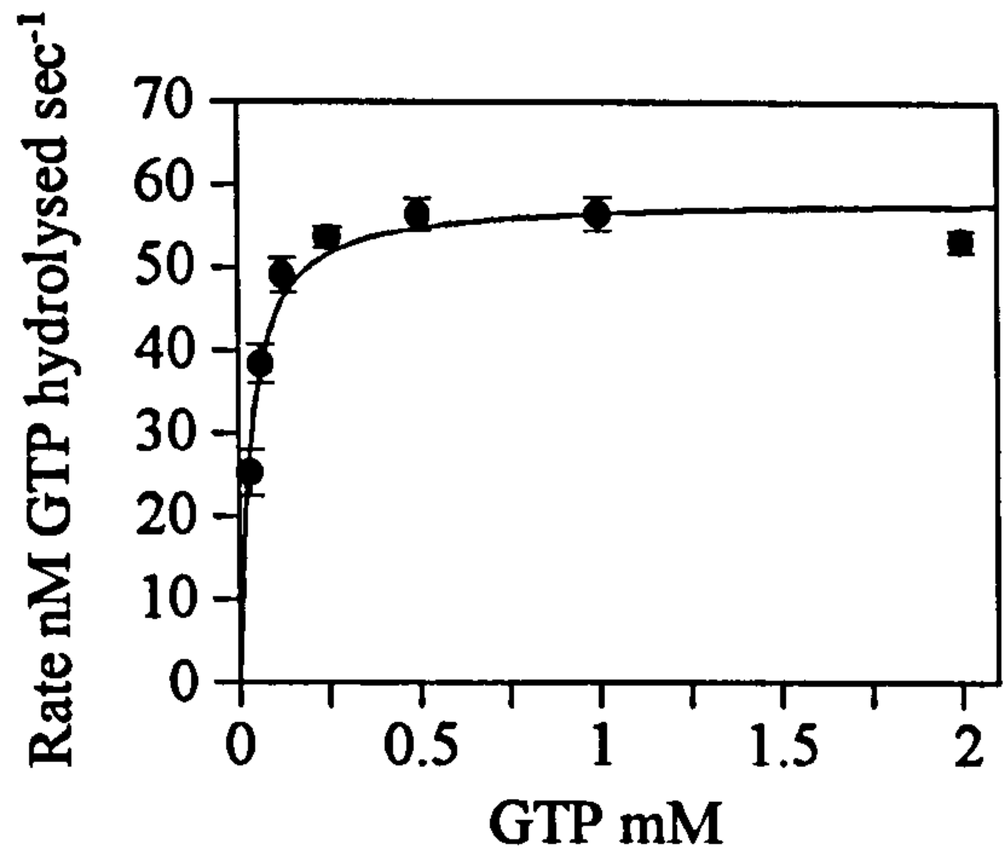

Figure 5.6 GTPase activity of wild-type UvrA.

GTP hydrolysis rates were calculated from data generated from nucleotide hydrolysis assays. Each assay contained the PK/LDH reagents, 50 nM UvrA and the indicated concentration of GTP in a final volume of 200 µl. The reactions were incubated at 37°C for one hour with readings taken every 15 seconds. The rates were calculated by measuring the steepest consecutive 30 minute period of the curve and then background degradation was subtracted. The rates shown are an average of at least three independent experiments (with standard deviation). A Michaelis-Menten curve was fitted to the data using GraFit software.

wild-type UvrB on wild-type UvrA needed to be determined for my proteins. On its own UvrB was, as expected, unable to hydrolyse GTP (data not shown) whilst UvrA could (see above).

The data obtained from reactions when both UvrA and UvrB were present did not fit the Michaelis-Menten equation and thus K_m and V_{max} values could not be calculated (Figure 5.7). The addition of UvrB to the UvrA nucleotide hydrolysis reactions caused a reduction in GTPase activity at saturating levels of GTP. As the UvrB concentration increased so did the level of GTPase inhibition. However at UvrB concentrations greater than 50 to 100 nM UvrB the level of inhibition was saturated and additional UvrB had no further detectable effect. This assay thus provided a way to detect the UvrA-UvrB interaction.

The stoichiometry of the UvrA-UvrB complex is believed to consist of a dimer of UvrA and either a monomer or dimer of UvrB (Orren and Sancar, 1989) (Verhoeven *et al.*, 2002). If it is assumed that the preparation of UvrA and UvrB had the same specific activity then the stoichiometry of the UvrA-UvrB complex can be calculated from the above inhibition data. If the UvrA-UvrB complex consisted of two molecules of UvrA and one molecule of UvrB then 25 nM UvrB would be sufficient to inhibit the GTPase activity of 50 nM UvrA. If the UvrA-UvrB complex consisted of two molecules of UvrA and two molecules of UvrB then 50 nM of UvrB would be required to inhibit the GTPase activity of 50 nM UvrA. The inhibition data indicated that between 50 and 100 nM UvrB was required to obtain inhibition saturation of 50 nM UvrA. This suggests that the UvrA-UvrB ratio in the UvrA-UvrB complex was at least one molecule of UvrB for each molecule of UvrA.

Effect of amino acid substitutions in UvrB on the GTPase activity of UvrA

An amino acid substitution within either UvrA or UvrB that prevented the formation of the UvrA-UvrB complex should prevent the inhibition of the UvrA GTPase activity by UvrB. $UvrB_{RE183}$, which was unable to interact with UvrA in pull-down assays (Truglio *et al.*, 2004), was therefore tested within this system as a control (Figure 5.8). At the same time $UvrB_{RA213}$ was also tested (Figure 5.8). $UvrB_{RE183}$ did not inhibit the GTPase activity of UvrA. $UvrB_{RA213}$ slightly inhibited the GTPase activity of UvrA but not to the level that wild-type UvrB could. The results indicated that the loss of the UvrA-UvrB interaction resulted in the loss of the UvrB inhibitory effect on the GTPase activity of UvrA. The

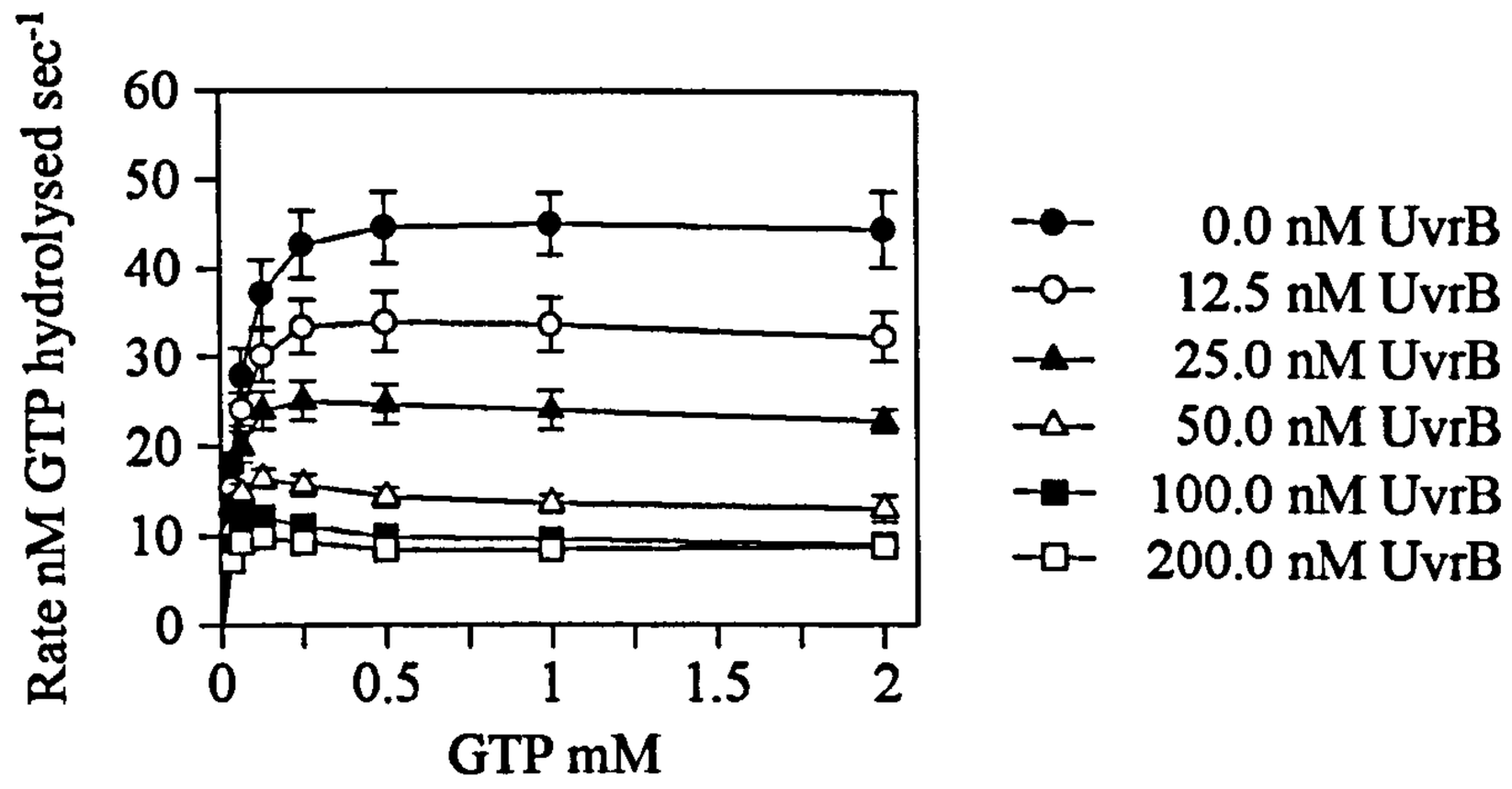

Figure 5.7 Effect of UvrB on the GTPase activity of UvrA.

GTP hydrolysis rates were calculated from data generated from nucleotide hydrolysis assays. Each assay contained the PK/LDH reagents, 50 nM UvrA, the indicated concentration of GTP and the indicated concentration of UvrB. The reactions were incubated at 37°C for one hour with readings taken every 15 seconds. The rates were calculated by measuring the steepest consecutive 30 minute period of the curve and then background degradation subtracted. The rates shown are an average of at least three independent experiments (with standard deviation).

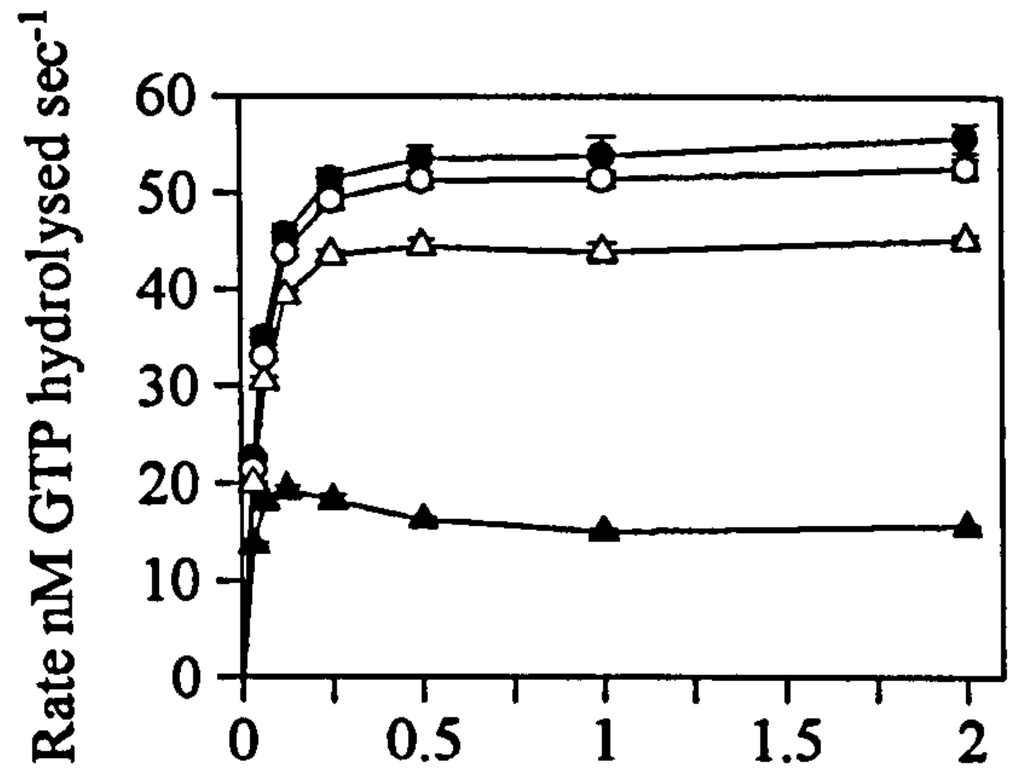

Figure 5.8 Effect of amino acid substitutions in UvrB mutants on the GTPase activity of UvrA.
GTP hydrolysis rates were calculated from data generated from nucleotide hydrolysis assays. Each assay contained the PK/LDH reagents, 50 nM UvrA, the indicated concentration of GTP and either 0 nM UvrB (black circles), 50 nM UvrB (black triangles), 50 nM $UvrB_{RE183}$ (white circles) or 50 nM $UvrB_{RA213}$ (white triangles) in a final volume of 200 µl. The reactions were incubated at 37°C for one hour with readings taken every 15 seconds. The rates were calculated by measuring the steepest consecutive 30 minute period of the curve and then background degradation subtracted. The rates shown are an average of at least three independent experiments (with standard deviation).

assay could therefore be used to determine which UvrA mutants were unable to form the UvrA-UvrB complex.

Effect of Mfd on the GTPase activity of wild-type UvrA

UvrB and Mfd share a region of sequence and structural homology that is believed to contain the UvrA interaction domain (Selby and Sancar, 1993) (Deaconescu *et al.*, 2006). It has been suggested that the same region of UvrA is involved in the UvrA-UvrB and the UvrA-Mfd interaction (Selby and Sancar, 1993). If this is true the GTPase activity of UvrA that was inhibited by UvrB may also be inhibited by Mfd.

Controls were carried out to confirm that Mfd could not hydrolyse GTP on its own. The nucleotide hydrolysis assay was carried out with and without Mfd in the presence of GTP. 200 nM Mfd was unable to hydrolyse GTP under these conditions (data not shown). This agreed with previous data in which Mfd was unable to utilise GTP to displace stalled elongation complexes which it could displace in the presence of ATP (Chambers, 2005).

Mfd (200 nM) was added to a nucleotide hydrolysis assay containing UvrA and GTP (Figure 5.9). The data generated was fitted to the Michaelis-Menten equation and K_m and V_{max} values calculated. The K_m values with and without Mfd were 47.0 and 46.6 μM GTP respectively. The V_{max} values with and without Mfd were 43.2 and 50.9 nM GTP sec^{-1} respectively. Despite the concentration of Mfd being four-fold in excess of the concentration of UvrB required for saturation the inhibition effect of Mfd on the GTPase activity of UvrA was small. Under the nucleotide hydrolysis conditions tested UvrB and Mfd did not have the same effect on UvrA.

The combined effect of UvrB and Mfd on the GTPase activity of UvrA

To understand the process of UvrA and UvrB recruitment within TCR it would be useful to know if UvrB and Mfd compete for the same site on UvrA. One way to investigate this is to determine if Mfd can alleviate the inhibitory effect caused by UvrB on the GTPase activity of UvrA.

At a fixed 2 mM GTP concentration combinations of UvrA, UvrB and Mfd were analysed for GTPase activity under the nucleotide hydrolysis assays conditions used previously (Table 5.2). As expected, UvrB inhibited the GTPase activity of UvrA whilst Mfd had

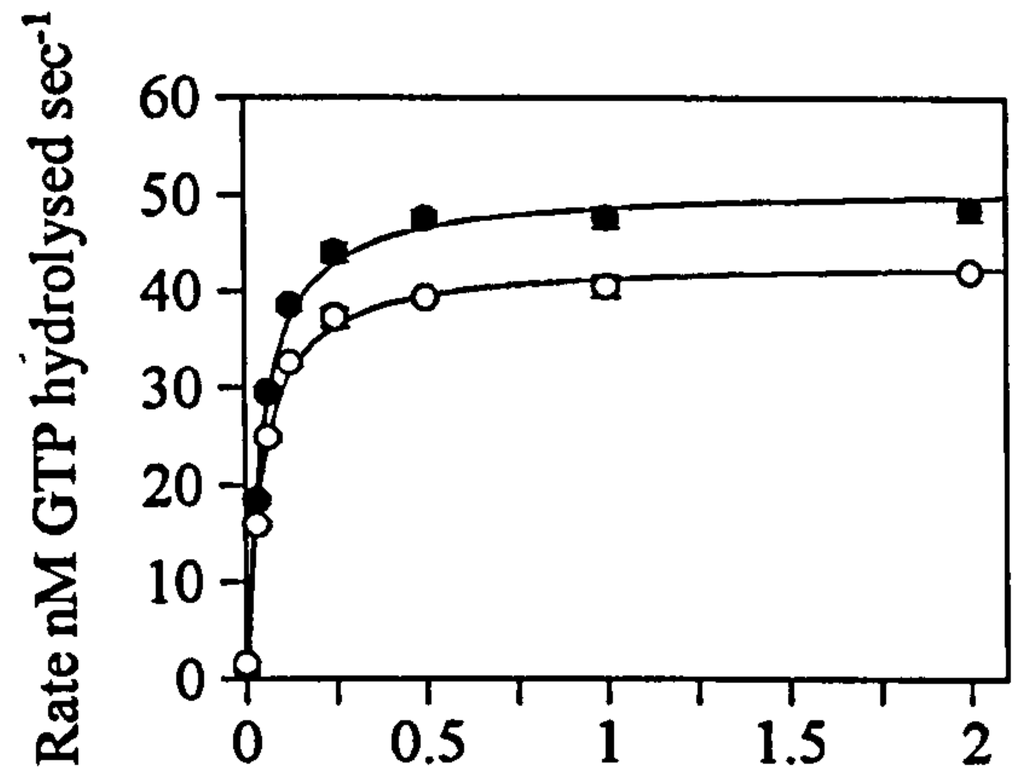

Figure 5.9 Effect of Mfd on the GTPase activity of UvrA.

GTP hydrolysis rates were calculated from data generated from nucleotide hydrolysis assays. Each PK/LDH reaction contained the PK/LDH reagents, 50 nM UvrA, the indicated concentration of GTP and either 0 nM Mfd (black circles) or 200 nM Mfd (white circles) in a final volume of 200 µl. The reactions were incubated at 37°C for one hour with readings taken every 15 seconds. The rates were calculated by measuring the steepest consecutive 30 minute period of the curve and then background degradation subtracted. The rates shown are an average of at least three independent experiments (with standard deviation). A Michaelis-Menten curve was fitted to the data using GraFit.

	0 nM UvrB		50 nM UvrB	
	Rate nM GTP hydrolysed sec-1	**Standard deviation**	**Rate nM GTP hydrolysed sec-1**	**Standard deviation**
0 nM Mfd	73.1	2.53	20.7	1.82
50 nM Mfd	69.2	1.59	21.0	0.183
500 nM Mfd	69.8	1.28	21.8	1.23

Table 5.2 Effect of Mfd and UvrB on the GTPase activity of UvrA.

GTP hydrolysis rates were calculated from data generated from nucleotide hydrolysis assays. Each assay contained the PK/LDH reagents, 50 nM UvrA, 2 mM GTP, the indicated concentration of Mfd and the indicated concentration of UvrB in a final volume of 200 µl. The reactions were incubated at 37°C for one hour with readings taken every 15 seconds. The rates were calculated by measuring the steepest consecutive 30 minute period of the curve and then background degradation subtracted. The rates shown are an average of at least three independent experiments.

relatively little effect. When all three proteins were present the rate of GTPase activity was comparable to the rate detected at the UvrA-UvrB inhibition level. Increasing the Mfd concentration to 500 nM did not alter this result despite being 10-fold in excess of the UvrB concentration. We conclude that under these conditions Mfd did not compete with UvrB for the UvrB binding site on UvrA. This may mean that Mfd binds UvrA at a distinct site or that under these conditions Mfd does not bind at all.

Characterisation of nucleotide hydrolysis activity of UvrA mutants

To determine if any of the identified UvrA amino acid substitutions affected nucleotide hydrolysis activity, ATPase, GTPase and GTPase inhibition experiments were repeated using the 15 UvrA mutants. Each experiment was carried out in triplicate, background rates deducted, the results averaged, Michaelis-Menten curves plotted and K_m and V_{max} values calculated where relevant.

Effect of amino acid substitutions in UvrA on ATPase activity

To determine if any of the 15 mutants were deficient in ATPase activity the ATPase nucleotide hydrolysis assays were used with each mutant replacing wild-type UvrA (Figure 5.10 and Table 5.1). The UvrA mutants can be split into those that have wild-type ATPase activity and those that have deficient (reduced) ATPase activity. ATPase K_m and V_{max} values for $UvrA_{FS064}$, $UvrA_{LH151}$, $UvrA_{KE159}$, $UvrA_{GD173}$, $UvrA_{YC174}$, $UvrA_{EV201}$ and $UvrA_{DG205}$ were within two-fold of the wild-type UvrA values. The ATPase K_m values for $UvrA_{LQ065}$ and $UvrA_{LP151}$ were between two and four-fold of the wild-type value whilst their V_{max} values were comparable to wild-type (less than two-fold different). $UvrA_{RL023}$, $UvrA_{SA038}$, $UvrA_{VD073}$, $UvrA_{SY080}$, $UvrA_{QL087}$ and $UvrA_{VE202}$ had ATPase K_m values at least four-fold in excess of the wild-type value and their V_{max} values were at least two-fold different from wild-type except for $UvrA_{SY080}$. As expected the N-terminal Walker A mutant, $UvrA_{SA038}$, was very poor at hydrolysing ATP. The ATPase k_{cat} value of 6.75 min^{-1} of $UvrA_{SA038}$ was two-fold lower than the reported k_{cat} value (15 min^{-1}) for the neighbouring Walker A mutant $UvrA_{KA037}$ (Myles and Sancar, 1991). It is not known if the amino acid substitutions in mutants that had reduced ATPase activity directly affected ATP binding, ATP hydrolysis, release of ADP or an upstream process such as UvrA dimerization.

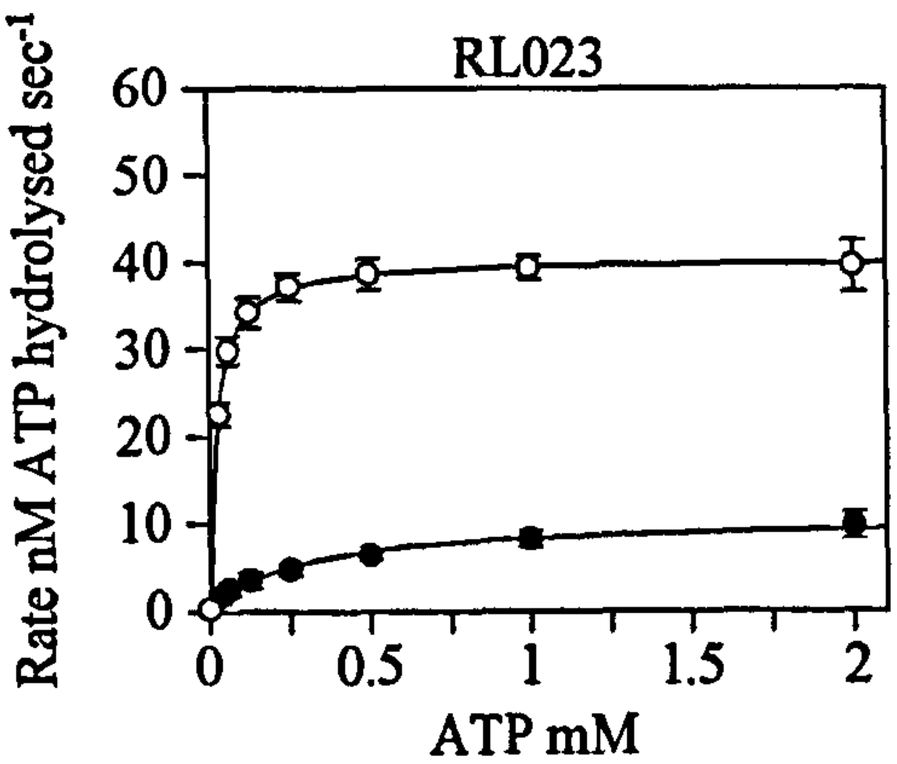

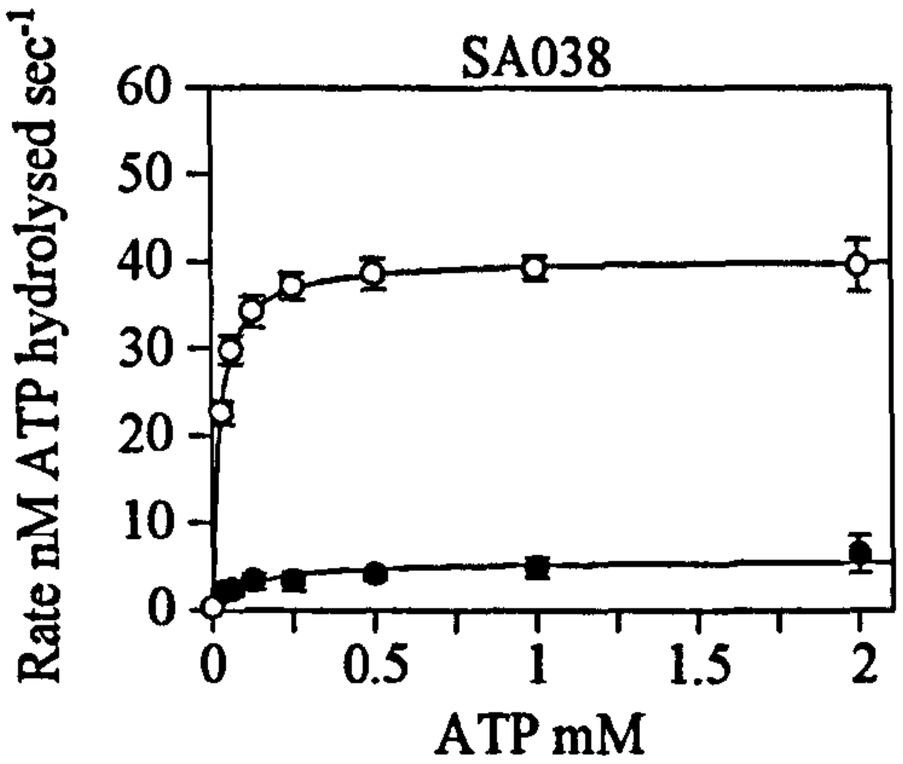

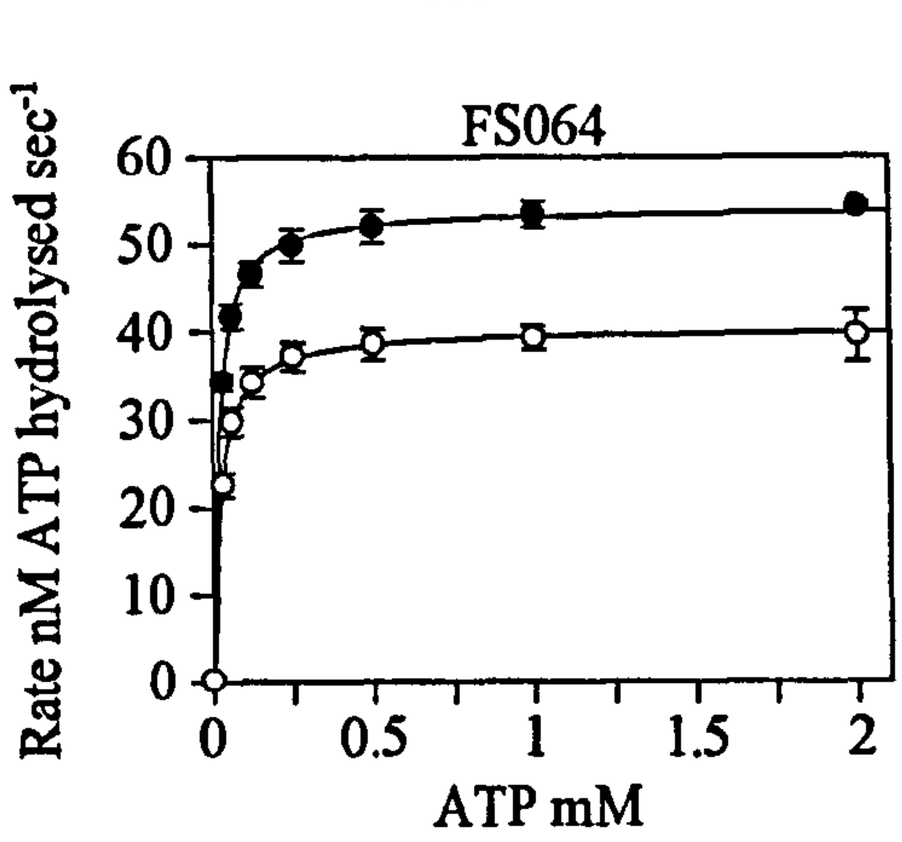

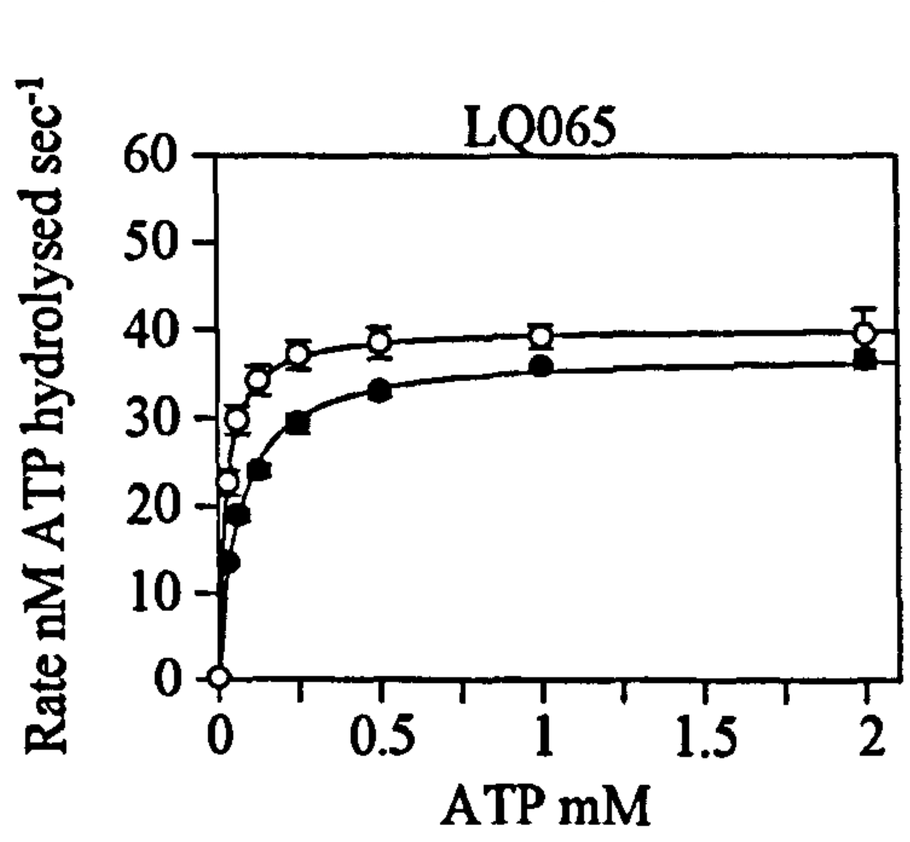

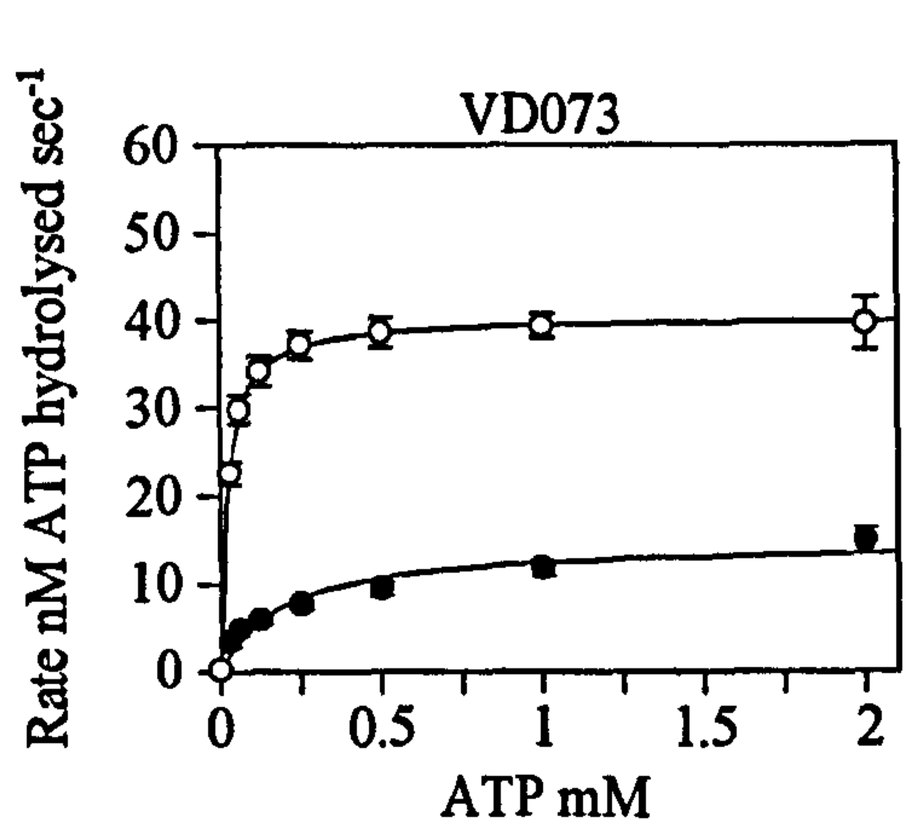

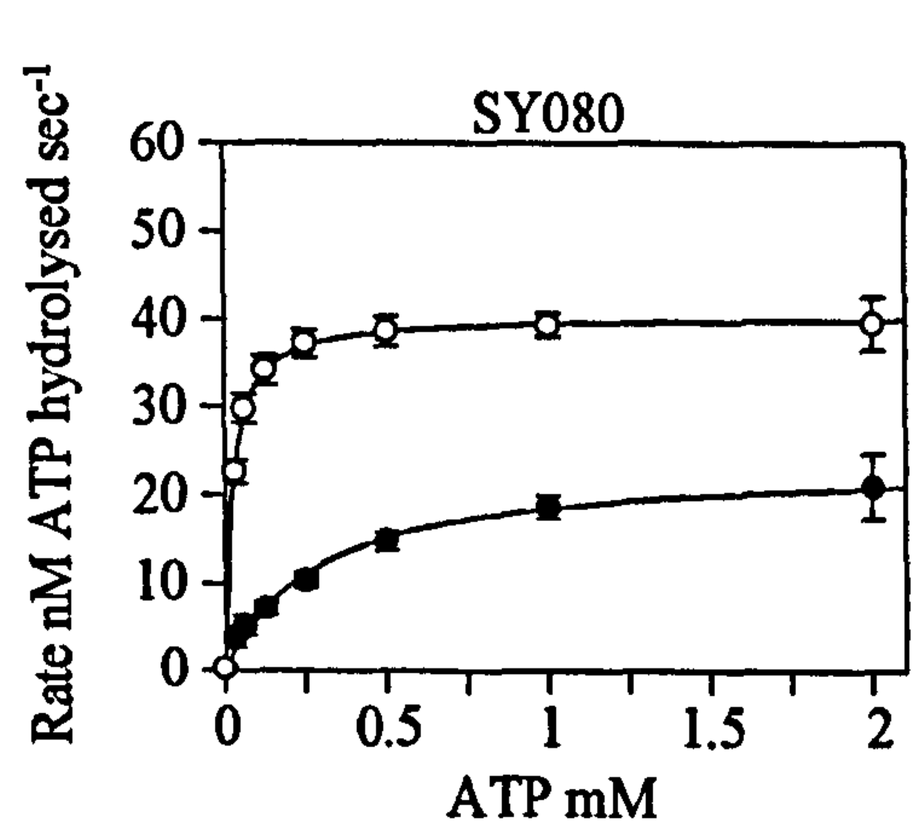

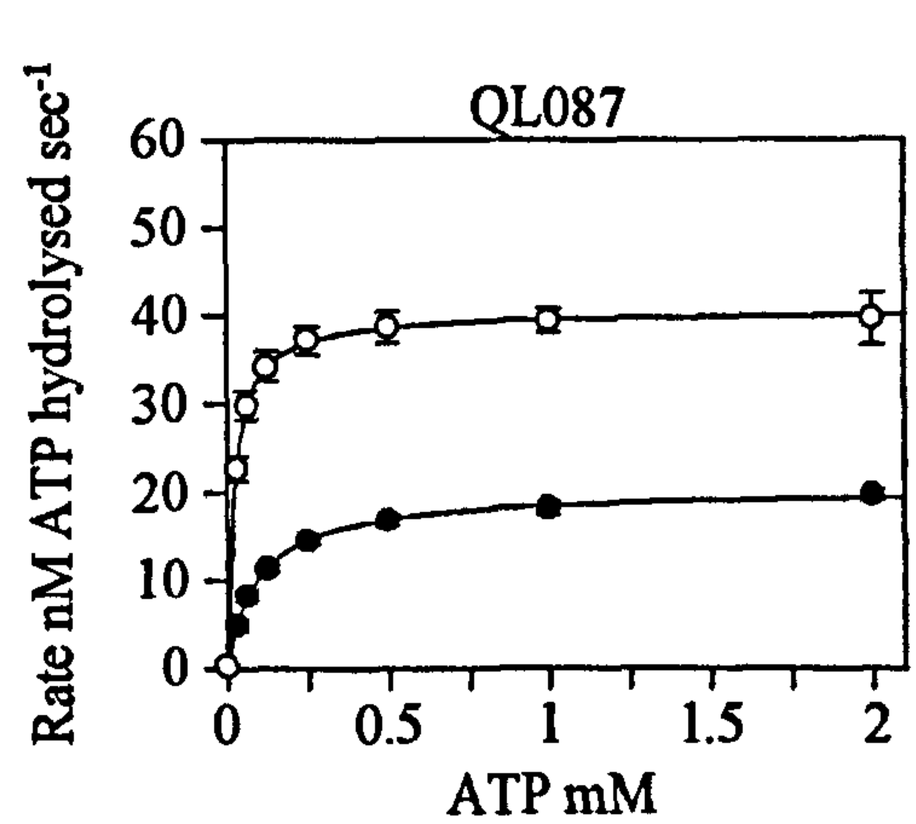

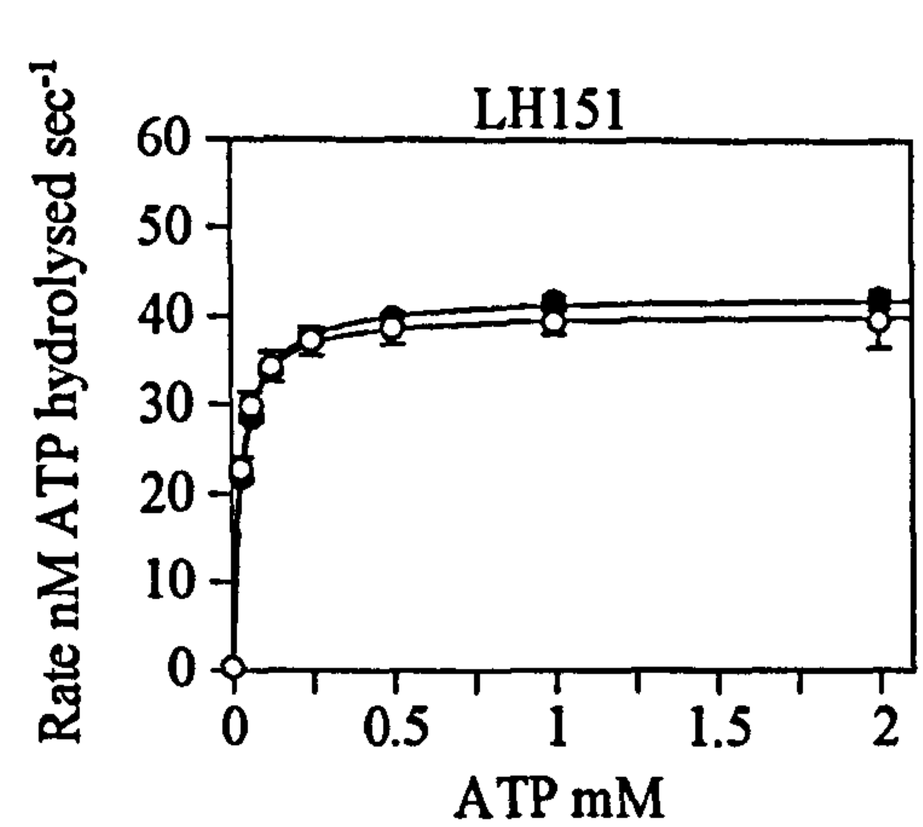

Figure 5.10 Page 1 of 2

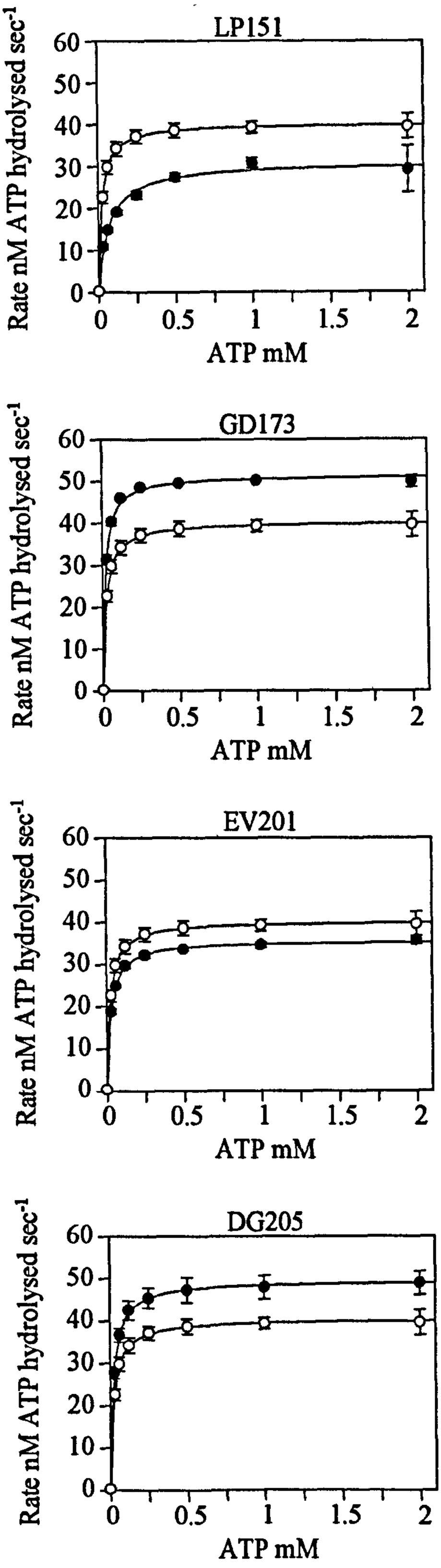

Figure 5.10 Page 2 of 2

Figure 5.10 Effect of amino acid substitutions in UvrA on the ATPase activity of UvrA.

ATP hydrolysis rates were calculated from data generated from nucleotide hydrolysis assays. Each assay contained 50 nM of the indicated UvrA mutant (black circles), the PK/LDH reagents and the indicated concentration of ATP in a final volume of 200 µl. The reactions were incubated at 37°C for one hour with readings taken every 15 seconds. The rates were calculated by measuring the steepest consecutive 30 minute period of the curve and then background degradation subtracted. The rates shown are an average of at least three independent experiments (with standard deviation). A Michaelis-Menten curve was fitted to the data using GraFit. The wild-type UvrA result (from Figure 5.5B) is on all mutant graphs for comparison (white circles).

Effect of amino acid substitutions in UvrA on GTPase activity

To ascertain the effect of the 15 substitutions on GTPase activity the GTPase nucleotide hydrolysis activity was assessed. The majority of the 15 UvrA mutants showed the same general trend as they had when tested for ATPase activity (Figure 5.11 and Table 5.1). Only $UvrA_{SA038}$ showed any difference. Its GTPase K_m value was comparable to wild-type unlike its ATPase K_m value, which was four-fold different. However the very low level of ATPase and GTPase activity seen with this mutant makes this observation unreliable.

Effect of UvrB on the GTPase activity of UvrA mutants

An interaction between UvrA and UvrB is necessary for the inhibition of the UvrA GTPase. Any mutant of UvrA that is unable to interact with UvrB should therefore maintain its GTPase activity upon addition of UvrB. The 15 UvrA mutants were therefore tested to determine which if any were able to maintain their GTPase activity when UvrB was present.

Each UvrA mutant was characterised using the nucleotide hydrolysis assay at 2 mM GTP with or without 100 nM UvrB (a concentration that saw maximum inhibition of 50 nM wild-type UvrA) (Table 5.3). Repression by UvrB on the GTPase activity of $UvrA_{SA038}$, $UvrA_{FS064}$, $UvrA_{QL087}$, $UvrA_{LH151}$, $UvrA_{KE159}$ and $UvrA_{EV201}$ was comparable to the repression by UvrB on the GTPase activity of wild-type UvrA. The GTPase activity of $UvrA_{RL023}$, $UvrA_{LQ065}$, $UvrA_{VD073}$, $UvrA_{SY080}$, $UvrA_{LP151}$, $UvrA_{GD173}$, $UvrA_{YC174}$, $UvrA_{VE202}$ and $UvrA_{DG205}$ was repressed less than wild-type UvrA upon addition of UvrB. However the effect of UvrB on the GTPase activity of $UvrA_{LQ065}$ and $UvrA_{YC174}$ was only marginally different from the effect of UvrB on wild-type UvrA and the GTPase V_{max} values without UvrB of $UvrA_{RL023}$, $UvrA_{VD073}$, $UvrA_{SY080}$ and $UvrA_{VE202}$ were more than two-fold lower than that of wild-type UvrA (Table 5.1).

The experiment was repeated for $UvrA_{LH151}$, $UvrA_{LP151}$, $UvrA_{GD173}$ and $UvrA_{DG205}$ with different concentrations of UvrB (Figure 5.12). The results confirmed that $UvrA_{LP151}$, $UvrA_{GD173}$ and $UvrA_{DG205}$ maintained a significant amount of GTPase activity when UvrB was added. The level of inhibition for $UvrA_{GD173}$ and $UvrA_{DG205}$ had not appeared to reach saturation at the highest concentration (100 nM) of UvrB tested. $UvrA_{LP151}$ was almost unaffected by the addition of UvrB unlike $UvrA_{LH151}$, which acted as wild-type UvrA.

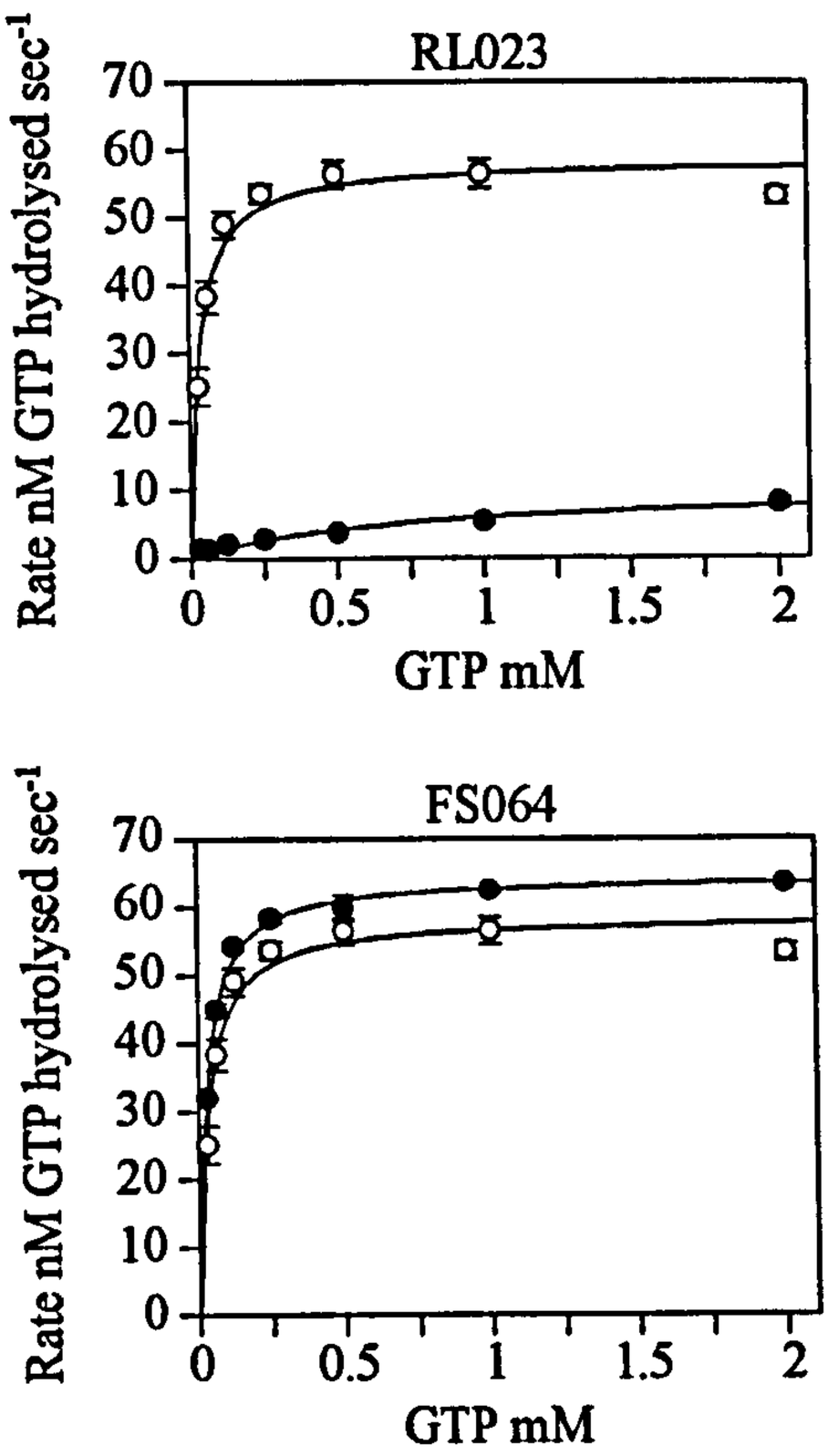

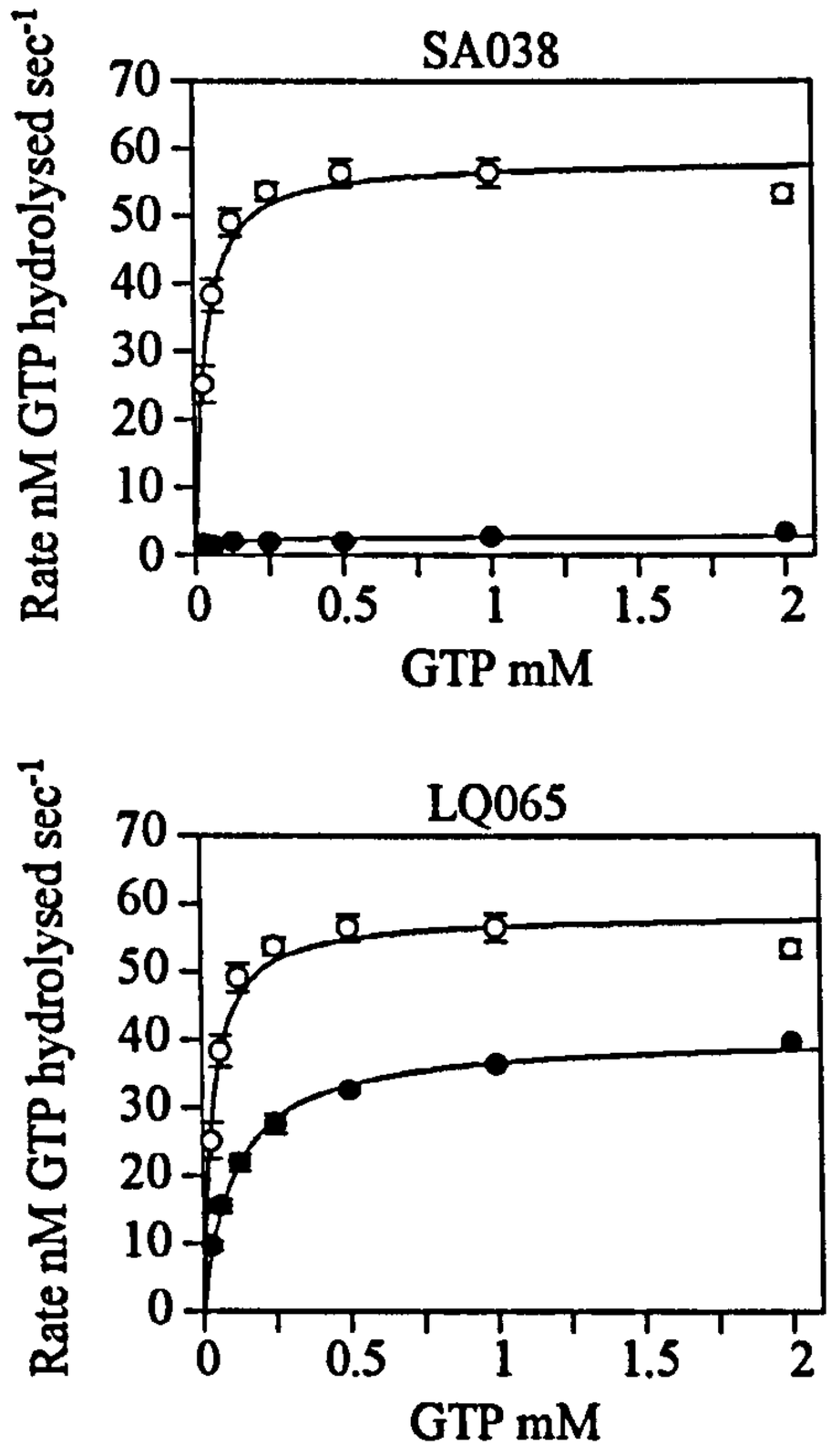

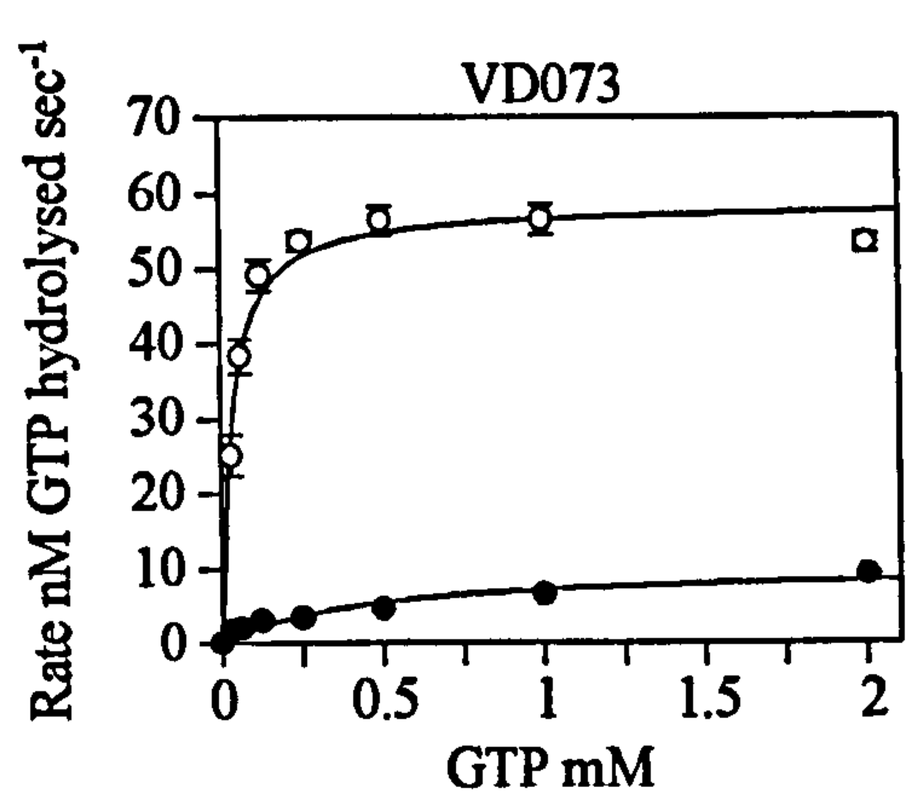

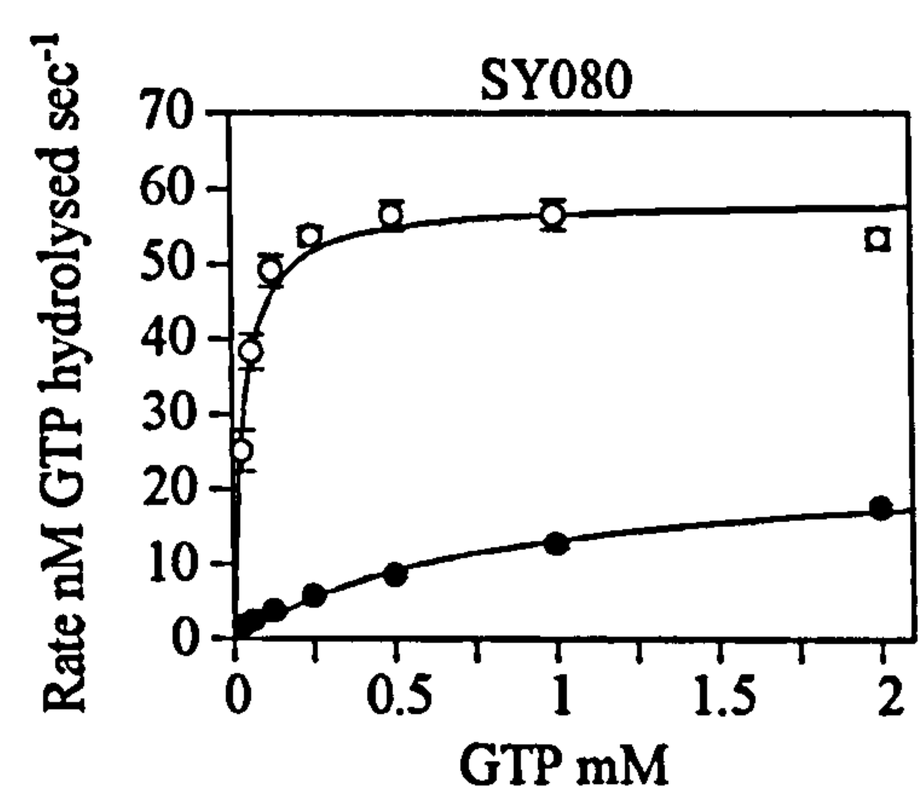

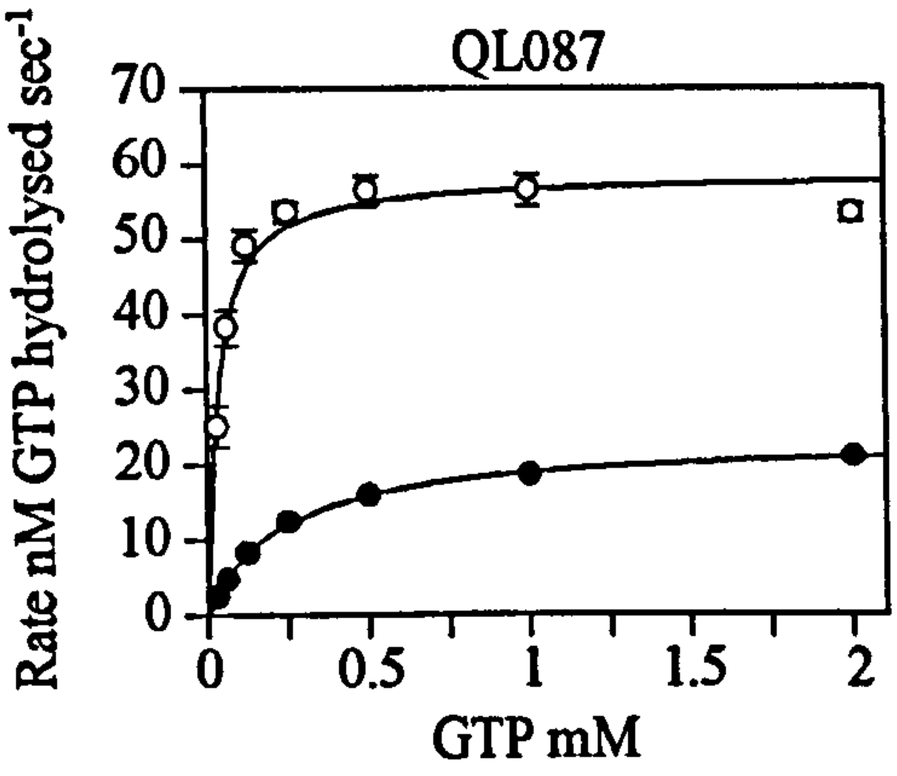

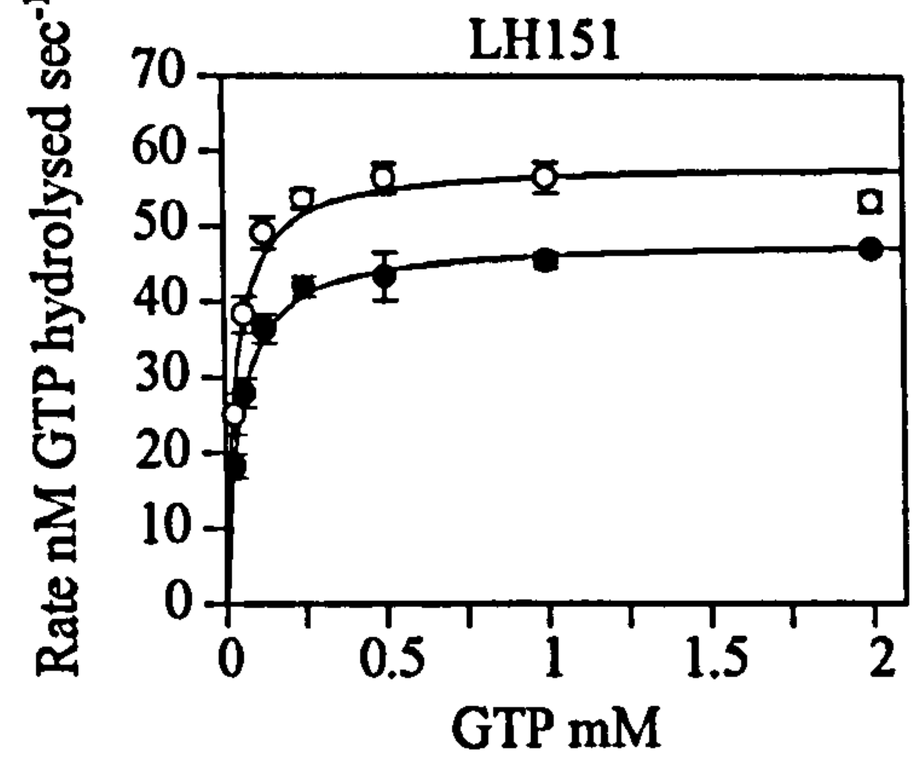

Figure 5.11 Page 1 of 2

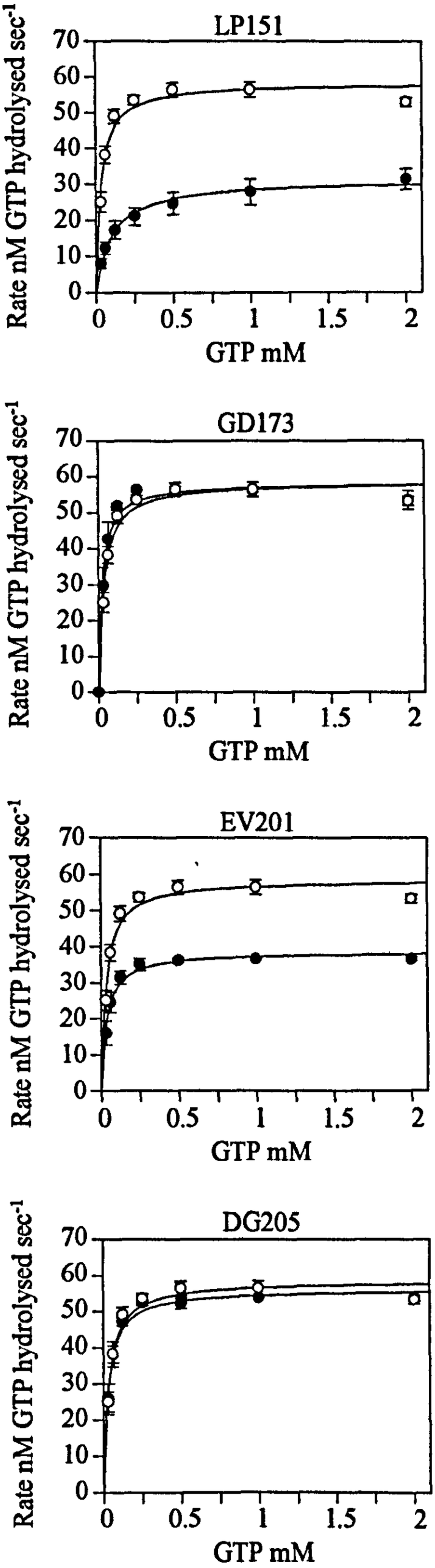

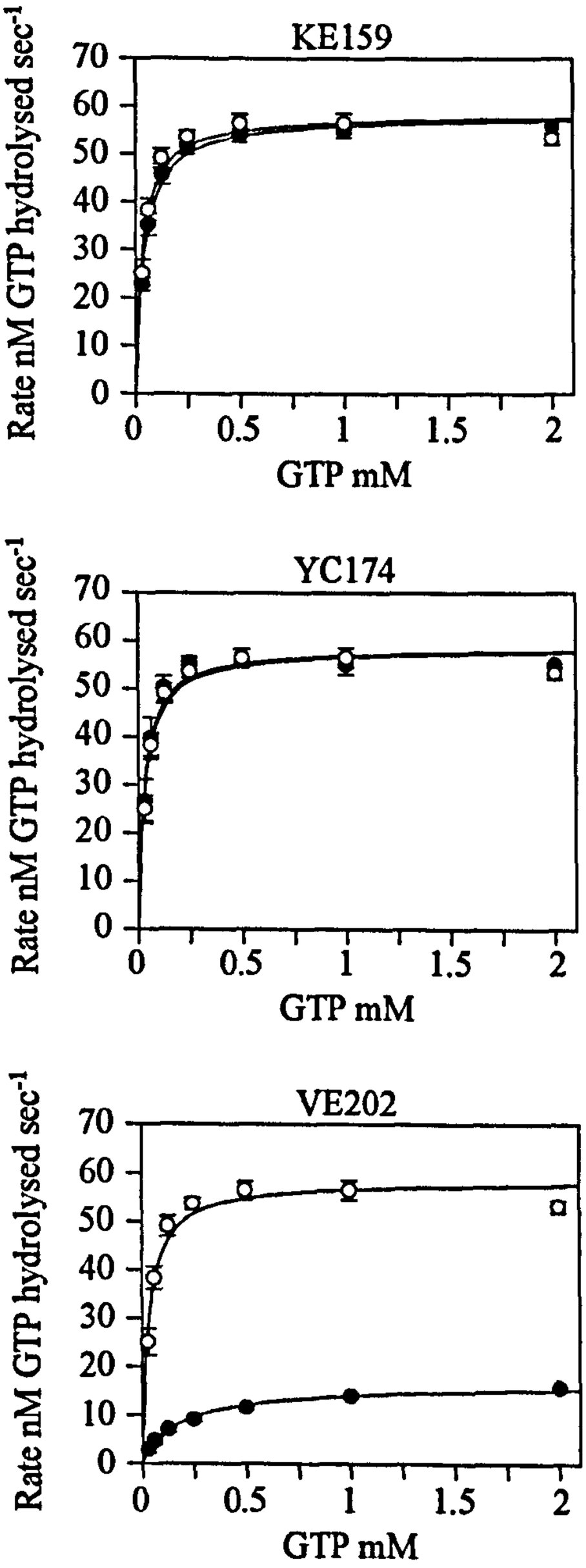

Figure 5.11 Page 2 of 2

Figure 5.11 Effect of amino acid substitutions in UvrA on the GTPase activity of UvrA.
GTP hydrolysis rates were calculated from data generated from nucleotide hydrolysis assays. Each assay contained 50 nM of the indicated UvrA mutant (black circles), the PK/LDH reagents and the indicated concentration of GTP in a final volume of 200 µl. The reactions were incubated at 37°C for one hour with readings taken every 15 seconds. The rates were calculated by measuring the steepest consecutive 30 minute period of the curve and then background degradation subtracted. The rates shown are an average of at least three independent experiments (with standard deviation). A Michaelis-Menten curve was fitted to the data using GraFit. The wild-type UvrA result (from Figure 5.6) is on all mutant graphs for comparison (white circles).

	0 nM UvrB		100 nM UvrB		Fold repression		
	Rate nM GTP hydrolysed sec^{-1} (Y)	**Standard deviation (y)**	**Rate nM GTP hydrolysed sec^{-1} (X)**	**Standard deviation (x)**	**Average**	**Max. Y+y X-x**	**Min. Y-y X+x**
Wt	54.6	12.1	12.1	2.76	4.51	7.13	2.86
RL023	5.49	0.05	3.86	0.61	1.42	1.71	1.22
SA038	2.63	0.80	2.63	1.63	1.00	3.41	0.43
FS064	56.7	2.80	16.4	0.79	3.45	3.81	3.13
LQ065	33.6	1.48	13.3	0.94	2.54	2.85	2.27
VD073	7.54	0.52	6.22	0.42	1.21	1.39	1.06
SY080	14.1	1.26	8.69	0.76	1.62	1.94	1.36
QL087	18.1	0.79	5.00	0.68	3.61	4.36	3.05
LH151	48.2	1.53	13.8	0.10	3.49	3.63	3.36
LP151	25.1	0.58	22.2	4.61	1.13	1.46	0.92
KE159	51.1	1.21	13.3	0.42	3.83	4.04	3.62
GD173	54.9	7.29	37.6	7.40	1.46	2.06	1.06
YC174	56.5	0.55	21.1	0.85	2.68	2.82	2.55
EV201	37.1	0.14	13.0	0.57	2.86	3.00	2.73
VE202	13.3	1.12	11.7	1.16	1.14	1.37	0.95
DG205	55.5	3.27	27.5	2.74	2.02	2.37	1.73

Table 5.3 Effect of UvrB on the GTPase activity of UvrA mutants.

GTP hydrolysis rates were calculated from data generated from nucleotide hydrolysis assays. Each assay contained 50 nM UvrA or the indicated UvrA mutant, 2 mM GTP and either 0 nM or 100 nM UvrB in a final volume of 200 µl. The reactions were incubated at 37°C for one hour with readings taken every 15 seconds. The rates were calculated by measuring the steepest consecutive 30 minute period of the curve and then background degradation subtracted. The rates shown are an average of at least three independent experiments (with standard deviation).

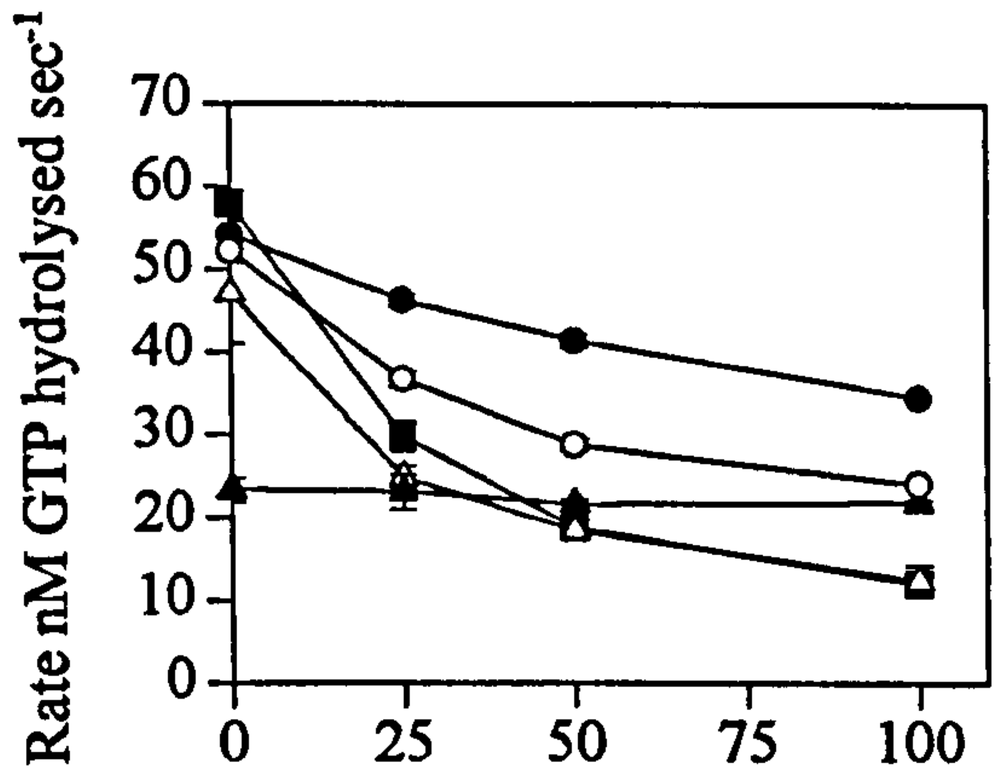

Figure 5.12 Effect of UvrB concentration on the GTPase activity of UvrA mutants.

GTP hydrolysis rates were calculated from data generated from nucleotide hydrolysis assays. Each assay contained the PK/LDH reagents, 2 mM GTP, the indicated concentration of UvrB and 50 nM of either UvrA (black square), $UvrA_{LH151}$ (white triangle), $UvrA_{LP151}$ (black triangle), $UvrA_{GD173}$ (black circle), or $UvrA_{DG205}$ (white circle) in a final volume of 200 µl. The reactions were incubated at 37°C for one hour with readings taken every 15 seconds. The rates were calculated by measuring the steepest consecutive 30 minute period of the curve and then background degradation subtracted. The rates shown are an average of at least three independent experiments (with standard deviation).

It can be concluded that the GTPase activity of $UvrA_{SA038}$, $UvrA_{FS064}$, $UvrA_{QL087}$, $UvrA_{LH151}$, $UvrA_{KE159}$ and $UvrA_{EV201}$ was inhibited by UvrB and therefore the UvrA-UvrB complex must presumably still form. However these mutants may have subtle changes in UvrB binding affinity that would not have been detected under this one set of conditions used to analyse them. The data indicated that the UvrA mutants $UvrA_{GD173}$ and $UvrA_{DG205}$ were still able to bind to UvrB as some inhibition was still detected. However it is not known if: the binding affinity has been reduced; the inhibitory effect of UvrB on UvrA has been affected; or whether both had. It would be beneficial to extend the experiment to include data points at higher UvrB concentrations to determine if the inhibitory effect would eventually reach that of wild-type UvrA. $UvrA_{LH151}$ and $UvrA_{LP151}$ had different characteristics within this assay. $UvrA_{LH151}$ acted as wild-type and as such is presumably able to interact with, and be affected by, UvrB. The results indicated that $UvrA_{LP151}$ was unable to bind UvrB or that once bound UvrB was unable to cause an effect on the GTPase activity. The replacement of leucine with the structurally altering proline residue within the mutant could have affected the UvrA structure and thus might affect many UvrA properties including its ability to bind and be affected by UvrB.

DNA binding activity of UvrA

Various complexes involving DNA are formed as part of the NER process. UvrA recognises and binds (psoralen) damaged DNA 10^3-fold more efficiently than undamaged DNA (Van Houten *et al.*, 1987). ATP is not essential for the UvrA-DNA complex formation (Mazur and Grossman, 1991). However ATP binding is required for the formation of a UvrA-UvrB-DNA complex which resolves to a UvrB-DNA complex upon ATP hydrolysis (Orren and Sancar, 1990). To further characterise the 15 UvrA mutants conditions needed to be established in which a UvrA-DNA complex could be detected.

DNA binding activity of wild-type UvrA

Many different substrates have been used to study the DNA binding properties of the NER proteins. These include oligonucleotides containing lesions such as cisplatin (Visse *et al.*, 1991), pyrimidine dimers (Reardon *et al.*, 1993) and fluorescein (DellaVecchia *et al.*, 2004).

A 50 base oligonucleotide was used in the DNA binding experiments. This oligonucleotide was designed to contain a single fluorescein molecule covalently attached to a thymine (Fld-dT) residue 29 bases from the 5′ end (Figure 5.13). The DNA sequence of the oligonucleotide was designed so that it would not homodimerize or form secondary structures such as hairpins.

To ascertain the effect of UvrA concentration on formation of a UvrA-DNA complex EMSAs were carried out with different concentrations of UvrA (Figure 5.14 (wild-type)). As expected the addition of UvrA shifted the DNA from the high mobility DNA-only band (band D) into the low mobility UvrA-DNA complex (band A). Increasing the concentration of UvrA resulted in the amount of the UvrA-DNA complex increasing whilst the amount of free DNA decreased. At the highest concentration of UvrA tested (100 nM) the majority of DNA had been shifted from the DNA-only band. A second and very faint third complex (band A^{+} and A^{++}) were also detected in reactions with high concentrations of UvrA. These bands had lower mobility than the UvrA-DNA complex and were believed to represent two or more dimers of UvrA bound to one molecule of DNA. A UvrA-DNA complex had therefore been identified that could act as a control in the characterisation of the UvrA mutants.

Effect of amino acid substitutions in UvrA on the formation of a UvrA-DNA complex

The effect that the 15 amino acid substitutions in UvrA had on formation of a UvrA-DNA complex was characterised. The EMSA was repeated using the UvrA mutants instead of wild-type UvrA (Figure 5.14). Of the 15 mutants $UvrA_{SA038}$, $UvrA_{FS064}$, $UvrA_{LQ065}$, $UvrA_{QL087}$ and $UvrA_{KE159}$ were all able to form a stable UvrA-DNA complex comparable to wild-type. In each of these cases the second UvrA-DNA complex (A^{+}) was also detected at the higher protein concentrations. $UvrA_{KE159}$ and to a lesser extent $UvrA_{QL087}$ formed the third complex (A^{++}) more predominantly than the second (A^{+}). $UvrA_{RL023}$, $UvrA_{VD073}$, $UvrA_{SY080}$, $UvrA_{LH151}$, $UvrA_{LP151}$, $UvrA_{GD173}$, $UvrA_{YC174}$, $UvrA_{EV201}$, $UvrA_{VE202}$ and $UvrA_{DG205}$ did not form a stable UvrA-DNA complex. In each of these cases the DNA-only band reduced as the concentration of the UvrA mutant increased. In some cases either one or both of the lower mobility bands (A^{+}/A^{++}) were detected, although in most

A

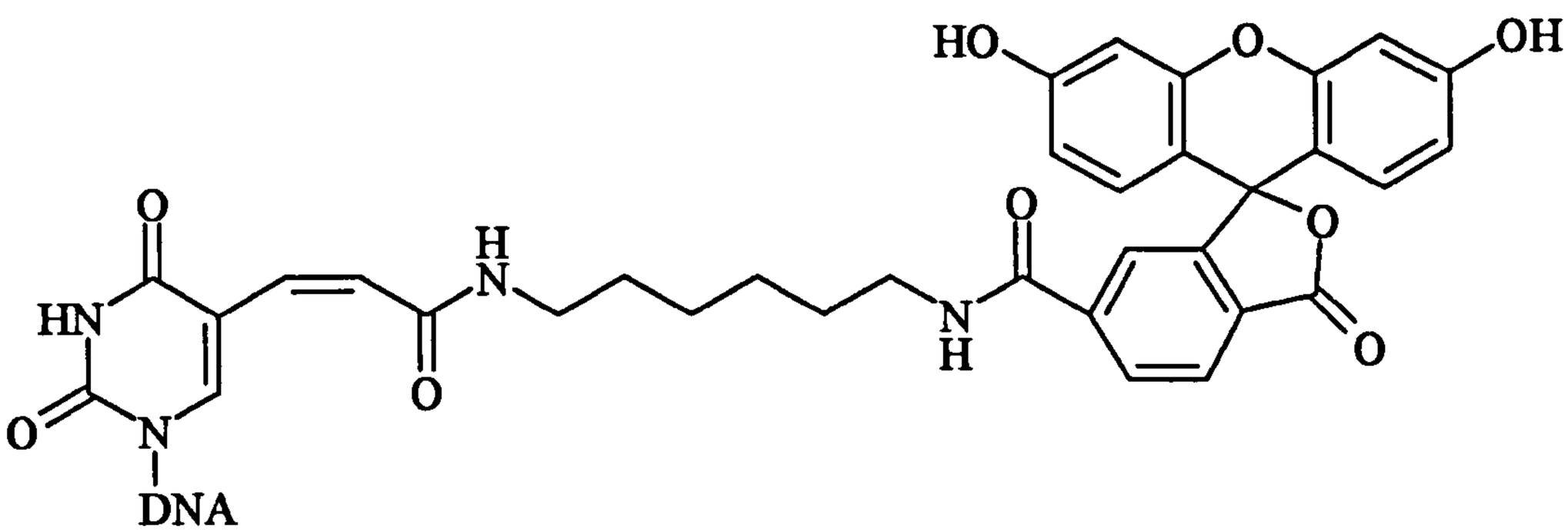

B

```
5' CTAGGATCGG ATAGCGCATG ACAGTGACTG GATCGACAGC GTCGTATGAG 3'
3' GATCCTAGCC TATCGCGTAC TGTCACTGAC CTAGCTGTCG CAGCATACTC 5'
```

Figure 5.13 Fluorescein-dT.

(A) The chemical structure of fluorescein covalently attached to thymine. **(B)** The DNA sequence of the oligonucleotide used in the EMSA experiments. The red letter indicates the base to which fluorescein had been covalently attached.

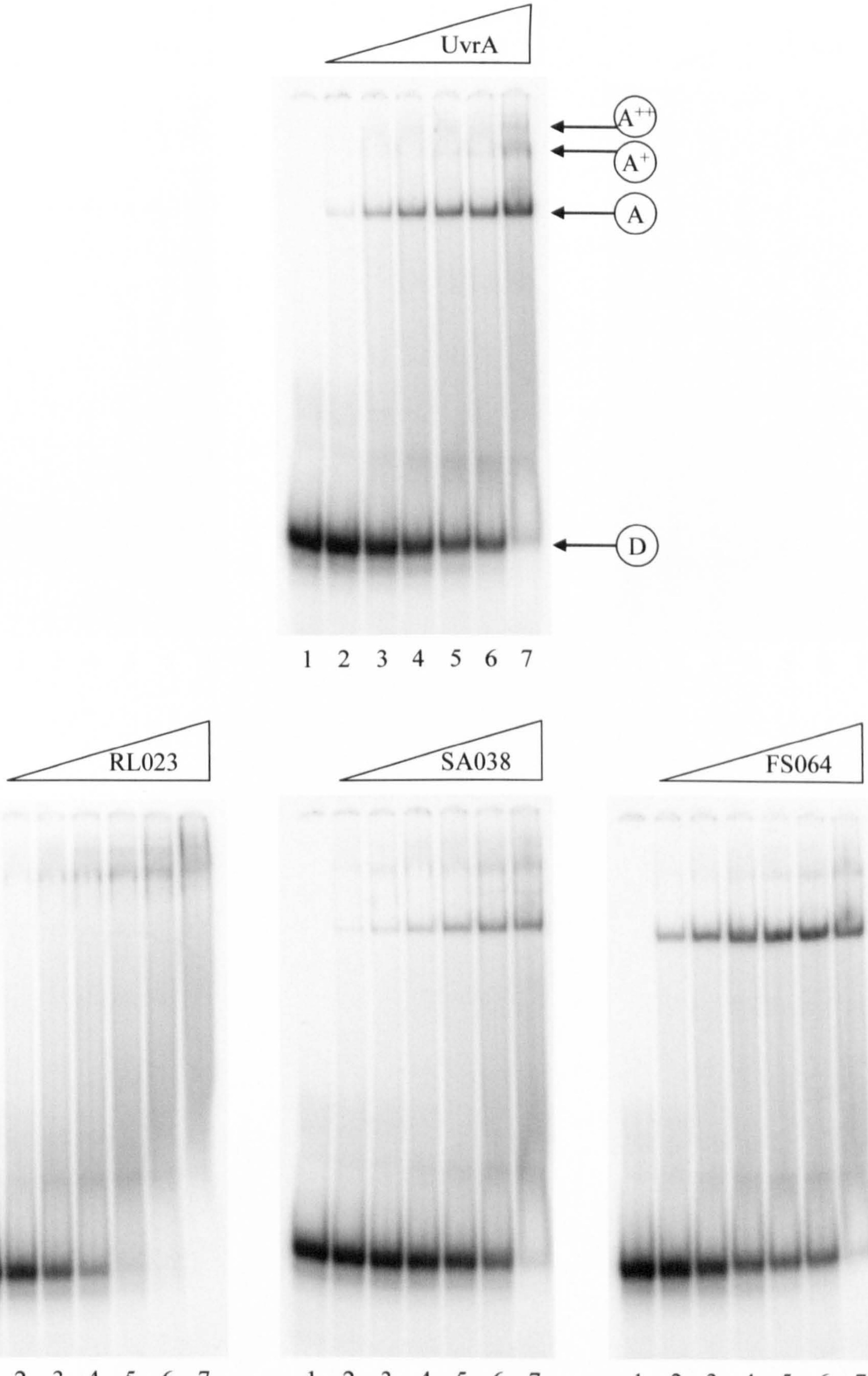

Figure 5.14 Page 1 of 3

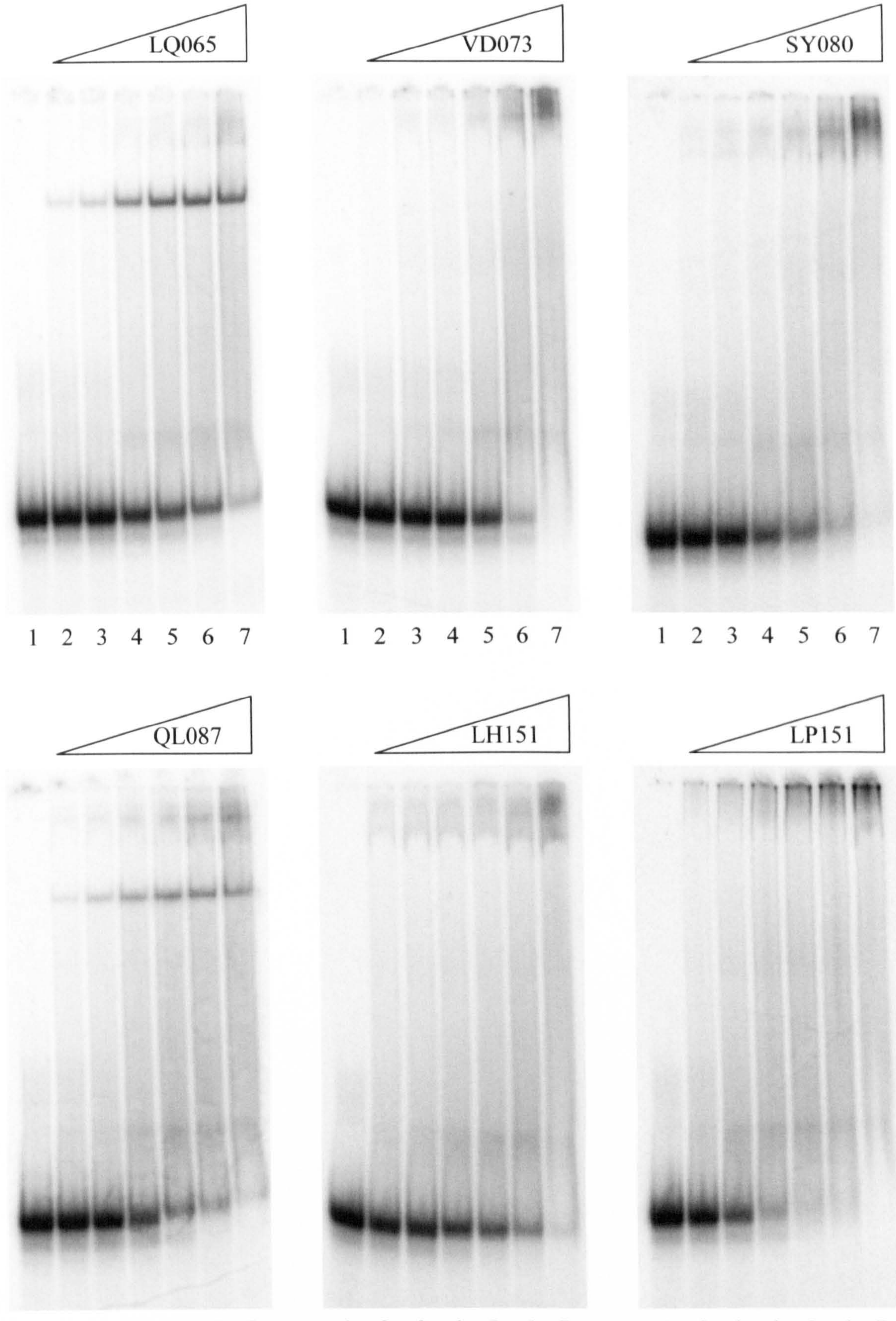

Figure 5.14 Page 2 of 3

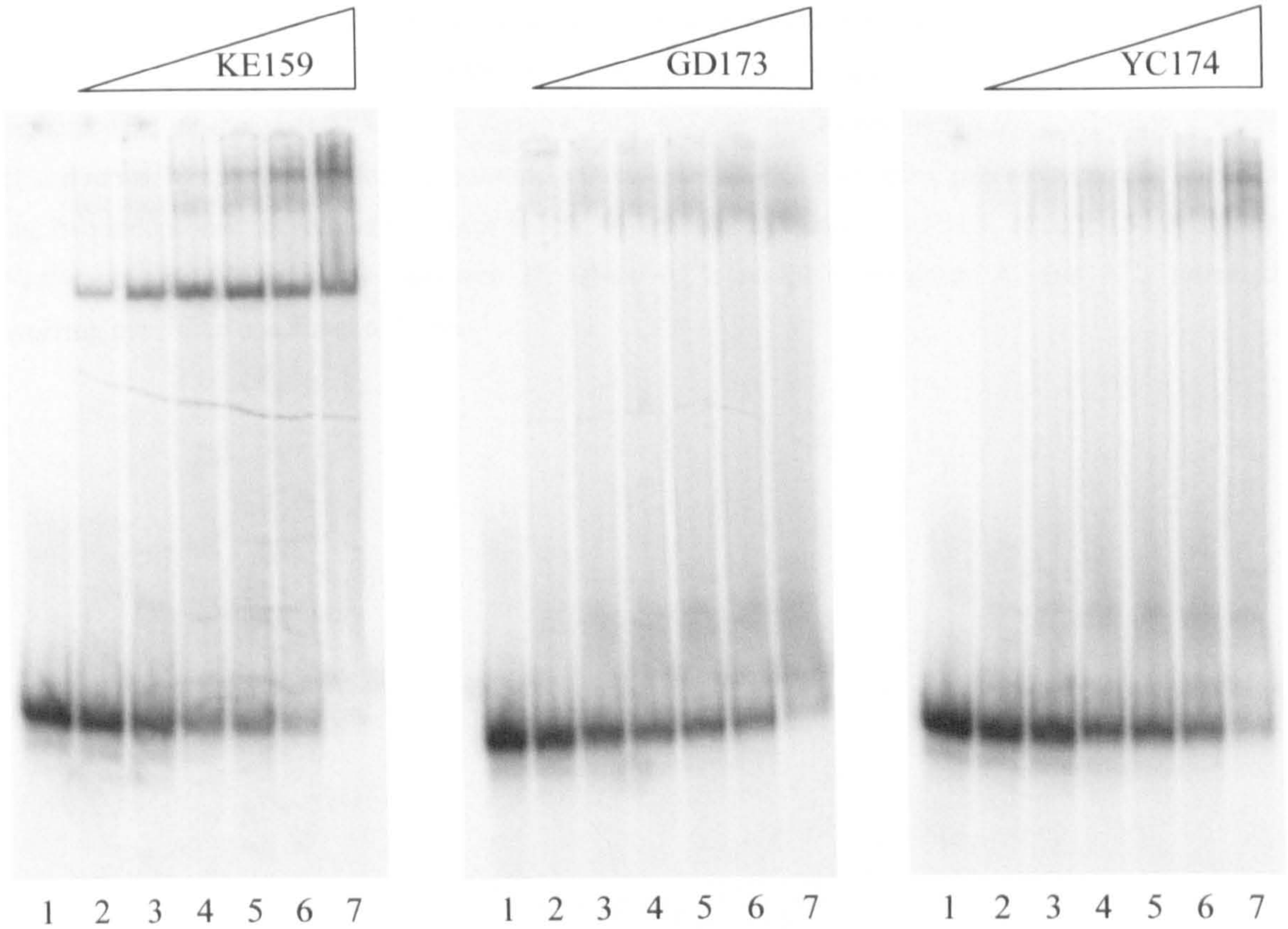

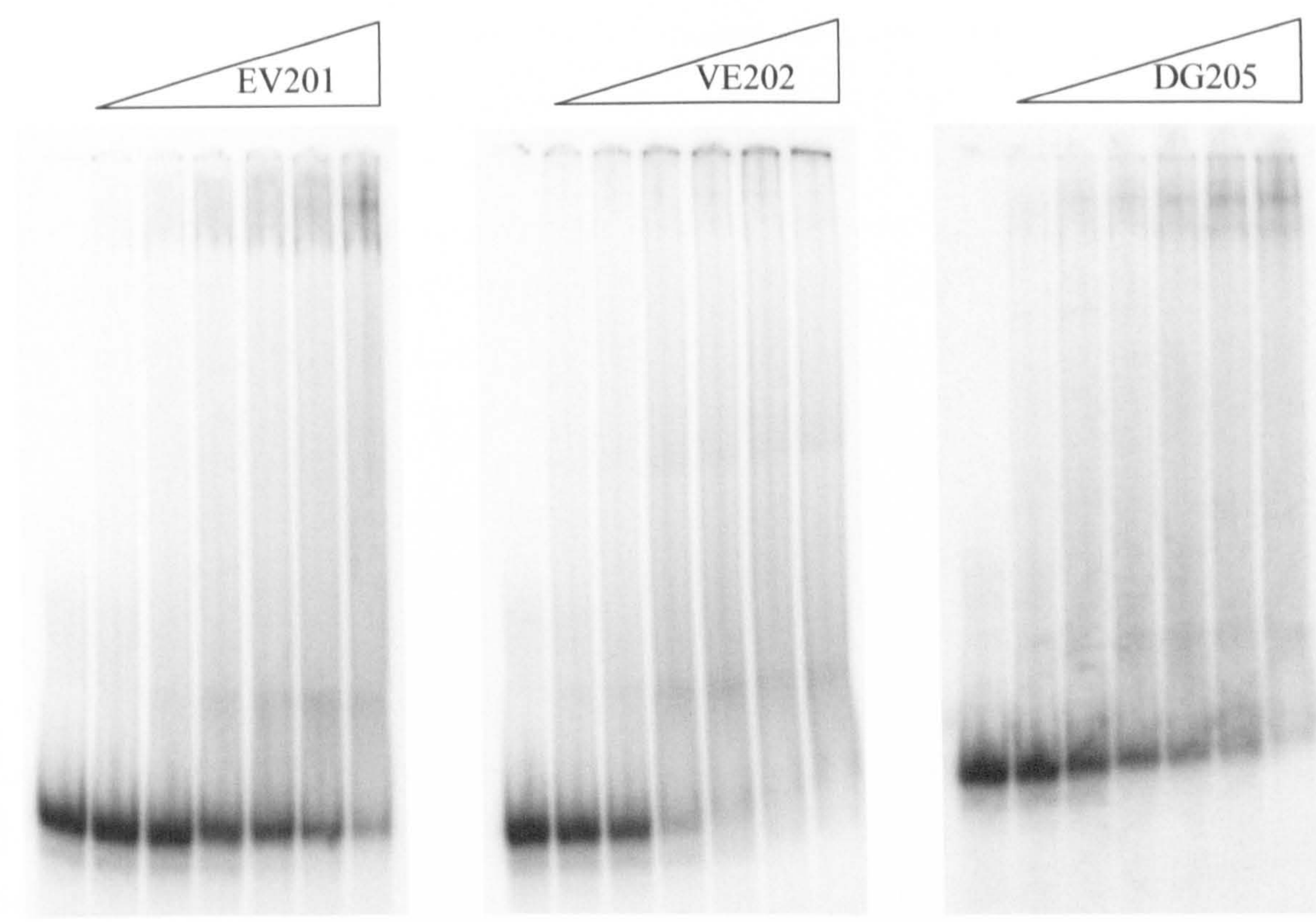

Figure 5.14 Page 3 of 3

Figure 5.14 Effect of amino acid substitutions in UvrA on the formation of a UvrA-DNA complex. UvrA (or the indicated mutant) was added to 1 nM Fld-dT DNA in the presence of 1 mM ATPγS. The reactions were incubated at 37°C for 30 minutes. Each reaction was loaded onto a 6% acrylamide, 1 x TBE gel and run at 40 mA (200 V) for approximately three hours at 4°C. The above gels are representatives of at least two independent experiments. Lanes 1, 2, 3, 4, 5, 6 and 7 contain 0, 3.1, 6.3, 12.5, 25, 50 or 100 nM UvrA respectively. The bands represent: D, DNA; A, UvrA-DNA complex; A^{+} and A^{++}, complexes involving more than one dimer of UvrA.

cases a smear was present at this position on the gel indicating some unstable specific or non-specific DNA binding.

The UvrA mutants fell into two main categories: those that bound DNA like wild-type; and those that were unable to form stable complexes under these conditions. It is not known if the UvrA mutants unable to form the UvrA-DNA complex were deficient in DNA binding or if they were deficient in an earlier step of the process such as UvrA dimerization. The formation of the higher order complexes (A^{+}/A^{++}) with mutants that were unable to form a stable UvrA-DNA complex is puzzling. It had been assumed that these complexes had formed by the addition of a UvrA dimer to the preformed UvrA-DNA complex. This may still be true if a second dimer is needed to stabilise the DNA binding activity of the first dimer.

UvrB binding activity of UvrA

Effect of UvrB on UvrA-DNA complexes

UvrA-DNA, UvrA-UvrB-DNA and UvrB-DNA complexes have previously been detected under various EMSA conditions (Moolenaar *et al.*, 2005) (Truglio *et al.*, 2004). During DNA binding, different steps in nucleotide hydrolysis must be completed to form the various protein-DNA complexes (Figure 5.15). UvrA can initially bind DNA in the presence or absence of ATP. However a UvrA-UvrB-DNA complex will only form upon ATP binding. The hydrolysis of ATP within this complex results in the loading of UvrB onto the damaged DNA by UvrA to form a UvrB-DNA complex.

The conditions in which I could detect a UvrA-UvrB-DNA complex and a UvrB-DNA complex needed to be identified (Figure 5.16). EMSAs were therefore carried out. On a 6% acrylamide gel in the absence of UvrA and UvrB the DNA formed a single band (lane 1). As seen previously upon addition of UvrA a band (band A) of lower mobility was detected (a UvrA-DNA complex) whilst the DNA-only band (band D) reduced in intensity (lanes 2 to 4 compared to lane 1). UvrB had no direct effect on the mobility of the DNA in the absence of UvrA (lanes 8 to 10 compared to lane 1). The combined effect of UvrA and UvrB depended on the cofactor added. In the absence or presence of ATP a band corresponding in position to the UvrA-DNA complex was detected (band A lanes 5 and 6). In the presence of ATPγS, a poorly hydrolysable analogue of ATP, a band with lower

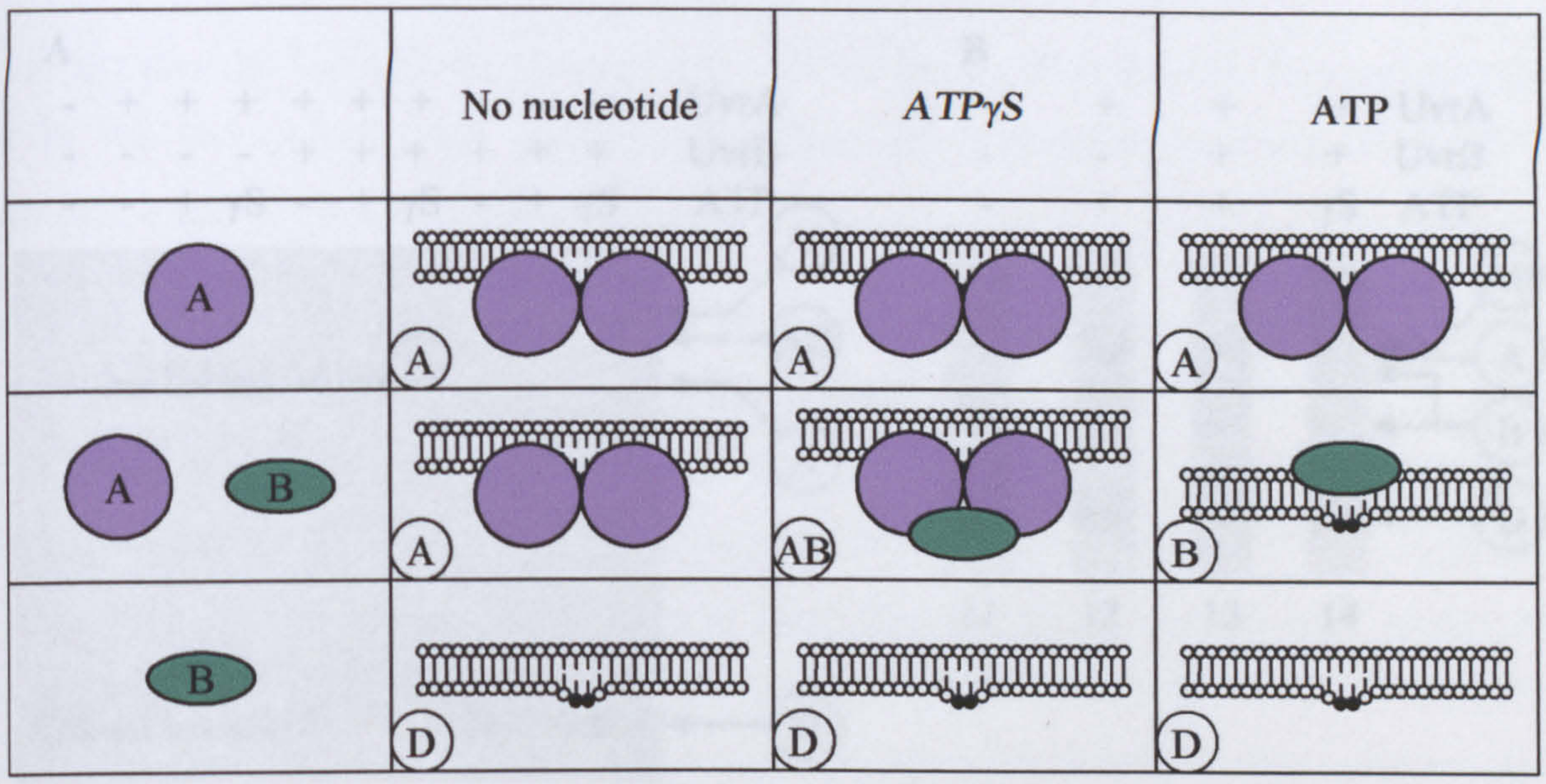

Figure 5.15 Nucleotide binding and hydrolysis requirements within NER.

Formation of the UvrA-DNA (A), UvrA-UvrB-DNA (AB) and the UvrB-DNA (B) complexes. Each complex indicates the furthest position in the NER cycle (Figure 5.1) that can be reached with the indicated proteins in the presence of no nucleotide, ATPγS or ATP. (D) indicates DNA.

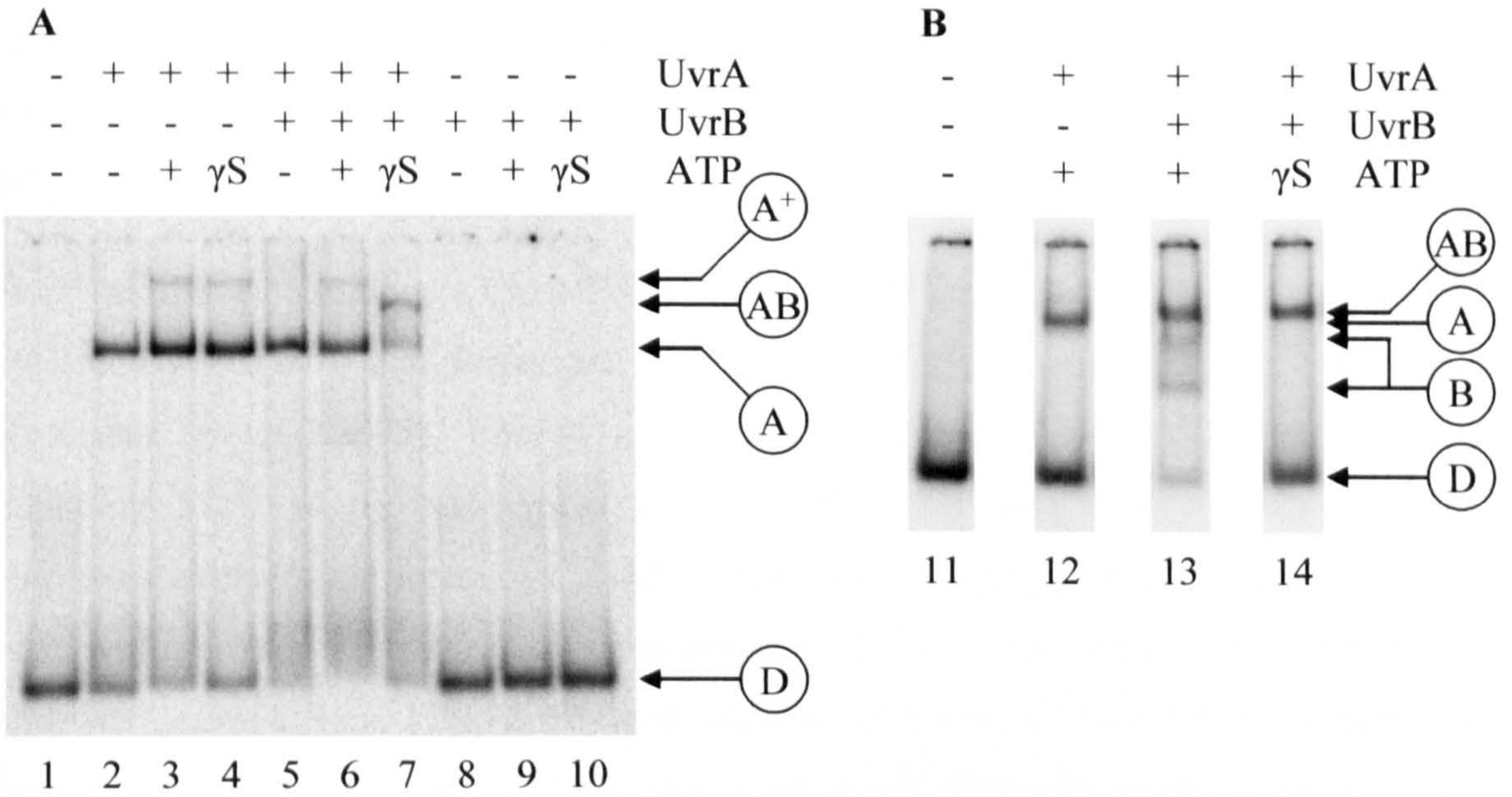

Figure 5.16 DNA binding properties of wild-type UvrA and UvrB proteins.

(**A**) Each reaction contained 1 nM Fld-dT annealed oligonucleotide and where indicated 100 nM UvrA, 100 nM UvrB and 1 mM ATP or ATPγS. The reactions were incubated at 37°C for 30 minutes. Each reaction was loaded onto a 6% acrylamide, 1 x TBE gel and run at 40 mA (200 V) for approximately three hours at 4°C. (**B**) Each reaction contained 1 nM Fld-dT annealed oligonucleotide and where indicated 50 nM UvrA, 200 nM UvrB and 1 mM ATP or ATPγS. The reactions were incubated at 37°C for 30 minutes. Each reaction was loaded onto a 4% acrylamide, 0.5 x TBE, 10 mM $MgCl_2$ gel and run at 40 mA (200 V) for approximately two hours at 4°C. Lanes 11 to 14 are from different parts a single gel. The bands in **A** and **B** represent: D, DNA; A, UvrA-DNA complex; AB, UvrA-UvrB-DNA complex; A^+, complexes involving more than one dimer of UvrA; and B, UvrB-DNA complexes.

mobility than the UvrA-DNA complex was detected (band AB in lane 7). This was thought to be the UvrA-UvrB-DNA complex. Therefore the conditions for UvrA-UvrB-DNA complex formation had been identified.

Under the above conditions a UvrB-DNA complex was not detected. Previous groups had detected UvrB DNA complexes on 4% acrylamide gels containing Mg^{2+} and ATP (Moolenaar *et al.*, 2005). EMSA were therefore resolved on 4% acrylamide gels containing Mg^{2+} to try and detect a UvrB-DNA complex (Figure 5.16). Different complexes were present when compared to those seen on the gel without Mg^{2+} (compare gel A with gel B in Figure 5.16). In the absence of UvrA and UvrB a single DNA-only band was detected (lane 11). Again upon addition of UvrA, a UvrA-DNA complex was formed (lane 12). The effect of UvrA and UvrB again depended on the cofactor. In the presence of ATPγS a UvrA-UvrB-DNA complex was detected (band AB lane 14) that had marginally less mobility than the UvrA-DNA complex (band A lane 12). In the presence of ATP two additional bands were detected along with the UvrA-UvrB-DNA complex (lane 13). Both bands had a higher mobility than the UvrA-DNA complex and were believed to be a UvrB-DNA and a $UvrB_2$-DNA complex. These complexes were only seen when UvrA, UvrB and ATP were all present in the reaction. This combination was known to lead to UvrB-DNA complex formation (Moolenaar *et al.*, 2005). The intensity of the UvrA-UvrB-DNA complex under these conditions was comparable to the same complex in the reaction containing ATPγS (band AB in lane 13 compared to lane 14) whilst the amount of free DNA had reduced. Under these conditions it would appear that once UvrA had loaded UvrB onto the DNA it was released. This enabled UvrA to restart the loading process. If further incubation had occurred it would be expected that all of the DNA would be within the UvrB-DNA complex. Therefore the conditions for UvrB-DNA complex formation had been identified.

The two different UvrB-DNA complexes were only formed when $MgCl_2$ was present within the gel (as well as in the reaction mix) indicating a requirement for Mg^{2+} to stabilise the UvrB-DNA complexes. The two UvrB complexes had only been previously detected in separate reactions that were run on acrylamide gels containing ATP (Moolenaar *et al.*, 2005) (Malta *et al.*, 2006).

Effect of UvrB concentration on the formation of a UvrA-UvrB-DNA complex

To enable differences in UvrA-UvrB binding affinity to be detected amongst the UvrA mutants the effect of UvrB concentration on the formation of the UvrA-UvrB-DNA complex was analysed. EMSA with different concentrations of UvrB were carried out in the presence of UvrA and ATPγS which would enable the formation of the UvrA-UvrB-DNA complex. As seen previously the addition of UvrB in the absence of UvrA had no effect on the mobility of the DNA (no UvrA gel Figure 5.17). As UvrB was titrated into reactions containing UvrA and ATPγS the amount of the UvrA-DNA complex (band A) reduced as the UvrA-UvrB-DNA complex (band AB) formed (wild-type gel Figure 5.17). Under the conditions used, 4 nM UvrB was sufficient to shift the majority of the UvrA-DNA complex into the UvrA-UvrB-DNA complex.

Effect of UvrA amino acid substitutions in UvrA on the formation of a UvrA-UvrB-DNA complex

If the UvrA mutants were unable to interact with UvrB then they would be unable to form a stable UvrA-UvrB-DNA complex. The above EMSA was repeated with each of the 15 UvrA mutants replacing wild-type UvrA (Figure 5.17). $UvrA_{SA038}$, $UvrA_{FS064}$, $UvrA_{LQ065}$, $UvrA_{QL087}$ and $UvrA_{KE159}$ all formed a UvrA-UvrB-DNA complex. $UvrA_{SY080}$, $UvrA_{LH151}$, $UvrA_{YC174}$, $UvrA_{EV201}$ and $UvrA_{DG205}$ also all formed a UvrA-UvrB-DNA complex despite the absence of a stable UvrA-DNA complex. $UvrA_{RL023}$, $UvrA_{VD073}$, $UvrA_{LP151}$, $UvrA_{GD173}$ and $UvrA_{VE202}$ all failed to form a stable UvrA-UvrB-DNA complex although some smearing near the top of the gel could be detected for some of these mutants.

$UvrA_{FS064}$, $UvrA_{LQ065}$, $UvrA_{QL087}$ and $UvrA_{KE159}$ appear to interact with UvrB as wild-type under the conditions tested. $UvrA_{SY080}$, $UvrA_{LH151}$, $UvrA_{YC174}$, $UvrA_{EV201}$ and $UvrA_{DG205}$ also appear to interact with UvrB despite their inability to form a stable UvrA-DNA complex. The ability of $UvrA_{RL023}$, $UvrA_{VD073}$, $UvrA_{LP151}$, $UvrA_{GD173}$ and $UvrA_{VE202}$ to interact with UvrB can not be confirmed in this assay due to the absence of both the UvrA-DNA and the UvrA-UvrB-DNA complexes.

$UvrA_{SA038}$ was confirmed to interact with UvrB as a UvrA-UvrB-DNA complex was detected. However quantification of the UvrA-DNA and the UvrA-UvrB-DNA complexes

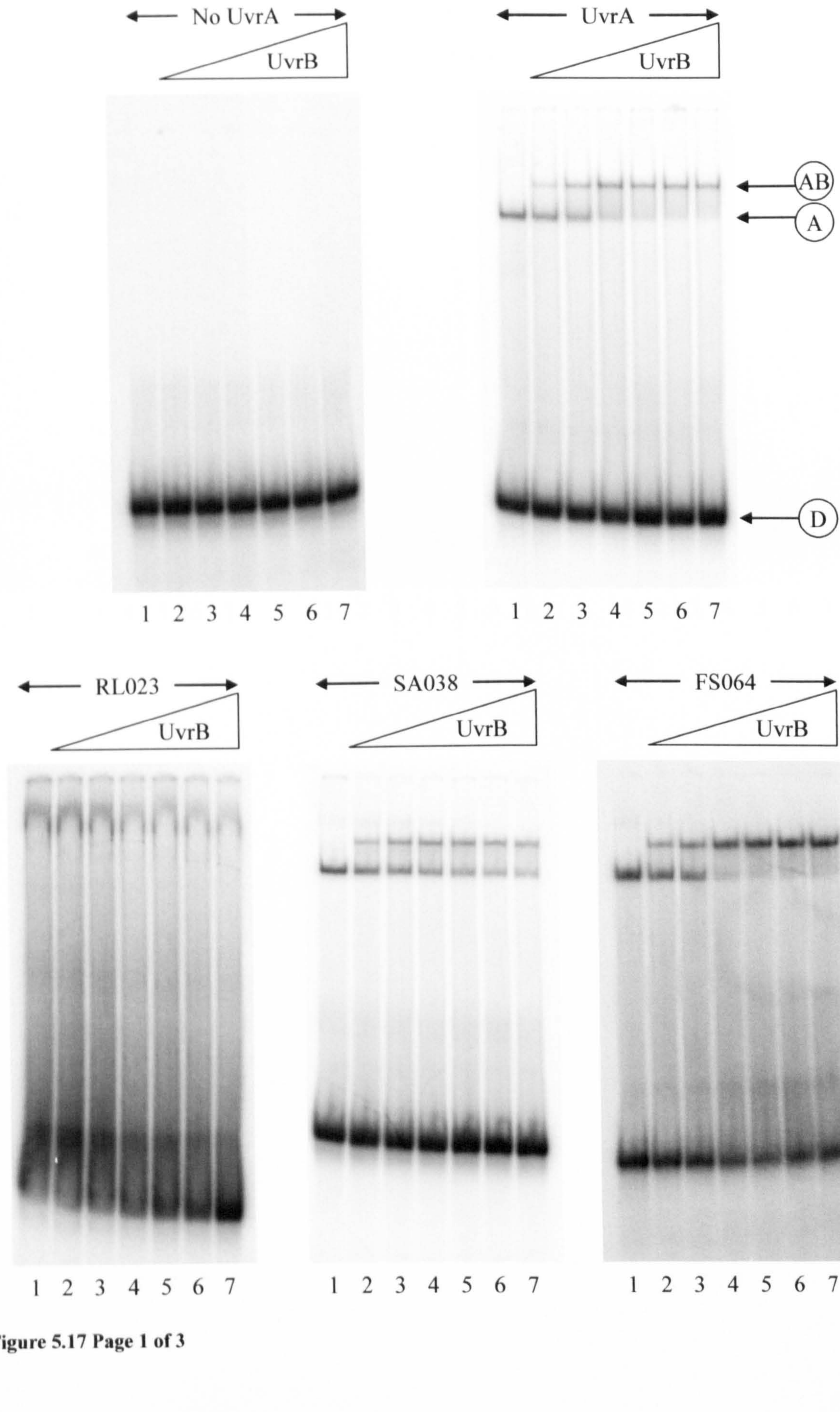

Figure 5.17 Page 1 of 3

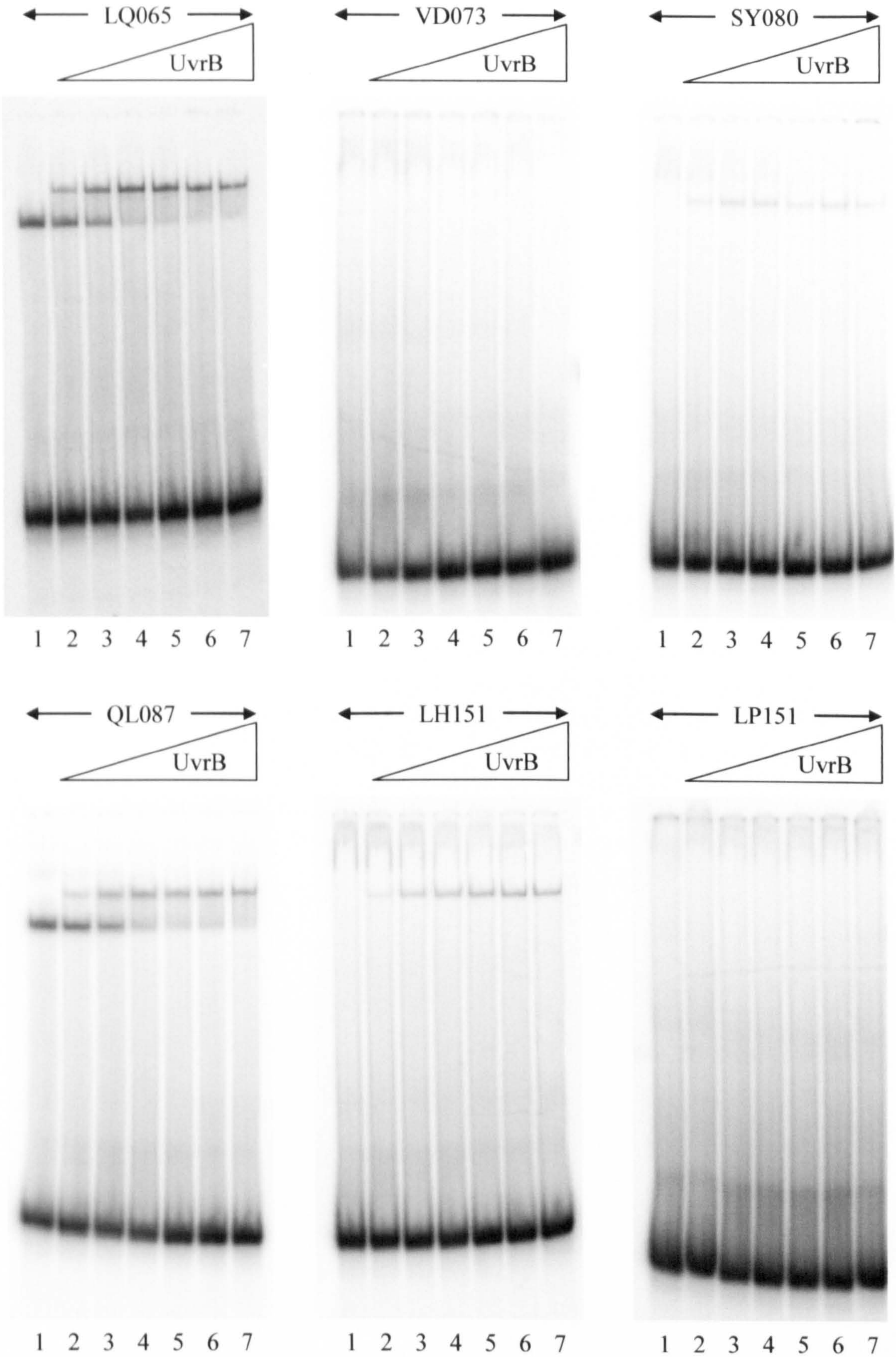

Figure 5.17 Page 2 of 3

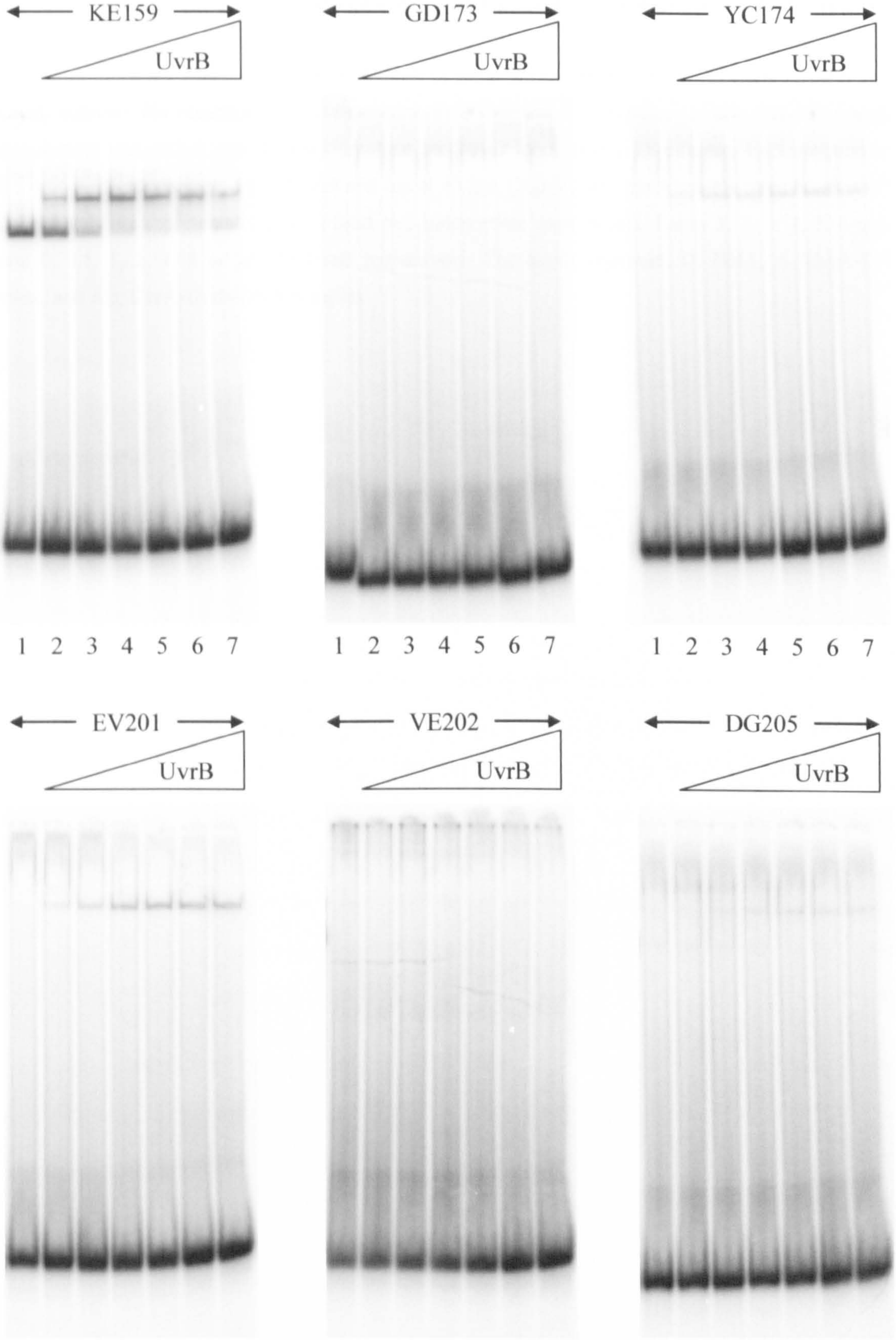

Figure 5.17 Page 3 of 3

Figure 5.17 Effect of amino acid substitutions in UvrA on the formation of a UvrA-UvrB-DNA complex.

Each reaction contained 1 mM ATPγS, 10 nM UvrA or the indicated UvrA mutant and UvrB (concentration indicated below). The reactions were incubated at 37°C for 15 minutes, 1 nM Fld-dT annealed oligonucleotide was added, and the reactions then incubated for a further 15 minutes. Each reaction was loaded onto a 6% acrylamide, 1 x TBE gel and run at 40 mA (200 V) for approximately three hours at 4°C. The above gels are representatives of at least two independent experiments. Lanes 1, 2, 3, 4, 5, 6 and 7 contain 0, 0.5, 1, 2, 4, 8 or 16 nM UvrB respectively. The bands represent: D, DNA; A, UvrA-DNA complex; and AB, UvrA-UvrB-DNA complex.

indicated that a maximum of 65% of the UvrA-DNA complex could be converted into the UvrA-UvrB-DNA complex. When the wild-type data was analysed almost 100% of the UvrA-DNA complex could be converted under the same conditions (Figure 5.18). The reasons for this are unclear but could indicate the presence of two species of UvrA-DNA complex. If this is the case the $UvrA_{SA038}$ amino acid substitution could prevent UvrB from interacting with one but not the other UvrA-DNA complex during the formation of a UvrA-UvrB-DNA complex.

Discussion

15 of the 20 amino acid substitutions of UvrA identified from the two screening procedures reported in chapter three have been successfully expressed and purified as N-terminal hexa-histidine tagged full-length UvrA mutants. Each of the UvrA mutants have been characterised *in vivo* and *in vitro* to understand the effect of each substitution on the properties of UvrA (summarised in Table 5.4).

UvrA is involved in the initial stages of NER and needs to: form homodimers; bind and hydrolyse ATP; bind DNA; bind UvrB and load UvrB onto damaged DNA. Its last step in the process is its dissociation from the UvrB-DNA complex to enable UvrC to bind UvrB and incise the DNA. Therefore within NER the role of UvrA is completed before the incision reactions occur. Each step preceding the 5′ cleavage, which includes all steps in which UvrA is involved, must be completed to allow the cleavage reaction to take place. UvrA mutants that are completely deficient in any essential NER property would therefore be unable to facilitate successful incision.

In combination wild-type UvrA, UvrB and UvrC proteins were able to incise biotinylated DNA eight and 15 phosphodiester bonds from the biotin site. Each of these wild-type proteins contained a histidine-tag at their N-terminus. The NER properties of my histidine-tagged wild-type NER proteins were comparable to previously published data for untagged NER proteins indicating that the histidine-tag did not appear to have any detectable effect on the initial stages of NER (up to and including incision).

Of the 15 UvrA mutants, 11 enabled the incision of the DNA to take place. $UvrA_{RL023}$, $UvrA_{VD073}$, $UvrA_{LP151}$, and $UvrA_{VE202}$ were unable to act as wild-type and enable incision of the DNA. At this stage it was not known if these four mutants were specifically

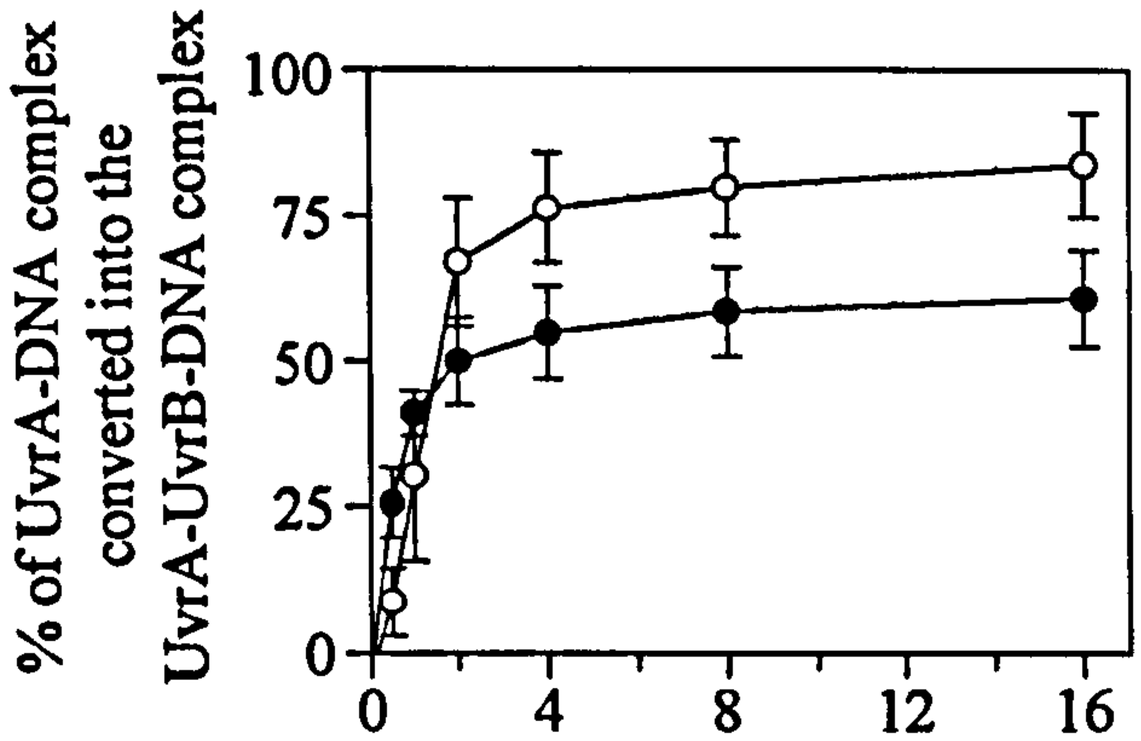

Figure 5.18 Effect of UvrA amino acid substitution SA038 on UvrA-UvrB-DNA complex formation. ImageQuant software was used to quantify the UvrA-DNA and the UvrA-UvrB-DNA complexes from the UvrA (white circles) and $UvrA_{SA038}$ (black circles) gels (an example of each in Figure 5.17). The proportion of the UvrA-UvrB-DNA complex (of the combined UvrA-DNA and UvrA-UvrB-DNA complex) was plotted on the graph. At least three individual experiments were quantified in this way and standard deviations are shown. A Michaelis-Menten curve fitting the data has been plotted.

			ATPase properties of UvrA		**GTPase properties of UvrA**					**Incision activity**	
	Bacterial two-hybrid	**UV sensitivity**	**K_m μM ATP**	**V_{max} nM ATP sec^{-1}**	**K_m μM GTP**	**V_{max} nM GTP sec^{-1}**	**Repression by UvrB on the GTPase activity of UvrA**	**UvrA-DNA complex formation**	**UvrA-UvrB-DNA complex formation**	**Primary 5′ incision**	**Secondary 5′ incision**
W/T	Y	N	23.4	40.4	33.5	58.5	4.51	Y	Y	Y	Y
RL 023	N/D	Y	288	10.7	737	10.2	1.42	N	N	N	N
SA 038	N/D	Y	106	5.62	48.6	2.70	1.00	Y	Y*	Y	Y
FS 064	N/D	Y	18.6	54.2	28.7	64.5	3.45	Y	Y	Y	Y
LQ 065	N/D	Y	63.2	37.5	107	40.5	2.54	Y	Y	Y	Y
VD 073	N/D	Y	190	14.7	426	10.1	1.21	N	N	N	N
SY 080	N/D	Y	290	23.8	820	24.1	1.62	N	Y	Y	N
QL 087	N/D	Y	97.5	20.1	229	23.2	3.61	Y	Y	Y	N
LH 151	N	N	30.6	42.4	45.9	48.3	3.49	N	Y	Y	N
LP 151	N/D	Y	70.5	31.1	106	31.5	1.13	N	N	N	N
KE 159	N/D	Y	24.6	49.2	41.4	58.2	3.83	Y	Y	Y	Y
GD 173	N	N	18.2	51.3	24.2	58.3	1.46	N	N	Y	N
YC 174	N	N	22.4	51.8	30.5	58.6	2.68	N	Y	Y	Y
EV 201	N	N	27.5	35.8	36.4	38.6	2.86	N	Y	Y	Y
VE 202	N	N	139	18.9	179	16.7	1.14	N	N	N	N
DG 205	N	N	23.0	49.5	30.9	56.2	2.02	N	Y	Y	Y

Table 5.4 Summary of the properties of UvrA mutants.

Red boxes indicates a difference from wild-type, Yellow boxes indicates similarity to wild-type. N/D Not measured. The star indicates that some UvrA-DNA complex always remained.

deficient in a particular NER step, reflecting an essential requirement for the amino acid that had been substituted, or if the amino acid substitutions had significantly altered the tertiary structure. Interestingly some of the 11 mutants that were able to facilitate the first 5′ incision were unable to support the second 5′ incision 15 phosphodiester bonds from the biotin site. This second 5′ incision reaction had previously been shown to require the nicked primary 5′ incision site, UvrB and UvrC, but not UvrA (Moolenaar *et al.*, 1998a). Therefore mutations within UvrA were not expected to have affected this secondary incision process. It is possible that the lack of incision at this site is due to changes in affinity or stability of protein-protein, protein-nucleotide or protein-DNA interactions and with more time the second incision would be detected. However the intensity of the band representing the first 5′ cleavage was comparable between mutants that do and do not have the second cleavage band. Another possibility is that UvrA normally stimulates this extra incision activity but this would contradict evidence that indicated that UvrA actually inhibited this reaction (Moolenaar *et al.*, 1998a). Finally it is possible that some of the UvrA mutants could not completely dissociate from the UvrB-DNA complex, and thus interfered with secondary incision. However the mutant would have to remain bound in such a way as to not interfere with UvrC binding and the initial incision events. The UvrA protein interacts with both the N- and C-terminal regions of UvrB whilst UvrC interacts with the C-terminal region (Hsu *et al.*, 1995). If the UvrA mutants were unable to dissociate from the N-terminal region of UvrB but were able to dissociate from the C-terminal region, UvrC would potentially be able to be bound to UvrB at the same time as UvrA. However UvrC would still need to cleave at the primary 3′ and 5′ incision sites and could be prevented by UvrA from cleaving at the secondary incision site if this theory is correct. It would be of interest to see if any of the UvrA mutants were able to inhibit the incision of the 15th phosphodiester bond when added to reactions containing UvrB, UvrC and a substrate prenicked at the eighth phosphodiester bond 5′ of the lesion (this assay was used by Moolenaar *et al.* (Moolenaar *et al.*, 1998a)).

Mutants that had subtle effects on the affinity of: UvrA dimerization; ATP binding; DNA binding; or UvrB binding could still be able to function within the incision assay without any noticeable defect. This was due to the incision reaction being analysed at a single time point. Stopping the assay at different time points would enable more information to be gained. However even when a defect was detected it was not possible to identify at which

stage the mutant was unable to function like wild-type. The individual steps of NER were assayed individually in order to identify steps in which amino acid substitutions in UvrA caused a noticeable defect.

Histidine-tagged wild-type UvrA was confirmed as both an ATPase and a GTPase in a series of nucleotide hydrolysis assays. The ATPase activity corresponded closely to the values reported from Sancar's lab however it differed from those reported from Grossman's lab (Myles *et al.*, 1991) (Caron and Grossman, 1988). The GTPase activity more closely resembled ATPase activity than previously published GTPase data (Caron and Grossman, 1988). The reaction conditions between the different labs differed in salt and magnesium concentration, temperature and UvrA concentration. It was therefore unsurprising that different K_m and k_{cat} values were measured.

Some of the amino acid substitutions within UvrA affected both the ATPase and GTPase activity. These mutants generally had an increased K_m and a decreased V_{max} values. The direct effect of the amino acid substitutions could be in: UvrA dimerization; NTP binding; NTP hydrolysis; or NDP release. Gel filtration or analytical ultracentrifugation (AUC) experiments would determine if these mutants were still able to dimerize. This would further localise the precise step in which these nucleotide hydrolysis deficient mutants were affected.

Under high UvrA concentrations UvrB was confirmed to inhibit the GTPase activity of UvrA, presumably via a direct UvrA-UvrB interaction. Interestingly the inhibition data also showed that in reactions where UvrA and UvrB were present high concentrations of GTP enhanced inhibition. This enhanced inhibition was more pronounced at the higher UvrB concentrations (Figure 5.7). This could indicate that under these conditions GTP was required for the formation of both the UvrA dimer and the UvrA-UvrB complex. If this is correct low GTP concentrations would stimulate the UvrA dimerization event but would be unable to promote the formation of the UvrA-UvrB complex. Thus the majority of UvrA would be in the dimerization state that can hydrolyse GTP. At high GTP concentrations there would be sufficient GTP to stimulate the formation of the UvrA-UvrB complex. The UvrA-UvrB complex is unable to hydrolyse GTP at the same rate as the UvrA dimer and thus the GTP hydrolysis rate would decrease. As the proportion of UvrA that was in a UvrA-UvrB complex increased the rate of hydrolysis would decrease.

The inhibition data indicated that at least one molecule of UvrB was present for each molecule of UvrA in the UvrA-UvrB complex. This agreed with scanning force microscopy (SFM) data from which a $UvrA_2UvrB_2$ complex was proposed (Verhoeven *et al.*, 2002). Damage is proposed to be recognised by the successful flipping of the nucleotide adjacent to the damaged site (whose stacking interactions within the double helix are reduced due to the neighbouring damage) (Malta *et al.*, 2006). If, as the inhibition data and published data suggested, there are two molecules of UvrB in the UvrA-UvrB complex then both strands could be scanned without the need for complex dissociation and rebinding which would help aid the overall repair rate within the cell (Verhoeven *et al.*, 2002).

Previous studies using GTPase assays to detect the UvrA-UvrB interactions indicated that the addition of UvrB had no effect on the overall GTPase activity (Truglio *et al.*, 2004). However the GTP concentration (100 μM) used in that assay was below the UvrA and the UvrA-UvrB K_m values for GTP (910 μM and 190 μM respectively) (Caron and Grossman, 1988). At 100 μM GTP the predicted GTP hydrolysis rates of UvrA and UvrA-UvrB were less than 1.3-fold different and thus it was not surprising that a difference in GTPase activity was not detected. At the 2 mM GTP concentration that I used the difference in GTPase activity was predicted to be 3.3-fold different and therefore a decrease in GTPase activity when UvrB was present would and is detected.

The repression of the GTPase activity of the majority of UvrA mutants by UvrB was investigated at a single UvrB concentration (100 nM). The assay was used for the detection of UvrA-UvrB contact mutants as the UvrB mutant $UvrB_{RE183}$ that was known to be deficient in the UvrA-UvrB interaction did not inhibit UvrA under these conditions. This mutant had previously been shown to slightly stimulate GTPase activity (Truglio *et al.*, 2004). $UvrA_{LP151}$, $UvrA_{GD173}$ and $UvrA_{DG205}$ were not affected by UvrB like wild-type UvrA was, and therefore were potentially UvrA-UvrB interaction mutants. $UvrA_{LP151}$ was completely unaffected by UvrB whilst $UvrA_{GD173}$ and $UvrA_{DG205}$ appeared to have a reduced UvrA-UvrB interaction affinity. Further experiments at higher UvrB concentrations are needed to determine if wild-type levels of inhibition can be achieved for these two mutants. The other UvrA mutants were either inhibited by UvrB under these conditions or were deficient in GTPase activity to begin with. However mutants that only slightly altered the UvrA-UvrB binding affinity would not have been detected in this assay

as the protein concentrations used were much higher than the 5 nM K_d value previously reported.

In TCR the NER proteins have been reported to be recruited to the damaged DNA via interactions with Mfd. The crystal structure of Mfd contained a region of structural similarity (amino acids 1 to 340) to UvrB (Assenmacher *et al.*, 2006) (Deaconescu *et al.*, 2006). This region extended beyond the region of sequence homology initially identified (amino acids 82 to 219) (Selby and Sancar, 1993). The corresponding region within UvrB has been linked with the interaction it makes with UvrA (Hsu *et al.*, 1995). Therefore it was suggested that this region of Mfd was involved in the Mfd-UvrA interaction (Selby and Sancar, 1993). UvrA has been shown to interact with Mfd bound to an affinity column (Selby and Sancar, 1993). Furthermore in pull-down assays UvrA interacted with the N-terminal region of Mfd (amino acids 1 to 378) (Selby and Sancar, 1995a).

If Mfd interacts with UvrA at the UvrB binding site it would be expected to compete with UvrB to bind UvrA, and might have a similar effect on GTPase activity. Despite predictions that Mfd interacts with UvrA in a similar manner to UvrB, Mfd was unable to inhibit the GTPase activity of UvrA under the conditions in which UvrB could. Mfd did not appear to compete with UvrB for the UvrA binding site as it was unable to alleviate the inhibition caused by the addition of UvrB to UvrA. However it could be possible that UvrB and Mfd bind different molecules of the same UvrA dimer to form a Mfd-$UvrA_2$-UvrB complex. A Mfd-$UvrA_2$-UvrB complex would help to explain the increased rate of repair in TCR compared to global NER as two of the six proteins required for complete NER (*in vitro*) would be localised to the damaged site without the need to scan the DNA for damage. However binding assays, in which UvrA and a UvrA-UvrB mix were placed on Mfd affinity columns, indicated that Mfd and UvrB were unable to bind UvrA at the same time (Selby and Sancar, 1993).

The results of the GTPase assays involving Mfd could indicate several things. Firstly it could indicate that Mfd interacts with a different region of UvrA than UvrB does. A Mfd-UvrA interaction away from the UvrB binding site would be unlikely to cause the same inhibitory effect as caused by the UvrA-UvrB interaction. Secondly it could indicate that the binding of Mfd to the UvrB interaction domain of UvrA does not have the same effect on GTPase activity. Thirdly it could indicate that the presence of the histidine-tag on UvrA could affect binding by Mfd. Although small the tag is located at the N-terminus

which is the region proposed to interact with Mfd. The tag did not affect the UvrA-UvrB interaction but could potentially affect the Mfd-UvrA interaction. Finally it could indicate that under the conditions used in these experiments Mfd was unable to interact with UvrA (with or without the histidine-tag).

The crystal structure of Mfd indicated that the UvrA interaction region of Mfd may be blocked by domain 7 (Figure 1.12B) (Deaconescu *et al.*, 2006). Within the UvrB crystal structure the UvrA interaction domain was clearly visible and not blocked by any other part of the protein (Truglio *et al.*, 2004). If the UvrA interaction domain of Mfd was blocked this would prevent an interaction between UvrA and Mfd and thus no GTPase inhibition would be detected. It has been proposed that due to conformational changes associated with the interaction Mfd makes with RNAP, domain 7 of Mfd moves (Deaconescu *et al.*, 2006). This movement was suggested to expose the UvrA interaction domain and thus enable a Mfd-UvrA interaction to form. It would be of interest to determine if the deletion of domain 7 would enable Mfd to interact and inhibit the GTPase activity of UvrA.

The DNA binding properties of the UvrA mutants varied with five able to bind DNA and nine unable to form the main complex that was seen with wild-type UvrA. Surprisingly some mutants that were unable to form the main UvrA-DNA complex were able to form a complex with lower mobility. This complex was originally assumed to be multiple dimers of UvrA bound to the same DNA molecule. Its appearance in lanes in which the original UvrA-DNA complex was not detected leads to the theory that some level of cooperation is required between dimers of UvrA for this complex to form. Alternatively it is possible that a higher order complex of UvrA such as a tetramer binds the DNA although no evidence for the formation of UvrA complexes greater than dimers has previously been published.

All of the UvrA mutants that bound DNA could also form a UvrA-UvrB-DNA complex. However, only 65% of the $UvrA_{SA038}$-DNA complex could potentially be converted to the UvrA-UvrB-DNA complex upon addition of any concentration of UvrB. This could indicate that two different UvrA-DNA complexes are formed. For example UvrA could bind specifically to the fluorescein section of the oligonucleotide or it could bind the DNA non-specifically away from the fluorescein site. The non-specific UvrA-DNA complex would not be a suitable target for UvrB loading and as such would be unstable and dissociate. The specific UvrA-DNA complex would be a suitable target for UvrB loading

and therefore a UvrA-UvrB-DNA complex would be formed. In this model any wild-type UvrA that bound non-specific DNA would dissociate and thus be able to rebind the DNA (either specifically or non-specifically). Once UvrA bound specifically UvrB would then bind. If $UvrA_{SA038}$ was unable to dissociate from the non-specific DNA then UvrB would be unable to bind and the $UvrA_{SA038}$-DNA complex would always be detected. The $UvrA_{SA038}$ that bound specifically could bind UvrB to form the UvrA-UvrB-DNA complex.

Some mutants that did not form the UvrA-DNA complex did form the UvrA-UvrB-DNA complex. Previous studies have indicated that the UvrA-UvrB-DNA complex is much more stable than the UvrA-DNA complex (Yeung *et al.*, 1983). Therefore the addition of UvrB could lead to the stabilization of UvrA-DNA interaction which would be detected on the gel as the appearance of the UvrA-UvrB-DNA complex. Other mutants were unable to form either the UvrA-DNA complex or the UvrA-UvrB-DNA complex.

Two UvrB mutants have been characterised. $UvrB_{RE183}$ was unable to inhibit the UvrA GTPase activity or support significant levels of incision on damaged DNA. $UvrB_{RA213}$ was unable to inhibit the GTPase activity of UvrA but was able to facilitate incision of the damaged DNA. This data reflected published date in which $UvrB_{RE183}$ was defective in a variety of *in vitro* assays including UvrA-UvrB interaction assays (Truglio *et al.*, 2004).

In summary, the UvrA mutants isolated in this work can be segregated into different groups depending on their *in vitro* and *in vivo* properties.

$UvrA_{RL023}$ and $UvrA_{VD073}$ were both identified from the UV sensitivity screen. In Δ*uvrA* cells both mutants were able to offer some UV resistance but not to the level seen when wild-type UvrA was present. Both mutants failed to display any wild-type *in vitro* property of those tested. This indicated that either the mutations have specifically affected the UvrA dimerization ability (the first step in NER) or the mutations have had a significant effect on the tertiary structure of the protein.

$UvrA_{VE202}$ was identified from the bacterial two-hybrid screen. It was able to complement Δ*uvrA* cells yet had no wild-type *in vitro* properties. It is likely that $UvrA_{VE202}$ did not maintain its tertiary structure during the purification process.

In contrast the UvrA mutants $UvrA_{FS064}$ and $UvrA_{KE159}$ acted as wild-type UvrA in all *in vitro* assays despite cells carrying these mutations being UV sensitive. An explanation for this is that these residues could affect a function of UvrA that is required *in vivo* but not *in vitro*. For example the residues could be involved in the recruitment of UvrA, as part of a macromolecular complex, to the inner membrane of *E. coli* upon exposure to UV light (Lin *et al.*, 1997).

$UvrA_{YC174}$ and $UvrA_{EV201}$ were unable to bind DNA without the assistance of UvrB. However this characteristic did not affect their ability to complement Δ*uvrA* cells and did not affect the overall incision activity *in vitro*. $UvrA_{Y174}$ and $UvrA_{E201}$ appear to be important for DNA binding but that this role is not essential for successful NER providing a UvrA-UvrB-DNA complex can be formed.

$UvrA_{SY080}$ had reduced nucleotide hydrolysis and DNA binding activity but was still able to form a UvrA-UvrB-DNA complex and enable incision of damaged DNA *in vitro*. The amount of the UvrA-UvrB-DNA complex formed was lower than that formed by wild-type UvrA. The reduced nucleotide hydrolysis rates could be the main cause of the UV sensitivity observed within cells expressing this protein. $UvrA_{S080}$ therefore appears to be important for ATP and GTP binding and/or hydrolysis but other residues must also be involved in these reactions.

$UvrA_{LQ065}$ and $UvrA_{QL087}$ both had poor nucleotide hydrolysis ability and were unable to complement Δ*uvrA* cells to the same extent as wild-type UvrA. However *in vitro* these mutants were able to bind DNA and UvrB and facilitate incision. Interestingly $UvrA_{QL087}$ was unable to enable the secondary incision reaction 15 phosphodiester bonds from the damage site. These results suggest that $UvrA_{L065}$ and $UvrA_{Q087}$ are involved in nucleotide binding or hydrolysis.

The two $UvrA_{L151}$ mutants had been identified from different screens. $UvrA_{LP151}$ was identified from the UV sensitivity screen in which it was unable to complement Δ*uvrA* cells. $UvrA_{LH151}$ was identified from the bacterial two-hybrid screen but unlike $UvrA_{LP151}$ could complement Δ*uvrA* cells. The difference in UV resistance phenotypes was reflected by the *in vitro* properties of these mutants. $UvrA_{LH151}$ was able to hydrolyse ATP and GTP whilst $UvrA_{LP151}$ had reduced K_m values. Both were unable to bind DNA but whilst $UvrA_{LH151}$ could form a UvrA-UvrB-DNA complex $UvrA_{LP151}$ was unable to do so.

Incision was detected when $UvrA_{LH151}$ was present but was not detected when $UvrA_{LP151}$ was present. The replacement of $UvrA_{L151}$ with proline or histidine appeared to have affected UvrA differently. Proline is often associated with large changes in tertiary structure due to the interaction of its side chain with the nitrogen residue of its backbone. Histidine is also dissimilar from leucine but would be unlikely to cause the same level of structural chaos as proline. $UvrA_{L151}$ is likely to be involved in DNA binding. UvrB did not have any effect on the GTPase properties of $UvrA_{LP151}$ whilst it did affect $UvrA_{LH151}$. It is likely that structural changes in $UvrA_{LP151}$ have affected residues involved in the UvrA-UvrB interaction either by altering their position or by blocking their availability. When and if a crystal structure of UvrA is published it would be interesting to determine if any residues near to $UvrA_{L151}$ could be involved in the UvrA-UvrB interaction.

$UvrA_{S038}$ is within the Walker A motif of UvrA. It was therefore predicted and subsequently proven that $UvrA_{SA038}$ would be deficient in nucleotide hydrolysis activity. This mutant was able to bind DNA which has previously been shown not to require nucleotide binding or hydrolysis (Caron and Grossman, 1988). It was also able to form a UvrA-UvrB-DNA complex. However not all the UvrA-DNA complex was converted into the UvrA-UvrB-DNA complex unlike it was with wild-type UvrA. It would appear that even at very high UvrB concentrations a maximum of 65% of the UvrA-DNA complex would be converted into the UvrA-UvrB-DNA complex whilst with the wild-type protein all would have been converted. The formation of a UvrA-UvrB-DNA complex requires ATP binding, not hydrolysis. As such it was expected that the $UvrA_{SA038}$ would be able to completely form the UvrA-UvrB-DNA complex which it did not.

$UvrA_{GD173}$ and $UvrA_{DG205}$ were both identified from the bacterial two-hybrid screens. Both were unable to interact with DNA. Both these mutants had normal nucleotide hydrolysis activities except that the addition of UvrB had a different effect compared to when it was added to wild-type UvrA. UvrB was unable to inhibit the GTPase activity of these UvrA mutant proteins to the same extent as it was able to inhibit the GTPase activity of wild-type UvrA. This strongly suggests that these residues play an important role in the UvrA-UvrB interaction. It would be of interest to see if the inhibition of these mutants by UvrB would eventually reflect the inhibition rate of wild-type UvrA if the protein concentration of UvrB was increased. Both mutants were able to support incision within

the DNA and both conferred UV resistance to Δ*uvrA* cells. $UvrA_{G173}$ and $UvrA_{D205}$ appear to be important for the UvrA-UvrB interaction.

Some of the six UvrA mutants identified from the bacterial two-hybrid screen were not defective in the UvrA-UvrB interaction under the GTPase inhibition assay conditions. In the original bacterial two-hybrid model transcription was proposed to be stimulated if the $\alpha UvrA_{1\text{-}252}$ and the $\lambda cIUvrB_{35\text{-}252}$ fusion proteins interacted. However *in vivo* full-length wild-type UvrB is proposed to interact with the dimeric form of UvrA. Thus the $\lambda cIUvrB_{35\text{-}252}$ truncation of UvrB may only interact with a dimeric form of $\alpha UvrA_{1\text{-}252}$. This alters the bacterial two-hybrid model with two interactions now being essential for transcription. Firstly $\alpha UvrA_{1\text{-}252}$ would have to dimerize and then $\lambda cIUvrB_{35\text{-}252}$ would have to bind UvrA, possibly in two positions (Figure 5.19B). The formation of the $\alpha UvrA_{1\text{-}252}$ dimer would be required to form the correct interface for UvrB binding. Two types of UvrA mutants would therefore be identified from this assay. These would be UvrA dimerization mutants and UvrA-UvrB interaction mutants (Figure 5.19C).

Previous work has identified that residues within $UvrA_{1\text{-}605}$ are required for UvrA dimerization (Myles and Sancar, 1991) (Claassen and Grossman, 1991). $UvrA_{1\text{-}230}$ was unable to dimerize (Claassen and Grossman, 1991). This indicates that at least one residue within $UvrA_{231\text{-}605}$ is essential for dimerization. There is one complete ABC ATPase motif within $UvrA_{1\text{-}680}$. In the absence of the complete ABC ATPase motif dimerization is likely to be compromised. However within the bacterial two-hybrid system the local concentration of $UvrA_{1\text{-}252}$ will be greatly increased as two $\alpha UvrA_{1\text{-}252}$ molecules will be tethered to one RNAP molecule. This may enable a dimer to form without all the necessary components.

If dimerization was required between the UvrA subunits in the bacterial two-hybrid screen then two $\alpha UvrA_{1\text{-}252}$ subunits would likely have to be part of the same RNAP complex. In Figure 3.9 it can be seen that levels of the endogenous full-length RNAPα subunit are greater then the levels of the $\alpha UvrA_{1\text{-}252.(mutants)}$ fusion proteins and therefore the majority of the RNAP complexes will either be in the wild-type form or be a hybrid with one full-length RNAPα subunit and one $\alpha UvrA_{1\text{-}252}$ subunit. Neither of these complexes would be proposed to interact with $\lambda cIUvrB_{35\text{-}252}$ in this model. This would help to explain the low level of β-galactosidase activity that was detected in comparison to other systems in which α and λcI fusion proteins have been used (Dove *et al.*, 1997).

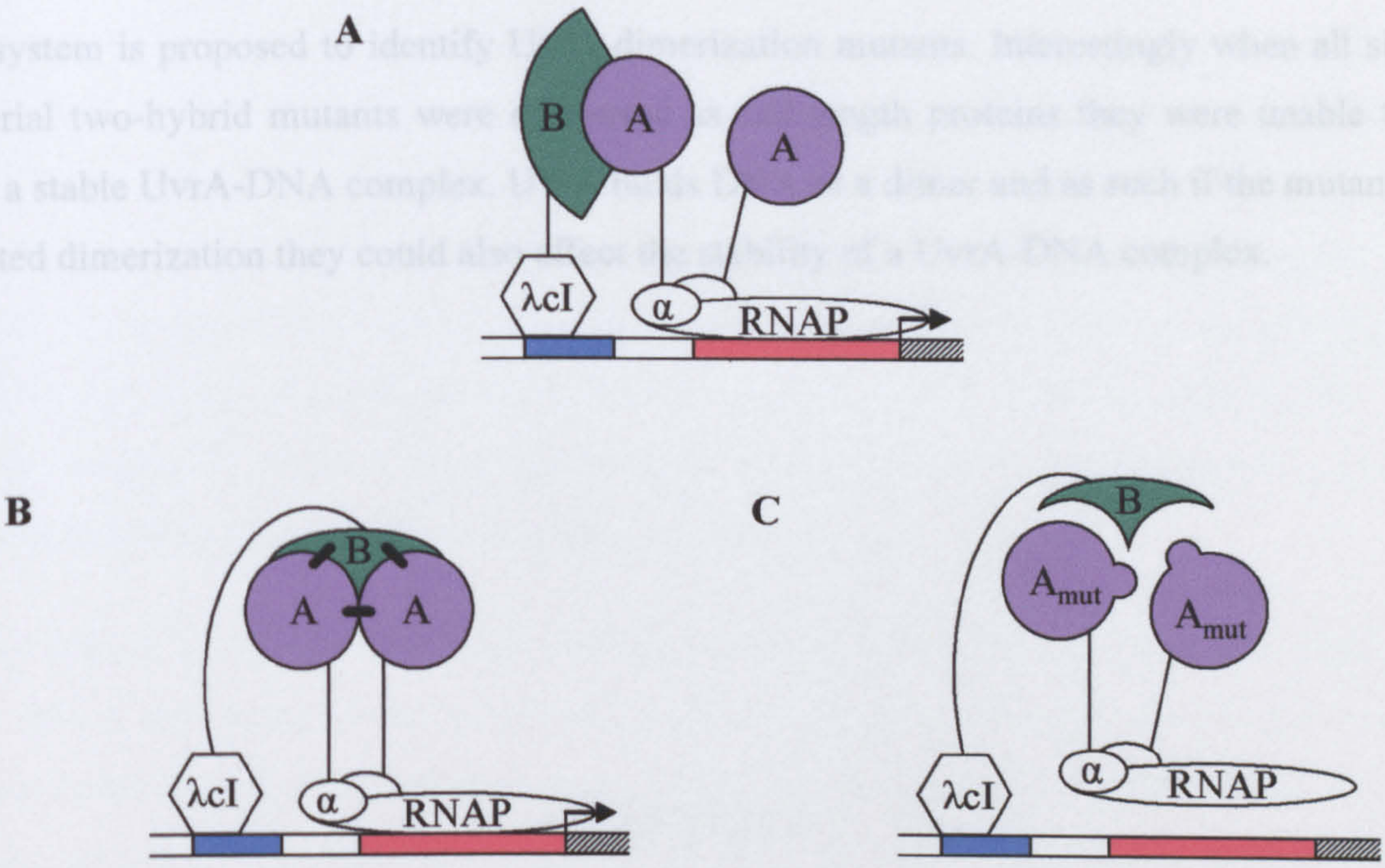

Figure 5.19 Revised model of bacterial two-hybrid interactions.

(**A**) The original model in which one molecule of UvrB interacted with one molecule of UvrA to recruit RNAP to the promoter to activate transcription. (**B**) The revised model in which UvrB will only bind to a UvrA dimer. The UvrA-UvrA and the UvrA-UvrB interaction are both necessary for the recruitment of RNAP to the promoter to activate transcription. The interactions necessary are indicated by thick black lines. (**C**) If UvrA is unable to dimerize then UvrB will not interact and RNAP will not be recruited to the promoter.

The system is proposed to identify UvrA dimerization mutants. Interestingly when all six bacterial two-hybrid mutants were expressed as full-length proteins they were unable to form a stable UvrA-DNA complex. UvrA binds DNA as a dimer and as such if the mutants effected dimerization they could also affect the stability of a UvrA-DNA complex.

CHAPTER 6
CONCLUSIONS

In summary, two genetic screens have been established to identify important residues within UvrA. The bacterial two-hybrid screen was specifically designed to identify residues of UvrA that interrupted the UvrA-UvrB or the UvrA-Mfd interaction. Six residues were identified from this screen as being important in the $UvrA_{1-252}$-$UvrB_{35-252}$ and the $UvrA_{1-252}$-Mfd_{1-219} interaction. The second screen was designed to identify UvrA residues that were essential for any aspect of UvrA function that was essential for its *in vivo* function. 12 residues were identified from this screen of which one ($UvrA_{L151}$) had been identified in the bacterial two-hybrid screen.

Hexa-histidine N-terminally tagged wild-type and mutant UvrA proteins were purified from Δ*uvrA* cells using a one column purification procedure. The tagged wild-type UvrA protein functioned as expected in all assays associated with the NER pathway, indicating that the tag had no effect on these properties of UvrA. Further work is needed to determine if the histidine tag effects the interaction that UvrA makes with Mfd.

Of the 20 identified UvrA mutants (17 residues), 15 (14 residues) were characterised *in vitro*. These mutants are deficient in a range of properties including ATP hydrolysis, DNA binding and overall support of incision activity. Of most interest to us are the two mutants that appear to affect the UvrA-UvrB interaction. $UvrA_{GD173}$ and $UvrA_{DG205}$ were both identified from the bacterial two-hybrid screen and are able to facilitate UV survival *in vivo*. Both mutants are able to hydrolyse GTP but unlike wild-type UvrA this GTPase activity is not strongly repressed by the addition of UvrB.

As part of this work a novel method of site-specifically introducing a lesion within a plasmid was used. SMILing DNA enabled a modification to be introduced within a large DNA fragment at a specific site on a specific strand. The introduced 6Baz modification contains a biotin molecule. Biotin had not previously been used a substrate for NER. The 6Baz modification acts as a NER substrate with similar cleavage patterns to other lesions repaired by NER.

CHAPTER 7
REFERENCES

Acharya, S., Foster, P.L., Brooks, P. and Fishel, R. (2003) The coordinated functions of the *E. coli* MutS and MutL proteins in mismatch repair. *Mol Cell*, **12**, 233-246.

Ahn, B. and Grossman, L. (1996) RNA polymerase signals UvrAB landing sites. *J Biol Chem*, **271**, 21453-21461.

Assenmacher, N., Wenig, K., Lammens, A. and Hopfner, K.P. (2006) Structural basis for transcription-coupled repair: the N terminus of Mfd resembles UvrB with degenerate ATPase motifs. *J Mol Biol*, **355**, 675-683.

Barnard, A.M., Green, J. and Busby, S.J. (2003) Transcription regulation by tandem-bound FNR at *Escherichia coli* promoters. *J Bacteriol*, **185**, 5993-6004.

Baumann, P. and West, S.C. (1998) Role of the human RAD51 protein in homologous recombination and double-stranded-break repair. *Trends Biochem Sci*, **23**, 247-251.

Blatter, E.E., Ross, W., Tang, H., Gourse, R.L. and Ebright, R.H. (1994) Domain organization of RNA polymerase alpha subunit: C-terminal 85 amino acids constitute a domain capable of dimerization and DNA binding. *Cell*, **78**, 889-896.

Blattner, F.R., Plunkett, G., 3rd, Bloch, C.A., Perna, N.T., Burland, V., Riley, M., Collado-Vides, J., Glasner, J.D., Rode, C.K., Mayhew, G.F., Gregor, J., Davis, N.W., Kirkpatrick, H.A., Goeden, M.A., Rose, D.J., Mau, B. and Shao, Y. (1997) The complete genome sequence of *Escherichia coli* K-12. *Science*, **277**, 1453-1474.

Bohr, V.A., Smith, C.A., Okumoto, D.S. and Hanawalt, P.C. (1985) DNA repair in an active gene: removal of pyrimidine dimers from the DHFR gene of CHO cells is much more efficient than in the genome overall. *Cell*, **40**, 359-369.

Boiteux, S. and Radicella, J.P. (1999) Base excision repair of 8-hydroxyguanine protects DNA from endogenous oxidative stress. *Biochimie*, **81**, 59-67.

Borukhov, S., Lee, J. and Laptenko, O. (2005) Bacterial transcription elongation factors: new insights into molecular mechanism of action. *Mol Microbiol*, **55**, 1315-1324.

Boyce, R.P. and Howard-Flanders, P. (1964) Release of ultraviolet light-induced thymine dimers from DNA in *E. coli* K-12. *Proc Natl Acad Sci U S A*, **51**, 293-300.

Caron, P.R. and Grossman, L. (1988) Involvement of a cryptic ATPase activity of UvrB and its proteolysis product, UvrB* in DNA repair. *Nucleic Acids Res*, **16**, 9651-9662.

Caron, P.R., Kushner, S.R. and Grossman, L. (1985) Involvement of helicase II (*uvrD* gene product) and DNA polymerase I in excision mediated by the uvrABC protein complex. *Proc Natl Acad Sci U S A*, **82**, 4925-4929.

Casadaban, M.J. and Cohen, S.N. (1980) Analysis of gene control signals by DNA fusion and cloning in *Escherichia coli*. *J Mol Biol*, **138**, 179-207.

Chambers, A.L. (2005) Transcription termination by a transcription-repair coupling factor. *PhD Thesis*.

Chambers, A.L., Smith, A.J. and Savery, N.J. (2003) A DNA translocation motif in the bacterial transcription-repair coupling factor, Mfd. *Nucleic Acids Res*, **31**, 6409-6418.

Chappell, C., Hanakahi, L.A., Karimi-Busheri, F., Weinfeld, M. and West, S.C. (2002) Involvement of human polynucleotide kinase in double-strand break repair by non-homologous end joining. *Embo J*, **21**, 2827-2832.

Cheng, X. and Roberts, R.J. (2001) AdoMet-dependent methylation, DNA methyltransferases and base flipping. *Nucleic Acids Res*, **29**, 3784-3795.

Christine, K.S., MacFarlane, A.W.t., Yang, K. and Stanley, R.J. (2002) Cyclobutylpyrimidine dimer base flipping by DNA photolyase. *J Biol Chem*, **277**, 38339-38344.

Churchill, J.J., Anderson, D.G. and Kowalczykowski, S.C. (1999) The RecBC enzyme loads RecA protein onto ssDNA asymmetrically and independently of chi, resulting in constitutive recombination activation. *Genes Dev*, **13**, 901-911.

Claassen, L.A., Ahn, B., Koo, H.S. and Grossman, L. (1991) Construction of deletion mutants of the *Escherichia coli* UvrA protein and their purification from inclusion bodies. *J Biol Chem*, **266**, 11380-11387.

Claassen, L.A. and Grossman, L. (1991) Deletion mutagenesis of the *Escherichia coli* UvrA protein localizes domains for DNA binding, damage recognition, and protein-protein interactions. *J Biol Chem*, **266**, 11388-11394.

Cooper, D.L., Lahue, R.S. and Modrich, P. (1993) Methyl-directed mismatch repair is bidirectional. *J Biol Chem*, **268**, 11823-11829.

Costa, R.M., Chigancas, V., Galhardo Rda, S., Carvalho, H. and Menck, C.F. (2003) The eukaryotic nucleotide excision repair pathway. *Biochimie*, **85**, 1083-1099.

Crowley, D.J. and Hanawalt, P.C. (1998) Induction of the SOS response increases the efficiency of global nucleotide excision repair of cyclobutane pyrimidine dimers, but not 6-4 photoproducts, in UV-irradiated *Escherichia coli*. *J Bacteriol*, **180**, 3345-3352.

Daniels, D.S., Woo, T.T., Luu, K.X., Noll, D.M., Clarke, N.D., Pegg, A.E. and Tainer, J.A. (2004) DNA binding and nucleotide flipping by the human DNA repair protein AGT. *Nat Struct Mol Biol*, **11**, 714-720.

Deaconescu, A.M., Chambers, A.L., Smith, A.J., Nickels, B.E., Hochschild, A., Savery, N.J. and Darst, S.A. (2006) Structural basis for bacterial transcription-coupled DNA repair. *Cell*, **124**, 507-520.

DellaVecchia, M.J., Croteau, D.L., Skorvaga, M., Dezhurov, S.V., Lavrik, O.I. and Van Houten, B. (2004) Analyzing the handoff of DNA from UvrA to UvrB utilizing DNA-protein photoaffinity labeling. *J Biol Chem*, **279**, 45245-45256.

Demple, B. and Linn, S. (1980) DNA N-glycosylases and UV repair. *Nature*, **287**, 203-208.

D'Ham, C., Romieu, A., Jaquinod, M., Gasparutto, D. and Cadet, J. (1999) Excision of 5,6-dihydroxy-5,6-dihydrothymine, 5,6-dihydrothymine, and 5-hydroxycytosine from defined sequence oligonucleotides by *Escherichia coli* endonuclease III and Fpg proteins: kinetic and mechanistic aspects. *Biochemistry*, **38**, 3335-3344.

Dillingham, M.S., Spies, M. and Kowalczykowski, S.C. (2003) RecBCD enzyme is a bipolar DNA helicase. *Nature*, **423**, 893-897.

Dixon, D.A. and Kowalczykowski, S.C. (1993) The recombination hotspot chi is a regulatory sequence that acts by attenuating the nuclease activity of the *E. coli* RecBCD enzyme. *Cell*, **73**, 87-96.

Donahue, B.A., Yin, S., Taylor, J.S., Reines, D. and Hanawalt, P.C. (1994) Transcript cleavage by RNA polymerase II arrested by a cyclobutane pyrimidine dimer in the DNA template. *Proc Natl Acad Sci U S A*, **91**, 8502-8506.

Doolittle, R.F., Johnson, M.S., Husain, I., Van Houten, B., Thomas, D.C. and Sancar, A. (1986) Domainal evolution of a prokaryotic DNA repair protein and its relationship to active-transport proteins. *Nature*, **323**, 451-453.

Douki, T. and Cadet, J. (2001) Individual determination of the yield of the main UV-induced dimeric pyrimidine photoproducts in DNA suggests a high mutagenicity of CC photolesions. *Biochemistry*, **40**, 2495-2501.

Dove, S.L. and Hochschild, A. (1998) Conversion of the omega subunit of *Escherichia coli* RNA polymerase into a transcriptional activator or an activation target. *Genes Dev*, **12**, 745-754.

Dove, S.L., Joung, J.K. and Hochschild, A. (1997) Activation of prokaryotic transcription through arbitrary protein-protein contacts. *Nature*, **386**, 627-630.

Dunderdale, H.J., Benson, F.E., Parsons, C.A., Sharples, G.J., Lloyd, R.G. and West, S.C. (1991) Formation and resolution of recombination intermediates by *E. coli* RecA and RuvC proteins. *Nature*, **354**, 506-510.

Eryilmaz, J., Ceschini, S., Ryan, J., Geddes, S., Waters, T.R. and Barrett, T.E. (2006) Structural insights into the cryptic DNA-dependent ATPase activity of UvrB. *J Mol Biol*, **357**, 62-72.

Essigmann, J.M., Croy, R.G., Nadzan, A.M., Busby, W.F., Jr., Reinhold, V.N., Buchi, G. and Wogan, G.N. (1977) Structural identification of the major DNA adduct formed by aflatoxin B1 *in vitro*. *Proc Natl Acad Sci U S A*, **74**, 1870-1874.

Fields, S. and Song, O. (1989) A novel genetic system to detect protein-protein interactions. *Nature*, **340**, 245-246.

Franklin, W.A. and Haseltine, W.A. (1984) Removal of UV light-induced pyrimidine-pyrimidone(6-4) products from *Escherichia coli* DNA requires the *uvrA*, *uvrB*, and *uvrC* gene products. *Proc Natl Acad Sci U S A*, **81**, 3821-3824.

Frederico, L.A., Kunkel, T.A. and Shaw, B.R. (1990) A sensitive genetic assay for the detection of cytosine deamination: determination of rate constants and the activation energy. *Biochemistry*, **29**, 2532-2537.

Friedberg, E., Walker, G., Siede, W., Wood, R., Schultz, R. and Ellenberger, T. (2006) *DNA repair and mutagenesis*. ASM Press, Washington DC.

Fronza, G. and Gold, B. (2004) The biological effects of N3-methyladenine. *J Cell Biochem*, **91**, 250-257.

Garcia-Diaz, M., Bebenek, K., Gao, G., Pedersen, L.C., London, R.E. and Kunkel, T.A. (2005) Structure-function studies of DNA polymerase lambda. *DNA Repair (Amst)*, **4**, 1358-1367.

Goosen, N. and Moolenaar, G.F. (2001) Role of ATP hydrolysis by UvrA and UvrB during nucleotide excision repair. *Res Microbiol*, **152**, 401-409.

Greene, J.M. (2002) Random mutagenesis by PCR. In Ausbel, F.M. (ed.), *Short protocols in molecular biology: a compendium for Current protocols in molecular biology*. John Wiley and Sons, Inc., pp. 8-7 to 8-12.

Haber, J.E. (1998) The many interfaces of Mre11. *Cell*, **95**, 583-586.

Hanawalt, P.C., Ford, J.M. and Lloyd, D.R. (2003) Functional characterization of global genomic DNA repair and its implications for cancer. *Mutat Res*, **544**, 107-114.

Henner, W.D., Grunberg, S.M. and Haseltine, W.A. (1982) Sites and structure of gamma radiation-induced DNA strand breaks. *J Biol Chem*, **257**, 11750-11754.

Hermanson-Miller, I.L. and Turchi, J.J. (2002) Strand-specific binding of RPA and XPA to damaged duplex DNA. *Biochemistry*, **41**, 2402-2408.

Hopfner, K.P., Karcher, A., Shin, D.S., Craig, L., Arthur, L.M., Carney, J.P. and Tainer, J.A. (2000) Structural biology of Rad50 ATPase: ATP-driven conformational control in DNA double-strand break repair and the ABC-ATPase superfamily. *Cell*, **101**, 789-800.

Hopfner, K.P. and Tainer, J.A. (2003) Rad50/SMC proteins and ABC transporters: unifying concepts from high-resolution structures. *Curr Opin Struct Biol*, **13**, 249-255.

Howard-Flanders, P., Boyce, R.P. and Theriot, L. (1966) Three loci in *Escherichia coli* K-12 that control the excision of pyrimidine dimers and certain other mutagen products from DNA. *Genetics*, **53**, 1119-1136.

Hsu, D.S., Kim, S.T., Sun, Q. and Sancar, A. (1995) Structure and function of the UvrB protein. *J Biol Chem*, **270**, 8319-8327.

Hsu, L.M. (2002) Promoter clearance and escape in prokaryotes. *Biochim Biophys Acta*, **1577**, 191-207.

Huffman, J.L., Sundheim, O. and Tainer, J.A. (2005) DNA base damage recognition and removal: new twists and grooves. *Mutat Res*, **577**, 55-76.

Husain, I., Griffith, J. and Sancar, A. (1988) Thymine dimers bend DNA. *Proc Natl Acad Sci U S A*, **85**, 2558-2562.

Husain, I., Sancar, G.B., Holbrook, S.R. and Sancar, A. (1987) Mechanism of damage recognition by *Escherichia coli* DNA photolyase. *J Biol Chem*, **262**, 13188-13197.

Husain, I., Van Houten, B., Thomas, D.C., Abdel-Monem, M. and Sancar, A. (1985) Effect of DNA polymerase I and DNA helicase II on the turnover rate of UvrABC excision nuclease. *Proc Natl Acad Sci U S A*, **82**, 6774-6778.

Husain, I., Van Houten, B., Thomas, D.C. and Sancar, A. (1986) Sequences of *Escherichia coli uvrA* gene and protein reveal two potential ATP binding sites. *J Biol Chem*, **261**, 4895-4901.

Karagiannis, T.C. and El-Osta, A. (2004) Double-strand breaks: signaling pathways and repair mechanisms. *Cell Mol Life Sci*, **61**, 2137-2147.

Karimova, G., Ullmann, A. and Ladant, D. (2001) Protein-protein interaction between *Bacillus stearothermophilus* tyrosyl-tRNA synthetase subdomains revealed by a bacterial two-hybrid system. *J Mol Microbiol Biotechnol*, **3**, 73-82.

Karran, P. and Lindahl, T. (1980) Hypoxanthine in deoxyribonucleic acid: generation by heat-induced hydrolysis of adenine residues and release in free form by a deoxyribonucleic acid glycosylase from calf thymus. *Biochemistry*, **19**, 6005-6011.

Kiianitsa, K., Solinger, J.A. and Heyer, W.D. (2003) NADH-coupled microplate photometric assay for kinetic studies of ATP-hydrolyzing enzymes with low and high specific activities. *Anal Biochem*, **321**, 266-271.

Kim, S.T., Malhotra, K., Smith, C.A., Taylor, J.S. and Sancar, A. (1994) Characterization of (6-4) photoproduct DNA photolyase. *J Biol Chem*, **269**, 8535-8540.

Kim, S.T. and Sancar, A. (1991) Effect of base, pentose, and phosphodiester backbone structures on binding and repair of pyrimidine dimers by *Escherichia coli* DNA photolyase. *Biochemistry*, **30**, 8623-8630.

Kim, S.T. and Sancar, A. (1993) Photochemistry, photophysics, and mechanism of pyrimidine dimer repair by DNA photolyase. *Photochem Photobiol*, **57**, 895-904.

Kleibl, K. (2002) Molecular mechanisms of adaptive response to alkylating agents in *Escherichia coli* and some remarks on O(6)-methylguanine DNA-methyltransferase in other organisms. *Mutat Res*, **512**, 67-84.

Klungland, A. and Lindahl, T. (1997) Second pathway for completion of human DNA base excision-repair: reconstitution with purified proteins and requirement for DNase IV (FEN1). *Embo J*, **16**, 3341-3348.

Korzheva, N., Mustaev, A., Kozlov, M., Malhotra, A., Nikiforov, V., Goldfarb, A. and Darst, S.A. (2000) A structural model of transcription elongation. *Science*, **289**, 619-625.

Krokan, H.E., Standal, R. and Slupphaug, G. (1997) DNA glycosylases in the base excision repair of DNA. *Biochem J*, **325 (Pt 1)**, 1-16.

Krummel, B. and Chamberlin, M.J. (1989) RNA chain initiation by *Escherichia coli* RNA polymerase. Structural transitions of the enzyme in early ternary complexes. *Biochemistry*, **28**, 7829-7842.

Kunkel, T.A. (1992) DNA replication fidelity. *J Biol Chem*, **267**, 18251-18254.

Kunkel, T.A. and Erie, D.A. (2005) DNA mismatch repair. *Annu Rev Biochem*, **74**, 681-710.

Lehmann, A.R. (2003) DNA repair-deficient diseases, xeroderma pigmentosum, Cockayne syndrome and trichothiodystrophy. *Biochimie*, **85**, 1101-1111.

Levin, J.D. and Demple, B. (1990) Analysis of class II (hydrolytic) and class I (beta-lyase) apurinic/apyrimidinic endonucleases with a synthetic DNA substrate. *Nucleic Acids Res*, **18**, 5069-5075.

Lieber, M.R., Ma, Y., Pannicke, U. and Schwarz, K. (2003) Mechanism and regulation of human non-homologous DNA end-joining. *Nat Rev Mol Cell Biol*, **4**, 712-720.

Lin, C.G., Kovalsky, O. and Grossman, L. (1997) DNA damage-dependent recruitment of nucleotide excision repair and transcription proteins to *Escherichia coli* inner membranes. *Nucleic Acids Res*, **25**, 3151-3158.

Lin, C.G., Kovalsky, O. and Grossman, L. (1998) Transcription coupled nucleotide excision repair by isolated *Escherichia coli* membrane-associated nucleoids. *Nucleic Acids Res*, **26**, 1466-1472.

Lin, J.J. and Sancar, A. (1992) Active site of (A)BC excinuclease. I. Evidence for 5' incision by UvrC through a catalytic site involving Asp399, Asp438, Asp466, and His538 residues. *J Biol Chem*, **267**, 17688-17692.

Lindahl, T. (1993) Instability and decay of the primary structure of DNA. *Nature*, **362**, 709-715.

Lindahl, T., Demple, B. and Robins, P. (1982) Suicide inactivation of the *E. coli* O6-methylguanine-DNA methyltransferase. *Embo J*, **1**, 1359-1363.

Lindahl, T. and Nyberg, B. (1972) Rate of depurination of native deoxyribonucleic acid. *Biochemistry*, **11**, 3610-3618.

Linton, K.J. and Higgins, C.F. (1998) The *Escherichia coli* ATP-binding cassette (ABC) proteins. *Mol Microbiol*, **28**, 5-13.

Liu, Y., Masson, J.Y., Shah, R., O'Regan, P. and West, S.C. (2004) RAD51C is required for Holliday junction processing in mammalian cells. *Science*, **303**, 243-246.

Loeb, L.A. and Preston, B.D. (1986) Mutagenesis by apurinic/apyrimidinic sites. *Annu Rev Genet*, **20**, 201-230.

Machius, M., Henry, L., Palnitkar, M. and Deisenhofer, J. (1999) Crystal structure of the DNA nucleotide excision repair enzyme UvrB from *Thermus thermophilus*. *Proc Natl Acad Sci U S A*, **96**, 11717-11722.

Mahdi, A.A., Briggs, G.S., Sharples, G.J., Wen, Q. and Lloyd, R.G. (2003) A model for dsDNA translocation revealed by a structural motif common to RecG and Mfd proteins. *Embo J*, **22**, 724-734.

Malta, E., Moolenaar, G.F. and Goosen, N. (2006) Base flipping in nucleotide excision repair. *J Biol Chem*, **281**, 2184-2194.

Matsunaga, T., Mu, D., Park, C.H., Reardon, J.T. and Sancar, A. (1995) Human DNA repair excision nuclease. Analysis of the roles of the subunits involved in dual incisions by using anti-XPG and anti-ERCC1 antibodies. *J Biol Chem*, **270**, 20862-20869.

Mazur, S.J. and Grossman, L. (1991) Dimerization of *Escherichia coli* UvrA and its binding to undamaged and ultraviolet light damaged DNA. *Biochemistry*, **30**, 4432-4443.

McMillan, S., Edenberg, H.J., Radany, E.H., Friedberg, R.C. and Friedberg, E.C. (1981) den V gene of bacteriophage T4 codes for both pyrimidine dimer-DNA glycosylase and apyrimidinic endonuclease activities. *J Virol*, **40**, 211-223.

Mellon, I. and Hanawalt, P.C. (1989) Induction of the *Escherichia coli* lactose operon selectively increases repair of its transcribed DNA strand. *Nature*, **342**, 95-98.

Mellon, I., Spivak, G. and Hanawalt, P.C. (1987) Selective removal of transcription-blocking DNA damage from the transcribed strand of the mammalian DHFR gene. *Cell*, **51**, 241-249.

Miller, J. (1972) *Experiments in Moleuclar Genetics*. Cold Spring Harbor Laboratory Press, Cold Spring Harbor, NY.

Mishina, Y., Duguid, E.M. and He, C. (2006) Direct reversal of DNA alkylation damage. *Chem Rev*, **106**, 215-232.

Moggs, J.G., Yarema, K.J., Essigmann, J.M. and Wood, R.D. (1996) Analysis of incision sites produced by human cell extracts and purified proteins during nucleotide excision repair of a 1,3-intrastrand d(GpTpG)-cisplatin adduct. *J Biol Chem*, **271**, 7177-7186.

Moolenaar, G.F., Bazuine, M., van Knippenberg, I.C., Visse, R. and Goosen, N. (1998a) Characterization of the *Escherichia coli* damage-independent UvrBC endonuclease activity. *J Biol Chem*, **273**, 34896-34903.

Moolenaar, G.F., Franken, K.L., Dijkstra, D.M., Thomas-Oates, J.E., Visse, R., van de Putte, P. and Goosen, N. (1995) The C-terminal region of the UvrB protein of *Escherichia coli* contains an important determinant for UvrC binding to the

preincision complex but not the catalytic site for 3'-incision. *J Biol Chem*, **270**, 30508-30515.

Moolenaar, G.F., Franken, K.L., van de Putte, P. and Goosen, N. (1997) Function of the homologous regions of the *Escherichia coli* DNA excision repair proteins UvrB and UvrC in stabilization of the UvrBC-DNA complex and in 3'-incision. *Mutat Res*, **385**, 195-203.

Moolenaar, G.F., Hoglund, L. and Goosen, N. (2001) Clue to damage recognition by UvrB: residues in the beta-hairpin structure prevent binding to non-damaged DNA. *Embo J*, **20**, 6140-6149.

Moolenaar, G.F., Monaco, V., van der Marel, G.A., van Boom, J.H., Visse, R. and Goosen, N. (2000) The effect of the DNA flanking the lesion on formation of the UvrB-DNA preincision complex. Mechanism for the UvrA-mediated loading of UvrB onto a DNA damaged site. *J Biol Chem*, **275**, 8038-8043.

Moolenaar, G.F., Schut, M. and Goosen, N. (2005) Binding of the UvrB dimer to non-damaged and damaged DNA: Residues Y92 and Y93 influence the stability of both subunits. *DNA Repair (Amst)*, **4**, 699-713.

Moolenaar, G.F., Uiterkamp, R.S., Zwijnenburg, D.A. and Goosen, N. (1998b) The C-terminal region of the *Escherichia coli* UvrC protein, which is homologous to the C-terminal region of the human ERCC1 protein, is involved in DNA binding and 5'-incision. *Nucleic Acids Res*, **26**, 462-468.

Moolenaar, G.F., van Rossum-Fikkert, S., van Kesteren, M. and Goosen, N. (2002) Cho, a second endonuclease involved in *Escherichia coli* nucleotide excision repair. *Proc Natl Acad Sci U S A*, **99**, 1467-1472.

Moolenaar, G.F., Visse, R., Ortiz-Buysse, M., Goosen, N. and van de Putte, P. (1994) Helicase motifs V and VI of the *Escherichia coli* UvrB protein of the UvrABC endonuclease are essential for the formation of the preincision complex. *J Mol Biol*, **240**, 294-307.

Mu, D. and Sancar, A. (1997) Model for XPC-independent transcription-coupled repair of pyrimidine dimers in humans. *J Biol Chem*, **272**, 7570-7573.

Myles, G.M., Hearst, J.E. and Sancar, A. (1991) Site-specific mutagenesis of conserved residues within Walker A and B sequences of *Escherichia coli* UvrA protein. *Biochemistry*, **30**, 3824-3834.

Myles, G.M. and Sancar, A. (1991) Isolation and characterization of functional domains of UvrA. *Biochemistry*, **30**, 3834-3840.

Nakamura, J., Walker, V.E., Upton, P.B., Chiang, S.Y., Kow, Y.W. and Swenberg, J.A. (1998) Highly sensitive apurinic/apyrimidinic site assay can detect spontaneous and chemically induced depurination under physiological conditions. *Cancer Res*, **58**, 222-225.

Obmolova, G., Ban, C., Hsieh, P. and Yang, W. (2000) Crystal structures of mismatch repair protein MutS and its complex with a substrate DNA. *Nature*, **407**, 703-710.

Oh, E.Y., Claassen, L., Thiagalingam, S., Mazur, S. and Grossman, L. (1989) ATPase activity of the UvrA and UvrAB protein complexes of the *Escherichia coli* UvrABC endonuclease. *Nucleic Acids Res*, **17**, 4145-4159.

Orren, D.K. and Sancar, A. (1989) The (A)BC excinuclease of *Escherichia coli* has only the UvrB and UvrC subunits in the incision complex. *Proc Natl Acad Sci U S A*, **86**, 5237-5241.

Orren, D.K. and Sancar, A. (1990) Formation and enzymatic properties of the UvrB.DNA complex. *J Biol Chem*, **265**, 15796-15803.

Orren, D.K., Selby, C.P., Hearst, J.E. and Sancar, A. (1992) Post-incision steps of nucleotide excision repair in *Escherichia coli*. Disassembly of the UvrBC-DNA complex by helicase II and DNA polymerase I. *J Biol Chem*, **267**, 780-788.

Pages, V. and Fuchs, R.P. (2003) Uncoupling of leading- and lagging-strand DNA replication during lesion bypass *in vivo*. *Science*, **300**, 1300-1303.

Park, J.S., Marr, M.T. and Roberts, J.W. (2002) *E. coli* transcription repair coupling factor (Mfd protein) rescues arrested complexes by promoting forward translocation. *Cell*, **109**, 757-767.

Park, J.S. and Roberts, J.W. (2006) Role of DNA bubble rewinding in enzymatic transcription termination. *Proc Natl Acad Sci U S A*, **103**, 4870-4875.

Pavlov, Y.I., Mian, I.M. and Kunkel, T.A. (2003) Evidence for preferential mismatch repair of lagging strand DNA replication errors in yeast. *Curr Biol*, **13**, 744-748.

Pearlman, D.A., Holbrook, S.R., Pirkle, D.H. and Kim, S.H. (1985) Molecular models for DNA damaged by photoreaction. *Science*, **227**, 1304-1308.

Phillips, D.H. (1983) Fifty years of benzo(a)pyrene. *Nature*, **303**, 468-472.

Pljevaljcic, G., Pignot, M. and Weinhold, E. (2003) Design of a new fluorescent cofactor for DNA methyltransferases and sequence-specific labeling of DNA. *J Am Chem Soc*, **125**, 3486-3492.

Pljevaljcic, G., Schmidt, F. and Weinhold, E. (2004) Sequence-specific methyltransferase-induced labeling of DNA (SMILing DNA). *Chembiochem*, **5**, 265-269.

Plotz, G., Raedle, J., Brieger, A., Trojan, J. and Zeuzem, S. (2003) N-terminus of hMLH1 confers interaction of hMutLalpha and hMutLbeta with hMutSalpha. *Nucleic Acids Res*, **31**, 3217-3226.

Ponticelli, A.S., Schultz, D.W., Taylor, A.F. and Smith, G.R. (1985) Chi-dependent DNA strand cleavage by RecBC enzyme. *Cell*, **41**, 145-151.

Poole, A., Penny, D. and Sjoberg, B.M. (2001) Confounded cytosine! Tinkering and the evolution of DNA. *Nat Rev Mol Cell Biol*, **2**, 147-151.

Rao, B.J. and Radding, C.M. (1993) Homologous recognition promoted by RecA protein via non-Watson-Crick bonds between identical DNA strands. *Proc Natl Acad Sci U S A*, **90**, 6646-6650.

Reardon, J.T., Nichols, A.F., Keeney, S., Smith, C.A., Taylor, J.S., Linn, S. and Sancar, A. (1993) Comparative analysis of binding of human damaged DNA-binding protein (XPE) and *Escherichia coli* damage recognition protein (UvrA) to the major ultraviolet photoproducts: T[c,s]T, T[t,s]T, T[6-4]T, and T[Dewar]T. *J Biol Chem*, **268**, 21301-21308.

Record Jr, M.T., Reznikoff, W.S., Craig, M.L., McQuade, K.L. and Schlax, P.J. (1996) *Escherichia coli* RNA polymerase (Esigma70), promoters, and the kinetics of the steps of transcription initiation. In Neidhardt, F.C. (ed.), *Escherichia coli and Salmonella cellular and molecular biology*. ASM Press, Washington DC, Vol. 1, pp. 792-820.

Riedl, T., Hanaoka, F. and Egly, J.M. (2003) The comings and goings of nucleotide excision repair factors on damaged DNA. *Embo J*, **22**, 5293-5303.

Rina, M. and Bouriotis, V. (1993) Cloning, purification and characterization of the BseCI DNA methyltransferase from Bacillus stearothermophilus. *Gene*, **133**, 91-94.

Sambrook, J. and Russell, D.W. (2001) *Molecular cloning a laboratory manual*. Cold Spring Harbor Laboratory Press, Cold Spring Harbor, NY.

Sancar, A., Clarke, N.D., Griswold, J., Kennedy, W.J. and Rupp, W.D. (1981a) Identification of the *uvrB* gene product. *J Mol Biol*, **148**, 63-76.

Sancar, A. and Hearst, J.E. (1993) Molecular matchmakers. *Science*, **259**, 1415-1420.

Sancar, A., Kacinski, B.M., Mott, D.L. and Rupp, W.D. (1981b) Identification of the *uvrC* gene product. *Proc Natl Acad Sci U S A*, **78**, 5450-5454.

Sancar, A. and Rupp, W.D. (1983) A novel repair enzyme: UVRABC excision nuclease of *Escherichia coli* cuts a DNA strand on both sides of the damaged region. *Cell*, **33**, 249-260.

Savery, N.J., Lloyd, G.S., Busby, S.J., Thomas, M.S., Ebright, R.H. and Gourse, R.L. (2002) Determinants of the C-terminal domain of the *Escherichia coli* RNA polymerase alpha subunit important for transcription at class I cyclic AMP receptor protein-dependent promoters. *J Bacteriol*, **184**, 2273-2280.

Savery, N.J., Lloyd, G.S., Kainz, M., Gaal, T., Ross, W., Ebright, R.H., Gourse, R.L. and Busby, S.J. (1998) Transcription activation at Class II CRP-dependent promoters: identification of determinants in the C-terminal domain of the RNA polymerase alpha subunit. *Embo J*, **17**, 3439-3447.

Scharer, O.D. (2003) Chemistry and biology of DNA repair. *Angew Chem Int Ed Engl*, **42**, 2946-2974.

Scharer, O.D. (2005) DNA interstrand crosslinks: natural and drug-induced DNA adducts that induce unique cellular responses. *Chembiochem*, **6**, 27-32.

Schendel, P.F., Fogliano, M. and Strausbaugh, L.D. (1982) Regulation of the *Escherichia coli* K-12 *uvrB* operon. *J Bacteriol*, **150**, 676-685.

Schofield, M.J., Brownewell, F.E., Nayak, S., Du, C., Kool, E.T. and Hsieh, P. (2001) The Phe-X-Glu DNA binding motif of MutS. The role of hydrogen bonding in mismatch recognition. *J Biol Chem*, **276**, 45505-45508.

Seeberg, E., Nissen-Meyer, J. and Strike, P. (1976) Incision of ultraviolet-irradiated DNA by extracts of *E. coli* requires three different gene products. *Nature*, **263**, 524-526.

Seeberg, E. and Steinum, A.L. (1982) Purification and properties of the uvrA protein from *Escherichia coli*. *Proc Natl Acad Sci U S A*, **79**, 988-992.

Selby, C.P. and Sancar, A. (1990) Transcription preferentially inhibits nucleotide excision repair of the template DNA strand *in vitro*. *J Biol Chem*, **265**, 21330-21336.

Selby, C.P. and Sancar, A. (1993) Molecular mechanism of transcription-repair coupling. *Science*, **260**, 53-58.

Selby, C.P. and Sancar, A. (1995a) Structure and function of transcription-repair coupling factor. I. Structural domains and binding properties. *J Biol Chem*, **270**, 4882-4889.

Selby, C.P. and Sancar, A. (1995b) Structure and function of transcription-repair coupling factor. II. Catalytic properties. *J Biol Chem*, **270**, 4890-4895.

Selby, C.P. and Sancar, A. (1997) Human transcription-repair coupling factor CSB/ERCC6 is a DNA-stimulated ATPase but is not a helicase and does not disrupt the ternary transcription complex of stalled RNA polymerase II. *J Biol Chem*, **272**, 1885-1890.

Selmane, T., Schofield, M.J., Nayak, S., Du, C. and Hsieh, P. (2003) Formation of a DNA mismatch repair complex mediated by ATP. *J Mol Biol*, **334**, 949-965.

Setlow, R.B. and Carrier, W.L. (1964) The disappearance of thymine dimers from DNA: an error-correcting mechanism. *Proc Natl Acad Sci U S A*, **51**, 226-231.

Shinagawa, H. and Iwasaki, H. (1996) Processing the holliday junction in homologous recombination. *Trends Biochem Sci*, **21**, 107-111.

Singleton, M.R., Scaife, S. and Wigley, D.B. (2001) Structural analysis of DNA replication fork reversal by RecG. *Cell*, **107**, 79-89.

Skorvaga, M., DellaVecchia, M.J., Croteau, D.L., Theis, K., Truglio, J.J., Mandavilli, B.S., Kisker, C. and Van Houten, B. (2004) Identification of residues within UvrB that are important for efficient DNA binding and damage processing. *J Biol Chem*, **279**, 51574-51580.

Slieman, T.A. and Nicholson, W.L. (2000) Artificial and solar UV radiation induces strand breaks and cyclobutane pyrimidine dimers in Bacillus subtilis spore DNA. *Appl Environ Microbiol*, **66**, 199-205.

Smith, A.J. and Savery, N.J. (2005) RNA polymerase mutants defective in the initiation of transcription-coupled DNA repair. *Nucleic Acids Res*, **33**, 755-764.

Snow, E.T., Foote, R.S. and Mitra, S. (1984) Base-pairing properties of O6-methylguanine in template DNA during *in vitro* DNA replication. *J Biol Chem*, **259**, 8095-8100.

Snowden, A. and Van Houten, B. (1991) Initiation of the UvrABC nuclease cleavage reaction. Efficiency of incision is not correlated with UvrA binding affinity. *J Mol Biol*, **220**, 19-33.

Sohi, M., Alexandrovich, A., Moolenaar, G., Visse, R., Goosen, N., Vernede, X., Fontecilla-Camps, J.C., Champness, J. and Sanderson, M.R. (2000) Crystal structure of *Escherichia coli* UvrB C-terminal domain, and a model for UvrB-UvrC interaction. *FEBS Lett*, **465**, 161-164.

Sonoda, E., Hochegger, H., Saberi, A., Taniguchi, Y. and Takeda, S. (2006) Differential usage of non-homologous end-joining and homologous recombination in double strand break repair. *DNA Repair (Amst)*, **5**, 1021-1029.

Strazewski, P. (1988) Mispair formation in DNA can involve rare tautomeric forms in the template. *Nucleic Acids Res*, **16**, 9377-9398.

Su, S.S., Lahue, R.S., Au, K.G. and Modrich, P. (1988) Mispair specificity of methyl-directed DNA mismatch correction *in vitro*. *J Biol Chem*, **263**, 6829-6835.

Sutherland, B.M., Bennett, P.V., Sidorkina, O. and Laval, J. (2000) Clustered DNA damages induced in isolated DNA and in human cells by low doses of ionizing radiation. *Proc Natl Acad Sci U S A*, **97**, 103-108.

Svejstrup, J.Q. (2002) Mechanisms of transcription-coupled DNA repair. *Nat Rev Mol Cell Biol*, **3**, 21-29.

Sweder, K.S. and Hanawalt, P.C. (1992) Preferential repair of cyclobutane pyrimidine dimers in the transcribed strand of a gene in yeast chromosomes and plasmids is dependent on transcription. *Proc Natl Acad Sci U S A*, **89**, 10696-10700.

Tang, M., Pham, P., Shen, X., Taylor, J.S., O'Donnell, M., Woodgate, R. and Goodman, M.F. (2000) Roles of *E. coli* DNA polymerases IV and V in lesion-targeted and untargeted SOS mutagenesis. *Nature*, **404**, 1014-1018.

Tantin, D. (1998) RNA polymerase II elongation complexes containing the Cockayne syndrome group B protein interact with a molecular complex containing the transcription factor IIH components xeroderma pigmentosum B and p62. *J Biol Chem*, **273**, 27794-27799.

Tapias, A., Auriol, J., Forget, D., Enzlin, J.H., Scharer, O.D., Coin, F., Coulombe, B. and Egly, J.M. (2004) Ordered conformational changes in damaged DNA induced by nucleotide excision repair factors. *J Biol Chem*, **279**, 19074-19083.

Terleth, C., van Sluis, C.A. and van de Putte, P. (1989) Differential repair of UV damage in *Saccharomyces cerevisiae*. *Nucleic Acids Res*, **17**, 4433-4439.

Theis, K., Chen, P.J., Skorvaga, M., Van Houten, B. and Kisker, C. (1999) Crystal structure of UvrB, a DNA helicase adapted for nucleotide excision repair. *Embo J*, **18**, 6899-6907.

Theis, K., Skorvaga, M., Machius, M., Nakagawa, N., Van Houten, B. and Kisker, C. (2000) The nucleotide excision repair protein UvrB, a helicase-like enzyme with a catch. *Mutat Res*, **460**, 277-300.

Thiagalingam, S. and Grossman, L. (1991) Both ATPase sites of *Escherichia coli* UvrA have functional roles in nucleotide excision repair. *J Biol Chem*, **266**, 11395-11403.

Thomas, D.C., Levy, M. and Sancar, A. (1985) Amplification and purification of UvrA, UvrB, and UvrC proteins of *Escherichia coli*. *J Biol Chem*, **260**, 9875-9883.

Todo, T. (1999) Functional diversity of the DNA photolyase/blue light receptor family. *Mutat Res*, **434**, 89-97.

Tornaletti, S. (2005) Transcription arrest at DNA damage sites. *Mutat Res*, **577**, 131-145.

Tremeau-Bravard, A., Riedl, T., Egly, J.M. and Dahmus, M.E. (2004) Fate of RNA polymerase II stalled at a cisplatin lesion. *J Biol Chem*, **279**, 7751-7759.

Truglio, J.J., Croteau, D.L., Skorvaga, M., DellaVecchia, M.J., Theis, K., Mandavilli, B.S., Van Houten, B. and Kisker, C. (2004) Interactions between UvrA and UvrB: the role of UvrB's domain 2 in nucleotide excision repair. *Embo J*, **23**, 2498-2509.

Truglio, J.J., Karakas, E., Rhau, B., Wang, H., Dellavecchia, M.J., Van Houten, B. and Kisker, C. (2006) Structural basis for DNA recognition and processing by UvrB. *Nat Struct Mol Biol*.

Truglio, J.J., Rhau, B., Croteau, D.L., Wang, L., Skorvaga, M., Karakas, E., Dellavecchia, M.J., Wang, H., Van Houten, B. and Kisker, C. (2005) Structural insights into the first incision reaction during nucleotide excision repair. *Embo J*, **24**, 885-894.

Urig, S., Gowher, H., Hermann, A., Beck, C., Fatemi, M., Humeny, A. and Jeltsch, A. (2002) The *Escherichia coli* dam DNA methyltransferase modifies DNA in a highly processive reaction. *J Mol Biol*, **319**, 1085-1096.

van der Kemp, P.A., Charbonnier, J.B., Audebert, M. and Boiteux, S. (2004) Catalytic and DNA-binding properties of the human Ogg1 DNA N-glycosylase/AP lyase: biochemical exploration of H270, Q315 and F319, three amino acids of the 8-oxoguanine-binding pocket. *Nucleic Acids Res*, **32**, 570-578.

van Gool, A.J., Verhage, R., Swagemakers, S.M., van de Putte, P., Brouwer, J., Troelstra, C., Bootsma, D. and Hoeijmakers, J.H. (1994) RAD26, the functional S. cerevisiae homolog of the Cockayne syndrome B gene ERCC6. *Embo J*, **13**, 5361-5369.

Van Houten, B. (1990) Nucleotide excision repair in *Escherichia coli*. *Microbiol Rev*, **54**, 18-51.

Van Houten, B., Croteau, D.L., Dellavecchia, M.J., Wang, H. and Kisker, C. (2005) 'Close-fitting sleeves': DNA damage recognition by the UvrABC nuclease system. *Mutat Res*, **577**, 92-117.

Van Houten, B., Gamper, H., Sancar, A. and Hearst, J.E. (1987) DNase I footprint of ABC excinuclease. *J Biol Chem*, **262**, 13180-13187.

Venema, J., Mullenders, L.H., Natarajan, A.T., van Zeeland, A.A. and Mayne, L.V. (1990) The genetic defect in Cockayne syndrome is associated with a defect in repair of UV-induced DNA damage in transcriptionally active DNA. *Proc Natl Acad Sci U S A*, **87**, 4707-4711.

Venema, J., van Hoffen, A., Karcagi, V., Natarajan, A.T., van Zeeland, A.A. and Mullenders, L.H. (1991) Xeroderma pigmentosum complementation group C cells remove pyrimidine dimers selectively from the transcribed strand of active genes. *Mol Cell Biol*, **11**, 4128-4134.

Verhoeven, E.E., van Kesteren, M., Moolenaar, G.F., Visse, R. and Goosen, N. (2000) Catalytic sites for 3' and 5' incision of *Escherichia coli* nucleotide excision repair are both located in UvrC. *J Biol Chem*, **275**, 5120-5123.

Verhoeven, E.E., Wyman, C., Moolenaar, G.F. and Goosen, N. (2002) The presence of two UvrB subunits in the UvrAB complex ensures damage detection in both DNA strands. *Embo J*, **21**, 4196-4205.

Verhoeven, E.E., Wyman, C., Moolenaar, G.F., Hoeijmakers, J.H. and Goosen, N. (2001) Architecture of nucleotide excision repair complexes: DNA is wrapped by UvrB before and after damage recognition. *Embo J*, **20**, 601-611.

Visse, R., de Ruijter, M., Brouwer, J., Brandsma, J.A. and van de Putte, P. (1991) Uvr excision repair protein complex of *Escherichia coli* binds to the convex side of a cisplatin-induced kink in the DNA. *J Biol Chem*, **266**, 7609-7617.

Visse, R., de Ruijter, M., Moolenaar, G.F. and van de Putte, P. (1992) Analysis of UvrABC endonuclease reaction intermediates on cisplatin-damaged DNA using mobility shift gel electrophoresis. *J Biol Chem*, **267**, 6736-6742.

Wakasugi, M., Kawashima, A., Morioka, H., Linn, S., Sancar, A., Mori, T., Nikaido, O. and Matsunaga, T. (2002) DDB accumulates at DNA damage sites immediately after UV irradiation and directly stimulates nucleotide excision repair. *J Biol Chem*, **277**, 1637-1640.

Walker, J.R., Corpina, R.A. and Goldberg, J. (2001) Structure of the Ku heterodimer bound to DNA and its implications for double-strand break repair. *Nature*, **412**, 607-614.

Wang, C.I. and Taylor, J.S. (1991) Site-specific effect of thymine dimer formation on dAn.dTn tract bending and its biological implications. *Proc Natl Acad Sci U S A*, **88**, 9072-9076.

Wang, J. and Grossman, L. (1993) Mutations in the helix-turn-helix motif of the *Escherichia coli* UvrA protein eliminate its specificity for UV-damaged DNA. *J Biol Chem*, **268**, 5323-5331.

Wang, J., Mueller, K.L. and Grossman, L. (1994) A mutational study of the C-terminal zinc-finger motif of the *Escherichia coli* UvrA protein. *J Biol Chem*, **269**, 10771-10775.

Ward, J.F. (1988) DNA damage produced by ionizing radiation in mammalian cells: identities, mechanisms of formation, and reparability. *Prog Nucleic Acid Res Mol Biol*, **35**, 95-125.

Warren, M.A., Murray, J.B. and Connolly, B.A. (1998) Synthesis and characterisation of oligodeoxynucleotides containing thio analogues of (6-4) pyrimidine-pyrimidinone photo-dimers. *J Mol Biol*, **279**, 89-100.

Weber, S. (2005) Light-driven enzymatic catalysis of DNA repair: a review of recent biophysical studies on photolyase. *Biochim Biophys Acta*, **1707**, 1-23.

Weinfeld, M., Xing, J.Z., Lee, J., Leadon, S.A., Cooper, P.K. and Le, X.C. (2001) Factors influencing the removal of thymine glycol from DNA in gamma-irradiated human cells. *Prog Nucleic Acid Res Mol Biol*, **68**, 139-149.

Welsh, K.M., Lu, A.L., Clark, S. and Modrich, P. (1987) Isolation and characterization of the *Escherichia coli* mutH gene product. *J Biol Chem*, **262**, 15624-15629.

Wyatt, M.D., Allan, J.M., Lau, A.Y., Ellenberger, T.E. and Samson, L.D. (1999) 3-methyladenine DNA glycosylases: structure, function, and biological importance. *Bioessays*, **21**, 668-676.

Yasui, A., Eker, A.P., Yasuhira, S., Yajima, H., Kobayashi, T., Takao, M. and Oikawa, A. (1994) A new class of DNA photolyases present in various organisms including aplacental mammals. *Embo J*, **13**, 6143-6151.

Yeung, A.T., Mattes, W.B. and Grossman, L. (1986a) Protein complexes formed during the incision reaction catalyzed by the *Escherichia coli* UvrABC endonuclease. *Nucleic Acids Res*, **14**, 2567-2582.

Yeung, A.T., Mattes, W.B., Oh, E.Y. and Grossman, L. (1983) Enzymatic properties of purified *Escherichia coli* uvrABC proteins. *Proc Natl Acad Sci U S A*, **80**, 6157-6161.

Yeung, A.T., Mattes, W.B., Oh, E.Y., Yoakum, G.H. and Grossman, L. (1986b) The purification of the *Escherichia coli* UvrABC incision system. *Nucleic Acids Res*, **14**, 8535-8556.

Yin, X. and Proteau, P.J. (2003) Characterization of native and histidine-tagged deoxyxylulose 5-phosphate reductoisomerase from the cyanobacterium Synechocystis sp. PCC6803. *Biochim Biophys Acta*, **1652**, 75-81.

Yoakum, G.H. and Grossman, L. (1981) Identification of *E. coli* uvrC protein. *Nature*, **292**, 171-173.

Yokoi, M., Masutani, C., Maekawa, T., Sugasawa, K., Ohkuma, Y. and Hanaoka, F. (2000) The xeroderma pigmentosum group C protein complex XPC-HR23B plays an important role in the recruitment of transcription factor IIH to damaged DNA. *J Biol Chem*, **275**, 9870-9875.